Production and characterisation of xylan degrading enzymes produced from *Penicillium chrysogenum* using agricultural biomass

Sadia Fida Ullah

Citation for published version (APA):
Ullah, S. F. (2019). Production and characterisation of xylan degrading enzymes produced from *Penicillium chrysogenum* using agricultural biomass: Postgraduate program in Molecular Biology, University of Brasilia

Link to publications: 1 and 2

ZIP: 70910-900
Brasilia DF, Brazil
www.unb.br

Production and characterisation of xylan degrading enzymes produced from *Penicillium chrysogenum* using agricultural biomass

Sadia Fida Ullah

Supervisor: Prof. Dr. Eliane Ferreira Noronha

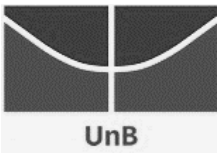

Thesis Submitted in total fulfilment requirements for the degree of

Doctor of Philosophy

Dedicated to Sir Alexander Fleming

Student agreement

I represent that my thesis /dissertation and abstract are my original work. Proper attribution has been given to all outside sources. I understand that I am solely responsible for obtaining any needed copyright permissions. I hereby grant to University of Brasilia and its agents the non-exclusive license to archive and make accessible my work in whole or in part in all forms of media, now or hereafter known including worldwide access. I understand that I may select some access restriction as part of the online submission of this thesis. I retain all ownership rights to the copyright of the thesis. I also retain the right to use in future works (such as articles or books) all or part of my thesis.

Review, approval and acceptance

Thesis entitled; "Production and characterisation of xylan degrading enzymes produced from *Penicillium chrysogenum* using agricultural biomass" was defended at 8th July 2019 in the presence of the thesis evaluation committee approved by the Graduate Program Coordination (PPG). This document has been reviewed and accepted by the supervisor and the thesis evaluation committee, and I verify that this is the final, approved version of my dissertation including all changes required by the evaluation committee.

Thesis evaluation committee

Prof. Dr. Eliane Ferreira Noronha
University of Brasilia

Prof. Dr. Marcelo Henrique Soller Ramada
Catholic University of Brasilia

Prof. Dr.Nádia Skorupa Parachin
University of Brasilia

Prof. Dr. Consuelo Medeiros Rodrigues de Lima
University of Brasilia

Dr. Caio de Oliveira Gorgulho Silva
Embrapa Agroenergy

Sadia Fida Ullah

Table of content

List of figures

List of tables

List of abbreviations

BSA	Bovine serum albumin
CAZy	Carbohydrate-Active enzyme
CBM	Carbohydrate binding module
CD	Circular dichroism
CFPs	Culture filtrate proteins
DNS	Dinitrosalicyl acid
DP	Degree of polymerization
EC	Enzyme Commission
GH	Glycoside hydrolase
HPAEC	High performance anion exchange chromatography
HPLC	High performance liquid chromatography
HX	Heteroxylan
MALDI TOF	Matrix assited laser desorption/ionisation
MS	Mass spectrometry
OSX	Oat spelt xylan
PcX	*Penicillium chrysogenum* xylanase
PNP	P-nitrophenyl
SCB	Sugarcane bagasse
SCS	Sugarcane straw
SDS-PAGE	Sodium dodecyl sulphate polyacrylamide gel electrophoresis
tCA	Transcinnamic acid
tFA	Transferulic acid
Trp	Tryptophan

Short definition of the techniques and terms used

I. Circular dichroism (CD)

Circular dichroism = $\Delta A\ (\lambda) = A\ (\lambda)$ LCPL − A (λ) RCPL, where λ is the wavelength. CD is a type of spectroscopy; widely use to observe the structure (secondary structure) of the molecules. Principle of CD involves the circular polarised light, which measure the difference in absorption of right and left-handed polarised light. CD exhibit absorption band of only optically active chiral molecule (molecules exist as pairs of mirror-image isomers).

II. Molar ellipticity

Molar ellipticity is the unit of CD that can be calculated using the formula;

$$[\theta] = 100 \times \theta / (C \times l \times n)$$

θ is the ellipticity in degrees

l is the optical path in cm

C is the concentration in mg/ml

M is the molecular mass, and

n is the number of residues in the protein

III. Florescence spectroscopy

Florescence spectroscopy involves the UV light pass through the sample to excite the electron in the molecules (fluorophore). These fluorophore absorb light (photon) and excite from the ground state to excited state. When coming back to the ground state, this electron emit/release energy in the form of fluorescence, which is light of a different wavelength (usually longer wavelength). The wavelength (light) that used to excite the molecule is called “excitation wavelength” and the fluorophore that emit the light during its return to ground state is called “emission wavelength”.

IV. Fluorophore

Fluorophore is the molecule (organic) that absorb light at shorter wavelength (excitation) and then emit light at longer wavelength (emission).

V. Fluorescence intensity

Fluorescence is the light emitted from the fluorophore that excited from the ground state by absorbing the shorter wavelength to exited state. Fluorescence or emission intensity is the measurement of emitted light.

VI. Intrinsic and extrinsic fluorophore

Intrinsic fluorophores are naturally occurring fluorescent molecules due to aromatic groups present in the amino acid side chains. Few examples of such compounds are tyrosine, tryptophan, phenylalanine and ferulic acid. Extrinsic fluorophores compounds are not naturally fluorescence. While fluorescence spectroscopy can be used for these compounds by attaching them to the intrinsic fluorophore compounds. Some examples of these are fluorescein, ethidium bromide and acridine orange.

VII. Red and Blue shift

Red shift in the emission spectra is the shift toward longer/higher wavelength (lower energy/lower frequency) While blue shift in the emission spectra is the shift towards shorter/lower wavelength (higher energy/higher frequency).

VIII. Quenching of fluorescence

Quenching is the decreased in the fluorescence/emission light (light emitted by fluorophore). Quenching can be occur due to solvent molecules or by the neighbouring residue located in proximity of fluorophore. The molecule that quench the fluorescence intensity is called Quencher. Quenching can be either collisional/dynamic or static. Small molecules bound to the fluorophore at the ground state and make it nonfluorescent is called static quenching. Dynamic/collisional quenching occur when the fluorophore interact with the quencher molecule at the excited state.

IX. Exciplexes

Exciplexis the complex between the fuorophore and the other moleucle formed during excited state.

X. Enzyme inhibition

Any molecule or substance that caused the inhibition of enzyme activity called the inhibitor. The loss of activity can be either reversible and irreversible. In reversible inhibitor the activity can be recovered after the removing the inhibitor.

i. Competitive inhibition

This inhibition occur when the both substrate and inhibitor compete for binding to the active site. Such inhibition occur at lower concentration of substrate and inhibition can be diminish

as the concentration of substrate increased. In competitive inhibition kinetics K_M (↑) for the substrate increased while Vamx (=) remained unchanged.

ii. Uncompetitive inhibition

In uncompetitive inhibition, the inhibitor binds only with the enzyme substrate complex. In competitive inhibition kinetics, K_M (↓) for the substrate decreased and Vamx (↓) of reaction decreased.

iii. Noncompetitive inhibition

In noncompetitive inhibition the, inhibitor to other than active called allosteric site. This binding facilitate the changes in the catalytic site, due to these changes the substrate not fit properly with the active sit that results in decreased of enzyme turnover rate (Kcat ↓). The increased concentration of substrate does not affect the inhibition.

Resumo

O fungo *Penicillium chrysogenum*, isolado de solo Cerrado, foi cultivado em meios de culturas contendo as biomass lignocelulósica bagaço de cana-de-açúcar (SCB)/palha (SCS), pele de laranja e avicel visando avaliar a produção de celobiohidrolase, endoglicanases, mananases, pectinase e xilanase. O tempo de produção de enzimas usando bagaço de cana foi avaliado por ensaio enzimático e eletroforese unidimensional por 10 dias consecutivos. A atividade máxima de endoglucanase (0.056 $U.mL^{-1}$) e celobihidrolase (0.24 $U.mL^{-1}$) foi maior no décimo dia de crescimento. Mananase e pectinase começaram a ser secretadas no segundo dia com um aumento gradual até o oitavo dia, atingindo a produção máxima de 0.11$U.mL^{-1}$ e 0.10$U.mL^{-1}$, respectivamente. A xilanase foi secretada no segundo dia de crescimento e a produção máxima (0.80$U.mL^{-1}$) foi observada após o sexto dia. Os filtrados protéicos dos meios de cultura (CFPs) foram utilizados para hidrólise enzimática de bagaço de cana-de-açúcar pré-tratado hidrotermicamente (ou submetido a pré-tratamento hidrotérmico), resultando na liberação de glicose (2.85$g.L^{-1}$), xilose (2.15$g.L^{-1}$) e celobiose (0.22$g.L^{-1}$). O zimograma para xilanase mostrou a presença de três isoformas, das quais duas xilanases (*PcX1* and *PcX2*) foram purificadas por cromatografia de troca iônica e gel filtração. A espectrometria de massas permitiu a identificação das enzimas, ambas endo-β-1, 4-xilanases. A enzima *PcX1* (MW 35kDa) apresentou atividade máxima a 30°C e em pH 5.0, mostrando maior afinidade por xilana farinha de aveia, o valor de K_M foi 1.2 $mg.mL^{-1}$ enquanto o K_M da xilana madeira de bétula foi 29.86 $mg.mL^{-1}$. A análise da estrutura secundária da *PcX1* por CD revelou as conformações α-helice, 45%, e folhas betas,10%, sendo consistente com a estrutura tridimensional predita. A *PcX1* mostrou-se tolerante a vanilia, ácidos gálicos e tânico. A orientação de Trp mudou o ambiente para polar pela adição do ácido transferúlico, os valores de K_M aumentaram e os valores de Vmax permaneceram inalterados, o que indica que o ácido ferúlico pode inibir a *PcX1* por competição. A *PcX2* possui massa de 23kDa, atividade ótima em pH 6.0 e 45ºC (termostabilidade de 1h). Os valores cinéticos de K_M e Vmax para *PcX2* foram 0.53 $mg.mL^{-1}$ para a xilana oat spelt. A estrutura terciária da *PcX2* ficou estável na faixa de pH 4.0 a 9.0. *PcX2* foi inibida por vanilia e pelo ácido 4-hidróxi-benzóico. As propriedades biofísicas mostraram que tFA e tCA não interferiram em sua conformação. *PcX2* reteve 77% de atividade na presença de 0.6 $mg.mL^{-1}$ ácido fenólico, a termoestabilidade bem como o aumento e a diminuição do K_M justificaram a afinidade de *PcX2* por seu substrato após a adição dos ácidos fenólicos. Ambas as xilanases foram sensíveis aos íos Cu^{+2} e Zn^{+2}. Este trabalho trouxe uma melhor compreensão na cinética das xilanases (GH10 e GH11), suas propriedades físico-químicas, aplicações na indústria e interação com ácidos fenólicos.

Palavras chaves: caracterização bioquímica, hidrólise enzimátic, xilanases GH10/GH11, cinética, biomassa lignocelulósica, compostos fenólicos, estrutura proteica.

Abstract

Penicillium chrysogenum collected from Cerrado soil cultured in media containing lignocellulosic biomass sugarcane bagasse (SCB)/ straw (SCS),orange peel and avicel aiming to evaluate the production of cellobiohydrolase, endoglucanase, mannanase, pectinase and xylanase. Time course production of enzymes using sugarcane bagasse was measured by activity assay and gel electrophoresis for ten constant days. Maximum activity (0.054 $U.mL^{-1}$) of endoglucanase and (0.24 $U.mL^{-1}$) cellobiohydrolase was recorded on the 10^{th} and 8^{th} day of growth. Mannanase and pectinase start to secrete on the 2^{nd} and 3^{rd} day of growth with a gradual increase until 8^{th} day, maximum yield recorded 0.11 $U.mL^{-1}$ and 0.10 $U.mL^{-1}$, respectively. Xylanase secreted on 2^{nd} of growth, maximum production (0.80 $U.mL^{-1}$) was observed after 6 days. These cultural filtrate proteins (CFPs) were employed for enzymatic hydrolysis of hydrothermal pre-treated SCB, resulted, in the liberation of glucose (2.85 $g.L^{-1}$), xylose (2.15 $g.L^{-1}$) and cellobiose (0.22 $g.L^{-1}$). Zymogram for xylanase showed the presence of three isoforms, while, two xylanases (*PcX1* and *PcX2*) were purified by gel filtration and anion exchange chromatography. Mass spectrometry (MALDI-TOF) identification revealed both enzymes were endo-β-1,4-xylanases. *PcX1* (MW 35kDa) was optimally active at pH 5.0 and 30°C, presented a half-life of 19 hours at 30°C and 6 hours at 40°C, showed a higher affinity for oat spelt xylan, K_M 1.2 $mg.mL^{-1}$ in comparison to birchwood xylan K_M 29.86 $mg.mL^{-1}$. Secondary structure contents 45% α-helix and 10% β-sheet of *PcX1* measured by CD were consistent with the predicted 3D structure. *PcX1* exhibited tolerance for vanillin, tannic and gallic acid. Orientation of Trp- changed to a polar environment by addition of transferulic acid (tFA), K_M values increased values of Vmax remained unchanged, which indicated the ferulic acid might competitively inhibiting the *PcX1*. GH11 xylanase *PcX2* containing MW 23kDa, has optimum activity at pH 6.0 and temperature 45ºC (thermostability 1hour). Kinetic values K_M and Vmax for *PcX2* were 0.53 $mg.mL^{-1}$ for oat spelt xylan. The tertiary structure of *PcX2* was stable over the pH range of 4.0 – 9.0. *PcX2* was inhibited by vanillin and 4-hydroxy-benzoic acid. Biophysical properties showed the tFA and tCA were not interfering with its conformation. *PcX2* retained 77% activity in the presence of 0.6 $mg.mL^{-1}$ of phenolic acids, thermostability as well increased and lower values of K_M justify the affinity of *PcX2* increased to its substrate after the addition of phenolic acids. Both xylanases were sensitive to Cu^{+2} and Zn^{+2}.This work presents the better understanding on xylanase (GH10 and GH11) kinetics, physicochemical properties, their industrial application and interactions with phenolic acids.

Keywords: Biochemical characterisation, enzymatic hydrolysis, enzyme kinetics, lignocellulosic biomass, xylanase GH10/GH11, phenolic compounds, protein structure

This page intentionally left blank

Literature review

Diversity and potential of lignocelluloses

Lignocellulose is the main constituent of the plant cell wall that represents the largest and most abundant biomass deposited in the world. The exploitable lignocellulosic resources are varied and come mainly from agricultural by-products (cereal straws, maize stalks, rape stalks, and sugarcane bagasse), residues from forest exploitations (woody substrates such as hardwoods and softwoods), waste from the wood and paper industry or from the crops of annual (triticale) plants or perennial species with rapid rotation (miscanthus, poplar, eucalyptus). These crops represent the greatest potential for biomass and are currently a significant challenge, due to their high level of production (YUAN et al., 2008). Renewed interest in lignocellulosic resources is linked to the so-called "renewable" nature of the carbon that constitutes them. Global desire is to limit the use of fossil petrochemical resources, in response to socio-economic concerns (scarcity and distribution unequal resources) and ecological impact (global warming). The valorisation of lignocellulosic biomass currently implies to the numerous applications, food industry, bioenergy (biofuels, biogas), chemistry (biomolecules, synthetic intermediates) and biomaterials, thanks to the developed concept of "biorefinery". According to this concept, the plant raw material (mainly cellulose, hemicellulose and lignin) is useable for the production of value-added products, in substitution for products derived from petroleum refineries. (HAYES, 2009; OCTAVE and THOMAS, 2009). Lignocelluloses are complex and diverse substrates, many research questions have been raises related to their organization in the plant, as well as, their pre-treatment methods to satisfy different uses (e.g., carbon source) Therefore, good knowledge of these substrates is an essential pre-requisite for their optimal assessment.

Plant cell wall composition

The plant cell wall is an organized and complex, semi-rigid and dynamic structure that encloses the cytoplasmic membrane of plant cells. It contributes to the rigidity of the plant, due to its structural and mechanical properties, supports cellular growth and constitutes a physical barrier protecting the cell against dehydration, osmotic or physical shocks and infections by pathogens. In general, lignocelluloses essentially correspond to the lignified plant cell wall that represents, about 80% of miscanthus composition and up to 90% of the wood composition. The nature, content and composition of lignocelluloses are functions of the plant species and nature of the plant organ (root, stem, and leaf), tissue and cell type, or the result of a spatial temporal

regulation linked to ecophysiological traits (maturation of tissues, plant development.) and genetic factors (HENRY, 2005HARRIS; SMITH, 2006b). The structural variability of lignocelluloses is particularly apparent in their organization and differential distribution according to cell and tissue types. For example, cereals parenchymal tissues in particular grasses, are practically devoid of lignin and contain mainly polysaccharides, unlike highly vascularised tissues. Although, the walls of different cell types are variable in terms of their chemical composition and structure (HARRIS; SMITH, 2006a). Lignocelluloses are complex assemblies of polysaccharides (mainly cellulose, hemicelluloses) infuse with phenolic compounds including lignins. The secondary cell wall represents the bulk of lignocellulosic mass (HATAKKA; HAMMEL, 2011).

Cellulose is the main constituent of lignocellulosic biomass, accounting for up to 50% of the dry matter of wood. It is a linear homopolymer formed of long β-linked chains of β-D-glucose β- (1,4). The successive units of glucose have a rotation of 180° between them, forming a repeating pattern of cellobiose (glucose dimer). The number of glucose units or degree of polymerization (DP) of cellulose chains varies considerably, depends on its origin as well as the isolation process. It can reach up to 15,000 units, especially for the secondary cell wall, cellulose is insoluble in water and some other solvents. Although the chemical composition of cellulose is simple, its three-dimensional structure is relatively heterogeneous and complex. Cellulose chains are stabilized by hydrogen bonds and intra- or intermolecular van der waal interactions, associate with each other to form microfibrils (O'SULLIVAN, 1997) that assemble together in macrofibrils (Fig 1). Hydrogen bonding network promotes the establishment of crystalline order, serving as a rigid and organized framework for the cell wall. In nature, native cellulose (named cellulose I) consists essentially two crystalline allomorphic phases Iα and Iβ. Cellulose-I may have other crystalline forms because of chemical or thermal treatments. The degree of crystallinity of the cellulose fibre varies between 40% and 60% depending on its origin and the nature of the treatment. Indeed, within the fibrils, highly crystalline regions alternate with amorphous regions that are less organised structured and prone to enzymatic or physicochemical degradation (MCNEIL et al., 1984).

Hemicellulose represents between 25 and 35% of the lignocellulosic biomass. Unlike cellulose, they are amorphous and heterogeneous polysaccharides, consisting of pentoses (xylose, arabinose), hexoses (mannose, glucose, and galactose) and uronic acids. The structure of hemicelluloses varies according to the plant origin, the cell type and the stages of tissues maturity (EBRINGEROVÁ; HEINZE, 2000). Depending on their composition, there are

essentially heteroxylan, xyloglucans and mannans. Xyloglucans represent up to 20% of the dry matter of the primary wall of dicotyledons.

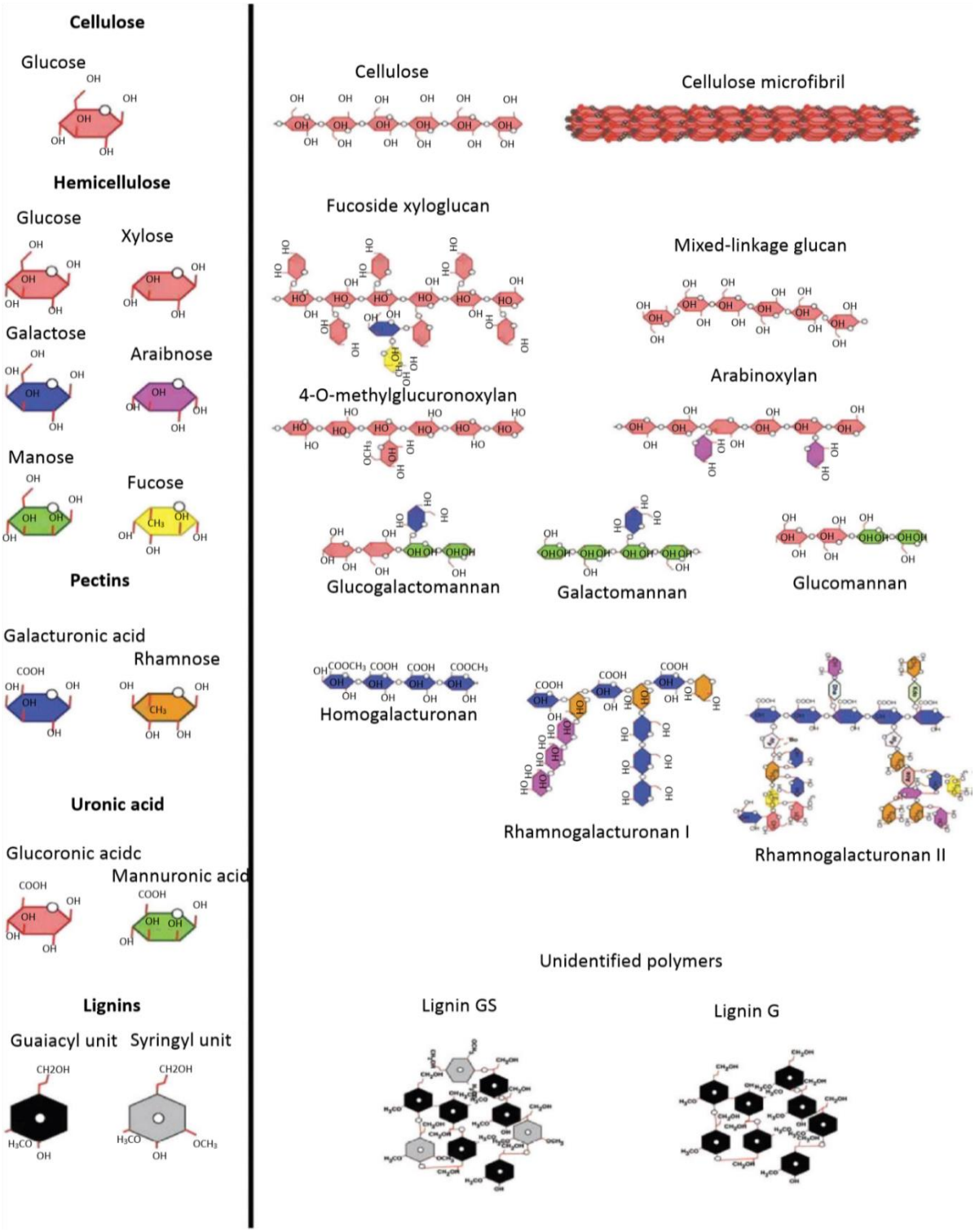

Figure-1 Chemical structure of the predominant building blocks of plant cell walls. Left panel: monomers. Right panel: a subunit of the respective polymers. (Recreated from vector image. Sarkar, P., Bosneaga, E., & Auer, M. (2009). Journal of experimental botany, 60(13), 3615-3635).

Heteroxylan is the main hemicellulose of lignocellulosic biomass (hardwood and annual plants), which can constitute up to 30% of the dry matter of plant secondary wall. In addition, mannans (glucomannans and galactoglucomannans), which are rarely present in angiosperms (grasses and cereals), are the hemicelluloses mainly found in the secondary walls of gymnosperms. In softwood, acetylated galactoglucomannans account for up to 25% of the dry matter (EBRINGEROVÁ, 2006). The primary and secondary cell walls of grasses are characterized by in situ presence of ρ-coumaric acid (pCA) (up to 3%) and ferulic acid (FA) (up to 4%) (Fig 2). Other hydroxycinnamic acids, less predominant, were also highlighted, such as sinapic and caffeic acids. Although quantitatively they poorly represented at the level of walls, these compounds play an important role in the cohesion and the physical resistance of plants. Due to their chemical structure, these phenolic acids have an antimicrobial potential and limit the degradation of the wall by insects, phytopathogens and bacteria (PÉREZ et al., 2002).

Lignin is an abundant polymer in nature, after cellulose and hemicelluloses, representing up to 20% of the dry matter of wheat straw. (BURANOV; MAZZA, 2008). In terms of their functions, lignin contributes to the mechanical support and impermeability of the plant wall and provide resistance from oxidative stress and pathogen attacks. They are amorphous aromatic polymers of heterogeneous structure, resulting from the oxidative copolymerization of the three phenylpropanoic alcohols (or monolignols) p-coumaryl, coniferyl and sinapyl, forming respectively the p-hydroxyphenyl (H), guaiacyl (G) and syringyl (S) (Fig 2). The structural arrangement of these monomeric units is irregular and complex. Their relative proportions vary according to their origin and type of tissue and stage of maturation. Lignin of gymnosperms (soft wood) consists essentially of G units while those of angiosperms are formed from G and S units in variable proportion. The lignin from grasses are more complex and mainly characterized by the presence of G and S units, and lower content of H units (CROZIER; CLIFFORD, 2006).
The increase in S/G ratio generally gives information about their origin and the maturity of the tissues. Many structural models have described the lignified plant wall as a natural nanostructured composite consisting a "framework" of cellulose microfibrils embedded in an amorphous matrix rich in hemicelluloses and encrusted with phenolic compounds including lignins, but also (glyco) proteins, lipids and mineral salts (JIM BIDLACK, MIKE MALONE, 1992 CARPITA; GIBEAUT, 1993). Constituents of plant cell wall interact via intra- and intermolecular covalent or non-covalent associations to form a complex and entangled network.

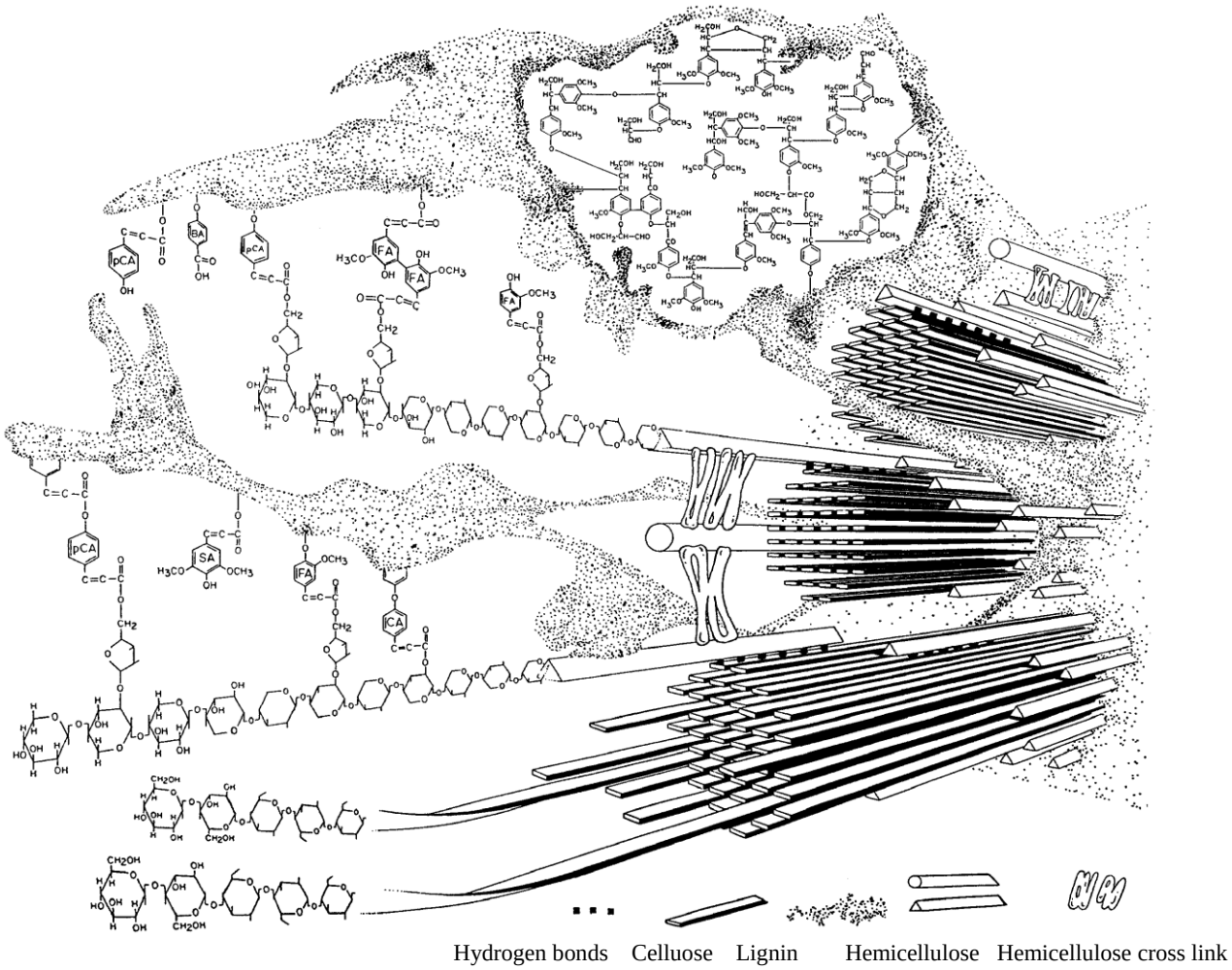

Figure-2 Lignified secondary plant cell wall. Interlink between cellulose and hemicellulose embedded in lignin. Phenolic acids include ferulic acid (FA), cinnamic acid (CA), ρ-coumaric acid (pCA), benzoic acid (BA, sinapic acid (SA) (From. JIM BIDLACK, MIKE MALONE, (1992). In Proceedings of the Oklahoma Academy of Science, 72, 51-56.

Associations with weak, but sometimes numerous, non-covalent bonds can be created between cellulose and hemicelluloses (xyloglucans, glucomannans, etc.), contributing to the cohesion/toughness of cell wall (WERTZ et al., 2017). In grasses, heteroxylans (GAX and/or AX) bridge the fibrils of cellulose. Indeed, the unbranched zones of these polymers are capable of creating inter-chain hydrogen bonds with cellulose. Moreover, the heteroxylans are likely to interact covalently with each other and with the other cell wall components, in particular to lignin via phenolic acids (TAVARES; BUCKERIDGE, 2015).

Phenolic acids, in particular, ferulic acid (FA) are not simply deposited in the cell wall, but play an important role in the covalent cross-linking of the parietal polymers and thus in the

structuring of lignocelluloses (FAULDS; WILLIAMSON, 1999). Indeed, it is "bifunctional" molecule that on the one hand can engage their carboxylic function in ester bonds and on the other hand their hydroxy-phenol group in ether bonds. Thus, ferulic acid is esterified with heteroxylan (AX or GAX) but also etherified with lignin. The oxidation of FA esters within the cell wall results in the formation of diferulic acid compounds (di-FA) or dehydrodimers, trimers and ferulic tetramers. These structures are covalent bridges cross-linking the chains of AX or GAX between them and /or with lignin, which could enhance their resistance against enzymatic hydrolysis. (Fig 2) These structures are also initiation points of lignification and thus play an important role in the organization of the walls of grasses. (RALPH et al., 1995)

Lignin being hydrophobic phenolic polymers, interlock with other cell wall components as they polymerize. The encrusting of the lignins would result in the release of water molecules and contribute to reinforcing the rigidity of the walls (DONALDSON, 2001). Many studies suggest that lignin monomers and oligomers are capable of aggregation with hemicelluloses, in particular via hydrophobic interactions, but also rapidly adsorb onto the surface of cellulose microfibrils by means of electrostatic interactions (ATALLA, 1998; BESOMBES; MAZEAU, 2005). In fact, lignification is a late phenomenon that takes place after the deposition of polysaccharides and proteins. Lignin deposition occurs primarily at the level of cellular junctions and then spreads tangentially in the middle lamella, the primary wall and the secondary wall.

Enzymatic degradation of lignocelluloses

The enzymatic deconstruction/degradation of lignocellulose faced challenged due to the structural complexity of plant cell wall, most "lignocellulolytic" microorganisms (phyto-pathogenic bacteria and fungi, saprophytes, symbionts, rumen bacteria) have developed various strategies to attack plant cell wall constituents (cellulose, hemicelluloses, polyphenols or lignin). Microorganisms produce these enzymes in two ways, majority of enzymes secretes in their immediate environment (such as plant and animal organ e.g. protease from papaya and amylase from animals) or mixtures of different enzymes produced/secrete according to the nature of the available substrate (RENNEBERG et al., 2017). Glycoside hydrolases play a central role in plant polysaccharides hydrolysis releasing mono/oligosaccharides directly assimilated by microbial metabolism. By taking inspiration from these natural strategies, the industrial processes of enzymatic degradation of lignocellulosic biomass are based on the development and implementation of in vitro enzymatic cocktails. However, the optimisation of these fractionation

tools requires a better understanding of the structure/function relationship of lignocellulolytic enzymes.

Glycoside hydrolases

Glycoside hydrolases can be classified according to their sequences, tertiary structure (folding), and type of substrate, mode and mechanism of action. Classification based on the type of substrate and reaction was proposed by the Enzyme Commission and is accepted by the International Union of Biochemistry and Molecular Biology (IUBMB). According to this classification glycosides hydrolases receive the general EC type number 3.2.1.x indicating the enzyme class, Hydrolase, Subclass (glycosidase), Sub-subclass (hydrolysing of O-glycosyl bond). So the first three digits indicate enzymes hydrolysing O-glycosyl linkages and the last (x) is variable and depends on the transformed substrate (for example: cellulases (3.2.1.4), xylanases (3.2.1.8). This classification system makes it possible to precisely name the substrate specificity of an enzyme.

Since 1991, a classification of the catalytic domains of glycoside hydrolases into families, based on amino acids sequence similarities, has been proposed to better reflect the structure of these enzymes (HENRISSAT, 1991). The similarities are appreciated by the HCA method ("Hydrophobic Cluster Analysis") or hydrophobic group analysis, which is based on the detection of structural segments constituting the hydrophobic core of globular proteins. With this approach, similarities in three-dimensional folding can be detected between proteins with very low sequence identities (< 20%). According to this classification, the glycoside hydrolases are grouped into families (denoted GH).

The interest of this classification is able to link the same family enzymes with the similar three-dimensional structure but with different activities and vice versa, highlighting convergent or divergent evolution phenomena as well as the presence of preferential structural patterns. At present, there are 115 families of glycoside hydrolases (GH) which approximately one third comprises poly-specific enzymes (Table I.1). Families of enzymes sharing the same three-dimensional folding are grouped into higher hierarchical levels, known as clans or super families (DAVIES; SINNOT, 2008). With regular update, this classification is accessible on the CAZy database (Carbohydrate-Active enZYmes) and is now extended to other classes of active enzymes on sugars, for example, glycosyltransferases or polysaccharides lyase.

Table-1 Clan and families of glycoside hydrolases

Clan	Folding	Clan family
GH-A	(β/α)8	1 2 5 10 17 26 30 35 39 42 50 51 53 59 72 79 51 86 113
GH-B	β−jelly roll	7 16
GH-C	β−jelly roll	11 12
GH-D	(β/α)8	27 31 36
GH-E	6-fold β-propeller	33 34 83 93
GH-F	5-fold β-propeller	43 62
GH-G	(α/α)6	37 63
GH-H	(β/α)8	13 70 77
GH-I	α + β	24 46 80
GH-J	5-fold β-propeller	32 68
GH-K	(β/α)8	18 20 85
GH-L	(α/α)6	15 65
GH-M	(α/α)6	8 48
GH-N	β-helix	28 49

Considering the catalytic reaction as a whole, the glycoside hydrolases can degrade their substrate according to two modes of action: an attack in the middle of the polysaccharide chain (endo mode), with the variant where the chain remains fixed (endo-process mode), or by attacking at the end of the chain (exo mode). However, the attribution of a mode of action is not exclusive, certain enzymes being able to exert endo or exo actions according to the available substrate (Fig 3).

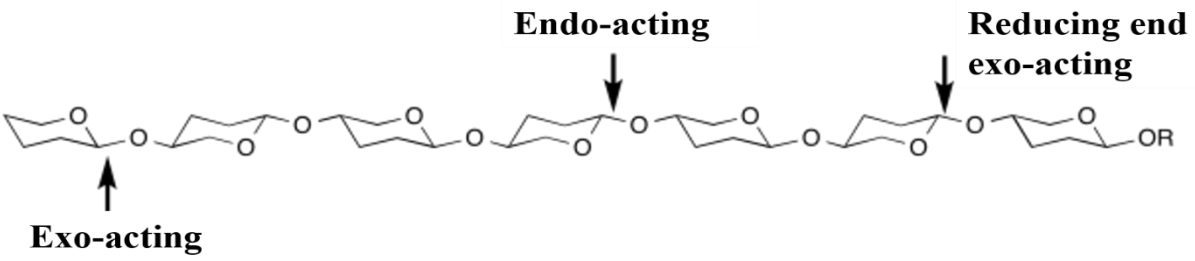

Figure-3 Exo- and endo-acting GH

The mode of action of an enzyme is dictated by the structure of the active site. Despite the diversity of the folds, the topology of the active sites of glycoside hydrolases belongs only to three different classes (DAVIES; HENRISSAT, 1995). Thus, endo enzymes have an open structure with an active site forming a cleft or groove of various sizes, which allows the attachment of several saccharide units (Fig 4).

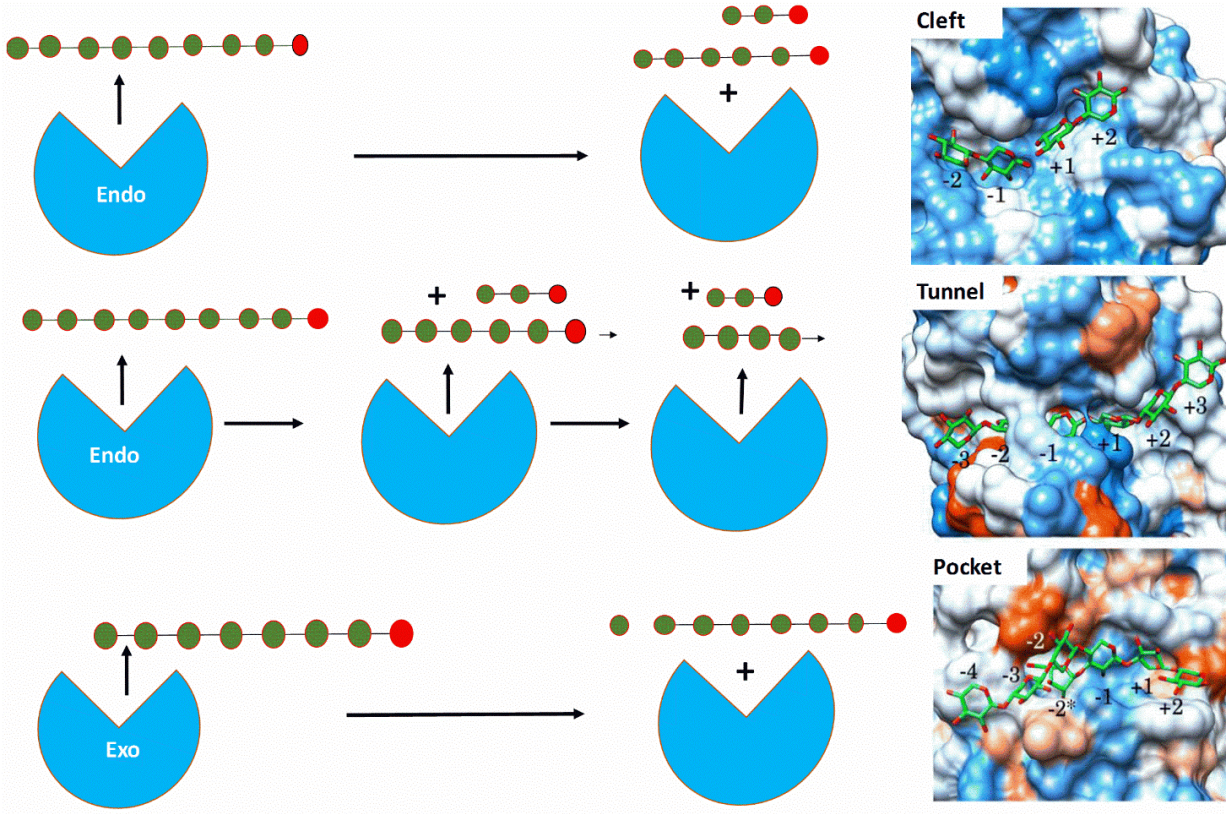

Figure-4 Active sites xylanases (a) the cleft (GH10, SoXynA10; PDB: 1V6U)) (b) the tunnel (GH11, TrXyn11A; PDB: 4HK8) (c) the pocket (GH5_34, CtXyl5A; PDB: 5LA2).

These GHs are capable of hydrolysing an oligo or polysaccharide chain randomly (for example, endoglucanases, endoxylanases). The endo-acting enzymes have the particularity, developed long loops that partially close the catalytic cleft to form a tunnel structure (Fig 4) This tunnel topology allows GHs to bind the polysaccharide chain and progressively process along it, from the reducing end to the non-reducing end, and from one cleavage site to another (by for example cellobiohydrolases). Finally, the exo-enzymes have a "pocket" structure, which is optimal for recognizing the non-reducing or reducing end of an oligo- or polysaccharide chain (for example, arabinofuranosidases).

Catalysis mechanism of glycoside hydrolases.

From the enzymatic catalysis point of view, the hydrolysis of the glycoside bond is carried out according to two major catalytic mechanisms: the retaining GHs and the inverting GHs (KOSHLAND.D.E., 1953). These are nucleophilic substitution mechanisms that result either in the inversion or in the retention of the configuration of the anomeric carbon (α or β) of the sugar units, involving two critical carboxylic acid residues from the active site of enzyme: one acting as an acidic residue while the other acts as nucleophilic / base residue. In most glycoside hydrolases, these residues are glutamate and/or aspartate residues (Fig 5).

The configuration retention of anomeric carbon during hydrolysis is the result of a two-step chemical double-shift mechanism (ARDÈVOL; ROVIRA, 2015). The sugar unit, located on the non-reducing side of the link to be hydrolysed, adopts a boat like conformation that places the inter glycoside oxygen in the vicinity of the proton donor catalytic residue (acid/base residue) and allows a trans-diaxial attack. In a first step (glycosylation), the acid/base residue acts as an acidic catalyst and protonates the glycosidic oxygen, whereas the nucleophilic residue effects a concomitant nucleophilic attack which results in the breakdown of the glycosidic bond and the formation of a glycosyl-covalent enzyme intermediate (ZECHEL; WITHERS, 2001).

Reaction is continued by second step (deglycosylation) where the acid / base residue acting this time as a base, activates a molecule of water (by capturing a proton) which then operates a nucleophilic attack of the anomeric carbon, hydrolyzing the glycosyl-enzyme intermediate and releasing a product of anomeric configuration identical to that of the starting substrate (MCCARTER; STEPHEN WITHERS, 1994b). The glycosyl enzyme formed and hydrolysed by the formation of an oxocarbanium ion. This second step may be a transglycosylation, if the nucleophilic group is derived from sugar (RO-) and not from water (HO-) molecule. In GHs acting, the distance separating the carboxylic groups from the catalytic residues is on average 5.5 Å (Fig 5).

In case of inversing GHs, hydrolysis reaction takes place via a single displacement during which the water molecule is simultaneously activated by the action of the nucleophilic/base residue (which acts as a base) and directly attacks the anomeric carbon resulting in the cleavage of the glycosidic bond with inversion of the configuration of the hydrolysis product. The two catalytic residues are generally distant 9.5 Å that allows accommodating the water molecule between the anomeric carbon and the residue "base"(McCaARTER; STEPHEN WITHERS; 1994; VASELLA et al., 2002).

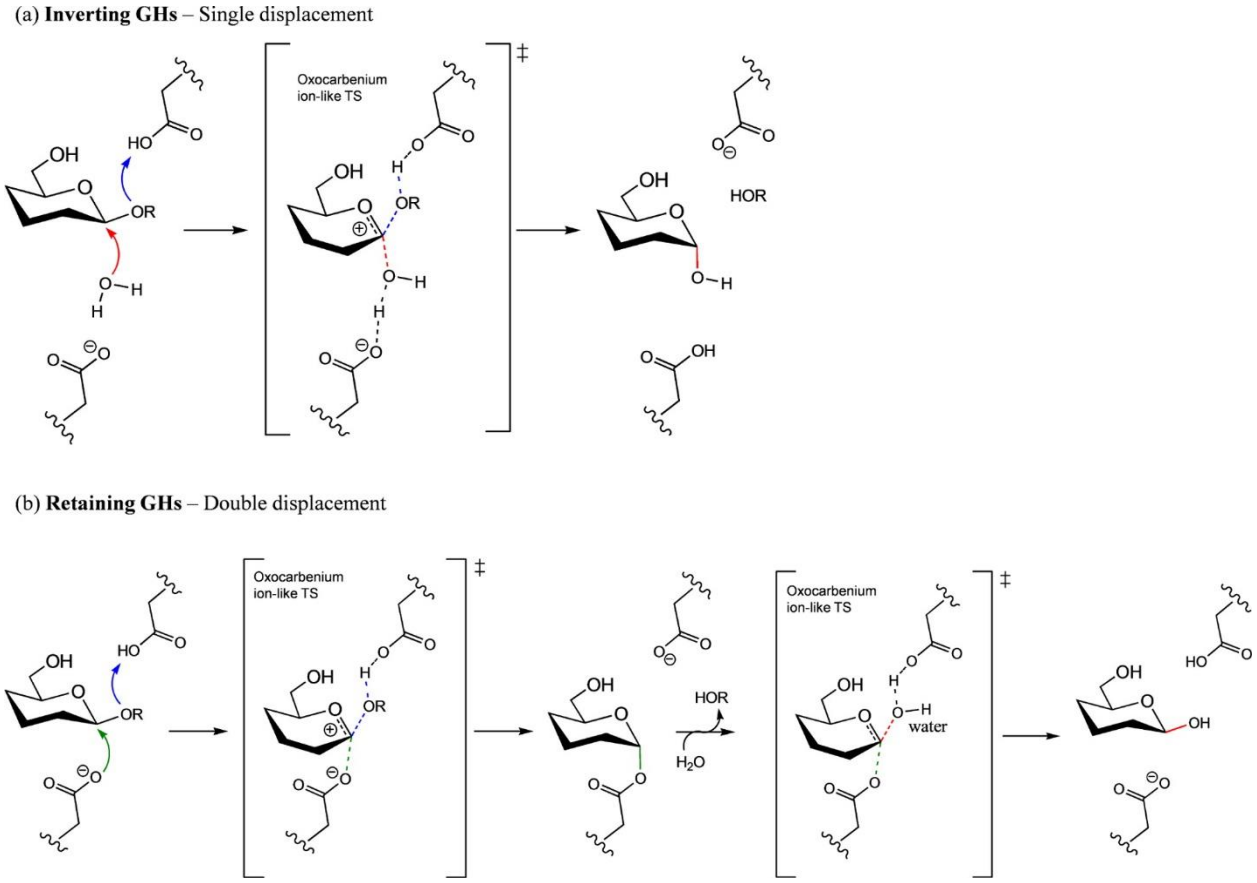

Figure-5 Generalized mechanisms for enzymatic glycoside hydrolysis: (a) inverting GHs and (b) retaining GHs (From. Ardèvol, A., & Rovira, C. (2015). Journal of the American Chemical Society, 137(24), 7528-7547.

Endoxylanases

Endo-β-1,4-xylanases, commonly known as xylanases, catalyse the breakdown of β-(1,4) bond between two β-D-xylopyranose residues of the main chain of heteroxylan. Endoxylanases are involved with other enzymes in the production/release of xylose, the primary source of carbon for the cellular metabolism of many microorganisms such as phytopathogenic bacteria and fungi, rumen bacteria (REN; SUN, 2010). In addition to producing a wide range of enzymes that degrade heteroxylan, most of these microorganisms produce several xylanases, which are variable by their structural properties (3D folding, presence or absence of domains such as CBM, etc.), and biochemical (optimal temperature and pH) and catalytic characteristics (substrate specificity). For example, *Aspergillus niger*, which secretes at least 15 different xylanases or *Trichoderma viride*, which produces 13 xylanases (PRATIMA BAJPAI, 2014) and *Penicillium chrysogenum* that contains 8 different types of xylanases (YANG et al., 2018a).

This diversity and multiplicity of xylanases would be the result of genetic redundancy and post-transcriptional modification and would constitute an adaptive strategy of "lignocellulolytic" microorganisms with respect to complexity, heterogeneity and problems of accessibility of xylosidic bonds within lignocelluloses (GUPTA et al., 2016). Given the huge diversity of sequences, structures and substrate specificities of xylanases, many classifications have been proposed. The first classification based on physicochemical properties, such as molecular weight (MW) and isoelectric point (*p*I) was introduced by (WONG; TAN; SADDLER, 1988). The endoxylanases were then separated into two classes: (i) low molecular weight (MW <30 kDa) and basic pI xylanases, and (ii) those of high molecular weight (MW> 30 kDa) and acidic *p*I.

However, this classification system is only valid for 70% of the xylanases, more complete classification based on the similarity of the catalytic domain sequences, accessible in the CAZy database, which is currently used for endoxylanases (HENRISSAT; GRENOBLE, 1991). According to this classification system, enzymes possessing xylanolytic activity, i.e having the EC 3.2.1.8 nomenclature, belong to families 5, 7, 8, 10, 11, 16, 26, 43, 52 and 62 (COLLINS; GERDAY; FELLER, 2005). The "true" endo-β-1,4-xylanases and the most studied and found in families 10 (formerly family F) and 11 (formerly family G). On the other hand, families 16, 52 and 62 actually contain bifunctional enzymes with two different catalytic domains. Finally, endo-β-1,4-xylanases with a single catalytic domain are limited to families 5, 7, 8, 10, 11 and 43.The vast majority of xylanases, especially those of families 5, 7, 10 and 11, catalysis the hydrolysis of xylan according to a configuration retention mechanism. The catalytic residues involved are generally two glutamic acids conserved from the active site.

In contrast, xylanases of families 8 and 43 typically function with inversion of the anomeric configuration, involving a glutamate residue and an aspartate residue Table I.2. summarizes the essential structural and catalytic properties of these families of enzymes. In general, most endoxylanases, especially families 10 and 11 are formed of a single catalytic domain. Nevertheless, some may have a multi-modular structure and contain in addition one (or more) CBM often dedicated to xylan fixation called xylan-binding domain (XBD). The presence of cellulose binding domain (CBD) has also been demonstrated in some cases of xylanases 11. In particular *Lentinula edodes* Xyn11A, or *Clostridium thermocellum* XynA, especially xylanases 10 such as *Cellvibrio japonicus* Xyn10A and *Pseudomonas fluorescens* (HAYASHI et al., 1999; RAGHOTHAMA et al., 2000; LEE et al., 2005)

These xylanases have the ability to bind to cellulose but are unable to hydrolyse it. Thus, CBDs would confer on xylanases the ability to attach to many sites on the plant wall and thus increase their chances of encountering in situ with their substrates. At present, the 3D structure of about 14 different XBDs associated with endoxylanases of families 10, 11 and 43 are known (CAZY database). Most of these are CBM type B (β-sandwich) belonging to families 2b, 4, 6, 9, 13, 15, 22, 35 and 36 (KITTUR et al., 2003). The nature and number of these XBDs affect the binding specificity of xylanases and their hydrolytic efficiency on both insoluble xylan and/or soluble xylan (MAMO; HATTI-KAUL; MATTIASSON, 2007). Indeed, XBDs have differential binding specificities depending on the degree of substitution of xylan.

Table-2 Xylanase glycoside hydrolase families presenting principle catalytic residue

Family	Clan	Structure	Catalytic Mechanism	Catalytic residues
5	GH-A	$(\beta/\alpha)_8$	Retention	Glu-Glu
7	GH-B	β - jelly roll	Retention	Glu-Glu
8	GH-M	$(\alpha/\alpha)_6$	Inversion	Glu-Asp
10	GH-A	$(\beta/\alpha)_8$	Retention	Glu-Glu
11	GH-C	β -jelly roll	Retention	Glu-Glu
43	GH-F	5-fold β-propeller	Inversion	Glu-Asp

(MCCARTNEY et al., 2006) showed that XBDs of families 4, 6, 15, and 22 similarly bind unsubstituted oat xylan (composed of about 93% xylose and 6% arabinose) and highly substituted rye arabinoxylan (AX) composed of about 50% xylose and 50% arabinose) while the XBDs of families 2b and 35 have a high affinity for low or no substituted xylan. Likewise, the XBDs of family 35 have the particularity of specifically recognizing glucuronoarabinoxylan.

Endo-xylanases of family 10

The family of glycoside hydrolases consists essentially of endo-β-1,4-xylanases (EC 3.2.1.8), but also endo-β-1,3-xylanases (EC 3.2.1.32) and cellobiohydrolases (EC 3.2.1.91). From the point of view of their structure, the endo-β-1,4-xylanases of the family 10 have, in general, a catalytic domain of high molecular weight and low pI with a characteristic three-dimensional folding in the barrel (β /α) (Fig 6). Many xylanases also have CBMs that are most often specific to xylan (XBD). Xyn10C xylanase from *Cellvibrio japonicus*, for example,

presents at its N-terminus an XBD belonging to the CBM family (type B) and capable of binding soluble xylan as well as xylooligosaccharides (Degree of Polymerization > 4).

In endo mode of action, the active site of GH10 xylanases housed in a long crevice that can accommodate four to seven xylose residues (COLLIN et al., 2005). Enzymatic catalysis occurs via a mechanism with retention of the anomeric configuration involving two glutamate residues. The endo-β-1,4-xylanases of the family 10 are distinguished by the versatility of their catalysis, compared to family xylanases 11. In fact, substrate specificity studies have shown that, in addition to xylan, xylanases are also active on low molecular weight cellulosic substrates, including aryl-cellobiosides and some cello-oligosaccharides (GILKES et al., 1991). Similarly, xylanases are able to cleave β-1,3 linkages in rhodymenan (β-1,3; β-1,4-xylan) and to hydrolyse xylan and highly branched oligosaccharides (BIELY et al., 1997)

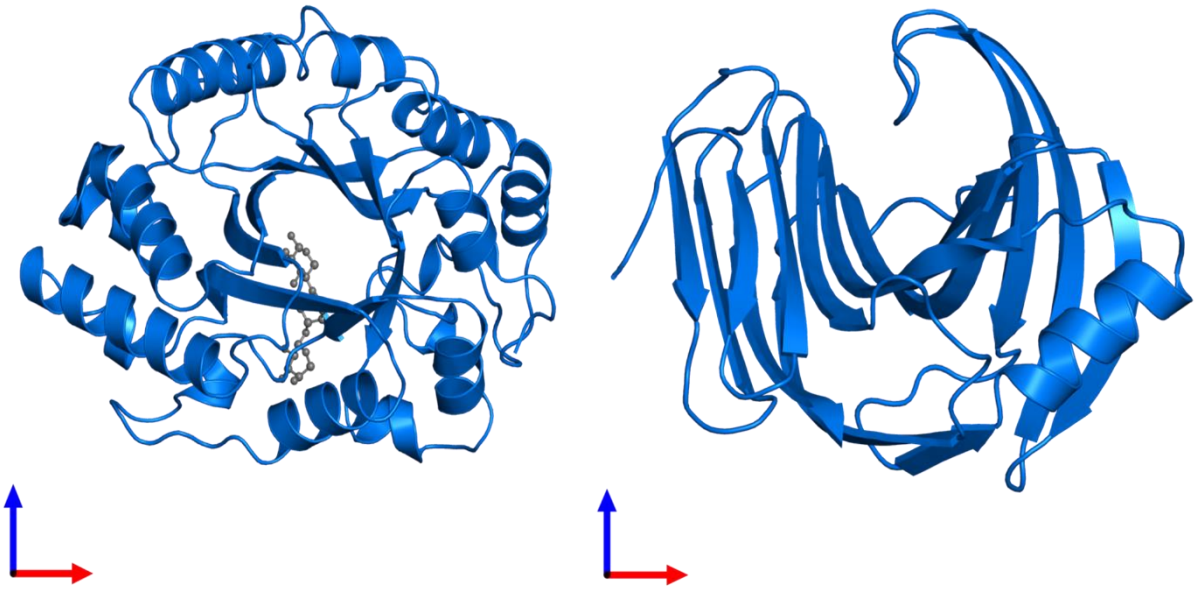

Figure-6 Structure of GH10 (*Penicillium simplicissimum*) and GH11 (*Penicillium funiculosum*) front view. (From Protein Data Base. OISE PAYAN et al., 2004; SCHMIDT; GÜBITZ; KRATKY, 1999)

Endo-xylanases of family 11

The majority of family 11 endoxylanases consist of a single globular functional domain (the catalytic domain). Some contain additionally one or more CBMs. These enzymes belong to clan C and have a characteristic three-dimensional folding in β-jelly-roll (Fig 6). The structure of their catalytic domain mainly comprises two antiparallel β sheets named A and B and α helix. The sheet A is on average composed of 5 strands β (A2-A6), the strand A1 being most often

replaced by a short loop. (Example, *Trichoderma reesei* xylanase TRX II) The β-strands of the B-sheet (B1-B9) have a twist of about 90° so that the sheet B is partially folded back on itself.

The hydrophobic faces of the two sheets A and B form a narrow and deep catalytic cleft. (Fig 6) Relatively short loops (of about 5 amino acid residues) join the secondary structure elements together. Nevertheless, 2 longer loops, of about 10 and 12 residues respectively, connect on the one hand strands B6 and B9 and on the other hand strands B8 and B7. Currently, there are more than 400 xylanases 11 primary sequences in the CAZy database. Study of 82 different xylanases 11, the catalytic domain sequences contain on average 175 to 233 amino acid residues and have a molecular weight ranging from 19 to 26 kDa. The strongest sequence similarities are obtained for strands B5, B6 and B8 as well as the C-ter end of α helix.

The N-ter end of xylanases 11 is weakly conserved. The xylanases XYNI and XYN respectively of *Trichoderma reesei* and *Bacillus circulans* do not contain B1 strand. Similarly, *Polypastron multivesiculatum* xylanase does not have B1 and B2 strands, indicating that their presence does not appear to be required for enzymatic activity. Weak sequence homology is observed for the loops respectively connecting the strands A3-B3, B3-B5 and B7-A6. From the point of view of their secondary structure, endoxylanases of family 11 have a very high level of conservation. Thus, of the 26 xylanase structures 11 known and deposited in the PDB (Protein Data Bank), the only notable variations reside in the presence or absence of the B1 strand at the N-ter end and the prolongation of the A4 strand in C-ter by a short loop (TÖRRÖNEN; ROUVINEN, 1997). In contrast, the primary structures of these enzymes appear more varied. The sequence identity within the GH11 family can range from 40 to 98%. Nevertheless, many functionally important amino acid residues (about 30 residues) are well preserved.

Specificity and selectivity of substrates

In contrast to other families of xylanases, especially family 10, family 11 is a monospecific family, acting exclusively on heteroxylan (HX). The mode of action of xylanases 11 is however largely influenced by the primary structure of heteroxylan, in particular by their degree of substitution (LIAB et al., 2000). Indeed, they are unable to cut a glycosidic bond between two branched xylose residues (by a residue of arabinose or glucuronic acid) or even adjacent to branched residues. Thus, the action of the xylanases 11 seems rather specific for the low substituted zones/regions of HXs, unlike the xylanases of the family 10 having more versatile catalysis and capable of hydrolyzing the arabinoxylans (AX) up to the branches (Fig 7). The action of the two major families of xylanases is essentially due to structural differences, the

catalytic domain of xylanases being more open and less concealed than that of xylanases 11, the jelly-roll which is more compact (CHÁVEZ et al., 2006).

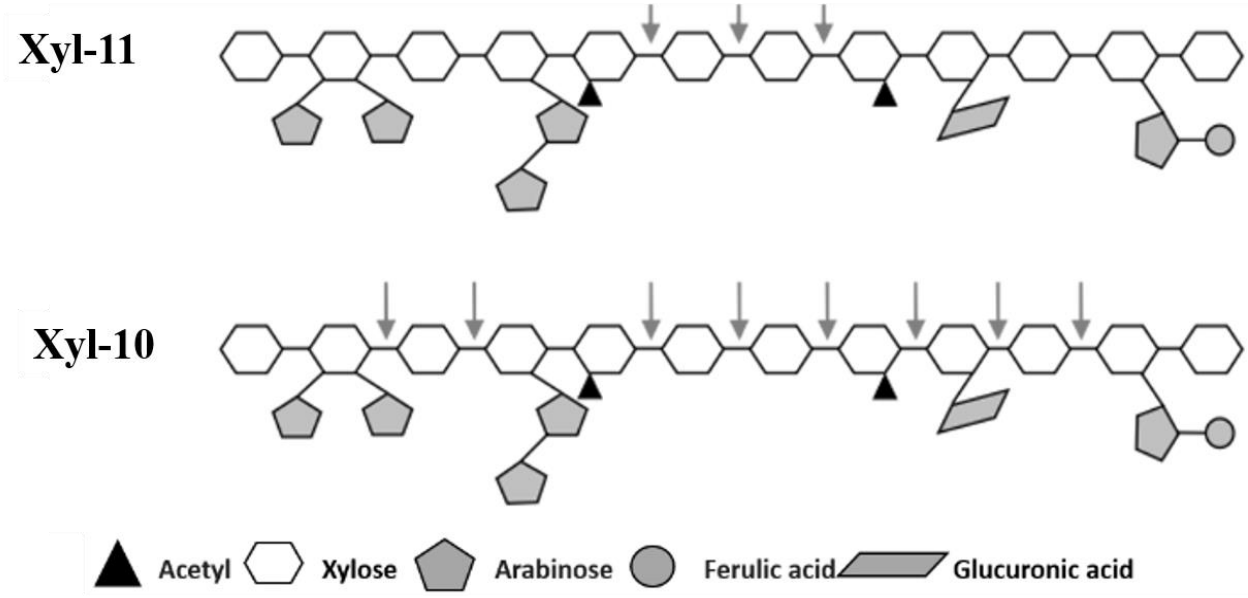

Figure-7 Differences in the mode of action of xylanases 10 and 11 on heteroxylan. Cleavage sites indicated by grey arrows

Similarly, the current classification of xylanases (in GH families) alone does not predict the ability of these enzymes to hydrolyse insoluble arabinoxylan (MOERS et al., 2005). At present, the biochemical and structural bases determining the selectivity of xylanases remain poorly known. Nevertheless, some data in the literature stipulate the involvement of certain surface residues.

In addition to the catalytic residues, the active site of the xylanases 11 contains aromatic residues (tryptophan, tyrosine and phenylalanine) which play an important role in the recognition, "docking" and fixation of the substrate. These residues form binding sub-sites making it possible to establish hydrophobic "stacking" interactions, Van der Waals interactions, as well as hydrogen bonds via their hydroxyl groups with the monomeric units of the sugars. According to the nomenclature introduced by (DAVIES et al., 1997), these subsites are marked (+1), (+2), and so on. Starting from the glycosidic bond that undergoes cleavage to the reducing side, and (-1), (-2), etc. to the non-reducing side, the subsites (-1) and (+1) presence on either side of the cut (Fig 8).

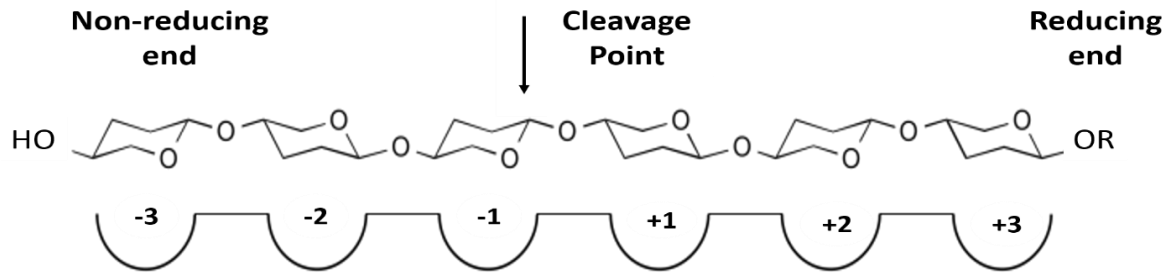

Figure-8 Sub-site nomenclature

Industrial application of endo-β, 1, 4-xylanases

Endo-β-1,4-xylanases are involved in a wide variety of industrial processes in food industries (human and animal), paper industry and lignocellulose biorefinery. In the food sector, xylanases are used in processes for baking and clarification of fruit juices. Their use as an additive in baking pastes, make possible to solubilize the heteroxylan (β-1,4-Xyl backbone) of the wheat flour, resulting in a redistribution of the water molecules that improve the dough elasticity, texture and also increase the bread volume (POLIZELI et al., 2005).

Xylanases are also used in animal feed. In particular, their use improves the nutritional value of feed by reducing the viscosity that increases the digestibility of cereal fibrous foods for monogastric and ruminant animals. Similarly, the oligosaccharides generated under the effect of these enzymes have prebiotic potential (SUBRAMANIYAN; PREMA, 2002).

In non-food industries, such as, textile, the most important application of xylanases is the bleaching of pulp (BUTT et al., 2008). In this sector, these enzymes used as an alternative to chemical bleaching traditionally used to remove lignin from Kraft pulp and employing highly toxic and polluting chlorine agents. The advantage of the use of xylanases consists of the solubilisation of heteroxylan and extraction of lignin without affecting the quality of the cellulose fibres (BUCHERT et al., 1994).

In addition, with the growth of biorefinery processes, the use of xylanases in the controlled fractionation and lignocellulose biorefinery is also growing. Indeed, the degradation of heteroxylan, major compounds of lignocellulose by an enzymatic pathway is more advantageous compared to conventional chemical processes. The reaction is more selective, and takes place under mild conditions, gives better yields, while consuming less energy, and does not cause partial or total degradation of certain constituents of the biomass (eg, cellulose). The saccharification of these polymers results in the release of products with high added values, including oligosaccharides and pentoses (xylose, arabinose, etc.). With regard to xylose, several possibilities for valuation are predicted (ISABIRYE et al., 2013).

In addition to xylitol (sweetener, sucrose substitute for diabetics), xylose is used for the manufacturing of surfactants and especially biofuels (2nd generation, such as ethanol) as a result of fermentation by appropriate fermentative systems (such as yeasts *Pichia stipitis* or *Candida shehate*).

Factors affecting the enzymatic fractionation of lignocelluloses

Although many enzymes (cellulases, hemicellulases) are described as performing for the hydrolysis of simple and soluble substrates (such as isolated polymers), they have very little effect on more complex and insoluble substrates such as lignocellulose. Their actions are influenced by various factors including factors related to their intrinsic catalytic properties (enzymatic catalysis proper) as well as factors related to the accessibility and arrangement of their target substrate at the same time within the plant walls. In addition, the plant walls are so diverse that it is not possible to envisage a single model of enzymatic degradation (DUTTA; WU, 2014).

However, despite the divergences, the plant walls have in common a structural complexity based on a set of macro- and simple molecules, closely associated by covalent or non-covalent bonds, forming a dense and entangled network (JIM BIDLACK, MIKE MALONE, 1992). Most studies on enzymatic catalysis in solid and heterogeneous media concern cellulose degradation by cellulase and few studies are directed to heteroxylan of the plant cell wall. Generalise model proposed for cellulases can nevertheless be applied to other enzymes in cell wall degradation (LEE; FAN, 1982). According to this model, enzymatic degradation of a substrate belonging to a plant wall can be established essentially in V steps: i) transfer of enzyme from aqueous medium to the substrate, ii) adsorption of enzyme on the substrate and the formation of enzyme-substrate complex, iii) hydrolysis of substrate, iv) transfer of products from substrate to aqueous medium, v) transfer of enzyme from aqueous medium to the substrate (step i). Lignocellulose is a porous material having accessible volumes to the circulating/surrounding molecules. However, these "pores" not presents in the form of uniform and regular tunnels, but rather cavities without precise form/shape connected to each other.

Various works have been carried out in order to define the range of accessible volumes of the wall. Most have used physical methods (gas sorption), or have implemented labelled molecules (including fluorescent probes) such as labelled dextran, polyethylene glycols or proteins of known molecular masses, using microscopy approaches allowing the study of the diffusion phenomenon (fluorescence microscopy, FRET, FRAP) (GRETHLEIN, 1985).

Others have used electronic microscopy methods for visualization and direct measurement of walls, using fast freezing techniques (deep freeze-drying) (MCCANN et al., 1990). However, the results obtained sometimes vary considerably depending on the methodology used. Some authors have suggested that the size of these pores would be approximately 3 to 5 nm. Thus, the diffusion of a molecule, in particular, protein is a function of the porosity of the wall, but also of its size, its structure (multi-modular or not), its conformation and the hydrodynamic volume that it occupies in the three-dimensional space. In addition to the notion of accessible pores, the accessibility of the substrate within the cell wall can be restricted. On the one hand because of the multiple intra- or inter-molecular bonds between the cell wall components (covalent crosslinking of heteroxylan via phenolic acids or their interlocking within lignin carbohydrate-complexes) and secondly because of non-specific interactions that may occur between the enzyme and certain compounds. Lignin, for example, is responsible for the non-specific adsorption of cellulases and xylanases via, presumably, hydrophobic interactions and thus clearly defined as limiting penetration and enzymatic degradation of the walls (KOTIRANTA et al., 1999).

For this reason, many biomass pre-treatment processes have been developed for reducing the lignin content in order to reduce these interactions and improve the yields of the enzymatic degradation (DE OLIVEIRA GORGULHO SILVA; FILHO, 2017). The formation of the enzyme-substrate complex (step 2) is the major step of in situ hydrolysis of the plant cell wall. Unlike isolated polymers, specific recognition and binding between enzymes and the insoluble substrate depend on various parameters, including its arrangement within the plant cell wall. Many enzymes have developed adaptive strategies, regarding the complexity of the plant cell wall by arming themselves with protein modules serving as specific probes for adsorption (CBM). These protein modules appear to enhance the recognition and specific binding of enzymes on their target substrate and play an important role in the biodegradation of lignocellulosic substrates (BORASTON et al., 2004)

In addition to transfer and recognition steps, enzymatic hydrolysis of the substrate within the lignocelluloses is subjected to catalytic constraints (as for the isolated polymers), such as the degree of crystallinity and the accessible surface cellulose fibres for cellulases, the degree of heteroxylan substitution for xylanases, or the presence of inhibitory molecules. Recent studies have shown that phenolic compounds (in particular phenolic acids) are the major bottleneck of biorefinery, because of their negative impact on both the enzymatic hydrolysis of plant cell walls and fermentation. These compounds are indeed the inhibitors of cellulases or hemicellulases and

have antimicrobial potential. Their mode of action, however, remains little known (PALMQVIST et al., 1996).

Penicillium chrysogenum

Alexander Fleming first discovered penicillin in 1929 in the culture of *Staphylococcus aureus* that contaminated by *Penicillium rubrum* (FLEMING, 1929), which was subsequently re-identified and designated as *Penicillium notatum*, a synonym of *Penicillium chrysogenum*/*Penicillium rubens* (HOUBRAKEN et al., 2011). Current industrial strains are derived from a single natural isolate of *P. chrysogenum*, NRRL1951, collected during WWII from an infected cantaloupe. Following ultraviolet irradiation of spores from a monoconidial isolate of the well-known strain X-1612 of *Penicillium chrysogenum*, a promising new strain, Wisconsin Q176, was obtained in June, 1945 (BACKUS et al.,1946). The genus *Penicillium* contains numerous significant ascomycetous fungi from the environmental, industrial, and medical perspectives. In 1809 Johann Heinrich Friedrich, first described *Penicillium* as a fungal family that produces brush like asexual proliferative structures called 'penicilli' a unique feature of this genus that used as a tool to recognise the *Penicillium* species. Penicillia are the most widespread filamentous fungi among the eukaryotic microorganisms, with over 350 described species (KIRK, 2008; VISAGIE et al., 2014)

Ubiquitous *Penicillium* species are well recognised as blue and green moulds that attack citrus fruits, some examples are *Penicillium digitatum* and *Penicillium italicum*. *Penicillium* species produced/secrete an enzyme cocktail to degrade and convert the plant cell wall polymers into oligo- and monomers. They are common contaminants of foods, indoor surroundings, and usually present in the soil ecosystem and colonize soil environments through their simple nutritional needs and growth competence (FRISVAD; SAMSON, 2004). *Penicillium* produces a wide range of active biomolecules that influence the life cycles of soil inhabitants. Penicillia survive by absorbing nutrients from plant biomass material and biodegradable organic substances using various extracellular enzymes (PANDA, 2011). These enzymes are also able to degrade xenobiotic compounds leading to soil-pollutant transformation and elimination (LEITÃO, 2009)

Morphological and molecular Identification of fungus

A number of micro-morphological specificities were used in the identification of the *Penicillium*. In addition to the characteristics such as cell-wall texture, the ornamentation of stalks and conidia, dimensions, arrangements and colours of the conidiophore segments (Fig 9).

Conidiophore branching patterns are important in identification that varies from simple (singular) phialides to complex ones (VISAGIE et al., 2014).

Most recognized patterns are: (i) Non-branched or monoverticillate, a group of phialides at the top of the stipe (ii) branched (symmetrical and asymmetrical) comprised of divaricate: simple to complex branching arrangements with several sub-terminal branches. Biverticillate: a cluster of branches, each bearing a cluster of phialides. Terverticillate: branches of conidiophores followed by a second order of branches carrying a cluster of phialides. Quaterverticillate: conidiophores with one additional level of branching beyond the terverticillate pattern.

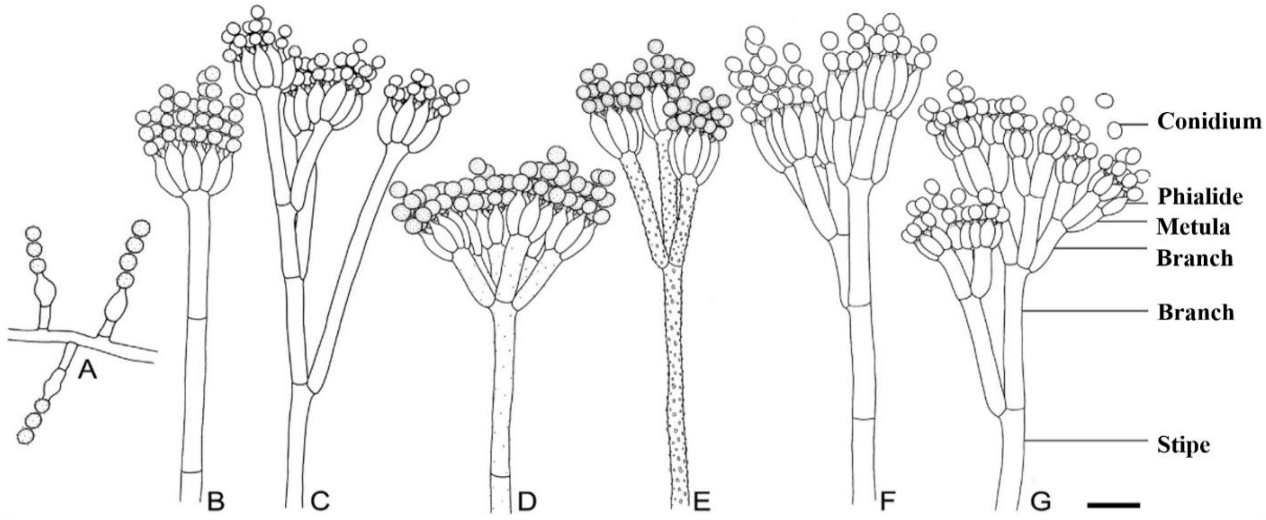

Figure-9 Conidiophore branching patterns of *Penicillium* spp. A). Conidiophores with solitary phialides B). Monoverticillate C). Divaricate. D and E). Biverticillate F). Terverticillate G). Quaterverticillate (From; Visagie et al., 2014. Studies in mycology, 78,343-371).

Molecular techniques of high accuracy, such as the sequencing of housekeeping genes, as well as ribosomal and mitochondrial DNA have been developed. In particular, to assign *Penicillium* sp. β-tubulin (BenA), calmodulin (CaM) as well as internal transcribed spacer (ITS) regions have been sequenced (BARRETOetal., 2011; VISAGIE et al., 2014; SAMSON, 2016) With the full genome sequence of Wis. 54-1255, *P. chrysogenum* has finally entered in the genomic era, opening up new opportunities for research (BERG et al., 2008). The genome (32.19 Mb) of *P. chrysogenum* comprises 12,960 open reading frames, all ORFs have been given a systematic name as follows: Pc for the organism, a two-digit supercontig number, followed by g for gene and a five-digit number matching the order of ORFS on the contig (i.e. Pc12g01520, ACVS).

P. chrysogenum produces various lignocellulolytic enzymes including cellulases (HOU et al., 2007a) and hemicellulases such as acetyl xylan esterase (YANG et al., 2017), arabinofuranosidase (SAKAMOTO et al., 2003), xylanase (HAAS et al., 1992), and mannanase (ZHANG; SANG, 2015). The genome includes genes encoding complete cellulases and numerous hemicellulases (BERG et al., 2008).

Table-3 Glycoside hydrolases produced from *P. chrysogenum*

Family	Enzyme Name	NCBI accession	Reference	Substrate
GH7	cellobiohydrolase (CbhI)	AAV65115	HOU et al., 2007	Avicel cellulose
GH10	endo-beta-1,4-xylanase (XylP)	AAA16427	HAAS et al., 1992	Oat spelt xlyan
GH11	endo-β-1,4-xylanase (Axs2)	BAG75460	Unreview	-
GH12	endo-beta-1,4-glucanase A	AM920431	Unreview	-
GH12	endoglucanase-1	AM920435	Unreview	-
GH15	glucoamylase	BAC82551	SUGIMOTO et al., 2004	Starch
GH27	α-galactosidase	AM920436	SAKAMOTO et al., 2013a	β-1,3-D-galactobiose
GH35	exo-β-1,4-galactanase (Galx35C)	BAM09150		exo-β-1,4-GALs
GH43	α-L-arabinofuranosidase (PcAbf43B)	BAQ35744	SHINOZAKI et al., 2015	arabinan,α-1,5-Ara2,
GH43	α-L-arabinofuranosidase (PcAbf43A)	BAM73651	SHINOZAKI et al., 2014	Branched arabinan
GH43	arabinan endo-α-1,5-L-arabinosidase	BAD15018	SAKAMOTO et al., 2012	Arabinopentaose/hexaose
GH43	endo-α-1,5-L-arabinanase (AbnS1)	BAD89094	SAKAMOTO et al., 2012	Arabinopentaose/hexaose
GH51	α-L-arabinofuranosidase (Afq1)	BAG71680	SAKAMOTO et al., 2013	Arabino-oligosaccharides
GH51	α-L-arabinofuranosidase (PcAbf51C)	BAQ35745	SHINOZAKI et al., 2015	Sugarbeet arabinan,α-1,5-Ara2, α-1,5-Ara3
GH53	endo-β-1,4-galactanase (Gal1)	BAG71683		β-1,4-Galactan, Arabinogalactan
GH54	α-L-arabinofuranosidase (AFS1)	BAG71681	SAKAMOTO et al., 2013b	sugar beet,wheat,soy bean
GH62	α-L-arabinofuranohydrolase (Axs5)	BAG71682	SHINOZAKI et al., 2015	Sugar Beet arabianan/ Wheat arabinoxylan
GH62	α-L-rhamnohydrolase (PcRGRH78A)	BAU45349	MATSUMOTO et al., 2017	RG4 (rhamnogalacturonan tetrasaccharide)
GH75	chitosanase (ChP;PgChP)	ADG96019	Martín et al., 2010	Chitosan
GH78	α-L-rhamnosidase (Pcrha78B)	BAU37009	MATSUMOTO et al., 2017	PNP-α-rhamnopyranoside, Naringin,
GH93	exo-α-1,5-L-arabinanase (AbnX)	BAC76689	SAKAMOTO et al., 2004	α-1,5-L-arabinoheptaose, α-L-Arabinofuranosi

Cazy database contains 485 proteins of *P. chrysogenum* genome among that 234 belongs to Glycoside Hydrolase family. *P. chrysogenum* consist of a larger number of enzymes involved in hemicellulose degration (10.1%) relative to those involved in cellulose degradation (4.2%). In addition, proteases and peptidases (8.1%), lipase (2.2%), proteins involved in chitin degradation (0.8%), pectin degradation (2.5%), and starch degradation (2.0%) were also detected (YANG et al., 2018b). Idientified glycosyl hydrolase enzymes from *Penicillium chrysogenum* are described in (Table I.3)

Industrial applications of *Penicillium* enzymes

The genus *Penicillium*, included over 300 species, plays important roles in biotechnological applications. The potential application ranges from bioremediation, low-cost production of antioxidant, vitamins, antibiotic and antifungal agents, due to the production of several classes of enzymes (GUPTA et al., 2016).

The enzymes have applications in the food, beverages, animal feeds, textile and detergent, pulp and paper, biorefinery and biofuels, wine and brewery industries and in the extraction of olive oil and pigments (CHÁVEZ; BULL; EYZAGUIRRE, 2006; SANDHU et al., 2018). Some examples of *Penicillium* sp. applications have been mentioned in Table I.4.

Recently published works on *Penicillium* sp. suggests the production of all three types of cellulases including an adequate amount of β-glucosidase, posing an advantage on *Trichoderma* (SANDHU et al., 2018). Some species of *Penicillium* such as; *P. brasilianum* produced a high yield of cellulase with the expression of five different cellulases (JØRGENSEN et al., 2005). Cellulases activities of *Penicillium funiculosum* were recorded three times of Trichoderma. The cellulase blend of *P. funiculosum* has been employed for the hydrolysis of cellulignin, yielded 16g/L of glucose (MAEDA et al., 2011).

On other hands, few species were identified covering a high number of hemicellulases. For instance, *P. oxalicum* reported containing eight different xylanases (LIAO et al., 2015). While *P. echinulatum* was rich in the production of both (cellulases and xylanases) showing a great potential to be used in the second generation ethanol with the hydrolysis yield of 82% glucose from sugarcane bagasse (AVER et al., 2014).

Table-4 Production of enzymes from *Penicillium* sp. and their application

Enzymes	Industrial applications	Producer(s)	References
Proteases	Food processing, beverages, textile, pulp and paper, detergent, feed, leather making and medicinal industries	*P. citrinum* *P. camemberti* *P. chrysogenum*	VAISHNAV et al., 2018 DRYJAŃSKI et al., 1995 BENITO et al., 2002
Amylases	Production of fructose and glucose by enzymatic conversion of starch, textile desizing, baking, detergent, paper, and biofuel production industries	*P. fellutanum* *P. purpurogenum* *P. chrysogenum* *P. expansum*	GOMES, 2014 CHÁVEZ et al., 2002 BALKAN; ERTAN, 2007 DOYLE et al., 1989
Pectinases	Fruits/vegetable, textile, wine, and animal or poultry feed, tea/coffee fermentations, extraction of vegetable oils, biobleaching of kraft pulp, and recycling of waste papers	*P. italicum* *P. oxalicum* *P. chrysogenum* *P. citrinum*	ALAÑA et al., 1990 PENG et al., 2004 RASHEEDHA et al., 2010 NG et al., 2010
Xylanases	Pulp biobleaching, removal of lignin residues from kraft pulp, increasing animal feed digestibility, production of biofuels from lignocellulose, food, and textile industries	*P. brasilianum* *P. funiculosum* *P. janthinellum* *P. simplicissimum* *P. janczewskii* *P. chrysogenum*	PANAGIOTOU et al., 2007 LAFOND et al., 2011 MILAGRES et al.,1993 SCHMIDT et al., 1999 TERRASAN et al., 2010 HAAS et al., 1992
Cellulases	Pulp and paper, textile (bio-stoning and biopolishing), biorefinery, wine and agricultural industries, food and feed processing, extraction of olive oil and pigments, waste management	*P. brasilianum* *P. echinulatum* *P. decumbens* *P. oxalicum* *P. glabrum* *P. chrysogenum*	JØRGENSEN, 2006 MARTINS et al., 2008 CHEN et al., 2010 SAINI et al., 2015 GUSAKOV, 2012 SILVA et al., 2019

Objectives and significance

The main aim of this thesis was to explore and characterise a fungal/bacterial strain that has the ability to degrade the agricultural biomass (raw sugarcane bagasse/straw, orange peel) used as an alternative source of carbon for the production of hydrolytic enzymes, further employed for the hydrolysis of biomass for the generation of fermentable sugars.

Hence, after testing a few strains, one fungal specie *P. chrysogenum* collected from the cerrado soil was screened and characterised for its ability to produce lignocellulose degrading enzymes. To optimise their applications, the enzymes were purified and Physicochemically characterised. To explore the hydrolytic efficiency of these enzymes, pre-treated sugarcane bagasse was hydrolysed.

The scope of present work was confined to the following objectives:

i. Evaluation of agricultural biomass for the production of cell wall degrading enzymes from *P. chrysogenum*

ii. Production of xylanases from *P. chrysogenum* using sugarcane bagasse as a carbon source

iii. Purification and identification of xylanases

iv. Physicochemical characterization of xylanases.

v. Application of enzymes produced from *P. chrysogenum* in the hydrolysis of pre-treated sugarcane bagasse

vi. Identify the inhibition mechanism or interaction between xylanases and lignocellulosic-derived phenolic compounds

Chapter I : Fungus isolation, screening, identification

Introduction

Penicillium is well known and one of the most commonly occurring fungi in nature. History of *Penicillium* sp. has largely acknowledged in the medicine; claim to fame production of Penicillin and distribution of economic impact, other are employed in the food industry for the production of speciality such as Camembert cheese. Currently, *Penicillium* is known for the production of novel enzymes due to their degradative abilities (VISAGIE et al., 2014).

Now it has been more than two hundred years since, the *Penicillium* meaning 'Bush' was introduced for *P. expansum* (described for the production of terverticillate penicili), *P. candidum* and *P. glaucum* (FRISVAD; SAMSON, 2004). Since then one thousand names were added to this genus. *P. chrysogenum* series was proposed in 1949 later; the penicillin producing family (variant of ancestral family NRRL 1951) known as 'Wisconsin' was investigated in 1954 (SAMSON; HADLOK; STOLK, 1977). At that time, the taxonomic identification was based on the micro- and macromorphology concept describing the colony colour characteristics on specific culture media, size, shape, and development of sexual/asexual spores and forming structures. (GREUTER, WERNER, 1993). With the advent of DNA based sequencing in 1990s, the name for the family *Trichocomaceae* accepted 223 species and omitted the others (GREUTER; PITT, 1993). Today the family contains 300 species of *Penicillium.*

Through this advancement, the PCR (polymerase chain reaction) become the lab routine, and species identified by using standardised short gene sequences called markers. Internal transcribed spacer (ITS) is the universally available marker, recently accepted the barcode for the identification of fungi (SCHOCH et al., 2012). Unfortunately, ITS marker is not reliable for the identification of *Penicillium* sp, as it failed to distinguish the closely related species, due to this limitation, the other sequencing makers β-tubulin (BenA) and Calmodulin (CaM) along with ITS were recommended to identify the *Penicillium* species accurately (HOUBRAKEN; FRISVAD; SAMSON, 2011b).

Preliminary identification based on morphology are used to date; by growing the fungus on specific media Czapek Yeast Autolysate agar (CYA), Yeast Extract Sucrose (YES) and Malt Extract agar (MEA). By employing these media VISAGIE et al., (2014) has recently re-identified the species of *Penicillium.* Extrolites of *P. chrysogenum* were also analysed by HPLC after the fungal growth on the described media.

Using the examples of previous literature, the *P. chrysogenum* in the present study was morphologically identified on YES, CYA, and MEA media and the molecular identification was accompanied by using the ITS sequencing marker with β-tubulin (BenA) and Calmodulin.

Methodology

Fungus Isolation and growth culture

The fungus was isolated from Brazilian cerrado soil. Soil samples were diluted (1:100) in autoclaved saline (0.9%) solution. A volume of 0.5 mL of each sample was inoculated on Malt yeast glucose (MYG) agar media plate prepared as describe (Table II.1). Plates were incubated at 28 °C for 7 days. After three rounds of purification, isolates were screened for lignocellulases activity.

Table I-1 Preparation of MYG media

MYG media	
Agar	2 g
Malt extract	1 g
Yeast extract	0.4 g
Glucose	0.4 g
MilliQ H_2O	100 mL
Mix well and autoclave at 121 °C for 15 min. pH 6.2 ± 0.2	

Screening for lignocellulases production

Isolates were screened for cellulose and xylan degradation on solid MYG agar medium supplemented with oat-spelt xylan (1% *w/v*) and CMC (2% *w/v*) as a substrate, 3 mm radius disks of seven days old culture was placed in the centre of the plate and grown at 28ºC for 10 days. Congo red 0.1% (*w/v*) was used to observe the clearance zone around.

Plates were flooded with congo red and shake slowly for 15 to 20 minutes and then 1 M NaCl was used to remove the excess of dye plates with NaCl were also put on a shaker for 15 to 20 minutes. Halo size and intensity were used as a criterion for fungi selection that used for cellulase and xylanase production (KASANA et al., 2008).

Identification of Fungus

Selected fungal isolates were identified on the morphology and molecular basis

Morphological Identification

Colony characters on specific media are important features for species identification. To identify the morphology, the fungus was grown on three different media Czapek Yeast Autolysate Agar (CYA) Malt Extract Agar (MEA) and Yeast extract sucrose agar (YES) prepared as described (VISAGIE et al., 2014). Protocol for trace elements solution has been described in the appendix.

Czapek Yeast Autolysate agar	
Czapek concentrate	1mL
Sucrose	3 g
Yeast extract (Difco)	0.5 g
K_2HPO_4	0. 1 g
Trace elements solution	100µL
Agar	2 g
Milli Q H_2O	100mL
Mix well and autoclave at 121 °C for 15 min. pH 6.2 ± 0.2	

Yeast Extract Sucrose (YES)	
Yeast Extract	2.25 g
Sucrose	17 g
$MgSO_4.7H_2O$	0.05 g
Trace elements solution	110µL
Agar	2 g
Milli Q H_2O	100mL
Mix well and autoclave at 121 °C for 15 min. pH 6.2 ± 0.2	

Malt Extract agar (MEA)	
Malt Extract	0.5 g
Trace element solution	100µL
dH_2O	100mL
Mix well and autoclave at 115 °C for 10 min. pH 5.2 ± 0.2	

Micromorphology

Microscope slide was prepared to observe the spores of the fungus. Sterilised slide (with 70% alcohol) was mounted with the lactophenol blue (indicator dye) and a small piece of fungal culture was gently mixed with the dye on the slide. Coverslip was placed on the slide by gently pressing it down. Spore characteristics were observed under a light microscope at 40x magnification.

Molecular Identification

For genomic DNA extraction, the fungi were grown on agar MYG media for 7 days at 28 °C and 5 mycelial disks of approximately 0.7 cm, were removed from the plate inoculate in MYG liquid medium. The fungi were cultured at 28 °C at constant agitation of 121rpm for 3 days, the mycelial mass was recovered by vacuum filtration and genomic DNA was extracted by the phenol-chloroform method. Approximately 50 mg of mycelia were homogenized in 500 µl extraction buffer (200 mM Tris HCl, 250 mM NaCl, 25 mM EDTA and 0.5% SDS pH 7.0). 350 µl of 150 µl phenol and chloroform were added. The suspension was centrifuged at 13,000 rpm for 30 minutes at room temperature. The upper aqueous phase was separated in another eppendrof and RNase (1U. uL^{-1}) was added and incubated at 37 °C for 10 minutes to degrade RNA. An equal volume of chloroform was added and stirred. At this stage, the residual proteins were eliminated. The material was centrifuged for 10 minutes at 13,000 rpm. The aqueous phase was transferred to a new eppendorf and isopropanol was added in a proportion of 54% of the volume of the sample for DNA precipitation.

The solution was centrifuged for 1 minute at speed 13000 rpm and the supernatant discarded. Pellet was precipitated using 70% ethanol at 4 °C to remove the salt. Again, it was centrifuged for 1 minute at 13,000 rpm and the supernatant was discarded. Residual ethanol was air dried on the bench. Genomic DNA was resuspended in 50 ul of TE buffer (10 mM Tris-HCl, pH 8.0 and 1 mM EDTA). After genomic DNA extraction, the ITS region of the rDNA was amplified using primers ITS1 and ITS4. The β-tubulin and calmodulin gene sequences were also amplified with primers Bt2a/Bt2b and CMD5/CMD6 as mentioned in Table I.2. The amplification was directed using a reaction mixture of 25 µL containing: $PCR10^{X}$ buffer 2.5 ul; Nuclease free H_2O, 15.15 µL; 1.5 µL of $MgCl_2$ (0.05 mM); Primers forward and reverse 0.4 uM (1.0 µL); 1.5 U Taq DNA polymerase recombinant (Invitrogen); 200 µM dNTPs; and 1.0 µl of genomic DNA (or template DNA).

Table I-2 Sequence of primer used for the molecular identification of fungus.

Internal Transcribed Spacer (ITS)		
ITS1	Forward	TCCGTAGGTGAACCTGCGG
ITS4	Reverse	TCCTCCGCTTATTGATATGC
β-tubulin (BenA)		
Bt2a	Forward	GGTAACCAAATCGGT GCTGCTTTC
Bt2b	Reverse	ACC CTCAGTGTAGTGACCCTT GGC
Calmodulin (CaM)		
CMD5	Forward	CCGAGTACAAGGARGCCTTC
CMD6	Reverse	CCGATRGAGGTCATRACG TGG

The PCR cycling conditions were as follows: 94 ºC for 5 minutes, 35 cycles of 94 ºC for 45 s: 55 ºC for 45 s and 72 ºC for 60s, and a final extension at 72 ºC for 7 minutes. PCR products were investigated by 0.8% agarose gel by mixing (4 µL molecular marker, 2 µL sample buffer and 5 µL of PCR product (sample).

The gel was stained with ethidium bromide and visualized by exposure to ultraviolet light and records were made with photo documenter. The products of PCR were purified by GeneJET PCR purification kit and sequenced by Macrogen, in Korea. DNA sequences obtained were analysed and trimmed using Geneious-R8 (v. 8.0.5). These DNA sequences were deposited in the NCBI database (GenBank) under the accession numbers listed in Table I.3.

Table I-3 Accession numbers of deposited gene sequences in GenBank

Gene	Accession No.
Internal Transcribed Spacer (ITS)	MG839059
β-tubulin (Bt2)	MG925671
Calmodulin (CMD)	MH018607

Phylogenetic analysis

Sequences were analyzed using Geneious-R8 (v. 8.0.5) (http://www.geneious.com) and compared against the collection of *P. chrysogenum* sequences from the Genbank database using BLASTn algorithm (SAMSON, 2016). The sequences with maximum coverage of query sequences were chosen. Multiple alignments of *P. chrysogenum* (similarities above 80%)

aligned in ClustalW. 3.8.31 (EDGAR, 2004). The phylogenetic tree was inferred by using the Maximum Likelihood method based on general time reversible mode in MEGA v.7.0.26 (TAMURA; NEI, 1993) with default parameters and 1000 bootstrap test (TAMURA; NEI, 1993)

Results and Discussion

Morphological identification

The morphological characteristics were recorded after 10 days of growth. Morphology of fungus colonies varied according to the growth medium. All four (MYG, YES, CYA, MEA) media were constructive for the growth of fungus; but the malt extract (MYG, and MEA media) favourable for growth and the production of yellow pigment (chrysogine) as well on the colony. Green velvety colonies were produced on the media containing yeast extract (YES). The production of yellow pigment was poor on both YES and Czapek media. Fungus morphology on all four media represented in Fig I.1.

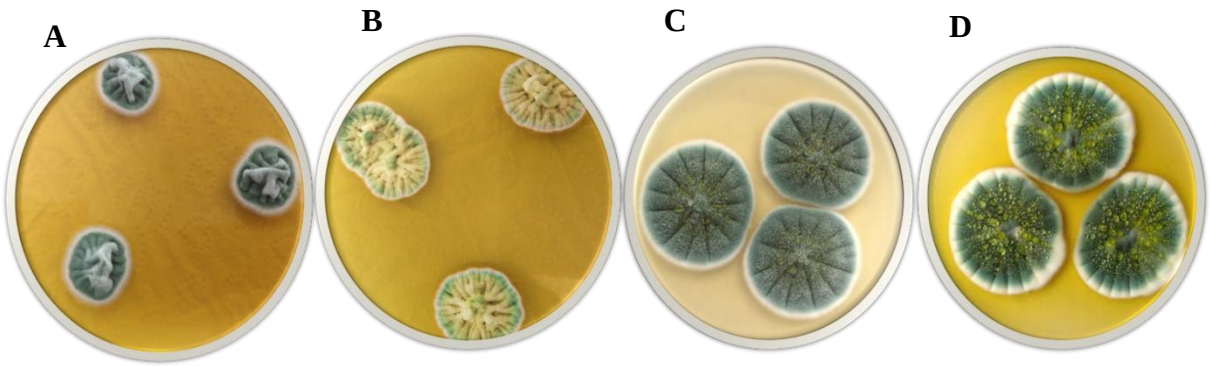

Figure I-1 *Penicillium chrysogenum* CCDCA10746. A) Yeast extract sucrose B) Czapek yeast autolysate agar C) Malt extract agar D) Malt yeast glucose

Similar morphology was previously observed from various studies of *P. chrysogenum* (HOUBRAKEN et al., 2011; VISAGIE et al., 2014). Houbraken et al., (2011) discussed the production of yellow pigment by using the Malt extract in the medium.

Results of the mentioned studies are in agreements to our morphological analysis, as observed in Fig I-1 the pigmentation was more prominent on the medium containing malt extract, that contained the glucose, peptones and a rich source of coenzymes and vitamins actually favour the growth of fungus and production of pigment (DA COSTA SOUZA et al., 2016). Another study described the pigment formation associated with the wild type fungus such as; NRRL 1951 and its X-ray mutant X-1612, that was further mutated by ultraviolet in the

Wisconsin university resulted in Q-176 mutant. All these mutants are pigmented strains, after the ultraviolet mutant of Q-176 that give rise to pigment less strain BL3D10 (BARREIRO et al., 2012).

Micromorphology

Lactophenol blue mount staining was used to check the morphology of spores under the light microscope at 40^{x} magnification (Fig I.2).

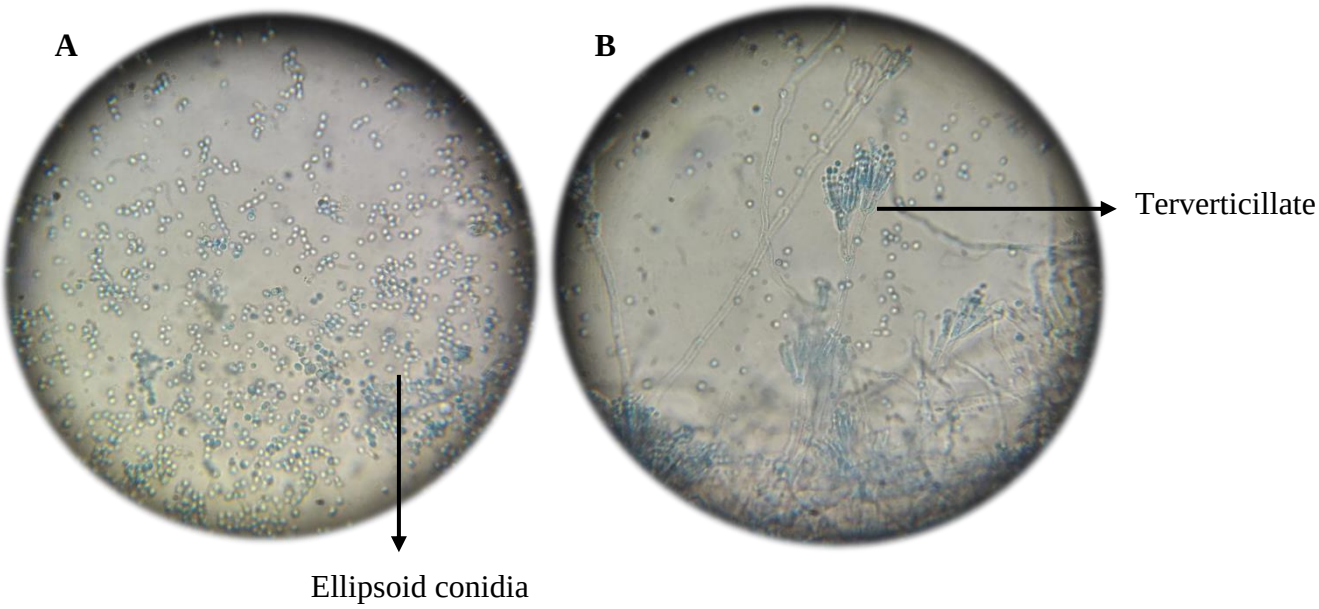

Figure I-2 Microscopic view of *Penicillium chrysogenum* spores, showing the terverticillate penicillia.

Branching pattern of terverticillate to quaterverticillate (containing two-staged branched conidiophore) was observed with the ellipsoidal shape of conidia. Microscopic characteristics are in accordance with the previous studies (FRISVAD; MYCOLOGY, 2004).

Molecular identification

The fungus was identified on species level by using the ITS, β-tubulin and calmodulin genes used as sequence markers.

Phylogenetic analysis

ITS marker amplified the gene of about 524bp long was sequenced. The sequence was highly conserved with other isolates deposited in NCBI GenBank (MG839059). The β-tubulin gene of about 402bp and 481bp long calmodulin gene were also amplified both sequences were

containing 3-exons. Sequences were deposited in GenBank under the accession number (MG925671) for β-tubulin and (MH018607) for calmodulin.

The combined phylogenetic relationship of the ITS, β-tubulin and calmodulin gene sequences of *P. chrysogenum* was inferred from the maximum likelihood based on the general time reversible model resulted in the tree presented in (Fig I.3). The tree is divided into two clades, one containing isolates from *P. digitatum* while other clade containing three distinct groups, containing isolates of *P. chrysogenum*, *P. rubens* and *P. allii sativi*

P.chrysogenum group containing three other *P. chrysogenum* have identical β-tubulin sequences with the difference of only three base pairs at position 197 – 199. The sequence was 98% identical with *P. chrysogenum* isolate KY469116.1. The phylogenetic tree represents the *P. ruben* into a distinct group containing three different isolates MH780064, KY469179, MN031392 sharing 97% sequence identity with *P. chrysogenum.* While *P.digitamum* AY674403 and FJ004403 sharing 89% sequence similarity.

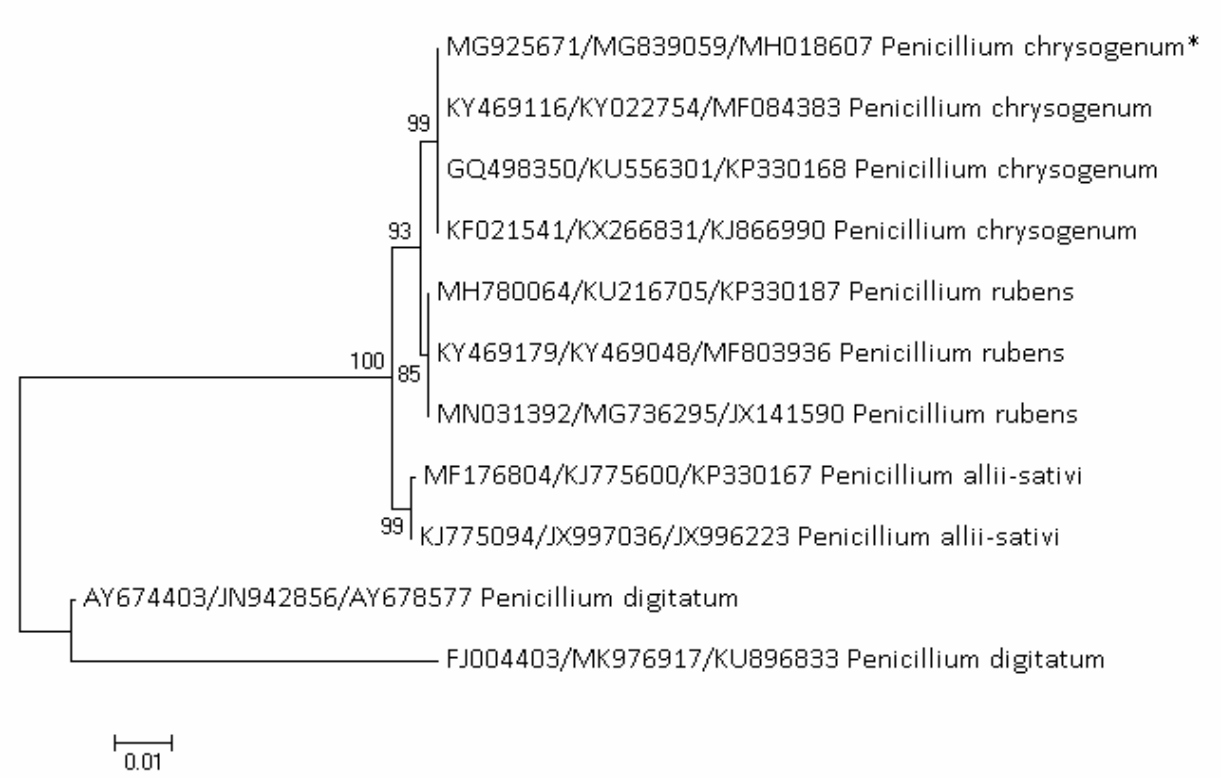

Figure I-3 Phylogenetic tree for β-tubulin (MG925671), ITS (MG839059) and calmodulin (MH018607) gene was inferred by using the Maximum Likelihood method based on the general time reversible model. The percentage of trees in which the associated taxa clustered together is shown next to the branches. Initial tree for the heuristic search was obtained automatically by applying Neighbor-Join and BioNJ algorithms to a matrix of pairwise distances estimated using

the Maximum Composite Likelihood (MCL) approach and then selecting the topology with superior log likelihood value. The tree is drawn to scale, with branch lengths measured in the number of substitutions per site.

For the calmodulin gene, *P. ruben* (KP330187) and *P.chrysogenum* sharing 100% sequence identity with no miss match. These results are align with the findings of VISAGIE et al., (2014), where CaM distinguishes the *P. chrysogenum* from *P. allii-sativi,* but not between *P. chrysogenum* and *P. rubens.*

Screening of xylanase and cellulase activity

The cellulases and xylanase production was screened from the *P. chrysogenum* isolate. As shown in (Fig I.4) low intensity (radius) clearance or hydrolysed zone on the plate containing CMC as a substrate. Positive results were obtained for the xylanase production; the production of cellulases was positive as well but the hydrolysed zone was lower compared to xylanase zone.

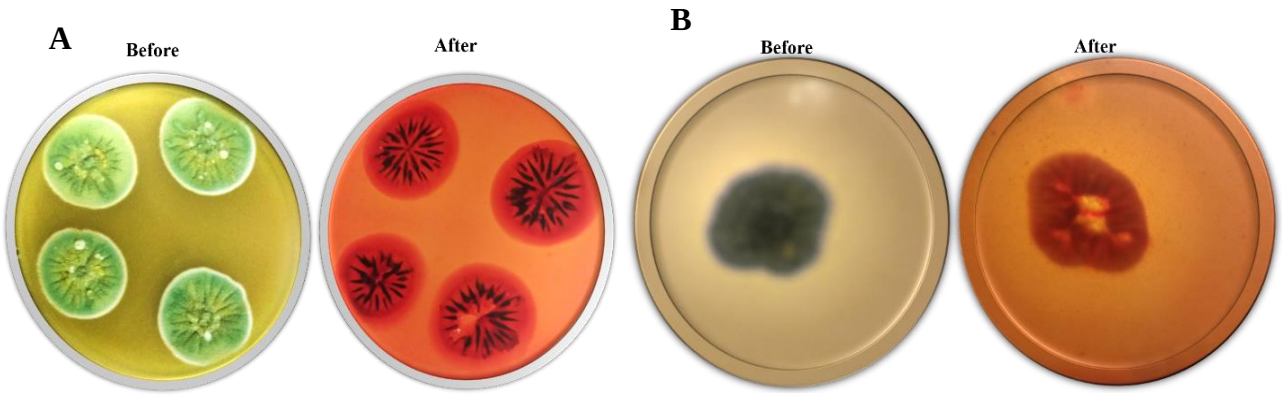

Figure I-5 Cellulase (A) and xylanase (B) activity predicted using agar pate. Plates were stained with 0.1% congo red (after).

Previously KASANA et al., (2008) found the successful activity zone of cellulases by staining the colonies of *P. chrysogenum* RS2 with 0.1% congo dye. *P.chrysogenum* was identified as a producer of both cellulases and hemicellulases, a property or skills required to achieve the objectives of this study.

International Journal of Biological Macromolecules 127 (2019) 385–395

Contents lists available at ScienceDirect

International Journal of Biological Macromolecules

journal homepage: http://www.elsevier.com/locate/ijbiomac

Structural and functional characterisation of xylanase purified from *Penicillium chrysogenum* produced in response to raw agricultural waste

Sadia Fida Ullah [a], Amanda Araújo Souza [b], Pedro Ricardo V. Hamann [a], Alonso Roberto P. Ticona [a], Gideane M. Oliveira [b], Joao Alexandre R.G. Barbosa [b], Sonia M. Freitas [b], Eliane Ferreira Noronha [a,*]

[a] Laboratory de Enzymology, Department of Cellular Biology, University of Brasilia, DF, Brazil
[b] Laboratory of Molecular Biophysics, Department of Cellular Biology, University of Brasilia, DF, Brazil

ARTICLE INFO

Article history:
Received 15 October 2018
Received in revised form 28 December 2018
Accepted 11 January 2019
Available online 14 January 2019

Keywords:
Biotechnological products
Lignocellulosic biomass
Phenolic compounds
Protein structural stability
Secondary structure
Xylanase

ABSTRACT

Commercial interest in plant cell wall degrading enzymes (PCWDE) is motivated by their potential for energy or bioproduct generation that reduced dependency on non-renewable (fossil-derived) feedstock. Therefore, underlying work analysed the *Penicillium chrysogenum* isolate for PCWDE production by employing different biomass as a carbon source. Among the produced enzymes, three xylanase isoforms were observed in the culture filtrate containing sugarcane bagasse. Xylanase (*PcX1*) presenting 35 kDa molecular mass was purified by gel filtration and anion exchange chromatography. Unfolding was probed and analysed using fluorescence, circular dichroism and enzyme assay methods. Secondary structure contents were estimated by circular dichroism 45% α-helix and 10% β-sheet, consistent with the 3D structure predicted by homology. *PcX1* optimally active at pH 5.0 and 30 °C, presenting $t_{1/2}$ 19 h at 30 °C and 6 h at 40 °C. Thermodynamic parameters/melting temperature 51.4 °C confirmed the *PcX1* stability at pH 5.0. *PcX1* have a higher affinity for oat spelt xylan, K_M 1.2 mg·mL^{-1}, in comparison to birchwood xylan K_M 29.86 mg·mL^{-1}, activity was inhibited by Cu^{+2} and activated by Zn^{+2}. *PcX1* exhibited significant tolerance for vanillin, *trans*-ferulic acid, *ρ*-coumaric acid, syringaldehyde and 4-hydroxybenzoic acid, activity slightly inhibited (17%) by gallic and tannic acid.

1. Introduction

Plant cell wall degrading enzymes (PCWDE) can be applied to different industrial processes. Therefore, there is a crescent demand of these enzymes, especially PCWDE presenting kinetic properties compatible with industrial processes. The alternative use of lignocellulosic biomass as a source of fermentable sugars to produce second generation ethanol and chemicals derived from lignocellulose and hemicelluloses also boost the search for PCDWE to deconstruct the feedstock [1]. Lignocellulosic biomass is daily produced and accumulated as a result of agro-industrial activities around the world and might be used as raw material to obtain a set of products with commercial value. Lignocellulose is composed of cellulose (45–60%), hemicellulose (20–40%), pectin (5–10%) and lignin (10–40%) [2]. Cellulose filaments are tightly linked and microfibrils are covered by hemicelluloses, pectin and lignin. It hampers their degradation and contributes to plant cell wall recalcitrance, one of the major limitation in the conversion of lignocellulosic biomass to value-added products [3]. Microorganisms are able to deconstruct lignocellulosic biomass by employing a consortium of enzymes, acts in synergism to depolymerise this complex material. At first, considered as accessory activities, hemicelluloses degrading enzymes including xylanases are essential to complete the deconstruction of lignocellulose [4].

Hemicelluloses hydrolysing enzymes are classified into *endo*-β-1,4-xylanases (EC 3.2.1.8), β-xylosidases (EC 3.2.1.37), and debranching enzymes, including α-glucuronidase (EC 3.2.1.139), L-arabinase, feruloyl esterase (EC 3.1.1.73) and *ρ*-coumaric esterase (EC 3.1.1.1). Endo-β-1,4-xylanases catalyse the hydrolysis of β-1,4 linkages of xylan backbone. This cleavage is not random and depends on the nature of substrate, size ramification of the chain, as well as the degree of branching [5]. These enzymes are classified into GH 10 and GH11 glycoside hydrolases families. In general, GH10 xylanases are characterised as a higher molecular mass (Mm > 30 kDa), lower *p*I values with a three-dimensional folding in barrel (β/α), whereas GH 11 presents a lower molecular mass (Mm < 30 kDa), higher *p*I value of xylanases and three-dimensional folding in β-jelly-roll [6].

Previous literature has largely debated the *Trichoderma* and *Aspergillus* species particularly efficient in the production of cellulases and their ability to deconstruct the lignocellulose [8,9]. However, other species are also focused of the research due to their potential to produce in addition to cellulases, hemicellulases and lignin active enzymes [7–10].

Penicillium species, such as *Penicillium chrysogenum*, studied previously as a source of antimicrobial activities, nowadays are gaining

* Corresponding author.
E-mail address: enoronha@unb.br (E.F. Noronha).

https://doi.org/10.1016/j.ijbiomac.2019.01.057
0141-8130/

attention as producer of glycoside hydrolases [11]. *P. chrysogenum* has been characterised as an efficient producer of xylanase rather than cellulases [12], ability which makes it a potential candidate to be used in the pulp and paper industries [13]. Xylan degrading enzymes and secretome from *P. chrysogenum* has also been described by employing corn stover and wheat straw as a carbon source [14]. However, its detailed enzymatic characterisation, which enables their industrial use, remained unclear. Including, the characteristics related to tolerance/stability to industrial processes conditions (pH, temperature, salt concentration) and compounds liberated during lignocellulosic biomasses deconstruction. Previous works have not comprehensively considered the structural or biophysical aspects (protein folding, thermodynamics, structural stability), an important and advanced topic in enzyme technology. In this context, the focus of the present study was to investigate the physicochemical, kinetics and structural features of GH10 *endo*-β-1,4-xylanase produced by *P. chrysogenum* (*PcX1*) using sugarcane bagasse as a carbon source, as well as the effect of lignocellulose-derived phenolic compounds on its activity. This basic knowledge could further be used in enzyme production to enhance its structural/functional stability for industrial utilities.

2. Material and methods

2.1. Agricultural residue preparation

Lignocellulosic biomass (sugarcane bagasse and straw) were obtained from local farms (Brasilia, Brazil), and orange peels from the local food market (University of Brasilia, Brazil). In brief, all three biomass were autoclaved for an hour at 121 °C. The resulted slurry was sieved and rinsed under tap water, and oven dried at 60 °C temperature until reaching a constant weight. Dried biomass was blended to a homogeneous fine powder using an industrial food blender (Skymsen, Brazil) which is used as a carbon source to supplement the liquid growth media.

2.2. Fungal collection/maintenance and enzyme production

P. chrysogenum was isolated from Brazilian Cerrado soil. Soil samples were diluted (1:100) in autoclaved saline solution (0.9%). A volume of 0.5 mL of each sample was inoculated on MYG media plate (Yeast extract 4 $g \cdot L^{-1}$, malt extract 10 $g \cdot L^{-1}$, glucose 4 $g \cdot L^{-1}$) and agar 2% (*w*/*v*), incubated at 28 °C for 7 days. After three rounds of purification, one of the fungal isolate presenting holocellulolytic activity was morphologically identified as *Penicillium chrysogenum* and deposited under the access code CCDCA10746 in fungal culture collection (CCDCA) at the Department of Food Sciences, Federal University of Lavras, Brazil.

Ribosomal DNA Internal Transcribed Spacer (ITS) regions, together with β-tubulin and calmodulin genes, were used as a conserved molecular marker to identify the fungus at specie level [15]. Genes were amplified and sequences deposited to NCBI under the accession number MG839059, MG925671, and MH018607, respectively. The spore concentration was determined by counting under a microscope with a Neubauer chamber, adjusted with a sterile saline solution (0.9%) to a final concentration of 10^6 spores $\cdot mL^{-1}$.

Enzyme production was carried out in liquid medium containing agriculture residues or avicel as a carbon source. Conical flasks containing 50 mL liquid media (0.7% KH_2PO_4, 0.2% K_2HPO_4, 0.05% $MgSO_4 \cdot 7H_2O$, and 0.16% $(NH_4)_2SO_4$) [16] supplemented with 1% (*w*/*v*) agriculture residues (sugarcane straw or sugarcane bagasse, orange peel), avicel ph101 (Sigma® USA). The culture was incubated at 28 °C and constant agitation of 120 rpm for 10 days. Aliquots were collected after every 24 h of incubation. Collected aliquots were filtered and centrifuged at 10,000*g* for 10 min at 4 °C to obtain cell-free supernatant (culture filtrate) and used as a protein source to estimate enzyme activity, protein concentration and electrophoretic analysis. All samples were overnight dialyzed against milli-Q water using 10 kDa cut off dialysis tube (Sigma® USA) and stored at 4 °C until further use.

2.3. Scanning electron microscopy

Sugarcane bagasse degradation was analysed through scanning electron microscope. Residual substrate from *P. chrysogenum* 10 days grown culture, was vacuum filtered and dried at 60 °C until achieved a constant weight. Residual biomass preparation and visualization by scanning electron microscope (SEM) was carried out as previously described [17]. Sugarcane bagasse of non-inoculated media was used as a control.

2.4. Enzyme assay and protein quantification

Endoglucanase and xylanase activities were evaluated by using carboxymethylcellulose (CMC) 2% (*w*/*v*) and oat spelt xylan 1% (*w*/*v*) as a substrate [17]. The enzymatic assay was standardised, by using 0.05 mL of samples mixed with 0.1 mL of substrates (0.05 M sodium acetate buffer pH 5.0). Hydrolysis was carried out for 30 min at 40 °C and the reaction was stopped by adding 0.3 mL of dinitrosalicylic reagent [18]. Reducing sugars were measured at 540 nm in SpectraMax® Plus (Molecular Devices, US). One unit of endoxylanase and CMCase activity was expressed as the enzyme quantity released 1 μmol of reducing sugar per minute of reaction, per millilitre of enzyme ($U \cdot mL^{-1}$) using xylose and glucose as a standard. All tests were performed in triplicate. Protein concentration was determined by Bradford assay using bovine serum albumin as a standard [19].

2.5. Enzyme purification

Culture filtrate (2.4 L) collected after four days of *P. chrysogenum* growth under sugarcane bagasse was lyophilised (Freeze Dryer Liobrás, Brazil). The lyophilised sample was resuspended in sodium acetate buffer (0.05 M) pH 5.0. Aliquot 10 mL of 16× concentrated sample was loaded onto Sephadex G-75 (68 × 2.25 cm) gel filtration system (GE Healthcare, UK). Acetate buffer (0.05 M) pH 5.0 with the addition of 0.15 M NaCl was used as mobile phase. Fractions (6 mL) were eluted isocratically at a flow rate of 0.3 $mL \cdot min^{-1}$, analysed for xylanase activity (540 nm) and protein content (280 nm). Fractions corresponding to xylanase activity were pooled and further purified in anion exchange chromatography using QFF-Sepharose (GE Healthcare, UK) column at a flow rate of 1 $mL \cdot min^{-1}$ on Äkta protein purification system (GE Healthcare, UK). Equilibration and elution were performed using 0.05 M acetate buffer pH 5.0, bound proteins were eluted with a linear gradient (NaCl 0.0–1.0 $M \cdot L^{-1}$). Fractions (2 mL) were collected and analysed for xylanase activity and protein content. Fractions containing xylanase activity were pooled and used in characterisation.

2.6. Electrophoresis and zymogram

Sodium dodecyl sulfate polyacrylamide gel electrophoresis (SDS-PAGE) 12% was used to analyse the protein profile. Protein samples were precipitated using 10% *v*/*v* trichloroacetic acid (TCA). Electrophoresis was carried out as previously described [20]. Resulting gels were stained with silver nitrate [21] and also with Coomassie G250. Molecular mass standards from Sigma (USA) were used as markers. Zymogram gels were prepared by using the same protocol except for copolymerization with oat spelt xylan 0.1% (*w*/*v*) [22].

2.7. Matrix-assisted laser desorption ionization/mass spectrometry

Purified *PcX1* was excised manually from the SDS-PAGE gel, stained with Coomassie G-250, and submitted to digestion using trypsin enzyme [23]. Resulting peptides were desalted using stage tips, prepared by packing 3 disks of C18 membrane (Empore™-3M) into the 200 μL tips [24] and eluted with acetonitrile 90% and tri-fluoro acetic acid

0.1% by centrifugation at 2000 rpm for 2 min. Tryptic peptides were loaded onto an Anchor-Chip plate mixed with 2 $\mu g \cdot \mu L^{-1}$ α-cyano-4-hydroxycinnamic acid (90% acetonitrile and 0.1% trifluoroacetic acid) and subjected to air dried [25]. Protein identification was carried out using peptide mass fingerprinting on MALDI-TOF/TOF mass spectrometer (MS) (Autoflex II, Bruker Daltonics, Bremen, Germany) in positive ion reflector mode (ion source 1: 20 kV) with a mass ranging from 500 to 4000 (m/z) and calibrated using the Starter kit peptide calibration standard for MALDI-TOF-MS (Bruker Daltonics). Resultant peptides were further fragmented and subjected to MS/MS by using LIFT technique [62]. Mass spectra were analysed using Flex Analysis software (Bruker Daltonics). Peptides were identified using Mascot 2.0 search engine (Matrix Science, London, UK). Protein search was performed against the National Centre of Biotechnology (NCBI) database. Search parameters were applied as; ±60 ppm mass tolerance and fragmentation mass tolerance of ±0.5 Da by applying no missed cleavage, carbamidomethylation of cysteine as fixed modification and oxidation of methionine and N-terminal acetylation as variable modifications.

2.8. Sequence alignment and structural analysis

Proteins with significant score value above 87 on the Mascot software from Matrix Science, were used for multiple sequence alignments using ClustalW and T-Coffee servers by applying the default parameters [26,27]. The BLAST algorithm was applied to search the sequence homology [28]. ESPript 3.0 was used to visualize the sequence alignment and the depiction of secondary structure [29]. The sequence and 3D structure of the template protein were retrieved from the PDB_1B30 (*Penicillium simplicissimum*) holding 80% sequence similarity with *PcX1*. Based on the high resolution crystal structure of the homologous protein, the model of *PcX1* was built using the homology modelling software MODELLER 9v18 [30]. The best Modeller model was chosen based on the QMEAN analysis [31]. The steric and geometric quality of the model was evaluated by MolProbity [32]. The structure depictions were generated using PyMol software [33]. The signal peptide of *PcX1* was predicted by signalP program (http://www.cbs.dtu.dk/services/SignalP/).

2.9. Fluorescence spectroscopy assay

Fluorescence measurements of the *PcX1* were performed using the Jasco Spectrofluorimeter FP-650 (Jasco Corporation, Tokyo, Japan) coupled with a Peltier-type temperature controller (Jasco Analytical Instruments, Japan). Conformational changes of the *PcX1* (0.046 $mg \cdot mL^{-1}$) were analysed at different pH values using 0.01 M sodium acetate buffer pH 4.0–5.5 and 0.01 M Tris HCl between pH 6.0–9.0 with a range difference of 0.5. The fluorescence emission was collected in the range of 300–400 nm, after excitation of the tryptophan at 295 nm, 25 °C. The excitation and emission slits were fitted at 5 nm.

2.10. Analysis of secondary structure and structural stability by circular dichroism

Circular dichroism (CD) measurements of *PcX1* (0.22 mg/mL in 2 × 10^{-3} M sodium acetate buffer ([pH 5.0] and 2 × 10^{-3} M Tris HCl buffer [pH 7.0 and pH 9.0]) were conducted using Jasco J-815 (Jasco Corporation, Tokyo, Japan) equipped with a Peltier temperature control system (Jasco Analytical Instruments, Japan). The Far-UV CD spectra were recorded using a 0.1 cm quartz cuvette in the range of 190–260 nm with data intervals of 0.2 nm at 25 °C. Five spectra were collected and the mean spectrum was considered after subtraction of the solvent spectra. The observed ellipticity was converted to molar ellipticity [θ] based on molecular mass per 115-Da residue [34]. The secondary structure content of the protein was estimated from the adjusted spectra using the CD Spectral deconvolution Vs 2.1 CDNN program [35].

The thermal stability assay of the *PcX1* was performed at pH values 5.0, 7.0 and 9.0. The change in ellipticity at λ_{222} nm was monitored at temperature ranging from 25 to 95 °C at a scan rate of 0.2 $°C \cdot min^{-1}$. In addition, the CD spectra were obtained in the far-UV region (190–260 nm), a step size of 0.2 nm at 10 °C intervals. The thermal denaturation curves were plotted as molar ellipticity [θ] versus temperature. The unfolded conformation of the protein (*fu*) was calculated by the Eq. (1)

$$fu = (yN - y)/(yN - yU), \quad (1)$$

where *yN* and *yU* represent the values of *y* characteristic of the folded and unfolded states, respectively. The *fu* values were used to plot a non-linear curve (Origin 8.1 software, Origin Lab Corporation, USA) used to define the melting temperature (T_m) [36].

2.11. Effect of pH and temperature on PcX1 activity and stability

PcX1 activity was evaluated using the standard enzyme assay (as described above) at pH ranging from 3.0 to 10, using four different buffers; sodium acetate (0.1 M pH 3.0, 4.0 and 5.0), sodium phosphate (0.1 M pH 6.0 and 7.0), Tris-HCl (0.1 M pH 8.0) and Glycine-NaOH (0.1 M pH 9.0 and 10). The temperature effect was assayed at temperature ranging from 30 to 70 °C. Thermal stability was determined by pre-incubating *PcX1* at 30 °C and 40 °C at regular interval ranging from 30 to 150 min.

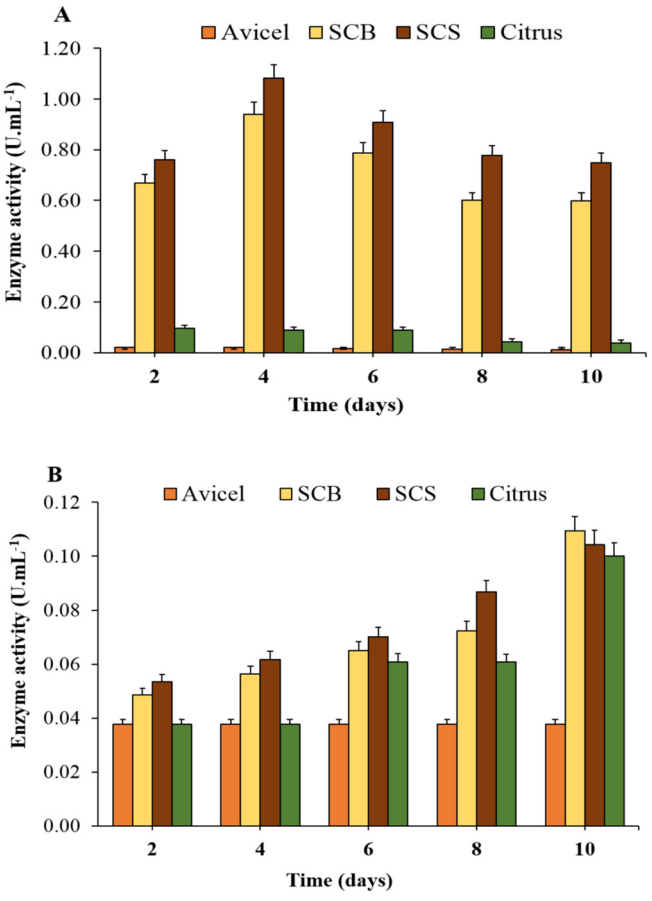

Fig. 1. Time course production of enzymes in raw biomass and avicel. (A) Xylanases (B) Endoglucanases (CMCase) activities by *P. chrysogenum* cultured in agricultural wastes (carbon source); Avicel, Sugarcane bagasse (SCB), Sugarcane straw (SCS), Citrus (orange peel).

2.12. Effect of lignocellulose derived phenolic compounds on PcX1 activity

The effect of phenolic compounds on the activity of *PcX1* was assessed by using vanillin, tannic acid, *trans*-ferulic acid, *trans*-cinnamic acid, *ρ*-coumaric acid, gallic acid, syringaldehyde and 4-hydroxybenzoic acid at a concentration of 1 $mg \cdot mL^{-1}$, as previously described [37]. Enzyme samples were incubated for 24 h at 28 °C in the presence as well as in the absence of each phenol compound and used to determine enzyme activities.

2.13. Effect of metal ions on PcX1 activity

The ions effect was determine by pre-incubation the enzyme with 1×10^{-3} M and 1×10^{-2} M solution of Ca^{2+}, Cl^{-}, Cu^{2}, Co^{2+}, Fe^{3+}, K^{+}, Mg^{2+}, SO_4^{2-}, Zn^{2+} and metal chelator EDTA for an hour at room temperature [38]. Residual activity was determined by stander assay as above described.

2.14. Kinetics parameters and substrate specificity

PcX1 kinetic parameters were determined using oat spelt and birchwood xylan as substrates. Each enzyme assay was carried out under optimal conditions using an enzyme solution containing 0.011 $mg \cdot mL^{-1}$ of protein and substrate concentration varied from 2.0 to 10 $mg \cdot mL^{-1}$ for oat spelt xylan and 5.3 to 26 $mg \cdot mL^{-1}$ for birchwood xylan. Kinetic constant K_M, Vmax and Kcat values were determined by Michaelis-Menten equation using Sigma Plot 12.0 software (Systat Software Inc., US).

Substrate specificity for exo-1,4-β-glucanase and β-D-xylosidase activities were tested with 5×10^{-3} M of *p*-nitrophenylcellobioside (pNPC) and *p*-nytrophenyl-β-D-xylopyranoside (pNPX), reaction

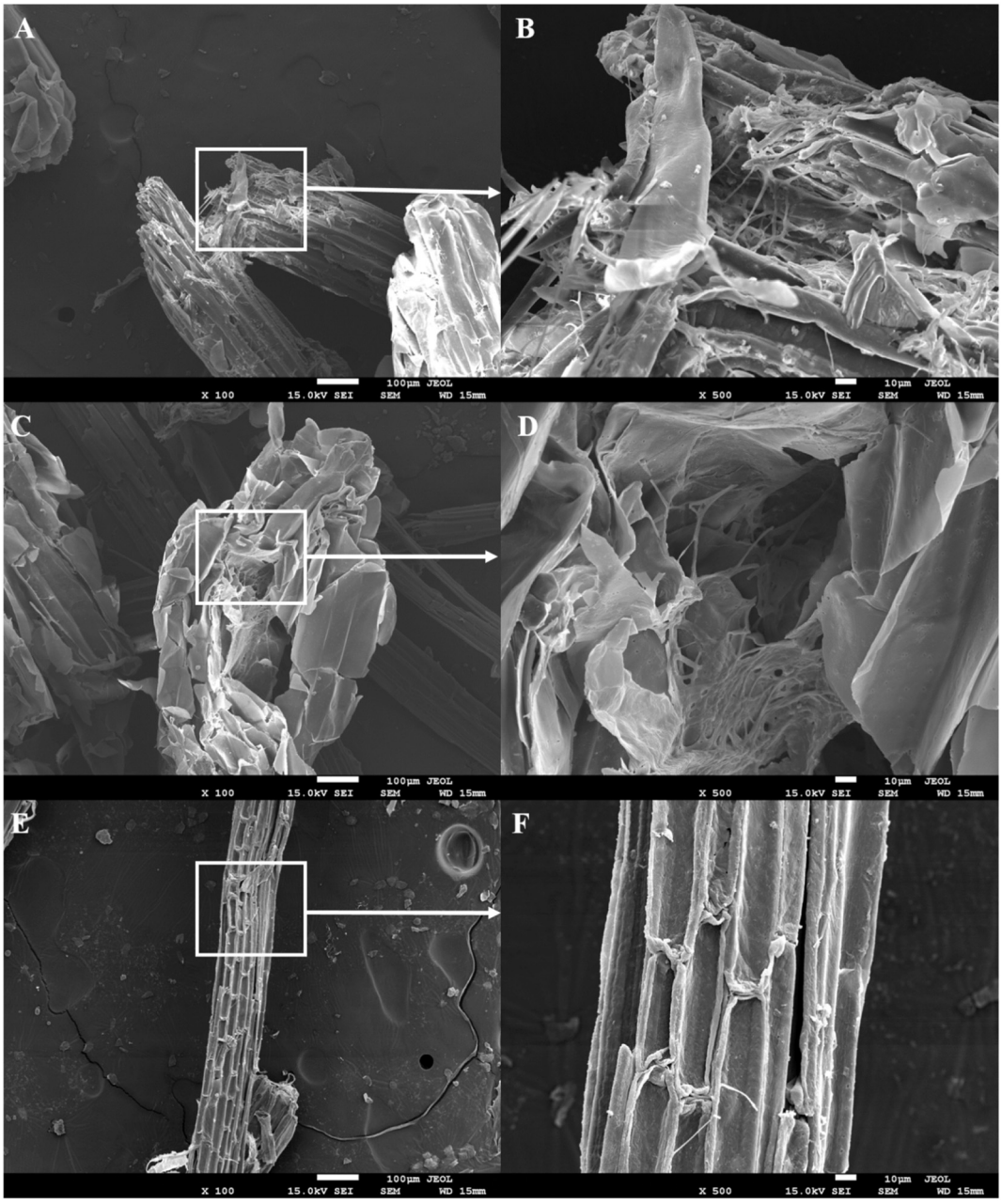

Fig. 2. Scanning electron microscope images of sugarcane bagasse. Biodegradation of raw sugarcane bagasse after ten days inoculation of *P. chrysogenum* (A, C) 100×, (B, D) 100× (E) 500× (F) are the control (without *P. chrysogenum*). White arrows indicate the magnification area.

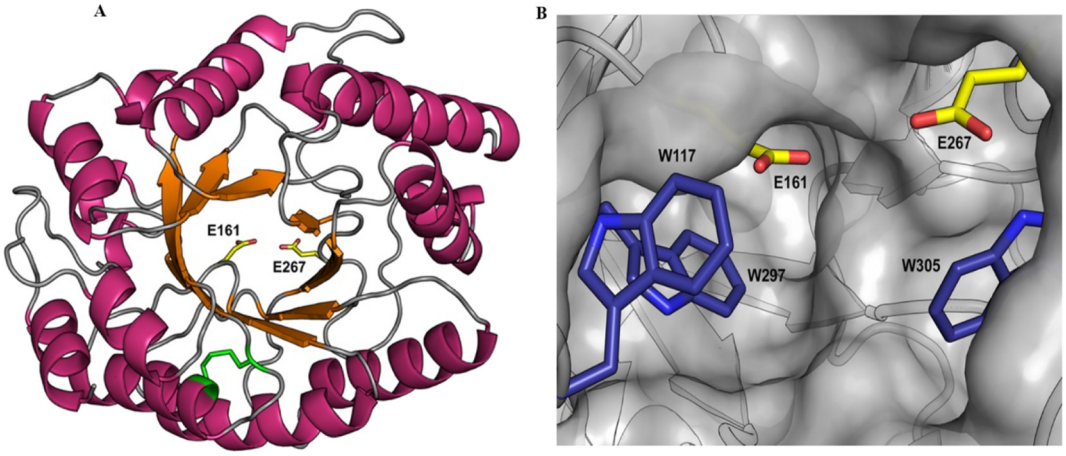

Fig. 3. Homology model of *PcX1*. (A) Alpha helices are coloured pink, beta strands, orange and the disulfide bond is in green sticks. The active site is coloured by atoms (C, yellow and O, red) and labelled (B) Surface of the *PcX1* showing the catalytic groove and the tryptophan triad (blue sticks) shielding the active site. (For interpretation of the references to colour in this figure legend, the reader is referred to the web version of this article.)

mixture was quenched by adding 2% of Na_2CO_3 and absorbance of the end product was measured at 405 nm. The activity against filter paper, carboxymethylcellulose (CMC), beechwood and birchwood xylan were analysed as described for xylanase by using the respective substrates. The hydrolysis reaction for all substrates was performed at pH 5.0 and 30 °C for 60 min and end products were interpolated against corresponding stander curves.

2.15. Statistical analysis

The experiments of phenolic compounds, effects of ions and EDTA were carried out in triplicate, and results were subjected to factorial ANOVA and Fisher LSD test for 5% or 1% level of significance ($P \leq 0.05$ or 0.01). All statistical analyses were performed using Origin version 8.5 and Microsoft office excel 2013.

3. Results and discussion

3.1. Enzyme production in response to lignocellulosic carbon sources

P. chrysogenum secreted xylanolytic activity after four up to ten days of growth in all the assayed complex substrates (biomass). Maximum activity values were 1.081 $U \cdot mL^{-1}$ and 0.940 $U \cdot mL^{-1}$ in the presence of sugarcane straw and sugarcane bagasse, respectively, after four days of growth (Fig. 1A). In comparison to previous works aiming to quantify the production of xylanases, the activity values described in the present paper are higher than those described for *Penicillium echinulatum* and *Aspergillus terreus*, 0.64 $U \cdot mL^{-1}$ and 0.096 $U \cdot mL^{-1}$ respectively, against sugarcane bagasse used as a carbon source [13,39]. CMCase activity was relatively lower than xylanase activities, maximum activity 0.162 $U \cdot mL^{-1}$ was detected in the presence of orange peels followed by 0.10 $U \cdot mL^{-1}$ in the presence of sugarcane bagasse/straw after 10 days of growth (Fig. 1B). In agreement to our results, secretome studies of *P. chrysogenum*-P33 stated the greater number of secreted hemicellulases (10.1% of the total proteins detect in the secretome) in comparison to cellulases (4.2% of the total proteins detect in the secretome) [14]. In many industrial processes, xylanases applications were carried out in the absence of cellulases, specifically for cellulose pulp bleaching processes, which require maximum cellulose recovery and elevate hemicellulose removal [40]. However, the secretome produced by *P. chrysogenum* in this study, demonstrated the presence of cellulases and hemicellulases, the co-occurrence of these enzymes could drive the use of this enzyme blend to holocellulose deconstruction and thus use of monomeric sugars into the biorefinery context.

Sugarcane bagasse degradation was visualised under scanning electron microscope (Fig. 2). The surface fibre (Fig. 2B) and pith (Fig. 2D) deconstructions were captured. Zones of partial biodegradation of

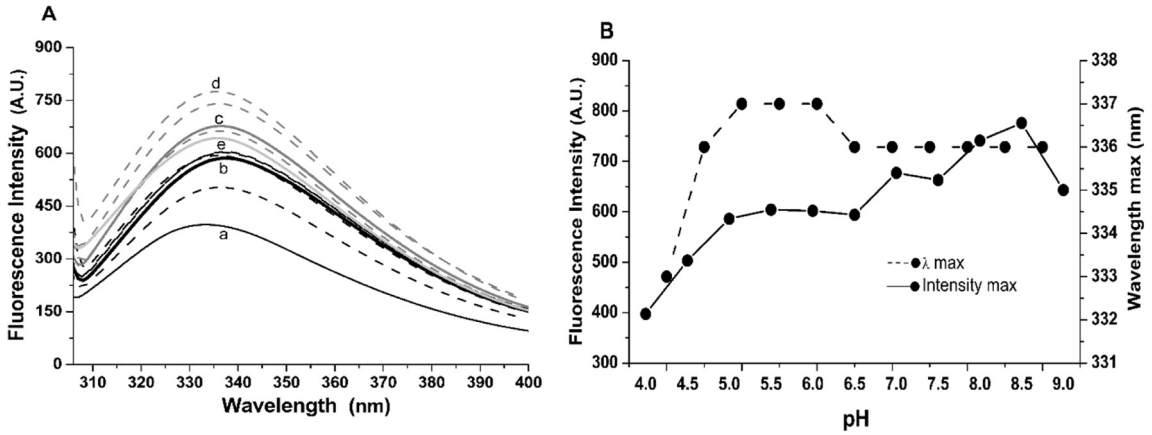

Fig. 4. Fluorescence of *PcX1* as function of pH. (A) The emission spectra presenting emission bands centred from ~332 to 338 nm. Spectra were presented as (a) pH 4.0, (b) pH 5.0, (c) pH 7.0, (d) pH 8.5 and (e) pH 9.0. (B) Fluorescence intensities (–●–) and centred emission bands from 332 to 338 nm (–●–). Fluorescence spectra red shifted by approximately 6 nm (332 to 338 nm) at pH 4.0 (332 nm), pH 5.0–6.0 (338 nm) and pH 6.5–9.0 (336 nm).

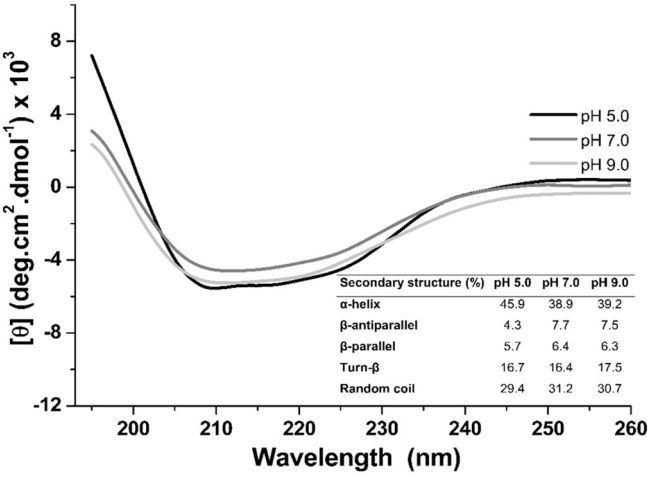

Fig. 5. Far-UV circular dichroism spectra of *PcX1*as a function of pH 5.0, 7.0 and 9.0 at 25 °C. The *PcX1* (0.22 mg·mL^{-1}) was solubilised in 2 × 10^{-3} M sodium acetate (pH 5.0) or 2 × 10^{-3} M Tris-HCl (pH 7.0 and 9.0). Inset: Secondary structure at pH 5.0, 7.0, and 9.0 estimated by CDNN deconvolution software.

sugarcane bagasse were observed after 10 days growth of *P. chrysogenum* that verified the efficiency of *P. chrysogenum* to deconstruct the hemicellulose. Similar biodegradation of sugarcane bagasse was mentioned by the enzymatic action of *S. cerevisiae* [41].

Table 1
Thermodynamic parameters of *PcX1* at pH.5.0 and pH 9.0.

pH	Tm (°C)	ΔH (Kcal·mol^{-1})	ΔS (cal/mol·K)	ΔG25 (Kcal·mol^{-1})
5.0	51.45 ± 0.03	57.09 ± 1.59	176.29 ± 8.34	4.65
9.0	45.32 ± 0.08	46.15 ± 0.57	145.05 ± 1.80	2.94

3.2. Enzyme purification

Xylanase was purified after two chromatographic procedures, gel filtration and anion exchange chromatography. At first, a single protein peak containing activity was eluted after fractionating on Sephadex G-75, a size exclusion chromatographic column (Fig. S1A). This peak presented three prominent protein bands with an estimated molecular mass ranging from 20 to 42 kDa (Fig. S1B). QFF-Sepharose chromatography column fractions resulted in two protein peaks, both containing *endo*-β-1, 4-xylanase activity (Fig. S1C). The second peak, fractions 19 to 21, presented one single protein band on SDS-PAGE (12%) with an estimated molecular mass of 38 kDa (Fig. S1D). Xylanolytic activity was confirmed in zymogram and purified xylanase was designated as *P. chrysogenum* xylanase1 (*PcX1*) (Fig. S1E). The purified enzyme corresponds to 17% of the total xylanolytic activity with purification fold of 5.83 (Table S1). Other xylanases from *Penicillium* sp. were purified by similar protocol with an additional step of ammonium sulfate precipitation. These xylanases have varying molecular masses ranges from 20 to 48 kDa; *P. brasilianum* (31 kDa), *P. glabrum* (21 kDa), *P. janczewskii* (30 kDa) *P. funiculosum* (48 kDa) [42–45].

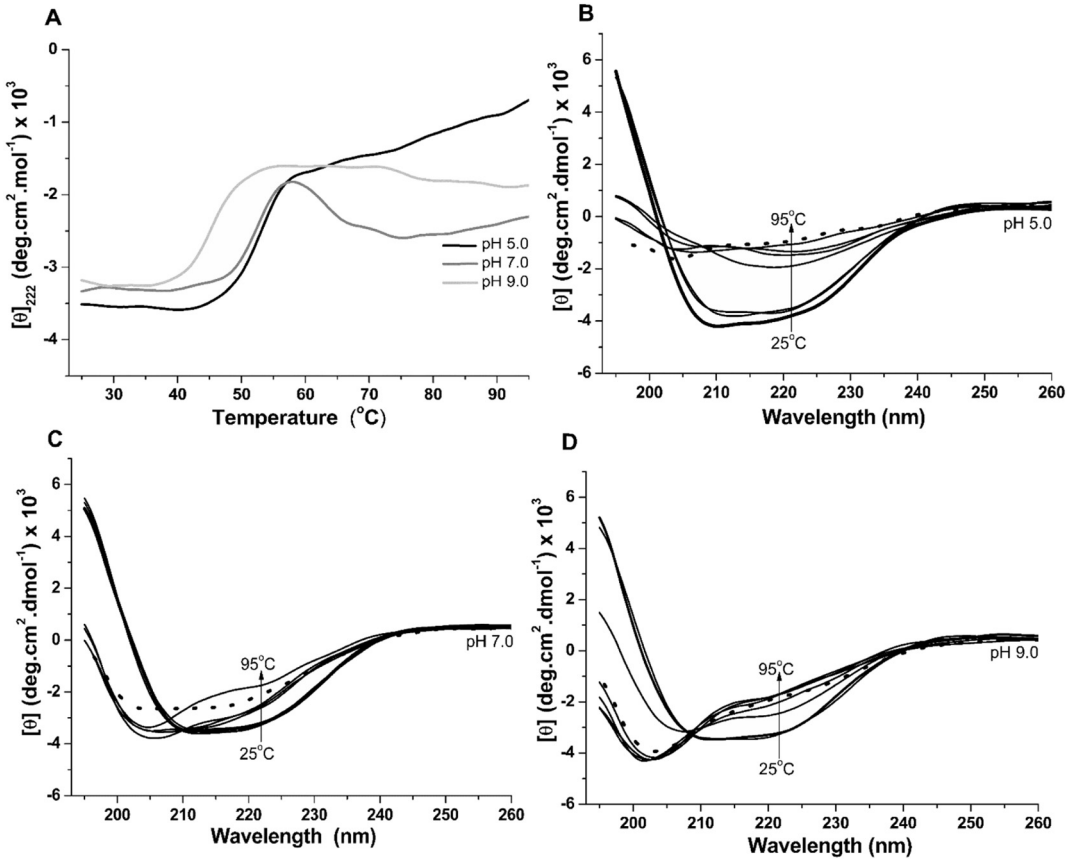

Fig. 6. Thermal denaturation profiles of *PcX1*. (A) Unfolding curves of *PcX1* (0.22 mg·mL^{-1}) were monitored by changes of [θ] at λ_{222} nm from 25 °C to 95 °C. The protein was solubilised in 2 × 10^{-3} M sodium acetate buffer pH 5.0 (black line) and Tris buffer to pH range 7.0 (gray line) and 9.0 (light gray line). (B–D) Unfolding profile of xylanase from 25 °C (solid line) to 95 °C (dashed line). Far-UV CD spectra of *PcX1* as function of increase of temperature ranging from 25 °C to 95 °C, at pH 5.0, 7.0 and 9.0, respectively. The arrow indicates the decrease in molar ellipticity as a function of increasing temperature.

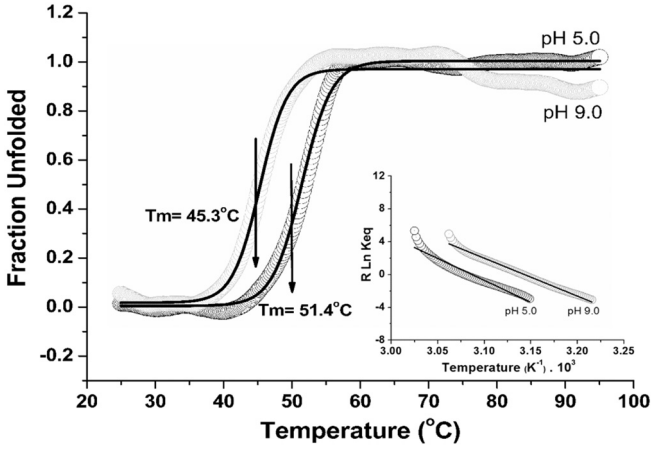

Fig. 7. Fraction of unfolded (*fu*). *PcX1* at pH 5.0 and pH 9.0 as a function of the temperature ranging from 25 °C to 95 °C. The arrow indicated the Tm 51.4 °C and 45.3 °C. Thermodynamic parameters calculated from fitted unfolded curves are presented in Table 1.

3.3. Sequence alignment and structure analysis

A total of thirty-six *PcX1* trypsin digested peptides were used in the search query against NCBI database. The spectrum and matched peptides were shown in Fig. S2. Significant matches (score values > 87), were obtained for different xylanases such as; *XylP* of *P. chrysogenum*-Q176 (P29417) matching eight peptides covering 20% of the protein sequence. The best hit with a score value of 112 was obtained in comparison to an unspecified xylanase of *P. chrysogenum*-31B (B6F253) matching of nine peptides that covers 27% of the total protein sequence (Fig. S3).

The entire protein is encoded within 1506 base pairs of genomic sequence; 10 exons encoding 331 amino acids of mature xylanase [46] having a monoisotopic mass of 35,548 Da and pI 4.9. *PcX1* was classified into GH10 family, according to its sequence similarity to other xylanase members of the family. *PcX1* shares 80% and 81% similarity with the xylanase of *P. simplicissimum* and *Aspergillus niger*, respectively. Sequence similarities between *PcX1* and other GH10 family xylanases were represented in the sequence alignment (Fig. S4). The structure of *PcX1* was modelled by using the *P. simplicissimum* structure (PDB_1B30, resolution of 2.25 Å) as a template. *P. simplicissimum* is the sole crystalline structure within genus *Penicillium* that exhibits 80% sequence similarity with *PcX1*, indicating that 1B30 is a good model to be used as a template. The *Pc*X1 is a high molecular weight xylanase that presents a TIM (α/β) barrel structural arrangement which is a common fold for the enzymes (Fig. 3A); one out of 10 enzymes is categorized in TIM barrel folding [47]. The barrel comprises three major secondary structural interfaces; the central β–barrel, α/β and α/α interfaces. All TIM-barrel enzymes exhibit conserved active site at the C-terminal [48]. *PcX1* might act as a retaining enzyme which hydrolyses glycosidic bonds via double displacement mechanism involving the conserved catalytic residues E161 and E267, one function as catalytic acid-base while other function as a nucleophile [49]. A single disulfide bond is formed between C285 and C291 (Fig. 3A). The secondary structure prediction from the model is in agreement with the secondary structure content obtained from CD experiment and predicted that the monomer has 16 helical segments corresponding to 45.9% of the amino acids and 19 β-turns corresponds to 16.7% amino acids. These values are close to *P. simplicissimum* structure contained 43% of

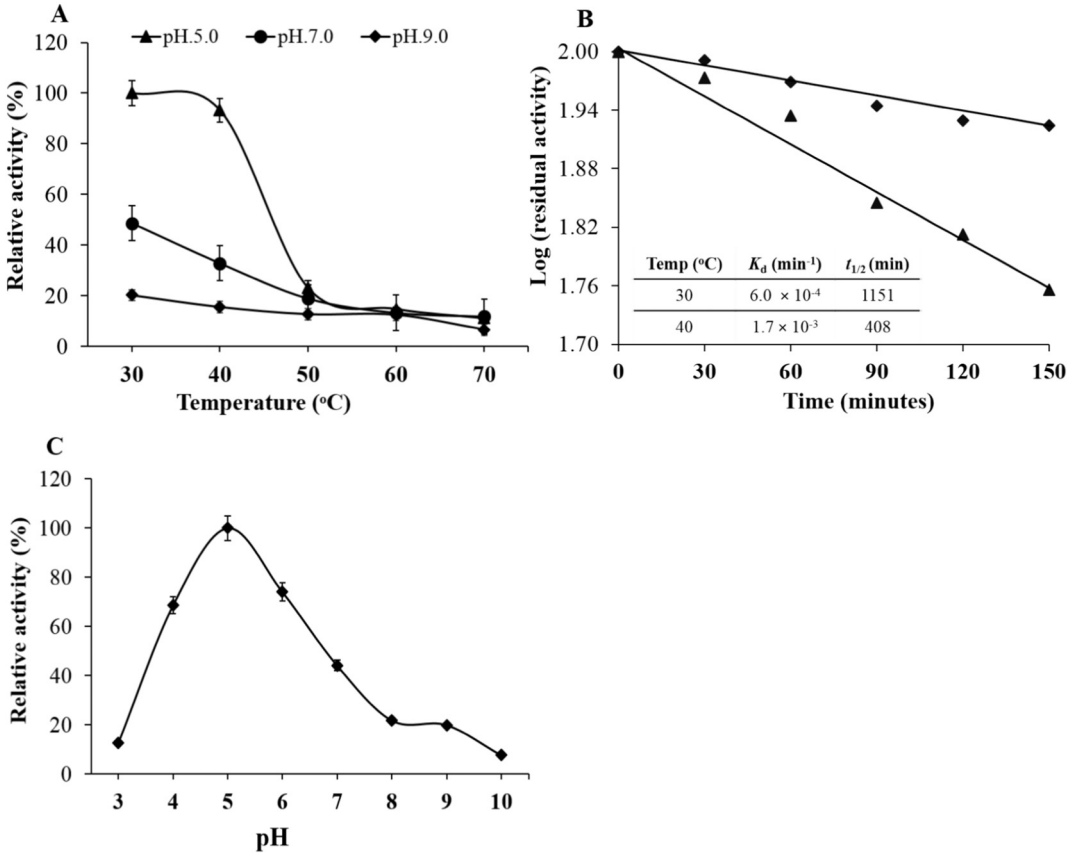

Fig. 8. Effect of temperature and pH on the activity of *PcX1* and its thermostability. (A) *PcX1* activity as function of thermal denaturation estimated by incubating the enzyme for 30 min in respective temperature at acidic (-▲-), neutral (–●–) and basic pH (–♦–). (B) Thermostability of *PcX1* measured at 30 °C (–♦–) and 40 °C (-▲-) (C) *PcX1* activity as a function of pH was estimated by incubating the enzyme in respective pH for 30 min at optimum temperature (30 °C).

α-helix and 16% of β-turn. Three aromatic residues, W117, W297 and W305, are located near the active site (Fig. 3B), these residues are strictly conserved in the GH10 family and also found at the same position in *P. simplicissimum* xylanases [49,50]. The GH10 domain is located from residue 50–330. The N-terminal of xylanase corresponds to signal peptide residues 1–23 (*MIPNITQLKT AALVMLFAGQ ALS*). The structure was validated using the Ramachandran plot, which has indicated 98% of the residues having their backbone Φ and Ψ angles presented in the favoured regions, while 1.7% and 0.3% of the residues were present in the allowed and outlier regions, respectively (Fig. S5). The calculated MolProbity score value of 2.31 implies that the *PcX1* model is in good agreement with X-ray structures available on the PDB.

3.4. Conformational changes analysis by fluorescence spectroscopy

Tryptophan fluorescence has been used to study the conformational changes and denaturation of protein, which is greatly influenced by the environmental factors such as temperature pH and polarity of the solvent [49]. Denaturation may cause by the disruption of the forces involved in stabilizing of the protein structure that can be monitored by displacement and intensity changes of the emission band of tryptophan residues [50].

The fluorescence spectra were recorded at 300–400 nm within the pH ranges from 4.0 to 9.0 (Fig. 4A). The emission band of the tryptophan at pH 4.0 was centred at 332 nm, which was red shifted to 338 nm and 336 nm, in the pH range of 5.0–6.0 and 6.5–9.0, respectively (Fig. 4B). Additionally, a gradual increase in emission intensity from 397 to 780 until pH 8.5 was noticed, with a decrease to 630 at pH 9.0 (Fig. 4B). The emission band at 336 nm remained constant over the pH range of 6.5–9.0, no further changes in the structure took place, and tryptophan remained partially in the polar environment (Fig. 4B). The red shift band from 332 nm (pH 4.0) to 338 nm (pH 5.0–6.0) indicates structural reorientation of the tryptophan from semi-buried environment to polar solvent exposed. Furthermore, the increase or decrease of the emission intensity reflects the significant conformational changes that can be attributed to the molecular rearrangement caused by the ionization of side chains of polar amino acids that surrounds the tryptophan residues. The conformational changes of the tryptophan to polar solvent exposed observed at pH 5.0 appeared to be important for the enzyme activity; hence the *PcX1* exhibits optimum activity at pH 5.0. This data can be associated with the tryptophan position that probably lies in the vicinity of amino acid residues that compound the catalytic site as shown in the 3D model of the *PcX1* (Fig. 3B).

3.5. Secondary structure analysis by circular dichroism

Several proteins present a well-characterised secondary structure under certain environmental conditions (pH, temperature, chemical, salt concentration), deviation from these conditions leads to an unfolded state or protein conformational changes. Most proteins have an intrinsic property to keep its native structure intact in a specific range of temperature, this property is defined by the sequence of its amino acid residues [51]. Several structural aspects of proteins, such as secondary structure, conformational changes and structural stabilities are investigated by circular dichroism spectroscopy.

FAR-UV CD spectra of the *PcX1* showed the difference in the secondary structure at pH 5.0 compared to neutral and basic pH at 25 °C (Fig. 5). The α-helix content decreased from 45% (pH 5.0) to about 39% at pH 7.0 and 9.0. However, the β-sheet parallel and antiparallel contents increased from 10% (pH 5.0) to 14% (pH 7.0 and 9.0) (Fig. 5 *inset*).These results corroborate with the findings associated with fluorescence assays that indicate higher conformational changes at pH 5.0 consistent with the optimum activity of the enzyme as well (Fig. 8C). Moreover, the secondary structure of *PcX1* is in agreement with the structure of xylanases deposited in the Protein Data Bank (PDB) such as; *Aspergillus niger* (4XUY_PDB code), *Penicillium simplicissimum* (1B30_PDB code) and *Thermoascus aurantiacus* (2BNJ_PDB code) which present higher α-helix contents (43%), following by β-sheets (19%).

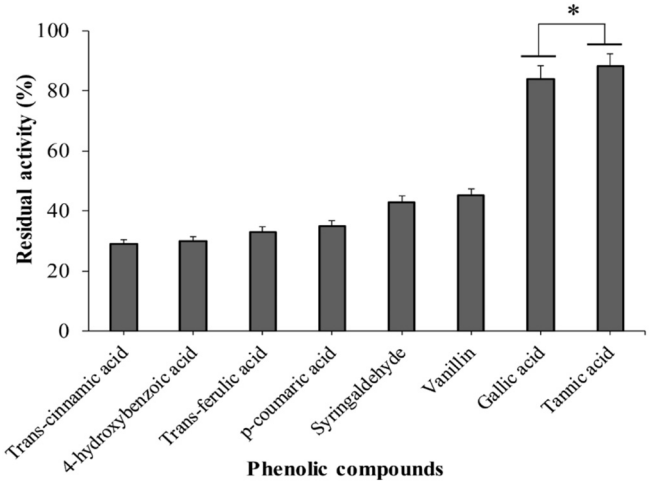

Fig. 9. Effect of phenolic compounds on the activity of *PcX1*. *Indicates not significantly different in LSD Fisher test.

Thermal unfolding assay of *PcX1* was monitored under the temperature range of 25 °C to 95 °C at acidic (pH 5.0), neutral (pH 7.0) and basic (pH 9.0) conditions. Gradual decrease of the dichroic signal of unfolding curves were noticed when the temperature increase from 45 to 50 °C that suggests the sensitivity of protein structure at temperature ranges 60–95 °C (Fig. 6A). At pH 5.0, protein unfolding started as the temperature exceeds 45 °C until 95 °C, decreasing the ellipticity signal at 222 nm from −3600 to −900 $mdg \cdot dmol^{-1} \cdot cm^2$ which was also observed in the spectra presented in the Fig. 6B. In case of pH 9.0, dichroic signal decrease from 3300 to 1800 approximately and gradual decrease of the negative bands closest to 208 nm, 218 and 222 nm indicates unfolding process, following the displacement of the dichroic band from around 222–218 nm to 200 nm, compatible with increase of unordered structure (Fig. 6D).

This displacement was also observed at pH 7.0 and temperature above 45 °C. The ellipticity of the unfolding curve reduced from −3600 to 1700 $mdg \cdot dmol^{-1} \cdot cm^2$ until 55 °C and increase as the temperature surpassed 60 °C (Fig. 6C). The spectra presented in the Fig. 5C, shows the signal decreased until 75 °C and increased from that, indicating partial structural rearrangement or protein aggregation. Consequently, the thermodynamic parameters characterising protein stability could not be calculated at pH 7.0. On the other hand, the thermodynamic parameters (Table 1) and Tm 51.4 °C and 45.3 °C calculated from the normalized unfolding curves (Fig. 7) indicate that *PcX1* is more stable at pH 5.0 than pH 9.0.

Table 2
Ions and EDTA effect on the activity of *PcX1*.

	PcX1 relative activity (%)	
	1×10^{-3} M	1×10^{-2} M
Control	100.00 ± 0.009	100.001 ± 0.029
$CuSO_4$	87.38 ± 0.017[a]	–
$ZnSO_4$	120.49 ± 0.024	–
$FeCl_3$	88.96 ± 0.032[a]	5.787 ± 0.034
$CoCl_2$	84.56 ± 0.071	81.42 ± 0.030
$MgCl_2$	106.74 ± 0.034[a]	73.69 ± 0.147
KCl	105.76 ± 0.020[a]	71.03 ± 0.029
$CaCl_2$	106.44 ± 0.113[a]	85.53 ± 0.036[a]
EDTA	116.28 ± 0.079	54.84 ± 0.035
$CuCl_2$	21.28 ± 0.030	–
$ZnCl_2$	105.49 ± 0.008[a]	63.23 ± 0.008

[a] Indicates not significantly different in LSD Fisher test. (–) no activity was observed.

Table 3
Kinetic parameters of *PcX1* against soluble oat spelt and birchwood xylan.

Xylan	K_M ($mg \cdot mL^{-1}$)	Vmax ($U \cdot mg^{-1}$)	Kcat (S^{-1})	Kcat/K_M ($S^{-1} \cdot mg^{-1} \cdot mL^{-1}$)
Oat spelt	1.20	0.0037	87.44	72.87
Birchwood	29.86	0.210	450.43	15.00

Protein stability is a function of numerous factors such as; the number of salt bridges, the disulfide bond and the hydrophobicity of the protein core. As shown *PcX1* contains single disulfide bond and 331 amino acid residues, among them 67 are charged. The maximum stability of the *PcX1* at pH 5.0 can be the attribute to this disulfide bond or the balance of the negative/positive charged side chains. The stability coinciding with pH near to its isoelectric point pI 4.9 could be due to the favourable electrostatic interactions among the charged groups on the surface of the protein. Furthermore, it is noteworthy that this stability appears to be essential for the optimal enzyme activity of the *PcX1* detected at pH 5.0.

3.6. Enzyme activity

The enzyme activity was tested as the function of pH/temperature. Maximum activity (100%) was recorded at pH 5.0 and temperature 30 °C that dropped to 93% at 40 °C. By changing to pH 7.0, maximum activity of 50% was obtained at 30 °C, which reduced to (30%) at 40 °C and gradually decrease with further increase of temperature (Fig. 8A). Enzyme exhibits 20% activity at pH 9.0 and at 30 °C, which further decreased and only 4% activity left at 40 °C. *PcX1* shows significant stability at 30 °C and 40 °C as shown (Fig. 8B). The enzyme half-lives ($t_{1/2}$) presented (Fig. 8B *inset*) confirmed the *PcX1* stability over the temperature range of 30–40 °C. Similar results were obtained from xyn10A of *P. oxilicum* that exhibits optimum activity at 40 °C and only 7% loss of activity was described at 30 °C [49]. Consistently the optima temperature of 40 °C and pH 5.0 of *P. chrysogenum* xylanase (*XylP*) are also in accordance with values obtained from *PcX1*. As *PcX1* exhibited around 75% activity in pH range 4.0–6.5, and maximal activity observed at pH 5.0 (Fig. 8C), activity decreases in neutral to basic pH about 50% loss in activity was noticed at pH 7.0 and 80% loss at pH 8.0 and 9.0. The biochemical results are coherent with conformational changes analysed by CD and fluorescence spectrometry.

3.7. Effect of lignocellulose derived phenolic compounds on PcX1

Trans-cinnamic acid strongly inhibited (77%) *PcX1* activity, *ρ*-coumaric acid, trans-ferulic acid 4-hidroxybenzoic inhibited 66–70% of activity, followed by vanillin and syringaldehyde that inhibit 55 and 58%, respectively. Gallic and tannic acid caused a minor effect with only 17% of *PcX1* inhibition (Fig. 9). Complete deactivation of *PcX1* was not detected for any of the phenolic compounds.

β-xylanases from *Aspergillus* sp. presented a high resistant for phenolic compounds in comparison to *PcX1*. For instance, the activity of *A. tamarii* endoxylanase was not effected under the influence of phenolic compounds [16]. Similar findings were referred from *A. terreus*; where two xylanases (*XylT1* and *XylT2*) were purified and both have displayed a different inhibition profile for phenolic compounds, *XylT1* was inhibited in the presence of some phenolics while *XylT2* was resistance to same phenolics [52]. Phenolic compounds have been reported to affect the biological function of proteins by changing their physicochemical properties. For instance, ferulic and *ρ*-coumaric acid were reported to binds covalently to the aromatic residues of a cellulase, inducing significant changes in protein tertiary structure [53]. The interactions between the phenolic compounds and protein are likely to involve residues located at the surface of the enzyme. *PcX1* might have some exposed aminoacid residues that favoured the interaction with phenolic compounds.

Interaction between *PcX1* and phenolic compounds could be further elucidated by kinetics and fluorescence studies. These results would be worth noticing because, in comparison to cellulases, less attention has been paid towards the inhibition or deactivation of hemicellulases.

Table 4
PcX1 activity against different substrates.

Substrates	Specific activity ($U \cdot mg^{-1}$)
Beechwood xylan	20.34
Birchwood xylan	17.99
Oat spelt xylan	22.16
Filter paper	1.17
Carboxymethylcellulose	1.23
pNP-β-D-cellbioside	0.60
pNP-β-D-xylopyranoside	0.00

3.8. Effect of ions on PcX1

About 75% activity was inhibited by Cu^{+2} (1×10^{-2} M), and 100% inhibition was observed for Zn^{+2} and Cu^{+2} at a concentration of 1×10^{-3} M. In opposite, activity was increased 25% by $ZnSO_4$ at 1×10^{-2} M, while Zn^{+2}, Mg^{+2}, K^{+}, Ca^{+2}, and EDTA did not influence the *PcX1* activity (Table 2). The Cu^{+2} ion is known to be a strong inhibitor of xylanases more likely by interacting with the active site residues [54,55]. It would be interesting that despite sharing the 91% sequence similarity with *PcX1* the activity of *Xylp* (*P. chrysogenum* xylanase) was not affected by Zn^{+2} or Cu^{+2} [12]. In consistence, to our results, the xylanase activity of *P. oxalicum* and *P. janczewskii* was inhibited in the presence of Zn^{+2} or Cu^{+2} [56,57].

3.9. Kinetics parameters and substrate specificity

PcX1 kinetics fit with Michaelis–Menten model. The enzyme presented more affinity towards soluble oat spelt xylan in comparison to birchwood xylan (Table 3), as previously described for other xylanases [58] and xylanase produced by *P. capsulatum* [59]. This feature can be a direct effect of varied ramifications and acetylating levels on xylan backbone. Altogether, these results indicate that *PcX1* is efficient in degrading hemicellulose from grass plants, rather than wood crops, representing potential in hydrolysing lignocellulosic residues such as sugarcane bagasse and straw.

Some activity ($0.02\ U \cdot mL^{-1}$) was noticed for the cellulose (FPase and CMCase) and pNPC. Previously purified *P. chrysogenum* xylanase (*Xylp*) was not active against cellulose but the hydrolysis of pNPC in fact consistence with *PcX1*. Apart from *PcX1*, a low activity on cellulose substrate was observed from *endo*-xylanases of *Penicillium capsulatum* and *Aspergillus niger* [59,60]. Similar findings were also described from *Caldicellulosiruptor bescii* a well-characterised specie for the production of PCWDE. The computational model of *C. bescii* xylanase (CbXyn10C), suggested the protein has an open cleft which usually observed in the endo- acting glycoside hydrolases that could accommodate the xylose and glucose configured substrates [61]. The activity of *PcX1* against CM-Cellulose was tested at pH 4.0 and 5.0. As expected the activity reduced to 40% at pH 4.0 (data not shown). The tertiary structure of *PcX1* was more relaxed or exposed at pH 5.0 in comparison to pH 4.0. However, we concluded that *PcX1* have affinity for β-l,4-1inkages required for activity, and the active site might be able to dock the carboxymethyl substituents (e.g., CM-cellulose). While the catalytic efficiency for cellulose was 95% less than those for xylan (Table 4), suggesting the weak interaction of glucose configured substrate with the binding site that was not optimise for cellulose substrate.

4. Conclusion

Functional and structural stability of proteins, especially enzymes, are of fundamental importance in several vital processes and have

been one of the most limiting factors for biotechnological applications. In the present work, our research group brought information about the effect of phenolic compounds on *P. chrysogenum* xylanase (*PcX1*) activity, as well as, a detailed enzymatic and structural characterisation of *PcX1*. Structural analysis linked to enzymatic characterisation contributed to understanding the interactions critical to the enzyme stability. The conformational changes of tertiary structure disclose the exposed tryptophan at pH 5.0. Interestingly maximum activity and thermal stability were obtained at pH 5.0, which justified that environment dictate the protein folding pathway to attain three dimensional conformation required for its physiological role. Indeed, information about biochemical and kinetic properties coupled to unfolding pathway could be helpful in further development of enzyme with improved stability for biotechnological applications.

Acknowledgments

The authors acknowledge the receipt of financial support from the Brazilian National Council for Scientific and Technological Development (CNPq), Coordination for the Improvement of Higher Education Personnel (CAPES).

Appendix A. Supplementary data

Supplementary data to this article can be found online at https://doi.org/10.1016/j.ijbiomac.2019.01.057.

References

[1] C. de Oliveira Gorgulho Silva, E.X.F. Filho, A review of holocellulase production using pretreated lignocellulosic substrates, Bioenergy Res. 10 (2017) 592–602, https://doi.org/10.1007/s12155-017-9815-x.
[2] V.O. Leitão, E.F. Noronha, B.R. Camargo, P.R.V. Hamann, A.S. Steindorff, B.F. Quirino, M.V. de Sousa, C.J. Ulhoa, C.R. Felix, Growth and expression of relevant metabolic genes of *Clostridium thermocellum* cultured on lignocellulosic residues, J. Ind. Microbiol. Biotechnol. 44 (2017) 825–834, https://doi.org/10.1007/s10295-017-1915-2.
[3] J. De Cassia Pereira, N. Paganini Marques, A. Rodrigues, T. Brito de Oliveira, M. Boscolo, R. Da Silva, E. Gomes, D.A. Bocchini Martins, Thermophilic fungi as new sources for production of cellulases and xylanases with potential use in sugarcane bagasse saccharification, J. Appl. Microbiol. 118 (2015) 928–939, https://doi.org/10.1111/jam.12757.
[4] V.K. Gupta, C.P. Kubicek, J.G. Berrin, D.W. Wilson, M. Couturier, A. Berlin, E.X.F. Filho, T. Ezeji, Fungal enzymes for bio-products from sustainable and waste biomass, Trends Biochem. Sci. 41 (2016) 633–645, https://doi.org/10.1016/j.tibs.2016.04.006.
[5] T. Collins, C. Gerday, G. Feller, Xylanases, Xylanase Families and Extremophilic Xylanases, 2005https://doi.org/10.1016/j.femsre.2004.06.005.
[6] G. Paës, J.G. Berrin, J. Beaugrand, GH11 xylanases: structure/function/properties relationships and applications, Biotechnol. Adv. 30 (2012) 564–592, https://doi.org/10.1016/j.biotechadv.2011.10.003.
[7] F. Ertan, B. Balkan, S. Balkan, T. Aktac, Solid State Fermentation for the Production of α-Amylase From *Penicillium chrysogenum* Using Mixed Agricultural By-Products as Substrate, 2006 657–661, https://doi.org/10.2478/s11756-006-0137-2.
[8] F. Zhang, X. Zhao, F. Bai, Improvement of cellulase production in Trichoderma reesei Rut-C30 by overexpression of a novel regulatory gene Trvib-1, Bioresour. Technol. 247 (2018) 676–683, https://doi.org/10.1016/j.biortech.2017.09.126.
[9] S.C. Nwodo, A.O. Uzoma, N.E. Thompson, I.O. Victoria, Xylanase production of *Aspergillus niger* and *Penicillium chrysogenum* from ammonia pretreated cellulosic waste, Res. J. Microbiol. 3 (2008) 246–253.
[10] W.M. Vangulik, M.R. Antoniewicz, W.T.A.M. Delaat, J.L. Vinke, J.J. Heijnen, Energetics of growth and penicillin production in a high-producing strain of *Penicillium chrysogenum*, Biotechnol. Bioeng. 72 (2001) 185–193, https://doi.org/10.1002/1097-0290(20000120)72:2<185::AID-BIT7>3.0.CO;2-M.
[11] M.P. Backus, J.F. Stauffer, M.J. Johnson, Penicillin yields from new mold strains, J. Am. Chem. Soc. 68 (1946) 152–153, https://doi.org/10.1021/ja01205a518.
[12] H. Haas, E. Herfurth, G. Stöffler, B. Redl, Purification, characterization and partial amino acid sequences of a xylanase produced by *Penicillium chrysogenum*, Biochim. Biophys. Acta Gen. Subj. 1117 (1992) 279–286, https://doi.org/10.1016/0304-4165(92)90025-P.
[13] L.R. De Souza Moreira, M. De Carvalho Campos, P.H.V.M. De Siqueira, L.P. Silva, C.A.O. Ricart, P.A. Martins, R.M.L. Queiroz, E.X.F. Filho, Two β-xylanases from *Aspergillus terreus*: characterization and influence of phenolic compounds on xylanase activity, Fungal Genet. Biol. 60 (2013) 46–52, https://doi.org/10.1016/j.fgb.2013.07.006.
[14] Y. Yang, J. Yang, J. Liu, R. Wang, L. Liu, F. Wang, H. Yuan, The composition of accessory enzymes of *Penicillium chrysogenum* P33 revealed by secretome and synergistic effects with commercial cellulase on lignocellulose hydrolysis, Bioresour. Technol. 257 (2018) 54–61, https://doi.org/10.1016/j.biortech.2018.02.028.
[15] C.M. Visagie, J. Houbraken, J.C. Frisvad, S.-B.B. Hong, C.H.W. Klaassen, G. Perrone, K.A. Seifert, J. Varga, T. Yaguchi, R.A. Samson, Identification and nomenclature of the genus *Penicillium*, Stud. Mycol. 78 (2014) 343–371, https://doi.org/10.1016/j.simyco.2014.09.001.
[16] A. Monclaro, Characterization of multiple xylanase forms from *Aspergillus tamarii* resistant to phenolic compounds, Mycosphere 7 (2016) 1554–1567, https://doi.org/10.5943/mycosphere/si/3b/7.
[17] P.R.V. Hamann, D.L. Serpa, A.S. Barreto da Cunha, B.R. de Camargo, K.O. Osiro, M. Valle de Sousa, C.R. Felix, R.N.G. Miller, E.F. Noronha, Evaluation of plant cell wall degrading enzyme production by *Clostridium thermocellum* B8 in the presence of raw agricultural wastes, Int. Biodeterior. Biodegrad. 105 (2015) 97–105, https://doi.org/10.1016/j.ibiod.2015.08.013.
[18] G.L. Miller, Use of dinitrosalicylic acid reagent for determination of reducing sugar, Anal. Chem. 31 (1959) 426–428, https://doi.org/10.1021/ac60147a030.
[19] M. Bradford, A rapid and sensitive method for the quantitation of microgram quantities of protein utilizing the principle of protein-dye binding, Anal. Biochem. 72 (1976) 248–254, https://doi.org/10.1016/0003-2697(76)90527-3.
[20] U.K. Laemmli, Cleavage of structural proteins during the assembly of the head of bacteriophage T4, Nature 227 (1970) 680–685, https://doi.org/10.1038/227680a0.
[21] H. Blum, H. Beier, H.J. Gross, Improved silver staining of plant proteins, RNA and DNA in polyacrylamide gels, Electrophoresis 8 (1987) 93–99, https://doi.org/10.1002/elps.1150080203.
[22] A. Sunna, J. Puls, G. Antranikian, Characterization of the xylanolytic enzyme system of the extreme thermophilic anaerobic bacteria *Thermotoga maritima*, *T. neapolitana*, and *T. thermarum*, Comp. Biochem. Physiol. A Physiol. 118 (1997) 453–461, https://doi.org/10.1016/S0300-9629(97)00006-6.
[23] J.V. Olsen, M. Mann, A. Shevchenko, H. Tomas, J. Havlis, In-gel digestion for mass spectrometric characterization of proteins and proteomes, Nat. Protoc. 1 (2007) 2856–2860, https://doi.org/10.1038/nprot.2006.468.
[24] J. Rappsilber, M. Mann, Y. Ishihama, Protocol for Micro-purification, Enrichment, Pre-fractionation and Storage of Peptides for Proteomics Using StageTips Protocol for Micro-purification, Enrichment, Pre-fractionation and Storage of Peptides for Proteomics Using StageTips, 2007https://doi.org/10.1038/nprot.2007.261.
[25] A.A. Souza, V.O. Leitão, M.H. Ramada, A. Mehdad, R.D.C. Georg, C.J. Ulhôa, S.M. De Freitas, *Trichoderma harzianum* produces a new thermally stable acid phosphatase, with potential for biotechnological application, PLoS One 11 (2016) 1–18, https://doi.org/10.1371/journal.pone.0150455.
[26] C. Notredame, D.G. Higgins, J. Heringa, T-Coffee: a novel method for fast and accurate multiple sequence alignment, J. Mol. Biol. 302 (2000) 205–217, https://doi.org/10.1006/jmbi.2000.4042.
[27] M.A.A. Larkin, G. Blackshields, N.P.P. Brown, R. Chenna, P.A.A. McGettigan, H. McWilliam, F. Valentin, I.M.M. Wallace, A. Wilm, R. Lopez, J.D.D. Thompson, T.J.J. Gibson, D.G.G. Higgins, Clustal W and Clustal X Version 2.0, vol. 23, 2007 2947–2948, https://doi.org/10.1093/bioinformatics/btm404.
[28] S. Altschul, T. Madden, A. Schäffer, J. Zhang, Z. Zhang, W. Miller, D. Lipman, Gapped BLAST and PSI-BLAST: a new generation of protein database search programs, Nucleic Acids Res. 25 (1997) 3389–3402.
[29] X. Robert, P. Gouet, Deciphering key features in protein structures with the new ENDscript server, Nucleic Acids Res. 42 (2014) W320–W324, https://doi.org/10.1093/nar/gku316.
[30] B. Webb, A. Sali, Protein structure modeling with MODELLER, Methods Mol. Biol. 1137 (2014) 1–15, https://doi.org/10.1007/978-1-4939-0366-5_1.
[31] P. Benkert, S.C.E. Tosatto, D. Schomburg, QMEAN: a comprehensive scoring function for model quality assessment, Proteins Struct. Funct. Bioinf. 71 (2008) 261–277, https://doi.org/10.1002/prot.21715.
[32] V.B. Chen, W.B. Arendall, J.J. Headd, D.A. Keedy, R.M. Immormino, G.J. Kapral, L.W. Murray, J.S. Richardson, D.C. Richardson, MolProbity: all-atom structure validation for macromolecular crystallography, Acta Crystallogr. Sect. D Biol. Crystallogr. 66 (2010) 12–21, https://doi.org/10.1107/S0907444909042073.
[33] W.L. DeLano, The PyMOL Molecular Graphics System, DeLano Scientific LLC, Palo Alto, CA, 2008.
[34] A.J. Adler, N.J. Greenfield, G.D. Fasman, Circular dichroism and optical rotatory dispersion of proteins and polypeptides, Methods Enzymol. 27 (1973) 675–735, https://doi.org/10.1016/S0076-6879(73)27030-1.
[35] G. Böhm, R. Muhr, R. Jaenicke, Quantitative analysis of protein far UV circular dichroism spectra by neural networks, Protein Eng. Des. Sel. 5 (1992) 191–195, https://doi.org/10.1093/protein/5.3.191.
[36] S.M. Kelly, T.J. Jess, N.C. Price, How to study proteins by circular dichroism, Biochim. Biophys. Acta Protein Proteomics 1751 (2005) 119–139, https://doi.org/10.1016/j.bbapap.2005.06.005.
[37] K.O. Osiro, B.R. de Camargo, R. Satomi, P.R.V. Hamann, J.P. Silva, M.V. de Sousa, B.F. Quirino, E.N. Aquino, C.R. Felix, A.M. Murad, E.F. Noronha, Characterization of *Clostridium thermocellum* (B8) secretome and purified cellulosomes for lignocellulosic biomass degradation, Enzym. Microb. Technol. 97 (2017) 43–54, https://doi.org/10.1016/j.enzmictec.2016.11.002.
[38] B.R. de Camargo, N.J. Claassens, B.F. Quirino, E.F. Noronha, S.W.M. Kengen, Heterologous expression and characterization of a putative glycoside hydrolase family 43 arabinofuranosidase from *Clostridium thermocellum* B8, Enzym. Microb. Technol. 109 (2018) 74–83, https://doi.org/10.1016/j.enzmictec.2017.09.014.
[39] M. Camassola, A.J.P. Dillon, Steam-exploded sugar cane bagasse for on-site production of cellulases and xylanases by *Penicillium echinulatum*, Energy Fuel 26 (2012) 5316–5320, https://doi.org/10.1021/ef3009162.
[40] S. Nagar, R.K. Jain, V.V. Thakur, V.K. Gupta, Biobleaching application of cellulase poor and alkali stable xylanase from *Bacillus pumilus* SV-85S, 3 Biotech 3 (2013) 277–285, https://doi.org/10.1007/s13205-012-0096-y.

[41] A.K. Chandel, F.F.A. Antunes, V. Anjos, M.J.V. Bell, L.N. Rodrigues, O.V. Singh, C.A. Rosa, F.C. Pagnocca, S.S. Da Silva, Ultra-structural mapping of sugarcane bagasse after oxalic acid fiber expansion (OAFEX) and ethanol production by *Candida shehatae* and *Saccharomyces cerevisiae*, Biotechnol. Biofuels 6 (2013) 1–15, https://doi.org/10.1186/1754-6834-6-4.
[42] H. Jørgensen, T. Eriksson, J. Börjesson, F. Tjerneld, L. Olsson, Purification and characterization of five cellulases and one xylanase from *Penicillium brasilianum* IBT 20888, Enzym. Microb. Technol. 32 (2003) 851–861, https://doi.org/10.1016/S0141-0229(03)00056-5.
[43] A. Knob, S.M. Beitel, D. Fortkamp, C.R.F. Terrasan, A.F. De Almeida, Production, purification, and characterization of a major *Penicillium glabrum* xylanase using brewer's spent grain as substrate, Biomed. Res. Int. 2013 (2013)https://doi.org/10.1155/2013/728735.
[44] C.R.F. Terrasan, B. Temer, M.C.T. Duarte, E.C. Carmona, Production of xylanolytic enzymes by *Penicillium janczewskii*, Bioresour. Technol. 101 (2010) 4139–4143, https://doi.org/10.1016/j.biortech.2010.01.011.
[45] M. Lafond, A. Tauzin, V. Desseaux, E. Bonnin, E.-H. Ajandouz, T. Giardina, GH10 xylanase D from *Penicillium funiculosum*: biochemical studies and xylooligosaccharide production, Microb. Cell Factories 10 (2011) 20, https://doi.org/10.1186/1475-2859-10-20.
[46] H. Haas, E. Friedlin, G. Stöffler, B. Redl, Cloning and structural organization of a xylanase-encoding gene from *Penicillium chrysogenum*, Gene 126 (1993) 237–242, https://doi.org/10.1016/0378-1119(93)90372-A.
[47] R.K. Wierenga, The TIM-barrel fold: a versatile framework for efficient enzymes, FEBS Lett. 492 (2001) 193–198, https://doi.org/10.1016/S0014-5793(01)02236-0.
[48] M.S. Vijayabaskar, S. Vishveshwara, Insights into the fold organization of TIM barrel from interaction energy based structure networks, PLoS Comput. Biol. 8 (2012) 18–24, https://doi.org/10.1371/journal.pcbi.1002505.
[49] L. Lo Leggio, S. Kalogiannis, K. Eckert, S.C.M. Teixeira, M.K. Bhat, C. Andrei, R.W. Pickersgill, S. Larsen, Substrate specificity and subsite mobility in *T. aurantiacus* xylanase 10A, FEBS Lett. 509 (2001) 303–308, https://doi.org/10.1016/S0014-5793(01)03177-5.
[50] A. Schmidt, G.M. Gübitz, C. Kratky, Xylan binding subsite mapping in the xylanase from *Penicillium simplicissimum* using xylooligosaccharides as cryo-protectant, Biochemistry 38 (1999) 2403–2412, https://doi.org/10.1021/bi982108l.
[51] K. Singh, M. Shandilya, S. Kundu, A.M. Kayastha, Heat, acid and chemically induced unfolding pathways, conformational stability and structure-function relationship in wheat α-amylase, PLoS One 10 (2015)https://doi.org/10.1371/journal.pone.0129203.
[52] L.R. De Souza Moreira, A. Da Cunha Morales Álvares, F.G. Da Silva, S.M. De Freitas, E.X.F. Filho, Xylan-degrading enzymes from *Aspergillus terreus*: physicochemical features and functional studies on hydrolysis of cellulose pulp, Carbohydr. Polym. 134 (2015) 700–708, https://doi.org/10.1016/j.carbpol.2015.08.040.
[53] Y. Tian, Y. Jiang, S. Ou, Interaction of cellulase with three phenolic acids, Food Chem. 138 (2013) 1022–1027, https://doi.org/10.1016/j.foodchem.2012.10.129.
[54] G.P. Maitan-Alfenas, M.B. Oliveira, R.A.P. Nagem, R.P. de Vries, V.M. Guimarães, Characterization and biotechnological application of recombinant xylanases from *Aspergillus nidulans*, Int. J. Biol. Macromol. 91 (2016) 60–67, https://doi.org/10.1016/J.IJBIOMAC.2016.05.065.
[55] X. Zhang, H. Liu, L. Ju, C. Liu, Exploring the effect of Cu2+ on sludge hydrolysis and interaction mechanism between Cu2+ and xylanase by multispectral and thermodynamic methods, Water Air Soil Pollut. 228 (2017) 99, https://doi.org/10.1007/s11270-017-3252-5.
[56] H. Liao, C. Xu, S. Tan, Z. Wei, N. Ling, G. Yu, W. Raza, R. Zhang, Q. Shen, Y. Xu, Production and characterization of acidophilic xylanolytic enzymes from *Penicillium oxalicum* GZ-2, Bioresour. Technol. 123 (2012) 117–124, https://doi.org/10.1016/j.biortech.2012.07.051.
[57] C.R.F. Terrasan, J.M. Guisan, E.C. Carmona, Xylanase and β-xylosidase from *Penicillium janczewskii*: purification, characterization and hydrolysis of substrates, Electron. J. Biotechnol. 23 (2016) 54–62, https://doi.org/10.1016/j.ejbt.2016.08.001.
[58] O.A. Vieira Cardoso, E.X. Ferreira Filho, Purification and characterization of a novel cellulase-free xylanase from *Acrophialophora nainiana*, FEMS Microbiol. Lett. 223 (2003) 309–314, https://doi.org/10.1016/S0378-1097(03)00392-6.
[59] E.X.F. Filho, J. Puls, M.P. Coughlan, Biochemical characteristics of two endo-beta-1,4-xylanases produced by *Penicillium capsulatum*, J. Ind. Microbiol. 11 (1993) 171–180.
[60] F.A. Ricardo, M.M. Frederick, J.R. Frederick, P.J. Reilly, Purification and characterization of endo-xylanases from *Aspergillus niger*. III. An enzyme of pl 3.65, Biotechnol. Bioeng. 27 (1985) 539–546, https://doi.org/10.1002/bit.260270422.
[61] X. Xue, R. Wang, T. Tu, P. Shi, R. Ma, H. Luo, B. Yao, X. Su, The N-terminal GH10 domain of a multimodular protein from *Caldicellulosiruptor bescii* is a versatile xylanase/β-glucanase that can degrade crystalline cellulose, Appl. Environ. Microbiol. 81 (2015) 3823–3833, https://doi.org/10.1128/AEM.00432-15.
[62] H. Steen, M. Mann, The ABC's (and XYZ's) of peptide sequencing, Nat. Rev. Mol. Cell Biol. 5 (9) (2004) 699.

Electronic Supplementary File I

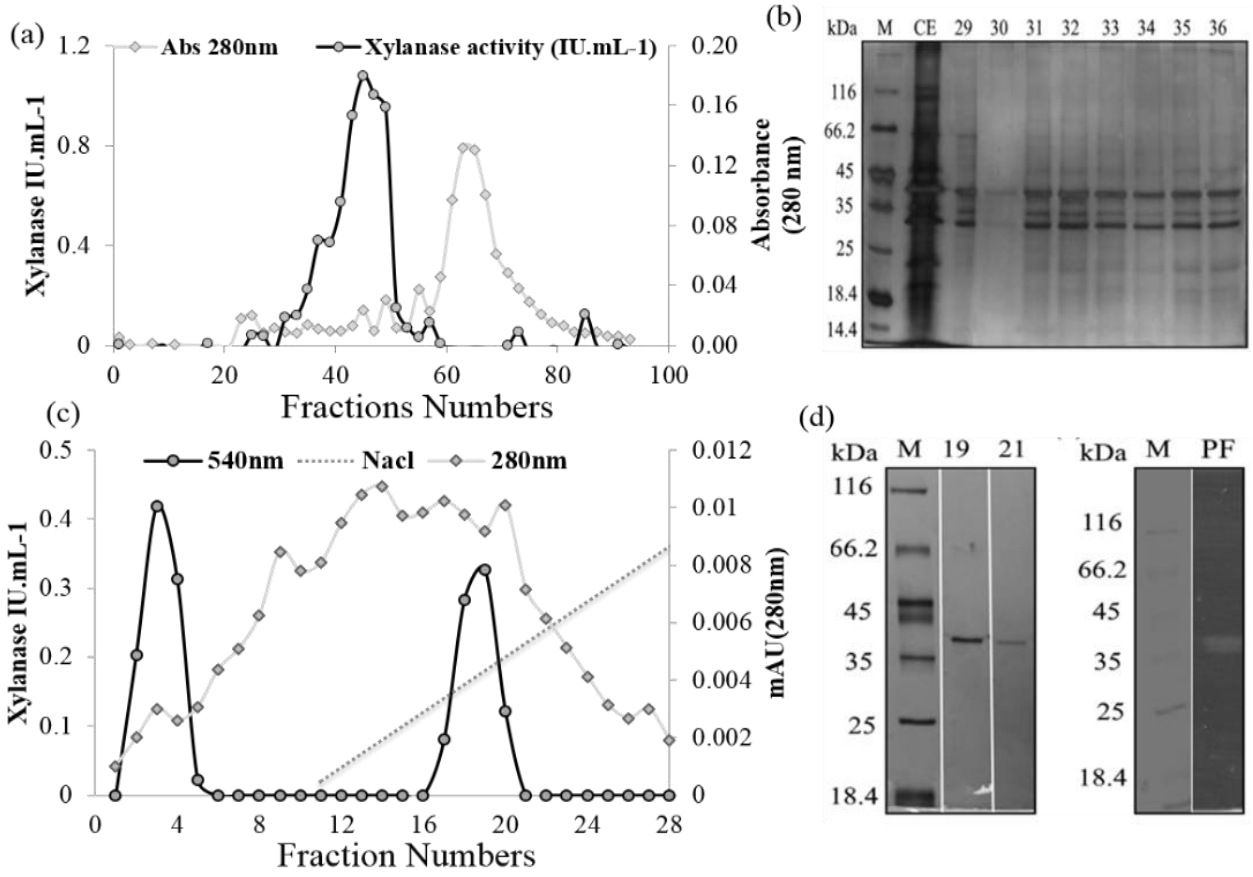

Supplementary Fig.1. Purification SDS and Zymogarm profile of *PcX1*

(a) Chromatographic profile of xylanase activity from *P. chrysogenum* crude extract applied on Sephadex G75 size exclusion chromatography. Grey squares represent UV (280 nm) protein detection, grey circle represent xylanase activity ($U.mL^{-1}$). (b) SDS-PAGE of crude extract and pooled fractions from size exclusion chromatography. (c) Äkta profile of QFF anion exchange chromatography (d) Silver stained SDS-PAGE of purified xylanase (*PcX1*) (e) zymogram analysis of purified collected fractions.

Electronic Supplementary File II

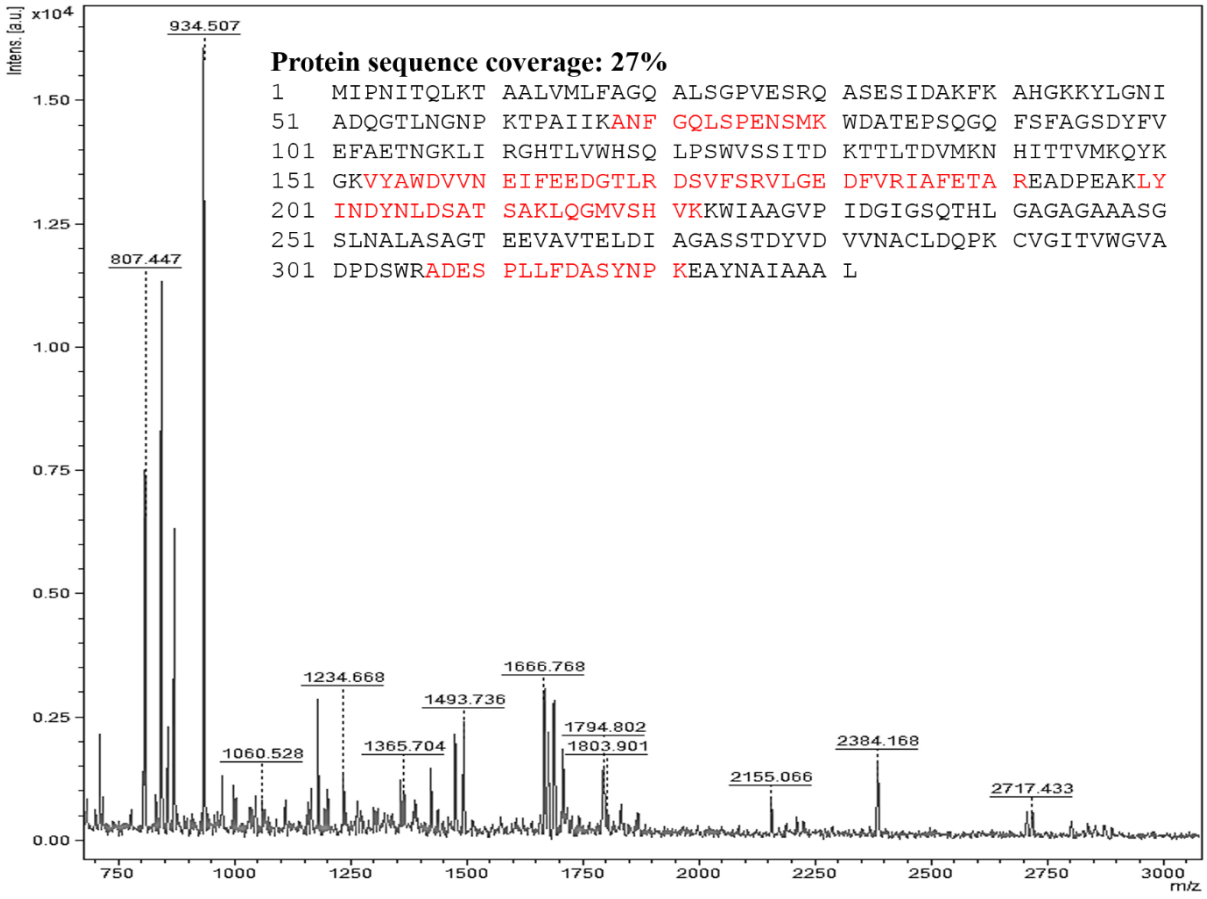

Supplementary Fig.2. Peptide spectra and amino acid sequence of *PcX1*

Spectrum of *PcX1* peptides after digestion with trypsin in MALDI-TOF. Sequence of *PcX1* based on MS and MS/MS analysis is presented *inset*. The identified peptides are highlighted in red

Electronic Supplementary File III

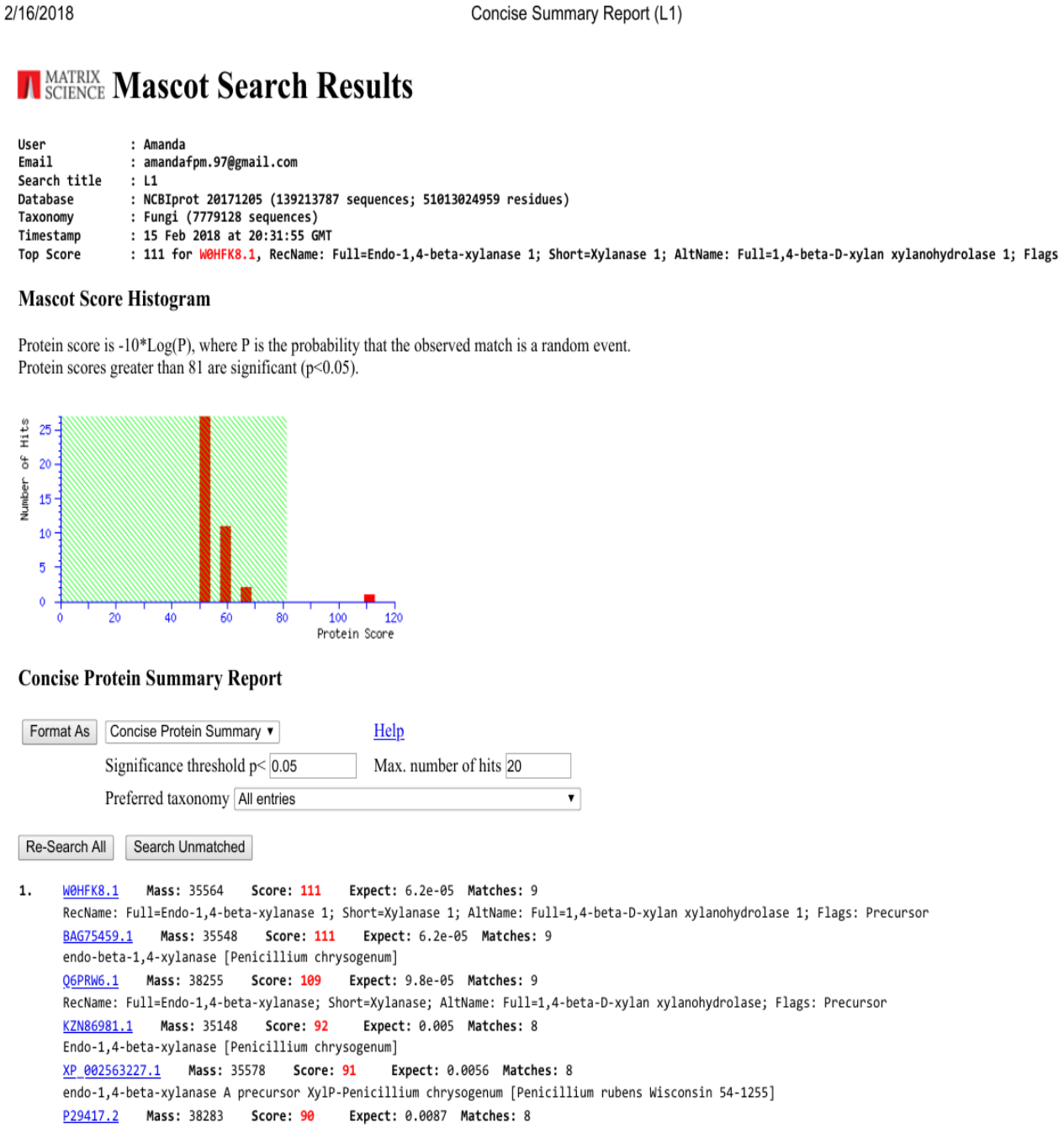

2/16/2018 Concise Summary Report (L1)

MATRIX SCIENCE **Mascot Search Results**

User : Amanda
Email : amandafpm.97@gmail.com
Search title : L1
Database : NCBIprot 20171205 (139213787 sequences; 51013024959 residues)
Taxonomy : Fungi (7779128 sequences)
Timestamp : 15 Feb 2018 at 20:31:55 GMT
Top Score : 111 for W0HFK8.1, RecName: Full=Endo-1,4-beta-xylanase 1; Short=Xylanase 1; AltName: Full=1,4-beta-D-xylan xylanohydrolase 1; Flags

Mascot Score Histogram

Protein score is -10*Log(P), where P is the probability that the observed match is a random event.
Protein scores greater than 81 are significant (p<0.05).

Concise Protein Summary Report

Format As Concise Protein Summary Help
Significance threshold p< 0.05 Max. number of hits 20
Preferred taxonomy All entries
Re-Search All Search Unmatched

1. W0HFK8.1 Mass: 35564 Score: 111 Expect: 6.2e-05 Matches: 9
RecName: Full=Endo-1,4-beta-xylanase 1; Short=Xylanase 1; AltName: Full=1,4-beta-D-xylan xylanohydrolase 1; Flags: Precursor
BAG75459.1 Mass: 35548 Score: 111 Expect: 6.2e-05 Matches: 9
endo-beta-1,4-xylanase [Penicillium chrysogenum]
Q6PRW6.1 Mass: 38255 Score: 109 Expect: 9.8e-05 Matches: 9
RecName: Full=Endo-1,4-beta-xylanase; Short=Xylanase; AltName: Full=1,4-beta-D-xylan xylanohydrolase; Flags: Precursor
KZN86981.1 Mass: 35148 Score: 92 Expect: 0.005 Matches: 8
Endo-1,4-beta-xylanase [Penicillium chrysogenum]
XP_002563227.1 Mass: 35578 Score: 91 Expect: 0.0056 Matches: 8
endo-1,4-beta-xylanase A precursor XylP-Penicillium chrysogenum [Penicillium rubens Wisconsin 54-1255]
P29417.2 Mass: 38283 Score: 90 Expect: 0.0087 Matches: 8

Supplementary Fig.3. Histogram and concise protein summary of Mass spectrometry

Figure showing the significant score value (>80). Below the blue underlines are the results obtained for matched peptides. WOHFK8.1 (*Rhizopus oryzae*), BAG7459.1 (*P. chrysogenum*-31B), Q6PRW6.1 (*P. chrysogenum*), KZN86981.1 (*Penicillium chrysogenum*-P2niaD18) XP_002563227.1 (*Penicillium rubens Wisconsin* 54-1255) P29417.2 (*Penicillium chrysogenum*-Q176)

Electronic Supplementary File IV

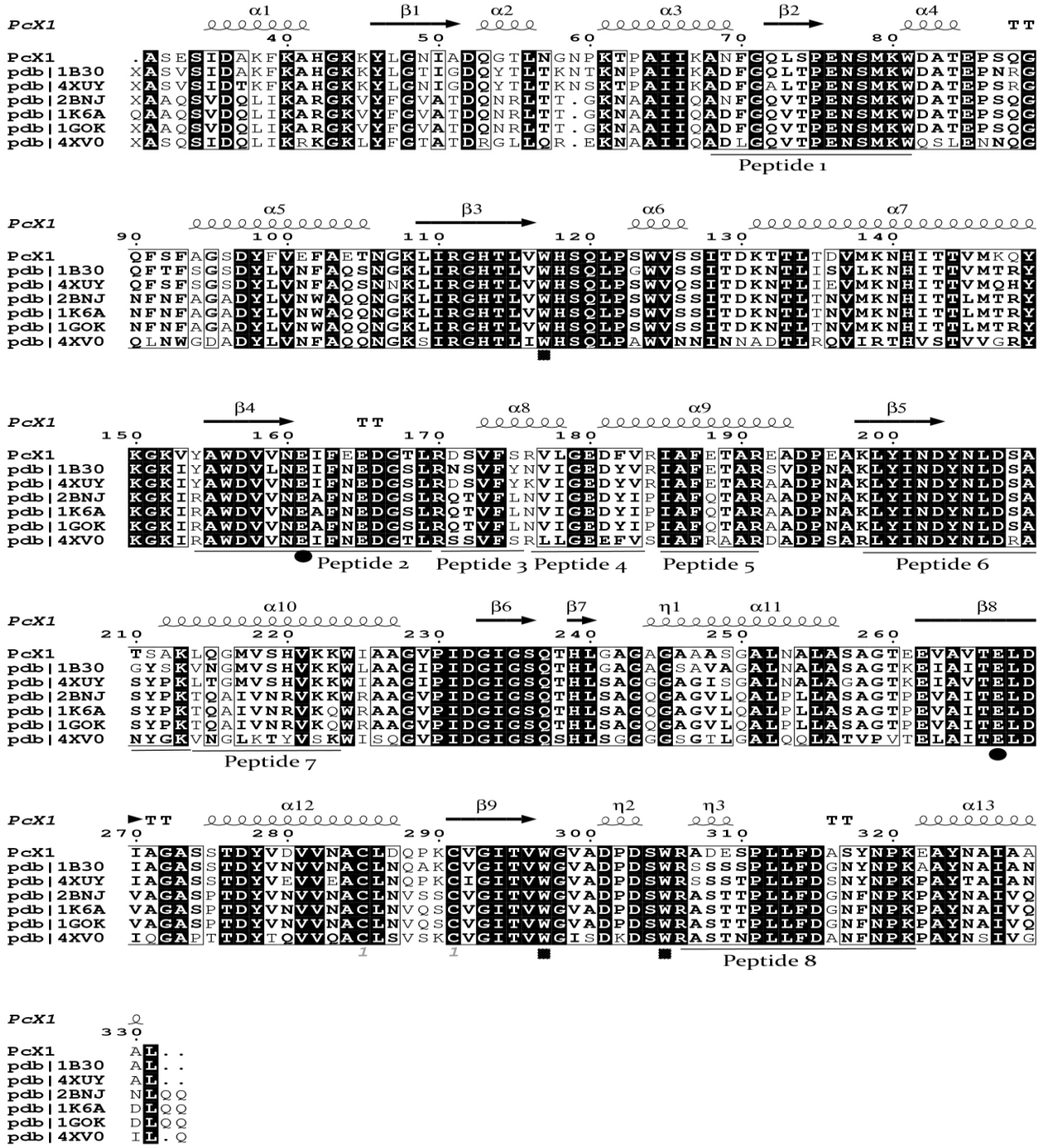

Supplementary Fig.4. Sequence alignment of *PcX1* and glycosyl hydrolase family10 xylanases available in PDB Secondary structures of *PcX1* are shown above alignment. Identical residues are shown in white letters on a black background, and similar residues are in bold black letters. Solid circles below residues indicate the catalytic pair. Solid squares below residues indicate the tryptophan triad. Cysteine that forms a disulphide bond is indicated by "1" in grey. α-helix are indicated by squiggles, β-sheets are indicated by arrows, turns are indicated by TT letters.

Electronic Supplementary File V

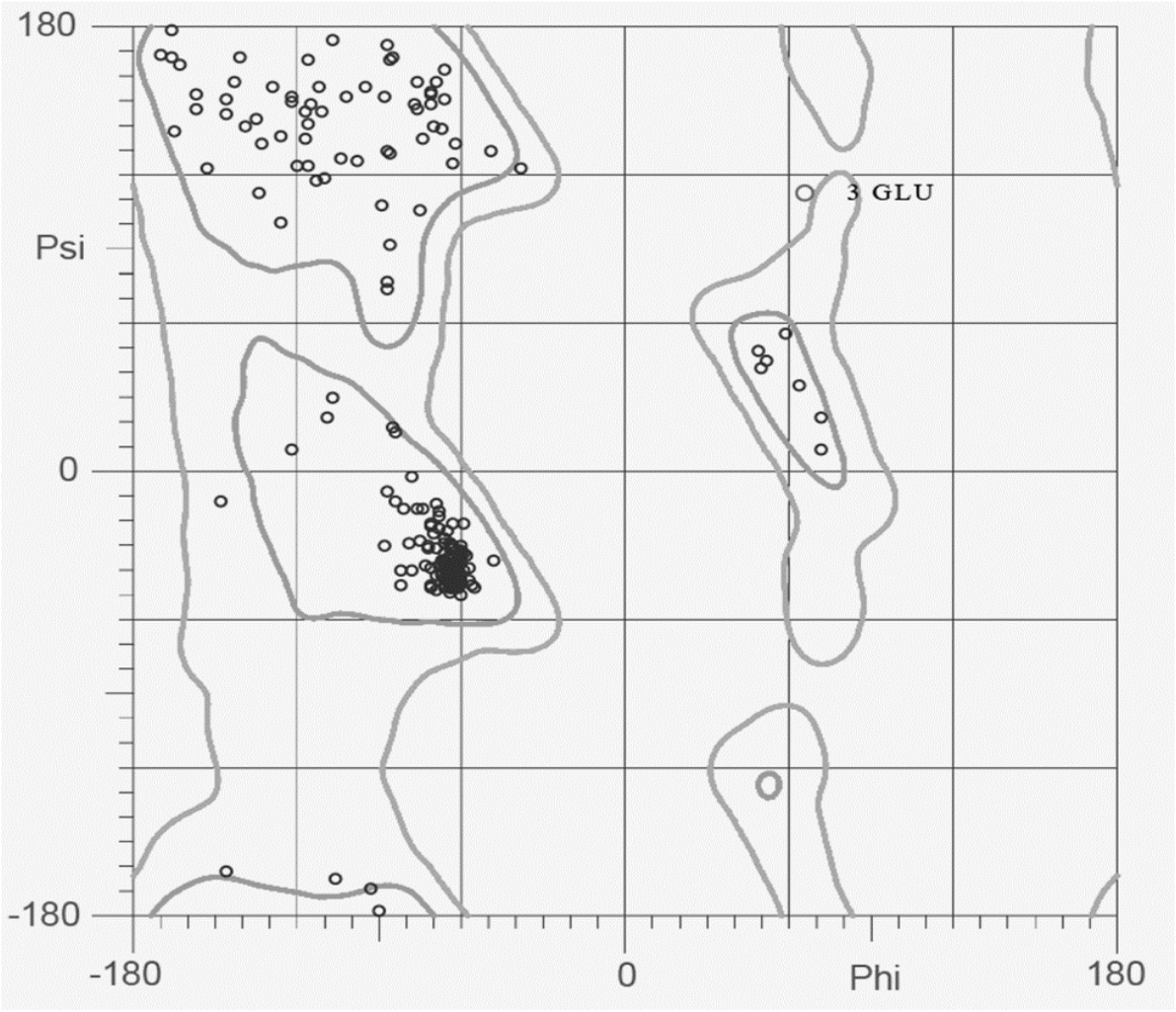

Supplementary Fig.5. Ramachandran Plot for *PcX1* solved by molecular homology modelling

98% of the residues have their backbone Φ and Ψ angles present in the favoured regions, 1.7% and 0.3% of the residues are present in the allowed region and outlier region, respectively.

Electronic Supplementary File VI

Table S1. Summary of purification steps of *PcX1*

Purification Steps	**Xylanase Activity (U)**	**Protein (mg)**	**Specific activity ($U.mg^{-1}$)**	**Purification Fold**	**Recovery (%)**
Culture Filtrate	34.00	3.28	10.37	1.00	100.00
Size exclusion Chromatography	12.51	0.22	56.34	5.44	36.79
FPLC/Anion exchange Chromatography	5.96	0.09	60.45	5.83	17.53

Chapter III : GH11 endo-β, 1, 4-xylanase from *Penicillium chrysogenum:* physicochemical properties and hydrolysis of pre-treated sugarcane bagasse

Abstract

Enzymes are the catalytic cornerstone of metabolism and focus of profound research for application in green industrial processes, as the conversion of lignocellulosic wastes to fuels and other molecules with industrial interest. In the present work, *Penicillium chrysogenum* CCDCA10746, an endo-β,1,4-xylanase (*PcX2*) was purified and characterized physicochemically. *P. chrysogenum* secreted three isoforms of endo-β,1,4-xylanases during growth in liquid media containing sugarcane bagasse as a carbon source. Purified *PcX2* presented estimated molecular mass 23kDa. *PcX2* was optimally active at pH 6.0 and temperature 45 ºC and CFPs (culture filtrate proteins) at pH 5.0 and temperature of 40 ºC. Half-life of *PcX2* and CFPs were 1.0 and 8.0 hours respectively, at 45ºC. Kinetic values K_M and Vmax of *PcX2* were 0.53 $mg.mL^{-1}$ and 0.21 $U.mg^{-1}$. Both (*PcX2* and CFPs) were sensitive to Cu^{+2} and Zn^{+2} and resistant to tannic acid. Xylanases were inhibited by vanillin, trans-cinnamic acid and 4-hydroxy-benzoic acid. *PcX2* was structurally stable over the pH range of 4.0 to 9.0. Glucose, xylose, and cellobiose were the major sugars liberated during enzymatic hydrolysis (CFPs) of hydrothermal pre-treated sugarcane bagasse.

Keywords: Enzymatic hydrolysis; GH11; sugarcane bagasse; Xylanases; protein conformation; biotechnological products

Introduction

Agricultural waste is renewable and abundantly available feedstock to employed for the production of cell wall degrading enzymes. Carbon source used in fermentation to produce microbial products also applied in industrial processes. The lignocellulosic biomass is composed of cellulose, hemicellulose, pectin and lignin (SILVA; VAZ; FILHO, 2018)

Cellulose is a linear polymer of glucose linked by β-1,4 glycosidic bonds comprising amorphous and crystalline structures. Cellulose deconstructed to its monomeric units by the action of exoglucanases, endoglucanases, and β-glucosidases (GILBERT; HAZLEWOOD, 1993). Hemicellulose is a branched heteropolymer, comprising pentoses (xylose and arabinose), hexoses (glucose, galactose and fructose) and uronic acids (such as glucuronic acid) linked by α or β (1-3, 1-4, and 1-6) glycosidic bond. The backbone is deconstructed to its monomeric unit by endo-1,4-β-D-xylanases and β-D-xylosidases, side chains and acetyl groups are removed by α-L-arabinofuranosidases, α-D-glucuronidases, and acetyl xylan esterases (COLLINS; GERDAY; FELLER, 2005).

Xylanases have promising potential for bioconversion or biodegradation of waste released from agro-industries, into value-added compounds. Enzymes with the catalytic properties to perform/work in industrial processes are favoured. Latest studies have seen successful use of xylanase in food, feed, textile, paper and pulp industries. Some wild-type *Candida shehatae*, *Pichia stipitis* and *Spathaspora passalidarum* were regarded for the production of ethanol from xylose (LONG et al., 2012; ZHANG; GENG, 2012; RODRUSSAMEE; SATTAYAWAT; YAMADA, 2018).

However, the degradation of biomass into fermentable sugars requires the combined action of glycosyl hydrolases (cellulases, xylanases, pectinases) acting individually or in consortium and protein accessories. Most recently, enzymes with oxidative activity (LPMOs) have been reported important contributors to cellulose deconstruction (FORSBERG et al., 2014). As well as, non-catalytic proteins with the ability to disrupt hydrogen bonds on cellulose fibres enhancing enzymes accessibility to the substrate were described (SALOHEIMO et al., 2002). Pre-treatment is another approach to avoid physical/chemical barriers, a biochemical process of lignocellulose, based on the sugar platform concept.

Various fungi secrete “free enzyme” cocktails, wherein many proteins diffuse and work synergistically to degrade the lignocellulosic biomass into fermentable sugars. Several fungi, *Trichoderma reesei and Aspergillus niger* produce a higher number of enzymes with

complementary activities to recycle the cellulose in nature (GUPTA et al., 2016). *Penicillium* sp. has also been reported as a good producer of cellulases and hemicellulases (YANG et al., 2018b). Regarding *Penicillium* species, *P. chrysogenum* has been described for its capability to produce industrial enzymes such as; lipases, amylases, cellulases and xylanases (FERRER et al., 2000; VANGULIK et al., 2001; ERTAN et al., 2006; NWODO et al., 2008; SILVA et al., 2019). Previously GH10 xylanase of *P. chrysogenum* produced using xylan as carbon source has been characterized (HAAS et al., 1992)

Most of the previous studies were focused on only one single aspect of xylanase technology. The objective of this study is to explore the functional and structural properties of GH11 endo-β-1,4-xylanase (*PcX2*) produced and purified from *P. chrysogenum*, and its potential to produce the xylose/glucose from hydrolysing the hydrothermal pre-treated sugarcane bagasse and the effect of lignin-derived phenolic compounds released during scarification of lignocellulosic biomass on the activity of xylanase.

Materials and methods

Fungal isolation, growth conditions

P. chrysogenum was previously isolated and identified (ULLAH et al., 2019) on MYG agar plates; containing yeast extract (4 g/L), malt extract (10 g/L), glucose (4 g/L) and agar 2% (*w/v*) and incubated for 7 days at 28 ^{o}C. Isolates were screened for xylan degradation on solid MYG agar media supplemented with oat-spelt xylan 1% (*w/v*) as a substrate, 3 mm radius disks of seven days old culture was placed in the centre of the plate and incubated at 28 ^{o}C for 10 days. Congo red 0.1% (*w/v*) was used to observe the clear zone around the colony. Halo size and intensity were considered as a criterion for fungi selection used for xylanase production.

Enzyme production and sample preparation

For enzyme production, 0.5L minimal medium (KH_2PO_4 (0.7%), K_2HPO_4 (0.2%), $MgSO_4.7H_2O$ (0.05%), and $(NH_4)_2SO_4$ (0.16%) was supplemented with 1% (w/v) raw sugarcane bagasse as sole carbon source. The medium was sterilized at 121 °C for 30 minutes and inoculated with 5 ml conidia suspension containing (1×10^6 conidia.mL^{-1}) and incubated at 28 °C for 10 days at constant agitation (120 rpm). During fermentation, an aliquot was decanted at a regular interval of 24 hours, sieved and centrifuged at 10,000 g for 10 minutes. The supernatant was filtered by a 0.22 µm membrane, dialyzed against 0.05 M sodium acetate buffer (pH 5.0) and used for enzyme activities and protein profiling.

Lignocellulosic residues (sugarcane bagasse) was collected from the local farms of Brasilia, Brazil autoclaved, filtered and washed thoroughly under tap water, and oven dried at 60 ^{o}C. The dried residues were blended to a homogeneous fine powder in an industrial food blender (Skymsen, Brazil); that was used to supplement liquid growth media. For enzyme purification, media with 1% sugarcane bagasse was fermented for 4 days at 30 ^{o}C and 120 rpm continuous agitation. On the 4th day, media was filtered and centrifuged (10,000 g) after confirming the activity by enzyme assay and in gel (zymogram) methods, the medium was subjected to lyophilisation (Freeze Dryer Liobrás, Brazil). The resultant powder was re-suspended in sodium acetate buffer 0.05 M (pH 5.0).

SDS-PAGE and zymogram analysis

Protein was profiled in the sterilizing solution using SDS-PAGE (12%) prepared as previously described (LAEMMLI, 1970). The xylanase activity was determined by zymogarm prepared by incorporating the 0.1% xylan with a polyacrylamide gel. The zymogram gel was stained with Congo red solution 0.1% (w/v) for 30 minutes followed by destaining with l M NaCl. Concentrated enzyme load 20 uL (from 1 mL sample size) was applied in each well.

Enzymatic hydrolysis and pre-treatment of sugarcane bagasse

Sugarcane bagasse was incubated at 170 ^{o}C for 30minutes in a bioreactor (SILVA et al., 2018). For enzymatic hydrolysis, 2% (w/v) pre-treated sugarcane bagasse was used by employing (4 mg/g of the substrate) crude enzymes (culture supernatant after 4 days of growth). Hydrolysis was performed at stranded enzymatic conditions (pH 5.0 and temperature 40 ^{o}C) at 200 rpm. The hydrolysate was collected after 3, 6, 12, 24, 36, 42 hours of incubation and reducing sugars were analysed using the DNS method and measured at A_{540} nm.

Analysis of sugar released by high-performance liquid chromatography (HPLC)

The concentrations of glucose and xylose were determined by high-performance liquid chromatography (HPLC) (Agillent) equipped with a column Aminex HPX-87H (Bio-Rad). The analysis was conducted by isocratic elution for 24 minutes, with 5 mM H_2SO_4 solution with a constant rate of 0.6 mL.min^{-1} at 45 °C. The curve calibration was obtained by measuring standard points with an increasing concentration from 0.0625 to 5.0 g.L^{-1} of glucose and xylose.

Hydrolysis Yield

Yield (%) was calculated by using an initial concentration of glucan, xylan of the pre-treated sugarcane bagasse by using the following formula;

$$Cellulose\ conversion = \frac{Glucose\ released\ \left(\frac{g}{L}\right) \times 0.9}{Cellulose\ added\ \left(\frac{g}{L}\right)} \times 100$$

$$Hemicellulose\ conversion = \frac{Xylose\ released\ \left(\frac{g}{L}\right) \times 0.8}{hemicellulose\ added\ \left(\frac{g}{L}\right)} \times 100$$

0.90 is the correction factor of anhydroglucose residue (or162/180); here 180 is molar mass of glucose and 162 is anhydrous molar mass of glucose calculated by removing the molar mass of H_2O (180 - 18 = 162) for C-6 sugars (glucose, galactose, and mannose). While 0.88 is the correction factor for anhydroxylose residue (or 132/150) for C-5 sugars (xylose and arabinose).

Protein purification

Aliquots (10 mL) of concentrated culture filtrate was fractioned on gel filtration chromatography. Sephadex G-75 (GE Healthcare, UK) and acetate buffer 0.05 M (pH.5.0) with the addition of 0.15 M NaCl were used as stationary and mobile phase, respectively. The flow rate was set at 0.3 $mL.min^{-1}$. Fractions (6 mL) were collected and analysed for xylanase activity, and protein content. Fractions containing xylanase activity were pooled loaded onto an anion exchange QFF-Sepharose (GE Healthcare, UK) column at a flow rate of 2 $mL.min^{-1}$ at Äkta protein purification system (GE Healthcare, UK). Equilibration and elution were performed with acetate buffer 0.05 M (pH 5.0).

Mass spectrometry/ MALDI-TOF

For mass spectrometry, the gel was stained with coomassie to avoid fixation and for intact recovery of protein. The band was excised with a sterile spatula and digested with trypsin (Protocol adapted from (OLSEN et al., 2007). Resultant peptides were identified in the Mass spectrometry (Autoflex II, BrukerDaltonics, Bremen, Germany). Prior to applying in MS, peptides were desalted by using C18-SD membrane described previously (RAPPSILBER; MANN; ISHIHAMA, 2007).

Homologous sequences were searched in the National Center for Biotechnology Information (NCBI) database using Mascot (Matrix Science, London, UK). The search

parameters were fixed at taxonomy fungi, enzyme trypsin, no missed cleavage, carbamidomethylation of cysteines as a fixed modification, oxidation of methionine as variable modification, peptide mass tolerance ± 200 ppm, and MS/MS fragmentation mass tolerance 0.4Da. The identification of the proteins was considered significant when the Mascot score was $P < 0.05$.

Signal peptides and sequence alignment

The signal peptide of *PcX2* was predicted with SignalP http://www.cbs.dtu.dk/services/SignalP/. The theoretical values of molecular mass and isoelectric point were retrieved from the Compute pI/Mw tool https://web.expasy.org/compute_pi/ according to predicted amino acid sequences. Multiple sequence alignment was carried out with the Clustal Omega tool https://www.ebi.ac.uk/Tools/msa/clustalo/. The BLAST algorithm was used to search the homology sequences. ESPript 3.0 online tool was employed to the depiction of secondary structure using *Penicillium funiculosum* (PDB_1TE1-B) xylanase as a template.

Enzyme activity and protein quantification

Endoglucanase and xylanase activities were evaluated by using carboxymethylcellulose (CMC 2% w/v) and oat spelt xylan (1% w/v) respectively, as a substrate. Activities of cellobiohydrolase, mannanase and pectinase were assessed using respective substrate, avicel (1% w/v) mannan (1% w/v), and pectin 1% (w/v). The enzymatic assay was standardised, by using 0.05 mL of samples mixed with 0.1 mL of substrates (all prepared in 0.1 M sodium acetate buffer pH 5.0). Hydrolysis was carried out for 30 minutes at 40 °C and the reaction was stopped by adding 0.3 mL of dinitrosalicylic reagent (MILLER, 1959).

Reducing sugars were measured at 540 nm in SpectraMax® Plus (Molecular Devices, US). One unit of endoxylanase and CMCase, avicelase, mannanase, and pectinase activity was expressed as the enzyme quantity released 1 µmol of reducing sugar per minute of reaction, per millilitre of the enzyme ($U.mL^{-1}$) using xylose and glucose, mannan and galacturonic acid as a standard. All tests were performed in triplicate. Bradford assay was prepared by applying bovine serum albumin as a standard (BRADFORD, 1976) used for protein quantification.

Effect of pH and temperature on the activity of xylanase

The enzyme activity under the influence of pH range (pH 3.0 – 10) was determined at standard conditions (45 ^{o}C for 30 minutes) using different (Acetate, phosphate, Tris-HCl,

Glycine NaOH) buffer systems. Temperature optima were determined by testing the activity in the temperature of range 25 ºC – 75 ºC. Thermostability of *PcX2* and CFPs was determined by incubating the enzymes at 45 ºC for 150 minutes, activity was measured after every 30 minutes interval. Half-life of enzyme was calculated by using the equation:

$$t_{1/2} = 0.693/ Kd \qquad (1)$$

where Kd is the rate constant of deactivation.

The deactivation energy was estimated using Arrhenius equation (2), activity data log ratio of Er (Enzyme residual activity)/E0 (Enzyme initial activity) was plotted as a function of time to obtain the deactivation rate constant (Kd) (AYMARD; BELARBI, 2000).

$$Kd = Kd_0 \exp^{-(Ed/RT)} \qquad (2)$$

The energy of deactivation (Ed) was the product of the slope of resultant straight-line times R, the universal gas constant.

Effect of ions on the activity of xylanase

The effect of salts, metal ions (Ca^{2+}, Fe^{3+}, Mg^{2+}, Cu^{2+}, Zn^{2+}, K^{+}, CO^{2+}, SO^{2-}_{4}, Cl^{-}) and EDTA the activity of the enzyme was investigated by measuring the residual activity at standard conditions after pre-incubation of the enzyme with each metal ion for 30 minutes at room temperature. Metal ions were prepared at 1 mM and 10 mM concentration in acetate buffer (pH 5.0).

Effect of phenolic compounds on the activity of xylanase

The effect of lignin-derived phenolic compounds (vanillin, tannic acid, trans-ferulic acid, trans-cinnamic acid, ρ-coumaric acid, gallic acid, syringaldehyde and acid-4-hydroxy-benzoic acid) on xylanases (0.023 $mg.mL^{-1}$ *PcX2* and 0.05 $mg.mL^{-1}$ CFPs) was evaluated by pre-incubating the enzyme with each phenolic compound for 24 hours at 28 ºC.

Residual activity under standard conditions was calculated after the enzyme was incubated (24 hours at 28 ºC) in the absence of phenolic compounds. Lignin-derive phenolic compounds were prepared in 1 $mg.mL^{-1}$ concentration (DE SOUZA MOREIRA et al., 2013). The ration between *PcX2*: phenolics was 1:44 while CFPs: phenolics 1:20.

Enzyme kinetics and statistical analysis

Enzyme kinetic studies were determined under optimal conditions at a varying concentration (0.2 to 4.0 mg.mL^{-1}) of oat spelt xylan. Kinetic constant K_M, Vmax and Kcat values were determined by Michaelis-Menten equation using the software Sigma Plot 12.0 (Systat Software Inc., US).

Assays for biochemical characterisation were performed in triplicates, and results were subjected to factorial ANOVA and post hoc test LSD Fisher Pairwise Comparison at 5% or 1% level of significance ($P \leq 0.05$ or 0.01). Statistical analysis was performed using Origin software version 8.5 (Origin Lab Corporation, EUA) and Excel 2013.

Conformational analysis by fluorescence spectroscopy

The conformational changes of (*PcX2*) under the function of pH were examined using fluorescence measurements on a Jasco Spectrofluorimeter FP-650 (Jasco Corporation, Tokyo, Japan) attached to a Peltier-type temperature controller (Jasco Analytical Instruments, Japan). Conformational changes of the enzyme (0.046 mg .mL^{-1}) were analysed by using 0.01 M sodium acetate buffer, pH 4.0 – 5.5 and Tris HCl pH 6.0 – 9.0 with a range difference of 0.5. The emission spectra of the tryptophan residue were recorded in the range of 300 – 400 nm, after excitation at 295 nm at 25 °C (SOUZA et al., 2016). The excitation and emission slits were set at 5.0 nm.

Results

Screening for glycoside hydrolase activity

The activity of xylanase was screened by the clear and prominent zones around the colonies indicating the production of xylanase. The selected fungal strain was able to grow on MYG agar media, transferred to liquid medium containing 1% sugarcane bagasse for the production of enzymes. Cell wall degrading enzymes having activities of cellobiohydrolase, endoglucanase, mannanase, pectinase and xylanase were estimated.

The activity of endoglucanase was relatively low during the initial days of growth; a gradual increase was noticed after 4 days of growth. Maximum activity (0.10 U.mL^{-1}) of endoglucanase was recorded on the 7th day of growth. A similar pattern of secretion was followed by cellobiohydrolase, activity was maximum (0.24 U.mL^{-1}) on the 9th day of growth and no activity was detected during the first 3 days of growth. The mannanase and pectinase start to secrete on the 2nd and 3rd day of growth with a gradual increase until the 7th day, recorded

maximum activity of 0.11 U.mL^{-1} and 0.10 U.mL^{-1}, respectively (Fig III.1). The xylanase activity was observed from 2.0 – 10 days of growth. *P. chrysogenum* showed the maximum xylanase activity of about 0.80 U.mL^{-1} and 0.084 mg.mL^{-1} protein after 6 days of growth.

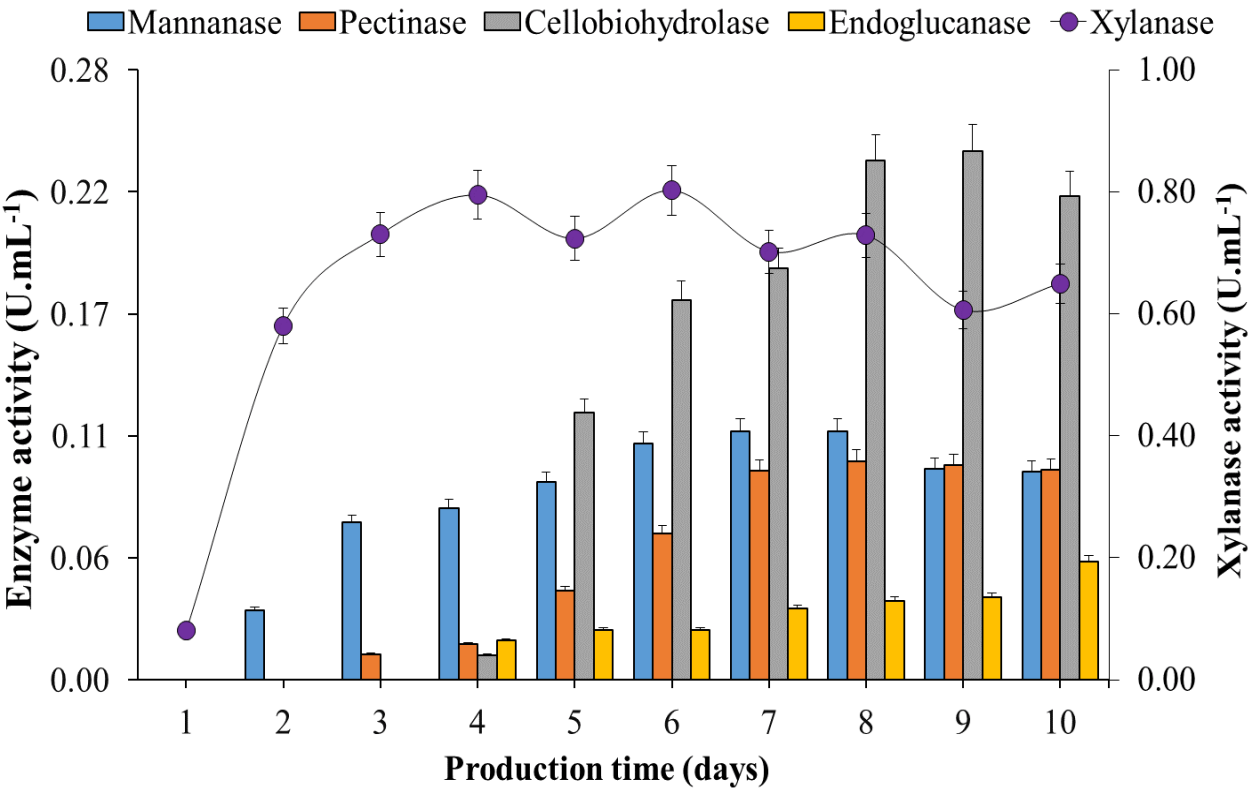

Figure III-1 Primary axis Enzyme production **Secondary axis** showing the xylanase production from *P. chrysogenum* by using sugarcane bagasse as a carbon source.

Protein profile and xylanase zymogram

Results of enzymatic activities were in line with the SDS-PAGE protein profile. As observed (Fig III.2A) number of bands and protein content increased proportionally with the time of growth, a maximum number of bands were obtained from day 7 – 10 days of growth, a similar array was followed by the protein content. The maximum amount (0.087 mg.mL^{-1}) of total secreted protein was estimated on the 7th day of growth.

In a separate experiment, xylanase activity was probed by zymogram and enzyme assays method. The in-gel activity of xylanase was obtained on the 2nd day of growth having a single band of xylanase with approximate molecular mass 23 kDa. From 3rd to 10th day of growth three bands of xylanase were consistence with approximate molecular mass values 23 kDa, 35 kDa, and 38 kDa (Fig III.2B).

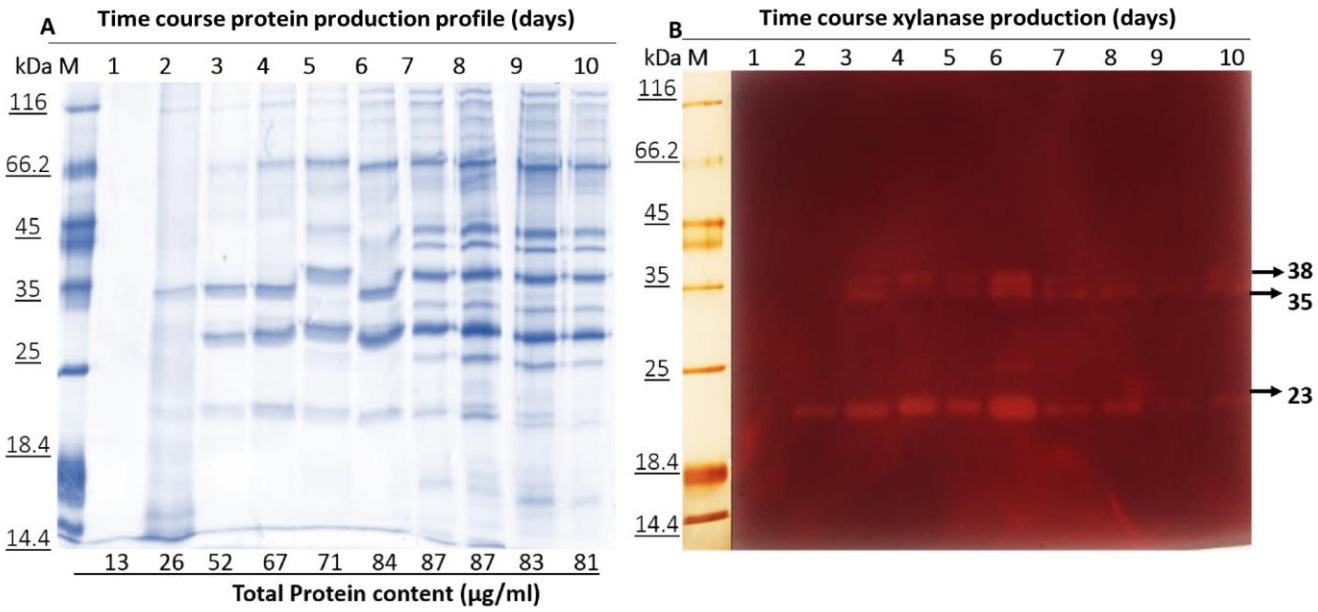

Figure III-2 Extracellular protein production profile (A), numbers above showing the days of fungal growth and numbers below showing the total protein content in the culture. (B) In-gel (zymogram) activity of xylanase produced during the fungal growth

Enzymatic hydrolysis of pre-treated sugarcane bagasse

The culture filtrate proteins (CFPs) containing above mentioned activities were applied for hydrolysis of hydrothermal pre-treated sugarcane bagasse. After the first 3 hours of hydrolysis, 0.67 mg.mL-1 of reducing sugars were release containing 0.25 mg.mL-1 glucose and xylose. The cellobiose 0.20 $mg.mL^{-1}$ was released after 6 hours of hydrolysis. The maximum yield of monosaccharides was obtained after 24 hours of hydrolysis, liberating 2.8 $mg.mL^{-1}$ glucose, 2.1 $mg.mL^{-1}$ xylose and 0.20 $mg.mL^{-1}$ of cellobiose (Fig III-3). HPLC spectra have shown in appendix.

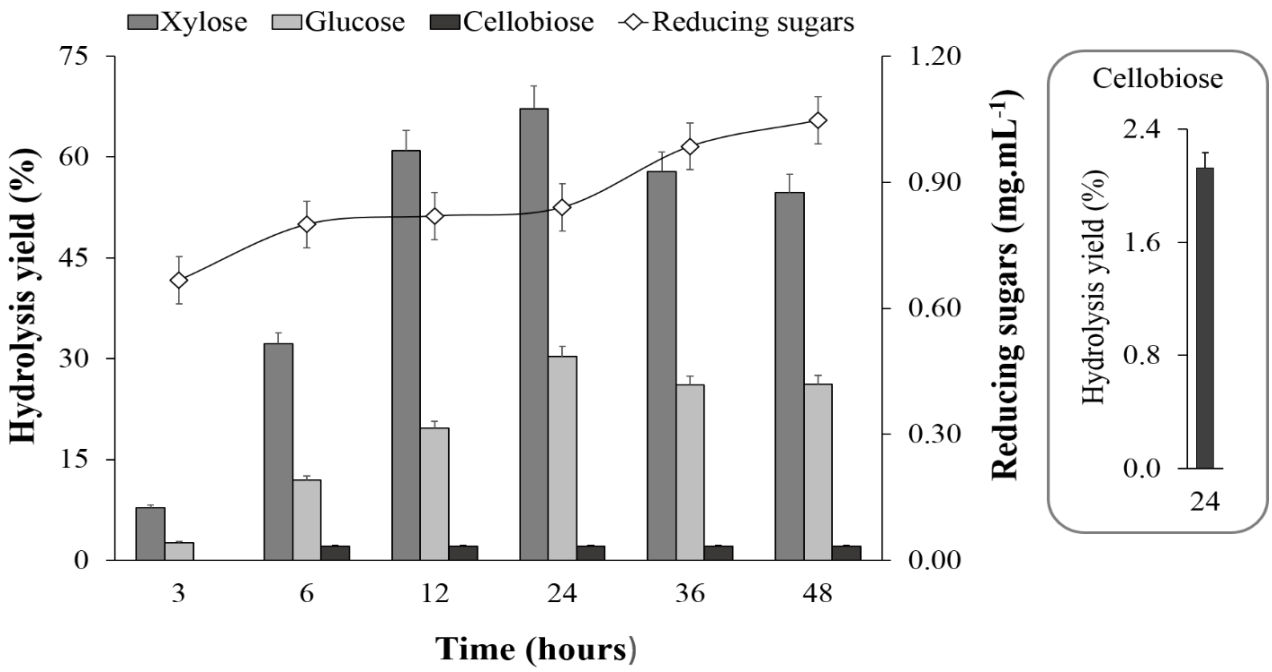

Figure III-3 Hydrolysis (hydrothermal pre-treated sugarcane bagasse) yield of reducing sugars obtained over different periods. Yield (%) calculated using an initial concentration of glucan, xylan in the pre-treated sugarcane bagasse.

Xylanase production and purification

The fermented broth was collected after 4 days of growth containing xylanase activity 34 $U.mL^{-1}$ and 3.28 mg of protein content. Purification of *PcX2* to apparent homogeneity as evidenced by SDS-PAGE (Fig III.4D) was achieved by the combination of gel filtration followed by ion-exchange chromatography.

Partial purification was attained after gel filtration chromatography having enzyme under molecular mass ranges from 38 to 20 kDa with total xylanase activity 12.51 $U.mL^{-1}$. Homogeneity was achieved by anion exchange chromatography, purification steps presented in (Fig III.4 inset table) the *PcX2* eluted before gradient (NaCl) in unbound fraction (Fig III.4C). The summary of xylanase.

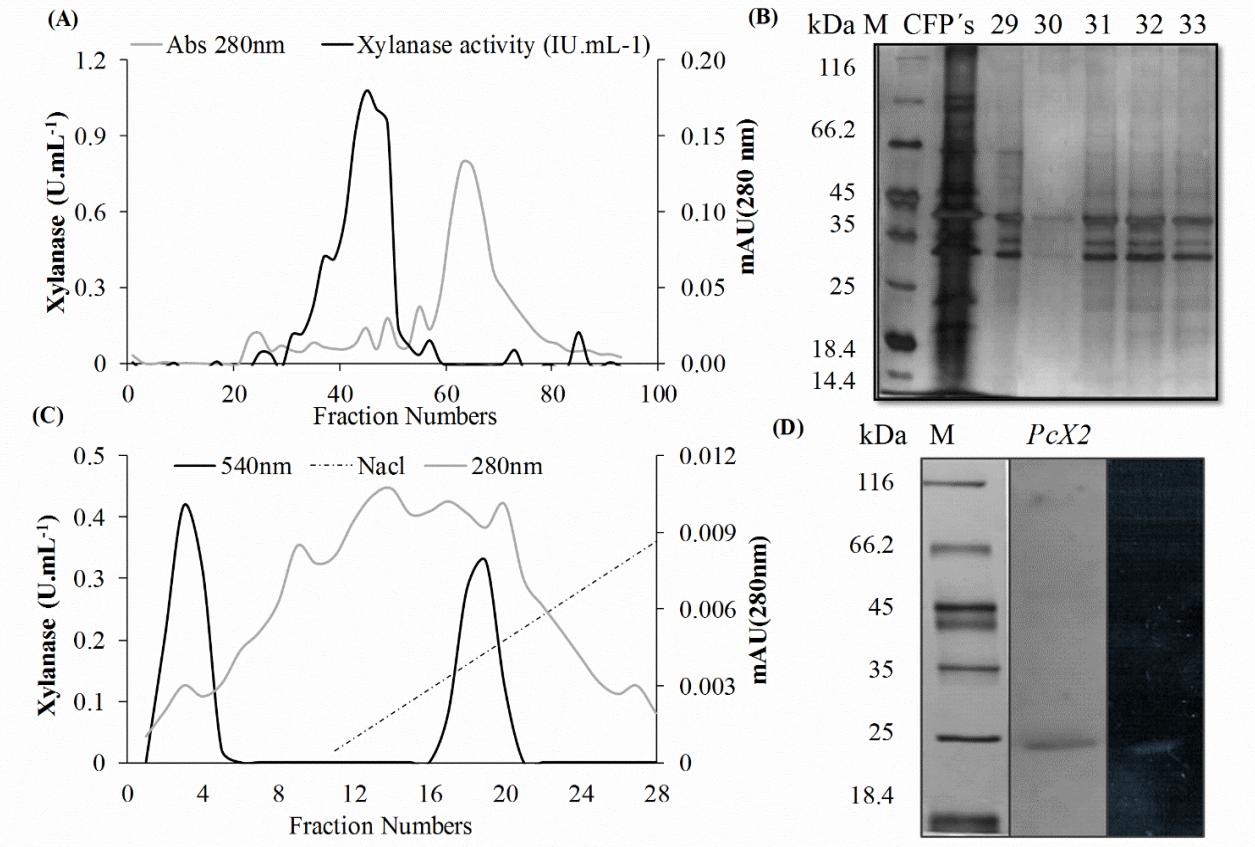

Purification steps	Total activity (IU)	Total protein (mg)	Specific activity (IU/mg)	Purification (Fold)	Yield (%)
Culture filtrate	34	3.28	10.36	1.00	100
Size exclusion	12.51	0.22	56.34	5.43	36.78
Anion exchange	0.629	0.007	92.25	8.90	1.824

Figure III-4 GH11 xylanase (*PcX2*) purification. (A) Chromatographic profile of xylanase activity from *P. chrysogenum* crude extract applied on Sephadex G75 size exclusion chromatography. Grey line represents UV (280 nm) protein detection, black line represent xylanase activity (U.mL^{-1}). (B) SDS-PAGE of culture filtrate proteins (CFP´s) and fractions from size exclusion chromatography. (C) Äkta profile of QFF anion exchange chromatography, showing two peaks. The first peak before gradient represents the *PcX2* activity (D) Silver stained SDS-PAGE of purified xylanase (*PcX2*) and zymogram analysis of purified.

Identification and sequence alignment of *PcX2*

Total thirteen peptides were obtained after trypsin digestion of *PcX2*. Spectrum and sequence are presented in the appendix. After stander calibration, ten peptides were validated for search query; four peptides covering 41% sequence of total protein were matched with

Penicillium rubens Wisconsin (Appendix). Matched peptides are highlighted in black bold letters (Fig III.5).

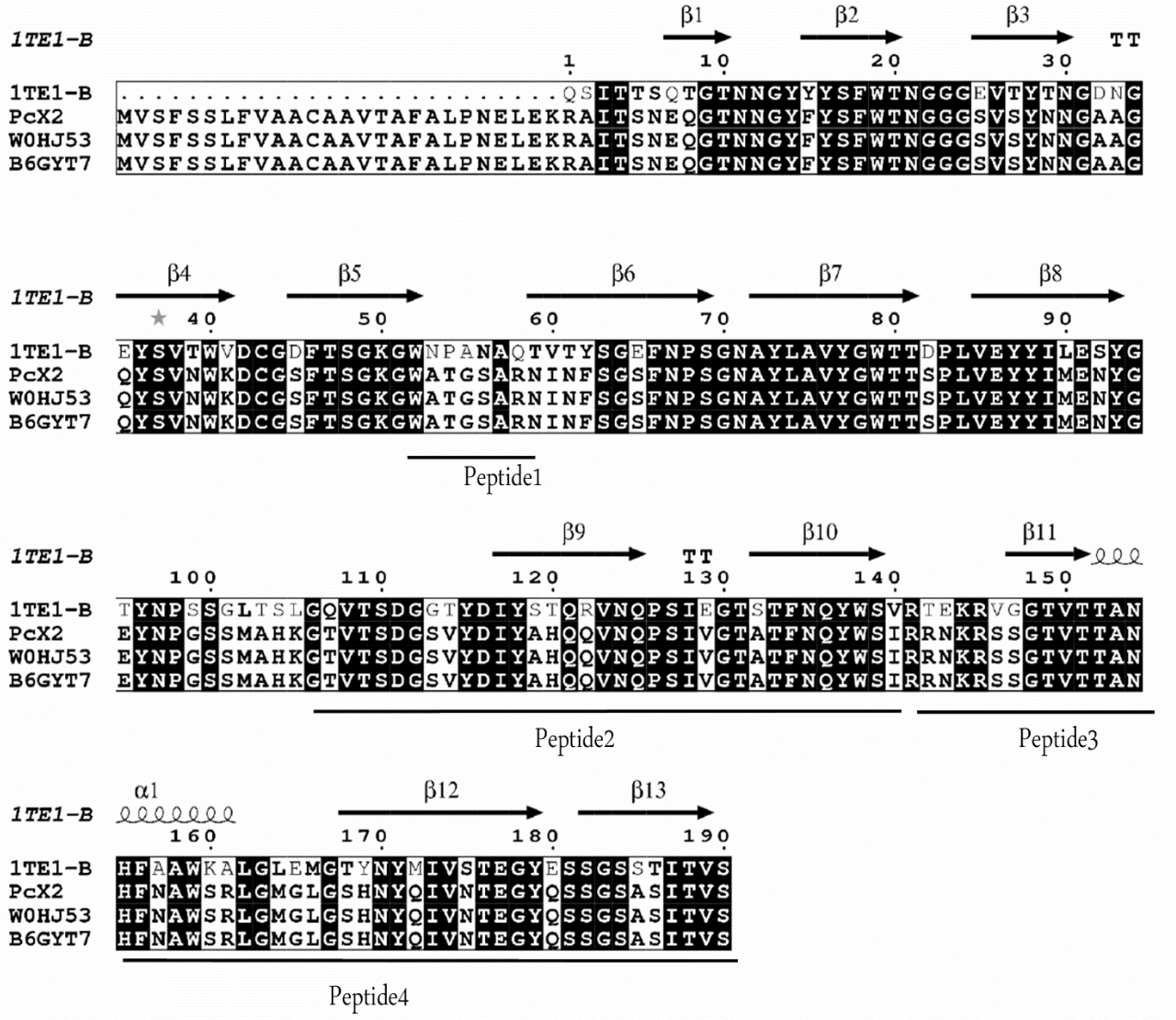

Figure III-5 Sequence alingment of similar xylanases (W0HJ53 *_Rhizopus oryzae*) (B6GYT7*_P. chrysogenum* B31), secondary structure predicted from 1TE1 *Penicillium funiculosum* (Q9HFH0). α-helix are indicated by squiggles, β-sheets are indicated by arrows, turns are indicated by TT letters. Solid circles below residues indicate the catalytic pair.

PcX2 predicted monoisotopic mass (M_r) 23361 Da and p*I* was 7.75. Multiple alignment analysis showed conservation between *PcX2* and other xylanase sequences such as; *Penicillium rubens and P. chrysogenum* B31 shares 100% similarity with *PcX2* (BERRIN et al., 2007). Secondary structure was predicted using *Penicillium funiculosum (Q9HFH0)* xylanase as a template, presenting 1 α-helix and 13 β-sheets. SignalP program specified N-terminus signal peptide at 1 – 19 residues (*MVSFSSLFVAACAAVTAFA*). Typical GH11 family catalytic residues

are located on the β-8 sheet (E85) and β-12 (E176) (Fig III.5). The nucleotide sequence of *PcX2* is 706bp long that encodes 216-amino acid residues

Xylanase characterization, Kinetics and stability

Purified (*PcX2*) and culture filtrate proteins (CFPs) were characterised biochemically by probing the effect of pH, temperature, ions, phenolic compounds and substrate kinetics. The activity of *PcX2* doubled in the presence of 1 mM concentration of Zn^{+2}, Mg^{+2} and Fe^{+3} while the CFPs activity not significantly ($P < 0.05$) change under these ions. The activity of both xylanases was strongly decreased in the presence of Cu^{+2} (Table III.1)

Table III-1 Ions and EDTA effect on the activity of CFPs, *PcX2*. Activity was compared with control value (100%) prepared in the absence of ions or EDTA

	PcX2 Relative activity (%)		CFPs Relative activity (%)	
Ions	1mM	10mM	1mM	10mM
$CuSO_4$	5.34 ± 0.049	21.28 ± 0.0297	56.18 ± 0.080	10.49 ± 0.007
$ZnSO_4$	247.6 ± 0.015	15.22 ± 0.126	82.97 ± 0.136*	20.26 ± 0.064
$FeCl_3$	284.3 ± 0.008	17.29 ± 0.003	78.55 ± 0.084*	13.25 ± 0.019
$CoCl_2$	21.71 ± 0.007	72.62 ± 0.034	73.10 ± 0.049	61.62 ± 0.045
$MgCl_2$	220.3 ± 0.063	46.09 ± 0.012	75.85 ± 0.097*	30.70 ± 0.044
KCl	124.7 ± 0.005	72.93 ± 0.029	40.37 ± 0.060	23.25 ± 0.026
$CaCl_2$	92.83 ± 0.004*	69.68 ± 0.030	58.85 ± 0.038	55.01 ± 0.018
EDTA	85.58 ± 0.006	97.81 ± 0.058*	52.26 ± 0.008	26.92 ± 0.016
$CuCl_2$	73.72 ± 0.040	14.83 ± 0.074	24.71 ± 0.019	2.580 ± 0.032
$ZnCl_2$	20.12 ± 0.053	100.6 ± 0.125*	72.06 ± 0.017	18.84 ± 0.019

(*) non-significant in LSD fisher test

Xylanase activity was observed from pH 5.0 – 7.0, with optimal activity at pH 6.0. The CFPs presented a broad range of acting pH 3.0 – 7.0 with optimal activity at pH 5.0 (Fig III.6C). In terms of temperature, *PcX2* was active at temperature ranges from 25 ^oC – 50 ^oC (Fig III.A), the maximum activity was observed at 45^oC and approximately 80% activity noticed at 25^oC. CFPs activity was optimum at 40 ^oC (Fig III.6B).

The culture filtrate proteins (CFPs) exhibited good thermostability in comparison to purified xylanase (*PcX2*) that was active for $t_{1/2}$ 463 minutes at 45 ^oC while (*PcX2*) was active for $t_{1/2}$ 66 minutes (Fig III.6D). Activities decreased about 50% after respective time. No activity

was observed from *PcX2* after 24 hours, though 15% relative activity was detected from CFPs after 48 hours of incubation.

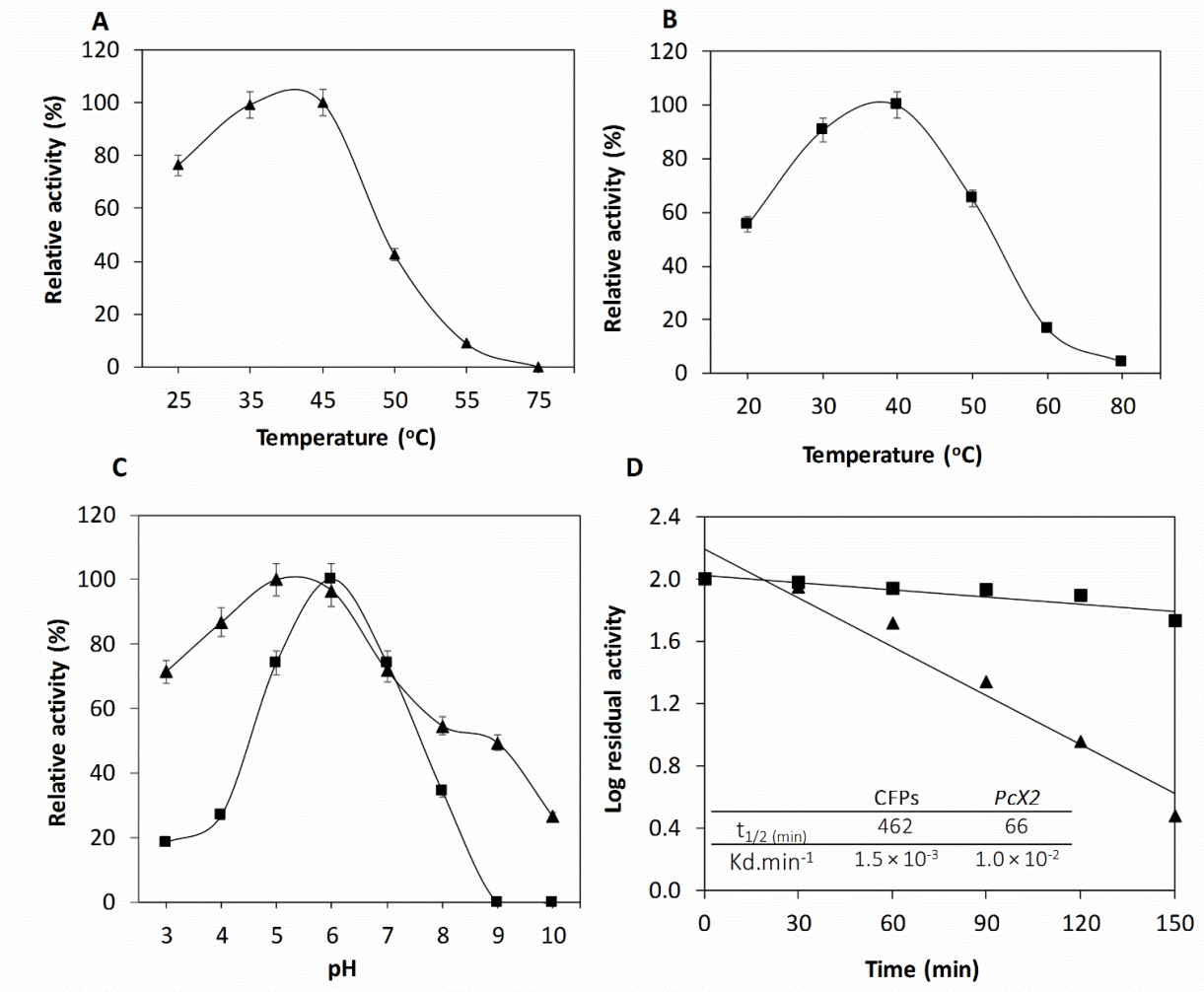

Figure III-6 Functional characterisation of *PcX2* (A) and CFPs (B) optimum temperature and pH (C) for the activity of *PcX2* (-▲-) and CFPs (-■-).Thermostability (D) of *PcX2* and CFPs (inset table showing the half life $t_{1/2}$ and energy of deactivation)

Influence of phenolic acids on the activity of both xylanases was examined. 4-hydroxybenzoic acid and vanillin resulted in strong inhibitors. Tannic acid caused no effect on the activity of both (crude and purified) xylanases. While ρ-coumaric acid strongly inhibited the activity of CFPs and *PcX2*, 40% activity of *PcX2* decreased (Fig III.7). *PcX2* kinetics showed the affinity towards oat spelt xylan having K_M value 0.537 mg.mL^{-1} and Vmax 0.21 U.mg^{-1}.

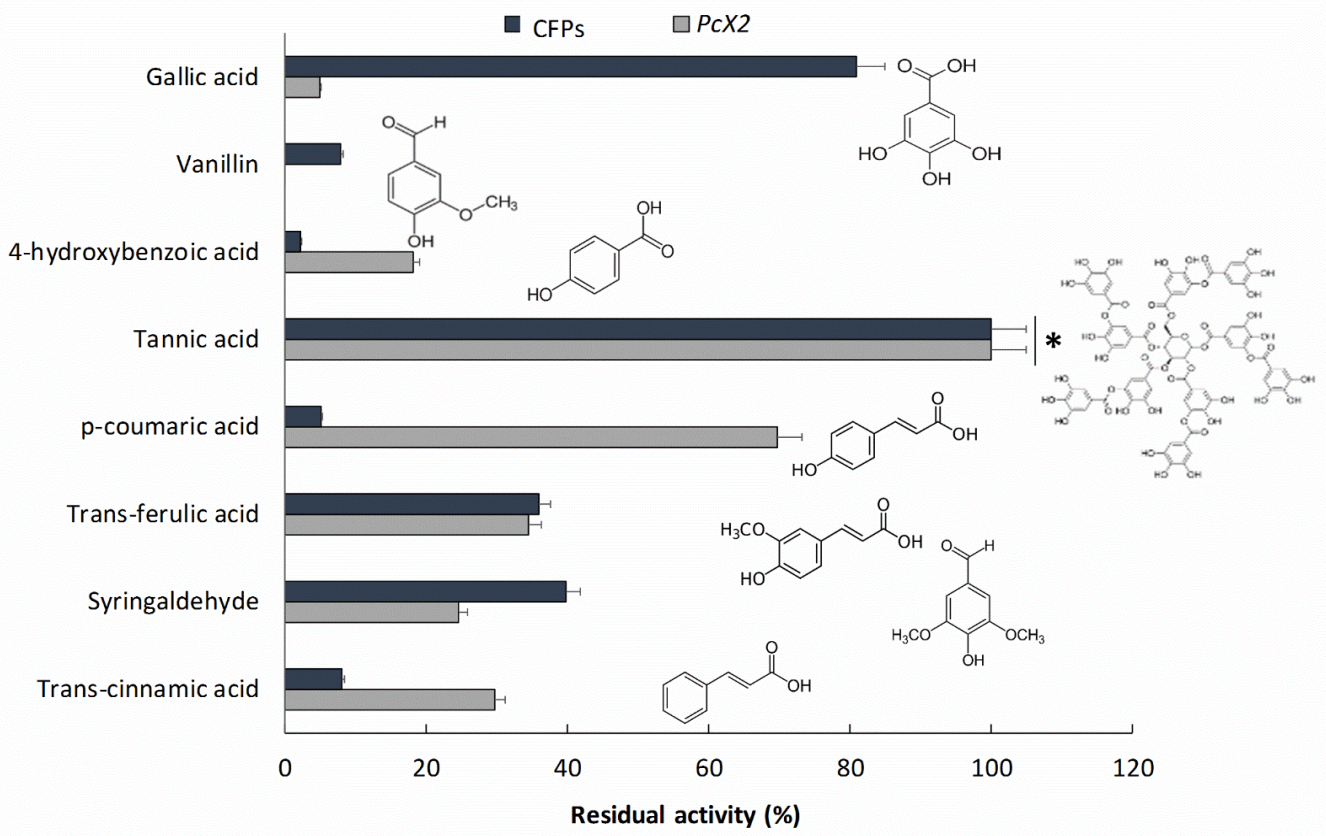

Figure III-7 Effect of lignin-derived phenolic compounds (1 mg) on the activity of *PcX2* and CFPs. Keeping the ratio 1:44 between *PcX2* and compound while 1: 20 between CFPs and compounds. Relative activity was compared from the control value (100%) prepared in the absence of phenolic acid. (* *indicates the values were not significantly different*)

Conformational analysis by fluorescence spectroscopy

The fluorescence emission was recorded at 300 – 400 nm in the pH range of 4.0 – 9.0. The emission fluorescence (λmax) values range from 327 to 329 nm. Maximum value λmax 329 was obtained for pH.7.0. At pH 5.5 the λmax 327 nm slightly blue-shifted (~1 nm) with respect to a native state that represents a minor change in the *PcX2* conformation (Fig III.8A).

The emission intensity observed at λmax 328nm remain constant over at pH range 4.0 to 5.5 and gradually decrease about 17% at pH 6.0 to 7.5, the maximum decrease in emission intensity was 67% at pH 9.0 (Fig III.8B). Decrease in the florescence intensity without any significant shift represents the ionization of any side group located close to tryptophan.

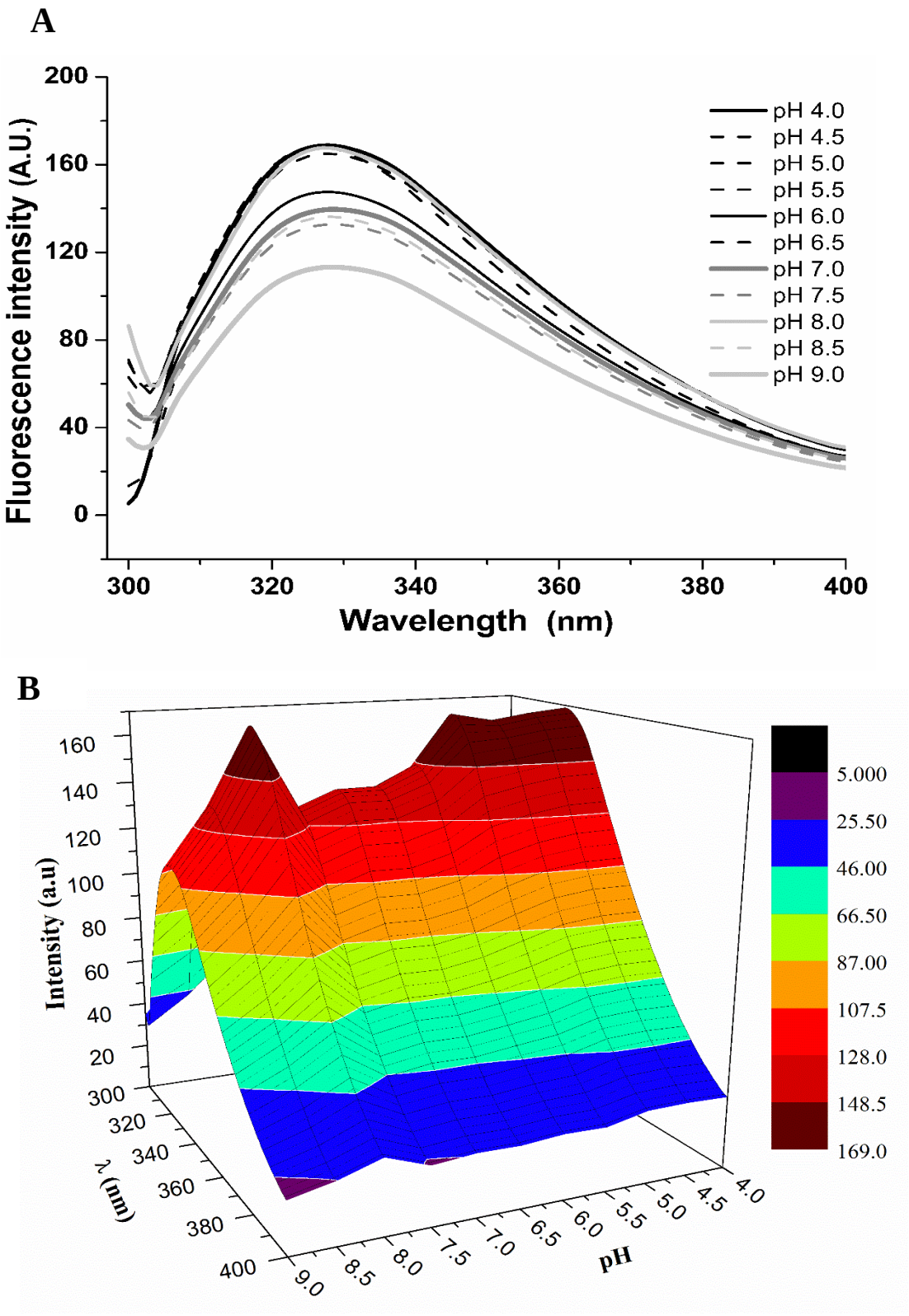

Figure III-8 Fluorescence spectra of *PcX2* (A) three-dimensional view of spectral projections (B) as a function of pH. Colour scale showing the range of fluorescence intensity, black (minimum) dark brown (maximum). Depression in the image indicating the intensity of tryptophan decreased in the pH range 6.0 – 8.0.

Discussion

P. chrysogenum strain CCDCA10746 isolated from soil in the central west of Brazil. The fungus was identified morphologically, for species identification ITS, β-tubulin and calmodulin were used as a molecular marker, that confirmed the strain CCDCA107476 belongs to *P. chrysogenum*. The fungus was screened for the production of cell wall degrading enzymes by using sugarcane bagasse as sole carbon source, with the specific interest of xylanase production. The culture filtrate of *P. chrysogenum* contained activities (Cellobiohydrolase, endoglucanase, mannanase, xylanase, and polygalacturonase) were monitored every day (Fig III.1).

Sugarcane bagasse constitutes a major proportion of cellulose and hemicellulose but lowers in pectin (GOMES et al., 2017). The activity yield can be correlated with the carbohydrate composition of sugarcane bagasse. Yield of pectinase was lower in comparison to other four activities, while xylanase and mannanase yield were higher in the culture filtrate that suggests the hemicellulose (xylan and mannan) barrier/ limits the cellulase accessibility to cellulose (KHATRI; MEDDEB-MOUELHI; BEAUREGARD, 2018). The delayed activity of cellobiohydrolase and endoglucanase further confirmed this argument. Similar production profile was noted for *P. echinulatum* and *P. janczewskii*, where the activities of cell wall degrading enzymes were carbon source dependent. The activity of xylanase was higher in the medium containing raw sugarcane bagasse on contrast the cellulase activity was higher in the medium containing pure cellulose as a carbon source (TERRASAN et al., 2010: CAMASSOLA; DILLON, 2012) On the other hand, CMCase activity of *Penicillium oxalicum* GZ-2 significantly increased when xylan was added to the cellulose medium. However, the culture containing xylan did not show any CMCase activity, that confirms the xylan was not inducing CMCase activity but it could be assumed, xylan or its derivative may act as regulatory factors that may enhance cellulase and hemicellulase expression or activity (LIAO et al., 2014). Complete hydrolysis of lignocellulose to fermentable sugars requires the consortium of cellulases (endo and exoglucanase, β-glucosidase), hemicellulases (β-xylosidases, endo-xylanases, and β-mannanases) to work in synergism. Sometimes enzyme mix contains accessory enzymes and proteins such as the lytic polysaccharide monooxygenases (GUPTA et al., 2016). The presence or addition of accessory enzymes that depolymerize pectin and cleave side chain substituents can enhance hydrolysis yield.

Culture filtrate containing holocellulases applied to hydrolyse the pre-treated sugarcane bagasse. After initial 3 hours of hydrolysis, 0.67 $mg.mL^{-1}$ of reducing sugars were

obtained, yield increased to 1.06 mg.mL^{-1} after 48 hours of hydrolysis. This amount considered significantly good by hypothetically comparing to the yield of *P. chrysogenum* P33 that release 1.30 mg of reducing sugars by using protein (secretome) concentration 4mg/g of the substrate (delignified corn stover) (YANG et al., 2018a). The hydrolysate contained three major (cellobiose, glucose, xylose) monomeric sugars. Hydrolysis yield (mg.mL^{-1}) of all three sugars was maximum after 24 hours of hydrolysis, converting 30% of glucan into glucose and 67% of xylan to xylose along with lower conversion 2% of glucan to cellobiose (Fig III-3). Presence of cellobiose in the hydrolysate indicates the possible presence of oligosaccharides (cellotetraose, cellopentaose), though were not analytically quantified. Cellobiose was not reported from *P. chrysogenum* P33 that account the liberation of xylose was 66% higher than the glucose during the hydrolysis of delignified corn stover containing 45% cellulose and 23% hemicellulose. While our results showed the xylose liberation was 44% higher than glucose, the difference could be due to the variation of lignocellulose content in the biomass (Table. III.2).

Table III-2 Chemical composition of Substrate (SILVA et al., 2019)

Sugarcane bagasse	Cellulose (%)	Hemicellulose (%)	Lignin (%)
Raw	43.46	22.43	24.41
Pre-treated	51.41	17.55	22.11

Our results indicate crude enzymes of *P. chrysogenum* could significantly be used with the commercial enzymes to enhance the hydrolysis yield as described in previous work (Yang et al., 2018). Where the liberation of reducing sugars increased to 75% by using commercial enzymes. Chemistry of enzymatic hydrolysis is described in Fig III.9. The extracellular proteins produced from *P. chrysogenum* were evaluated on the gel. A higher number of protein bands were obtained after 6 days of growth, the band's assembly interestingly associated with the enzyme production and the amount of protein content that as well increased after 6 days of growth. In comparison to the first five days, not only more protein bands but also the increased abundance of protein bands were observed. On the other hand, hemicellulose profile for the production of xylanase was analysed from the zymogram that has an advantage to the traditional colorimetric method, it not only measure enzymatic activity but also visualize the hydrolytic activity. As observed, in gel activity of three xylanases were consistence from 2 to 10 days of growth (Fig. III-2). Similar findings were quoted for the secretome of *P. chrysogenum* P33 produced three xylanases against complex (corn stover) biomass (YANG et al., 2018b).

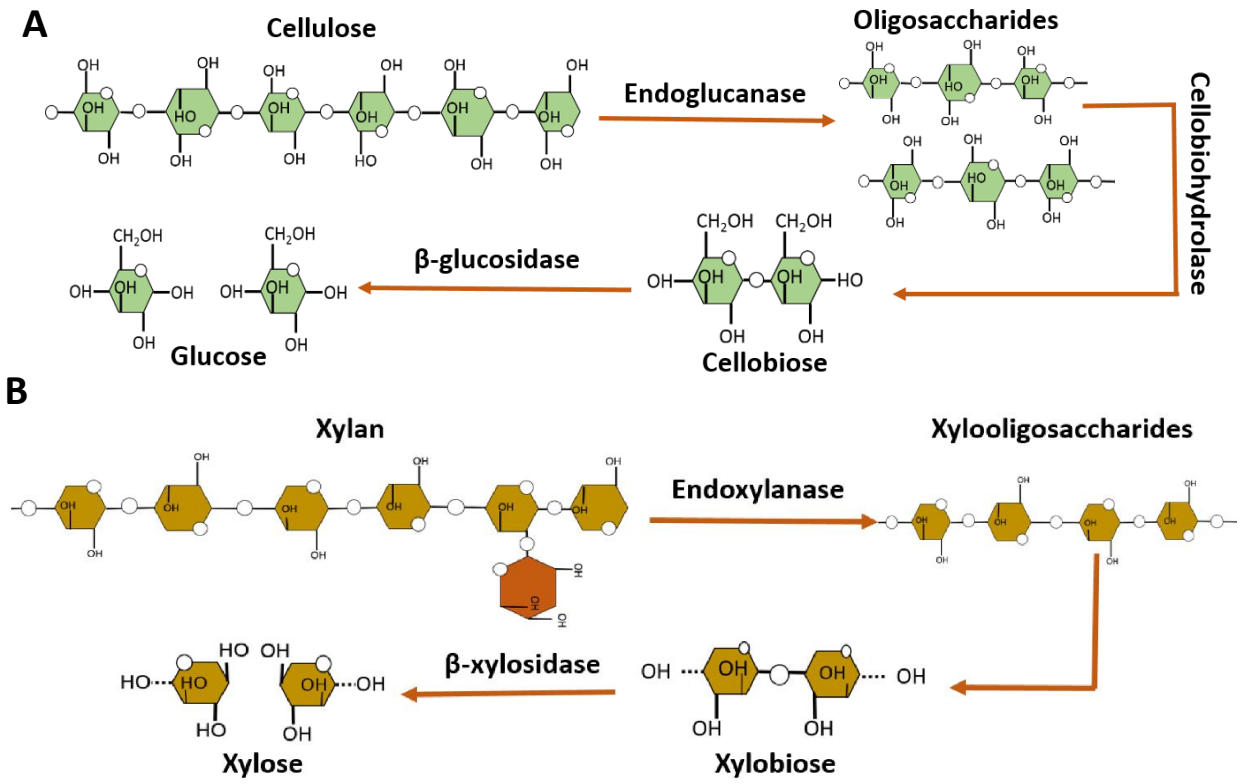

Figure III-9 Enzymatic hydrolysis of sugarcane bagasse. (A) Hydrolysis of cellulose (B) hydrolysis of hemicellulose

The specific xylanase activity determines by enzyme assay was higher on the 4th day of growth consider for enzyme purification. The homogenised band was confirmed on a gel and excised for the identification of peptides. The nucleotide sequence of *PcX2* is 706bp long that encodes 216-amino acid residues, the presence of signal peptide at N-terminal suggests the extracellular secretion. The amino acid sequence of *PcX2* shares 100% similarity with xylanase of the fully sequenced genome of *P .rubens*, 94% and 85% similarity shared with the xylanases of *P. nalgiovense* and *P. polonicum*, respectively.

The molecular size of protein was estimated 23 kDa that is close to previously identified xylanases from *Penicillium herquei*, *Penicillium purpurogenum* and *Penicillium glabrum* (FUNAGUMA et al., 1991: BELANCIC et al., 1995; KNOB et al., 2013). Although having a similar molecular mass, the biochemical characteristics of these enzymes are different from *PcX2*, all three xylanases are acidic and showing the optimum activity at pH 3.0. On the other hand, *PcX2* has optimum activity at pH 6.0 and retained 75% activity at pH 5.0 and 7.0. The temperature optima for *P. herquei* and *P. purpurogenum* xylanase was 50 ^{o}C while the *P. glabrum* activity was optimum at 60 ^{o}C, contrary to all three xylanases *PcX2* activity was optimum at 45 ^{o}C. In terms of thermostability, after incubation at 45 ^{o}C for an hour, the activity

of *PcX2* decrease to 50%, that is considered stable in comparison to *P.oxalicum* xylanases (xyn10A, xyn11A and xyn11B), where the activity of all three xylanases was decreased to 80% after 30 mintues of incubation (LIAO et al., 2015).

In the presence of 1mM inorganic salts (K^{+}, Mg^{+2}, Zn^{+2}) the activity of *PcX2* increased, similar behaviour was noticed by *P.herquei* and *P.oxalicum* GZ-2 xylanase (Xyn11A), while the activity from *P.glabrum* xylanase was not affected by such salts. The low concentration (1 mM) of trivalent ion (Fe^{3+}) doubled the activity of *PcX2*. Contrary to the activity of *P. oxlicum* that was strongly inhibited in the presence of Fe^{3+}. Inorganic salts possibly bind to the ionic side chains of a protein. Such interactions, although not affect the three-dimensional structure of enzyme but presence of divalent or metal ion make it easier for a substrate molecule to locate or bind to the active site of the enzyme (VAAJE - KOLSTAD, 2011). Thus, the presence of the ion in optimum concentrations could change the rate of the reaction. In the case of Cu^{+2} ion, the activity of *PcX2* was inhibited; such inhibitions were also observed from the xylanases of *P. janczewskii* and *P. oxalicum.* Previously, the interaction of Cu^{+2} ion with commercial xylanase was analysed, Cu^{+2} ion formed a complex (xylanase-Cu^{+2}) with the catalytic residues of xylanase that caused structural change and ultimately affect the activity (ZHANG et al., 2017).

PcX2 activity was deactivated by vanillin, 4-hydroxybenzoic acid and strongly inhibited by gallic acid. While 70% inhibition was caused by trans-ferulic acid, syringaldehyde and trans-cinnamic acid and ρ-coumaric acid caused only 30% inhibition, no effect on activity was observed by tannic acid. Similar deactivation of xylanase was previously described for vanillin. Some phenolic such as ferulic acid and ρ-coumaric acid were reported to covalently interact with the protein (TIAN; JIANG; OU, 2013). The interaction changes the protein conformation that results in either increase or decrease of enzyme activity. Another scenario of deactivation mechanism could be the competitive or non-competitive interaction of phenolic with the aromatic or catalystic residues of protein (BOUKARI et al., 2011).

The aromatic residues of protein molecule have long been used as an intrinsic fluorophore to study the conformational changes in the protein, specifically the tryptophan indole double ring that has a dual physical nature. On one hand, it has a great hydrophobic van-der-Waals surface area and on the other, it possessed a polar NH-group. Changes in the tryptophan emission band can occur in response to protein conformational changes, protein-protein association, ligand binding, and denaturation (ULLAH et al., 2019). Burstein and co-workers proposed a model postulates the coexistence in the protein of three classes of tryptophan residues that have distinct fluorescent value emanating from the discrete local environment: Class A (λmax 308nm) Trp

buried no exciplexes. Class S (λmax 316nm) Trp buried but form exciplexes 1:1 stoichiometry. Class I (λmax 331nm) Trp buried but form 2:1 exciplex in the interior. Class II (λman 340-342nm) on surface Trp in contact with water and Class III (λmanx 340nm – 353nm) fully exposed Trp in contact with mobile water (RESHETNYAK; BURSTEIN, 2001). By assuming this scheme, *PcX2* results presented the side chains of tryptophan were buried in the non-polar environment; by varying the pH, the orientation of tryptophan has slightly changed but not exposed to the surface or unfolded.

GH11 xylanase possessed jelly roll structure that contains 95% β-sheet, considered a more rigid unit than α-helix. Rigidity affects the activity of enzyme due to low conformation changes and poor adaptability to pH change (PAËS; BERRIN; BEAUGRAND, 2012; PERTICAROLI et al., 2013). The protein primary structure contained 7-tryptophan residues, the emission intensity of Trp showed the enfolding (buried) of all Trp in the interior of protein (apolar environment) possibly contribute to the stability of the protein. This decreased /increased in the emission intensity with the change of the solvent polarity is likely due to the ionization of side chains, located in the proximity of tryptophan or catalytic residue. For instance, the side group of histidine ionized at pH 6.0 (Appendix). Sequence alignment of *PcX2* revealed the presence of four histidine residues and H155 on α-helix is present close to W159, both residues are present at the same position in *Penicillium funiculosum* (Uniprot: Q9HFH0; PDB: ITE1) sharing 63% sequence identity with *PcX2*.

This study concludes the *P. chrysogenum* secrete holocellulases (cellobiohydrolase, endoglucanase, mannanase, xylanase) active towards sugarcane bagasse. These activities were used to hydrolyse the pre-treated sugarcane bagasse and the release of monomeric sugars (G1, G2 and X1) signify its potential for the biofuel industry. The release of Cellobiose (G2) confirms the presence of β-glucosidase. *PcX2* was resistant to five (tannic acid, trans-ferulic acid, trans-cinnamic acid, ρ-coumaric acid, syringaldehyde) to phenolic acids while CFPs was resistance to syringaldehyde, ferulic, tannic and gallic acid. The culture filtrate proteins (CFPs) of *P. chrysogenum* were thermostable and have a broad range of acting pH (3.0 to 9.0) and temperature (25 ^{o}C – 50 ^{o}C). While purified xylanase was structurally stable in different pH and showed thermostability in the wide range of temperature (25 ^{o}C – 50 ^{o}C), suitable for textile and food industries. Hydrolytic properties could further be improved by the increase of enzyme load or the addition of commercial enzymes. The findings provide the ground to design and development the enzymes using the green route for biotechnological applications.

Chapter IV : Probing the enzyme-phenolic interaction using kinetic and fluorescence spectroscopic approach

Introduction

The environmental and economic concern is gaining attention, linked to Man's dependency on fossil fuels. This attention deriving the force to explore an alternative source, such as; biofuels or use of plant biomass as carbon source or feedstock. To achieve this objective, the development of cost-effective methods are necessary. Methods that allow the production of bioethanol from sugars liberated from cellulose and hemicellulose along with the substantial conversion of lignin and hemicellulose into value-added products(CARDONA; SÁNCHEZ, 2007). Today the conversion of biomass into ethanol stands on the basic concept of enzymatic hydrolysis, biomass pre-treatment and fermentation (CANILHA et al., 2012). Enzyme technology employing the mixture of enzymes (cocktail) contained all the essential activities of cellulases (endoglucanases, cellobiohydrolases, glucosidases), hemicellulases (mainly endoxylanases) and lignin-degrading enzymes required for the degradation of biomass (SILVA, 2018).

Complex structure and presence of lignin or phenolic acids in the plant cell wall, recalcitrant the degradation of biomass, which introduced the concept of pre-treatment (DE OLIVEIRA et al., 2018). However, the concept is indispensable and increases the accessibility of cellulose to enzymes but the process of pre-treatment often modified the native structure of lignin. This change resulted in undesirable demethylation, generation of exposed/free phenolic moieties, the formation of soluble by-products (furfural and aromatics) and generation of phenolic oligomers (tannin, ferulic and ρ-coumaric acid) (XIMENES et al., 2010).

The effects of phenolic compounds on the activity of glycoside hydrolases have been largely discussed. SHARMA et al., (1985) reported the inhibition of crude xylanase from *Aspergillus japonicus* in the presence of vanillin and ρ-coumaric acid. Contrary, KAYA et al., (2000) reported the positive activation effect of vanillin and guaiacol on the activity of commercial xylanase, increased the rate of hydrolysis of xylan. XIMENES et al., (2010) found the effect of 4-hydroxy benzoic acid was more severe on β-glucosidase from *T. reesei* than β-glucosidase from *A. niger*. SILVA et al., (2019) described the effect of phenolic compounds on *P. chrysogenum* enzymes was concentration dependent, more than half of activity reduced at

higher concentration, interestingly low concentration increased the activity. In another study, purified xylanase of *P. chrysogenum* was resistant to tannic and gallic acid (ULLAH et al., 2019).

Regardless, few works proposed that phenolic hydroxyl groups might interact with the proteins through non-covalent interaction, an important element in the inhibition potency of lignin-derived aromatics towards enzymes (BOUKARI et al., 2011), these details are incomprehensive to understand the inhibition or interaction mechanism between enzyme and phenolics. Therefore, accession of new information is prerequisite in enzyme technology for the optimisation of biorefining processes.

In the present study, the mechanism of inhibition GH10 and GH11 endo-β-1,4-xylanases from *Penicillium chrysogenum* by phenolic acids (ferulic and cinnamic acids) has been probed. Kinetic analyses and fluorescence spectrophotometric study provide a comprehensive insight into the interactions between the xylanases and phenolic acids. Results procure from this study advanced the understanding of how hemicellulases might be inhibited in biorefining processes by lignin degradation products.

Methodology

Effects of Phenolic acids on the activity of xylanase

Enzyme samples *PcX1* 0.038 $mg.mL^{-1}$ (~ 1.1 µM) and *PcX2* 0.025 $mg.mL^{-1}$ (~1.1 µM) were prepared in sodium acetate buffer (0.1 M, pH 5.0). In the eppendorf different concentrations 0.2 – 1.0 $mg.mL^{-1}$ of transferulic (1.0 – 5.0 mM) and transcinnamic acid (1.3 – 6.7 mM) were prepared and pre-incubated with enzymes. *PcX1* at 30 °C and *PcX2* was incubated at 45 °C for 10 minutes.

Activity assay

Oat spelt xylan (2%, 0.1M, pH 5.0) was added into each eppendorf and incubated at 30 °C (*PcX1*) and 45 °C (*PcX2*) for 30 minutes. After a respective time, eppendorf were kept in boiling water for 10 minutes to inactivate the enzyme, and then cooled on ice and centrifuged at 8000g for 10 minutes. The reducing sugars in the supernatant were determined at A_{540} using the DNS method.

Inhibition kinetics

Inhibition kinetics was determined by varying the oat spelt substrate concentration 0.8, 1.6, 2.4, 3.2 and 4.0 $mg.mL^{-1}$ in two different concentrations minimum 0.2 mg (tCA 1.3 mM and

tFA 1.0 mM) and maximum 0.8 mg (tCA 5.4 mM and tFA 4.0 mM) phenolic acid (TIAN; JIANG; OU, 2013). The assay was performed by interacting the xylanase with each phenolic acid for 10 minutes prior to addition of substrate. To check the activity standard activity assay was followed as mentioned above.

Effect on thermostability

Thermostability of both xylanases in the absence and presence of phenolic acids (0.2 mg) was determined by incubating the enzymes at optimum temperatures (*PcX1* at 30 ^{o}C and *PcX2* at 45 ^{o}C) with phenolics for 150 minutes. Aliquots were collected after every 30 minutes and activity was tested by using the substrate xylan oat spelt.

Analysis of enzyme–phenolic acid compound interactions using fluorescence spectrophotometry

Effect of Phenolic concentrations on PcX1

Fluorescence analysis was performed on *PcX1* 50 µg.mL^{-1} (~1.37 µM) with different (0 – 0.67 mM) concentrations of the transcinnamic acid and (0 – 1.7 mM) of transferulic acid (WU et al., 2017).

Effect of Phenolic concentrations on PcX2

Fluorescence analysis was performed on *PcX2* 53 µg.mL^{-1} (~2.3 µM) with (0 – 0.67 mM) concentrations of the transcinnamic acid and (0 – 0.036 mM) of transferulic acid.

Fluorescence assay

The absorption spectroscopy of *PcX1* and *PcX2* was performed at 25 ^{o}C. The fluorescence measurements were performed at pH (5.0, sodium acetate buffer; 1mM) using a Jasco FP-6500 spectrofluorimeter (Jasco, Tokio, Japan) coupled to a Peltier system with water circulation. The excitation and the emission slits were set to 5.0 nm. The tryptophan excitation wavelength was fitted at 295 nm and emission collected at 300 – 400 nm (DE SOUZA MOREIRA et al., 2015). The averages of fluorescence spectra were recorded and processed by the program "Spectra Manager" (Jasco, Tokyo, Japan). The binding constants (K_b) for *PcX1* and *PcX2* with increased concentration (titaration) of two phenolic compounds were calculated according to Equation 1.

$$log\ (F_0 - F/F) = log\ K_b + n\ log[Q] \qquad \text{(Equation 1)}$$

where F and F_0 are the fluorescence intensities in the presence and absence of quencher, respectively, K_b is the binding constant and n is the number of binding sites per xylanase and Q is the concentration of the quencher (OJHA et al., 2012)

Results and Discussion

Effect of phenolic concentration on the activity of xylanase

The activity of xylanase decrease in the presence of phenolic acids (transcinnamic acid and transferulic acid). The inhibitory effect on *PcX1* was strong in comparison to *PcX2* (Fig. IV.1).

Effect of transferulic acid on the activity of xylanase

In the presence of 0.4 mg of transferulic acid (tFA), *PcX1* retained 75% activity. While activity reduced to 35% and 25 % at concentration 0.6 and 0.8 mg, respectively (Fig IV.1A). On another hand, *PcX2* retained approximately 58% activity at maximum concentration of 1.0 mg of transferulic acid. Whereas, only 23% activity was inhibited in the presence of 0.6 mg (IV.1B).

Ratio	*PcX1*	
Enzyme: Phenolic	tFA	tCA
1: 5	103±0.05	78±0.02
1: 11	75±0.12	75±0.05
1: 18	35±0.02	70±0.07
1: 24	26±0.01	40±0.02
1: 31	19±0.02	20±0.02

Ratio	*PcX2*	
Enzyme: Phenolic	tFA	tCA
1: 8	102±0.04	100±0.04
1: 16	103±0.03	84±0.17
1: 24	78±0.05	77±0.15
1: 32	68±0.02	54±0.02
1: 40	58±0.05	51±0.01

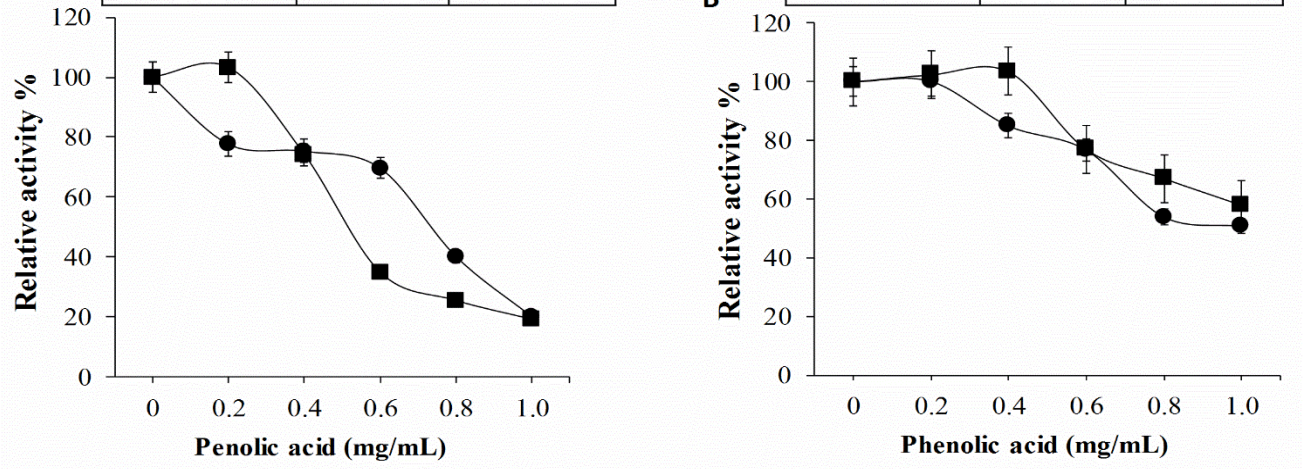

Figure IV-1 Effect of transferulic acid (–■–) and transcinnamic acid (–●–) on the activity of *PcX1* (A) and *PcX2* (B). Inset table is showing the ratio between enzyme (constant concentration) and phenolic acid (varying concentration).

Effect of transcinnamic acid on the activity of xylanase

PcX1 retained 70% activity at concentration of 0.6 mg of transcinnamic acid (tCA), but maximum concentration 1 mg caused 80% inhibition. Similarly, *PcX2* retained 77% activity at concentration of 0.6 mg. Contrarily to *PcX1; PcX2* retained 50% activity at maximum concentration 1.0 mg concentration of transcinnamic acid (IV.1B).

Effect of Phenolic acids on thermostability

Transferulic and transcinnmaic acid at 0.2 mg effected (decreased) the thermal stability of *PcX1*. The decrease in activity caused by transcinnmaic acid was far greater than ferulic acid, 78% and 45% of inhibition after incubation for 150 minutes, respectively.

On the other hand, thermostability of *PcX2* increased after the interaction of tFA, 76% activity retained after 150 minutes of incubation. Transcinnamic acid as well not considerably effect the thermostability in comparison to control. In fact, the half-life time of *PcX2* increased from 91miuntes to 114 minutes and 289 minutes, in the presence of tCA and tFA, respectively (Table IV.1).

Table IV-1 Half-life and thermal deactivation (Kd) constant in the presence of phenolic acids concentration transcinnmaic acid (1.3 mM) transferulic acid (1mM). Control was assayed in the absence of phenolic acids.

Xylanase	**Transcinnamic acid**		**Transferulic acid**		**Control**	
	$t_{1/2}$ (min^{-1})	$Kd.min^{-1}$	$t_{1/2}$ (min^{-1})	$Kd.min^{-1}$	$t_{1/2}$ (min^{-1})	$Kd.min^{-1}$
PcX1	63	1.1×10^{-2}	144	4.8×10^{-3}	408	1.7×10^{-3}
PcX2	114	6.1×10^{-3}	289	2.4×10^{-3}	91	7.6×10^{-3}

Inhibition kinetics

Inhibition kinetics of PcX1

Inhibition kinetics determine under varying concentration (0.8 mg – 4.0 $mg.mL^{-1}$) of oat spelt xylan. The K_M value of *PcX1* was increased after the addition of transferulic acid while the Vmax not obviously effected.

In the presence of 1.3 mM (0.2 mg) transcinnmaic acid the value of K_M and Vmax increased, and both values decrease at higher concentration 5.3 mM (0.8 mg) indicated the tCA

increase the affinity between enzyme and substrate but not favour the product formation. The values of catalytic efficiency (Kcat/K_M) were decrease in comparison to control (Table IV.2).

Table IV-2 Phenolic acid inhibition kinetics of *PcX1*. Control was assayed in the absence of phenolic acids (volume was adjusted with assayed buffer).

35kDa/GH10	**Transcinnamic acid**		**Transferulic acid**		**Control**
	1.3 mM	5.4 mM	1.0 mM	4.0 mM	
Xylan mg.mL^{-1}	Rate (mg/mL.min^{-1})				
0.8	0.0093	0.0060	0.0127	0.0114	0.0090
1.6	0.0175	0.0121	0.0236	0.0194	0.0246
2.4	0.0220	0.0128	0.0352	0.0296	0.0294
3.2	0.0259	0.0139	0.0384	0.0326	0.0305
4.0	0.0288	0.0168	0.0402	0.0330	0.0337
Kinetics Parameters					
K_M (mg.mL^{-1})	3.20	2.21	3.35	3.40	2.73
Vmax (mg.mL.min^{-1})	0.05	0.02	0.07	0.06	0.06
Kcat (S^{-1})	20.0	5.7	20.2	20.0	20.0
Kcat/K_M (S^{-1}.mg^{-1})	6.25	2.60	6.0	5.85	7.3
R2	0.93	0.91	0.97	0.92	0.97

Inhibition kinetics of PcX2

In case of, *PcX2* the values of K_M and Vmax decreased in the presence of phenolic acids (Table IV.3). These results represent the transferulic (tFA) and transcinnamic acids (tCA) are noncompetitive inhibitors of *PcX2.*

Table IV-3 Phenolic acid inhibition kinetics of *PcX2.* Control was assayed in the absence of phenolic acids (volume was adjusted with assayed buffer).

23kDa/GH11	**Transcinnamic acid**		**Transferulic acid**		**Control**
	1.3 mM	5.4 mM	1.0 mM	4.0 mM	
Xylan mg.mL^{-1}	Rate (mg/mL.min^{-1})				
0.8	0.0044	0.0029	0.0075	0.0067	0.0076
1.6	0.0073	0.0039	0.0080	0.0158	0.0113
2.4	0.0082	0.0076	0.0138	0.0181	0.0133
3.2	0.0102	0.0067	0.0129	0.0204	0.0190

4.0	0.0101	0.0068	0.0119	0.0227	0.0178
Kinetics Parameters					
K_M (mg.mL^{-1})	2.24	2.18	0.92	2.43	2.71
Vmax (mg.mL.min^{-1})	0.016	0.011	0.016	0.036	0.033
Kcat (S^{-1})	6.32	4.30	6.07	14.65	12.28
Kcat/K_M (S^{-1}.mg^{-1})	2.87	2.00	6.74	5.87	4.69
R2	0.98	0.77	0.75	0.98	0.92

Effect of Phenolic acids on the structure of *PcX1* (GH10) and *PcX2* (GH11)

Effect of Transcinnmaic acid

To understand the binding of phenolic acids to *PcX1* and *PcX2* fluorescence spectroscopy was used. The sensitivity of tryptophan indole ring to its microenvironment makes it an ideal choice for studying the protein conformation changes and to analyse the interactions with other molecules. The excitation and emission were set at 295nm and 300 – 400 nm, respectively. The fluorescence emission of the tryptophan was detectable for both xylanases in the presence of transcinnmaic acid.

In case of *PcX1*, the emission maximum was quenched and red shifted from 328 nm to 338 nm (of 10 nm) at the concentration of 0.02 mM, another red shift observed from 338 to 340 nm in the presence of 0.40 mM concentration (Fig IV.2A).

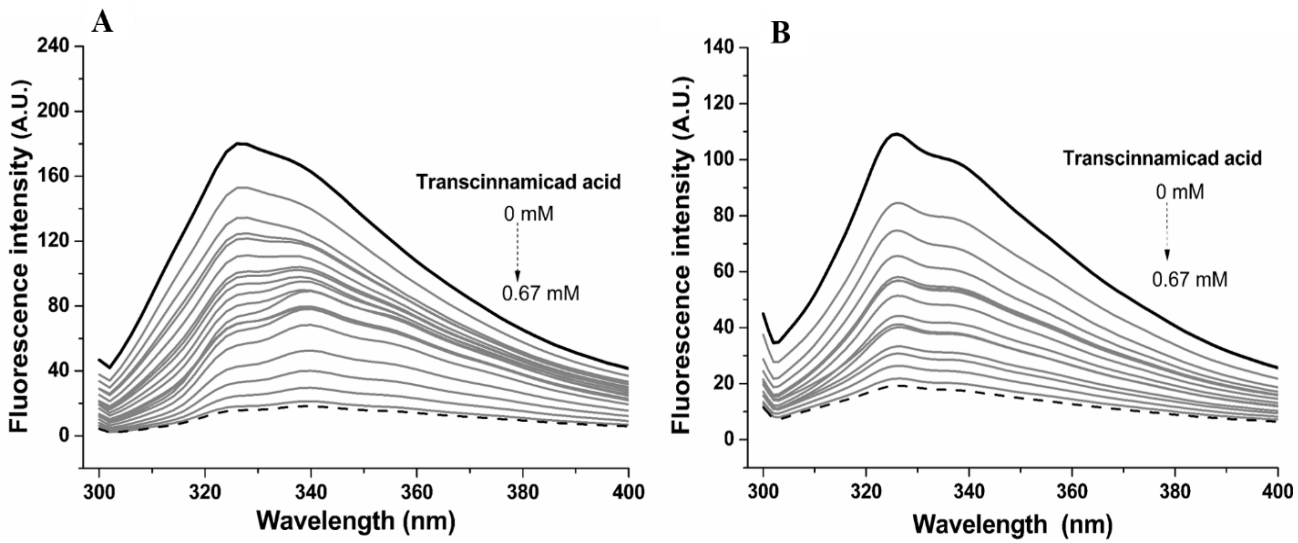

Figure IV-2 Fluorescence emission spectra of (A) *PcX1* (1.9 µM) and (B) *PcX2* (2.3 µM) in the absence and the presence of increasing amounts (from 3.7×10^{-5} to 6.7×10^{-4} M) for *PcX1* and

for *PcX2* (from 8.4×10^{-5} to 6.7×10^{-4} M) of transcinnamic acid in 1mM sodium acetate buffer, pH 5.0. The excitation wavelength was 295 nm.

No further shift was noticed above this concentration, while emission intensity quenched constantly with the increased concentration. Although, the emission maximum for *PcX2* was constant at 326 nm in the concentration ranges from 0.08 mM to 0.67 mM of transcinnmaic acid, and fluorescence intensity quenched by increasing the concentration. Maximum quenching was obtained at 0.67 mM concentrating (Fig IV.2B).

The results obtained from the attenuation of fluorescence emission assay for enzymes *PcX1* and *PcX2* in the presence of transcinnamic acid showed that there was a reduction in the emission for both enzymes correlate with the increasing concentration (titration) of inhibitor (Fig IV-2). However, *PcX1* showed displacement of tryptophan emission band to a polar environment, exposing the Trp residues to the solvent. The binding constant, as well as the number of inhibitor binding sites, were calculated for the enzymes at pH 5.0 at 25 °C. The value of Kb determined for *PcX1* was higher than that calculated for *PcX2*, on the 10-folds scale, showing that *PcX1* shows a higher affinity for this phenolic compound (Fig IV-3 and Table IV-4).

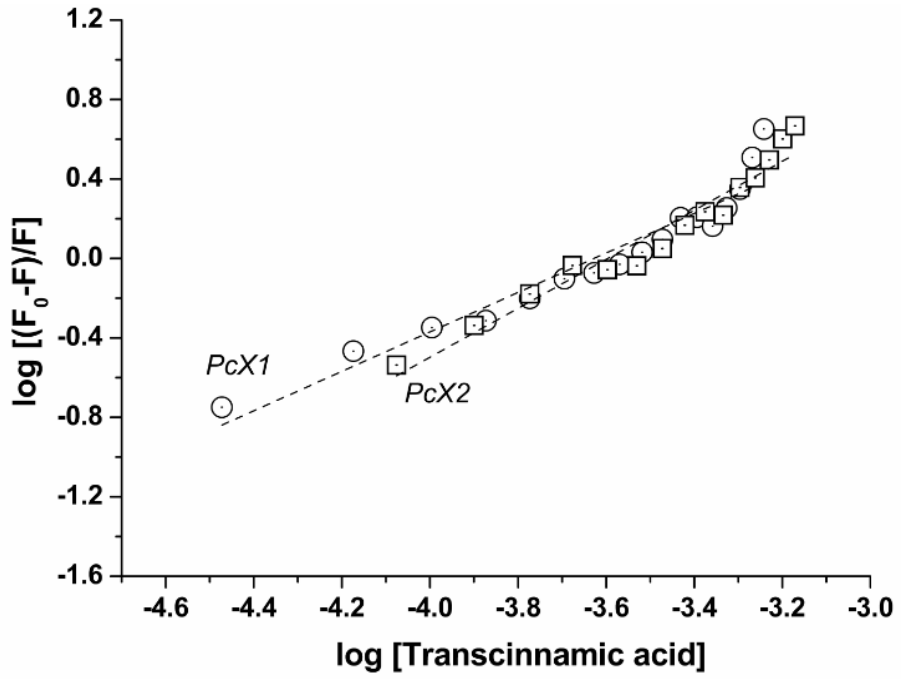

Figure IV-3 Plots of Log (F_0-F/F) vs. Log [Transcinnamic acid] in pH 5.0 at 25 ºC. *PcX1* (circle) and *PcX2* (square) in the presence of increased concentration of the transcinnamic (from 0 at 6.7×10^{-4} M).

The value of n showed that both enzymes have a single site of interaction with this inhibitor (Table IV-4). The results may be associated with biochemical inhibition assays, which showed that *PcX1* activity (80%) inhibited by transcinnamic acid when compared to *PcX2* activity (49%).

Table IV-4 Binding constants (K_b) values and number of sites (n) per molecule of *PcX1* and *PcX2* for transcinnamic acid in pH 5.0 at 25ºC.

	Transcinnamic acid		
	K_b x 10^4 (M^{-1})	*n*	R^2
PcX1	0.40 ± 0.04	0.99	0.96
PcX2	0.03 ± 0.01	1.23	0.97

Effect of Transferulic acid

The emission intensity of both xylanases was quenched in the presence of transferulic acid. In case of *PcX1*, emission intensity was constant at 338 nm at the concentration 0.101 mM to 0.094 mM of transferulic acid, by increasing the concentration at 0.102 mM emission maximum slightly red shift to 340 nm (Fig IV.4A). When analysed the *PcX2*, emission maximum observed at 326 nm for the concentration of 0.010 and 0.016 mM of transferulic acid. As the concentration further increased, an isosbestic point was notice and emission maximum was shifted to 400 nm (Fig IV.4B).

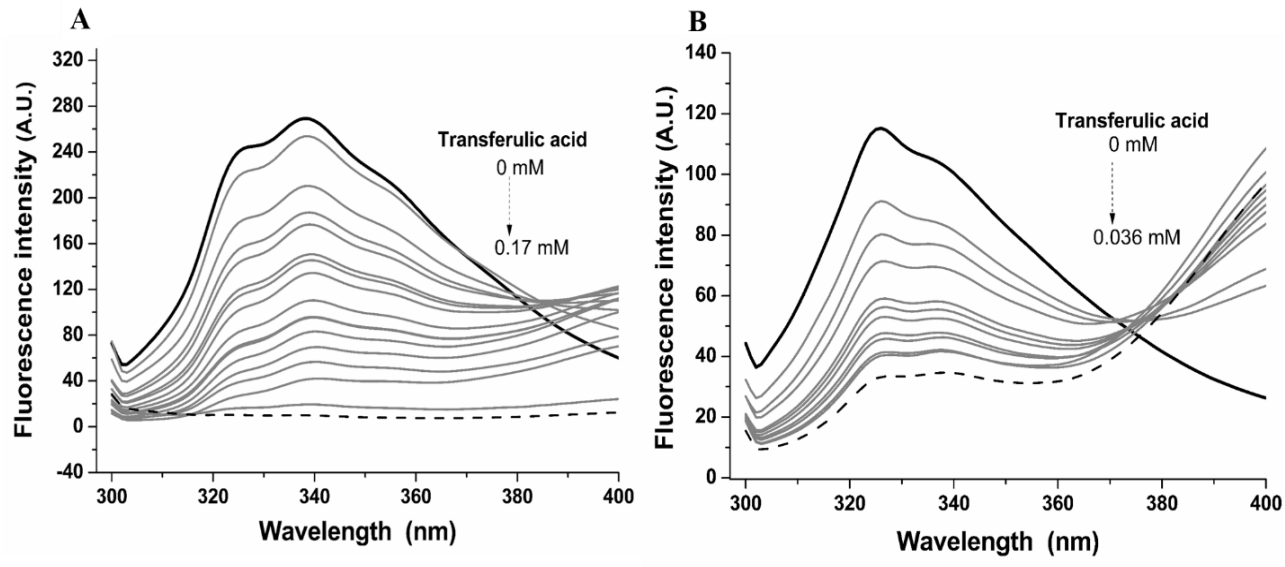

Figure IV-4 Fluorescence emission spectra of (A) *PcX1* (2.9×10^{-6} M) and (B) *PcX2* (3.5×10^{-6} M) in the absence and the presence of increasing amounts (from 1.7×10^{-5} to 1.7×10^{-4} M) of

transferulic acid for *PcX1* and (from 1.0×10^{-5} to 3.6×10^{-5} M) for *PcX2* in 1mM sodium acetate buffer, pH 5.0. The excitation wavelength was 295 nm.

The results obtained from the attenuation of fluorescence emission assay for enzymes *PcX1* and *PcX2* in the presence of transferulic acid showed that there was a reduction in emission intensity for both enzymes, with the increasing concentration of ferulic acid (Fig. IV-4). However, *PcX1* showed displacement in the tryptophan emission band to a more hydrophilic environment (340 nm), exposing the tryptophan residue to the solvent.

The binding constant, as well as the number of inhibitor binding sites, were calculated for the enzymes at pH 5.0 at 25 °C. The value of Kb determined for *PcX1* was lower than that calculated for *PcX2*, on a 10-fold scale, showing that *PcX2* has a higher affinity for transferulic acid (Fig IV-5 and Table IV-4).

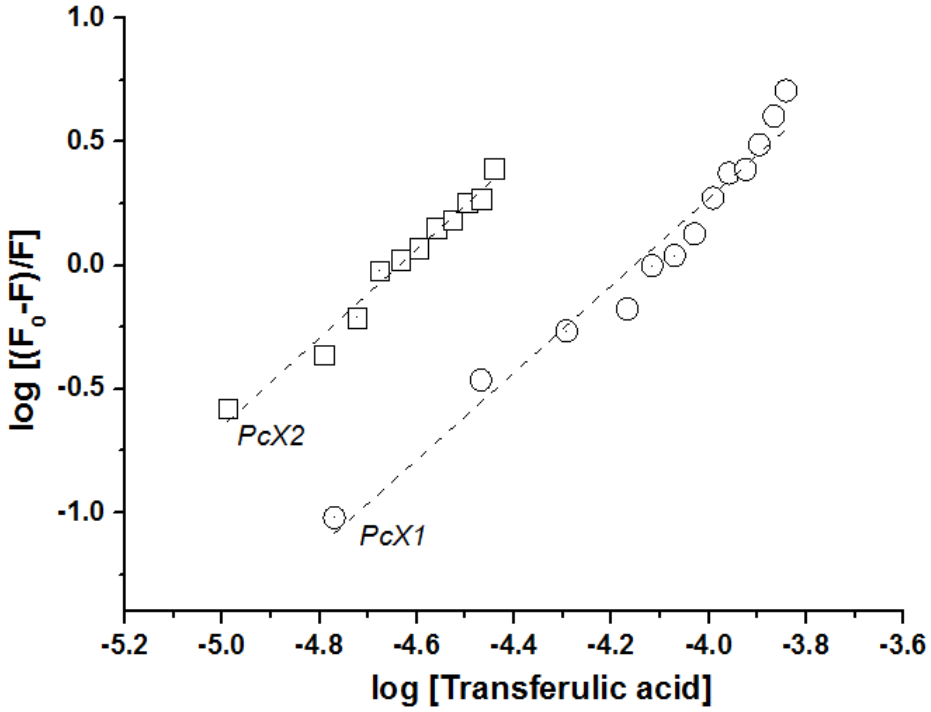

Figure IV-5 The plots of Log (F_0-F/F) vs. Log [Transferulic acid] in pH 5.0 at 25 ^{o}C. *PcX1* (circle) and *PcX2* (square) in presence of increase concentration of the transferulic at *PcX1* (from 0 to 1.7×10^{-4} M) and *PcX2* (from 0 to 3.6×10^{-5} M).

Results from the inhibition assay for *PcX2* showed that a noncompetitive inhibition occurred, suggesting that the complex formed between *PcX2*-tFA can happen at more than one binding site, and not only at the active site of the enzyme. The value obtained for n showed that both enzymes may present more than one site of interaction for this phenolic compound, which may be associated with the results obtained in the biochemical inhibition assays for *PcX2* (Table

IV-5). The initial binding of tFA at high affinity binding site influence the further binding and the phenolic compound bind at low affinity site.

Table IV-5 Binding constants (*Kb*) values and number of sites (n) per molecule of *PcX1* and *PcX2* for transferulic acid in pH 5.0 at 25^{o}C.

	Transferulic acid		
	K_b x 10^8 (M^{-1})	***n***	**R^2**
PcX1	0.20 ± 0.01	1.76	0.98
PcX2	2.03 ± 0.04	1.79	0.98

The activity of both xylanases was influenced by increasing the concentration of transcinnamic and transferulic acid. The concentration 0.2 was not inhibitory for both xylanases, in fact, the activity of *PcX1* and *PcX2* increased (2%) in the presence of 0.2 mg transferulic acid. *PcX1* activity enhancement was attained only in the presence of 0.2 mg of ferulic aid, 20% activity inhibited at the same concentration of transcinnmaic acid. Activity reduction was 65% in the concentration of 0.6 mg of transferulic acid, contrary, the reduction was 30% when the same concentration of transcinnmaic was applied. Thermostability was also decreased in the presence of both phenolic acids.

By comparing the overall inhibition of both xylanases, *PcX2* showed more tolerance towards phenolic acids by retaining more than 50% activity at a maximum concentration of 1.0 mg.mL^{-1}. On the other hand, the activity of *PcX1* reduced about 80 % at 1.0 mg.mL^{-1} concentration of phenolic acids. As observed for activity, the thermostability of *PcX2*, as well, increased with the addition of phenolic acids at concentration 0.2 mg. The half-life of *PcX2* was almost doubled when the enzyme was incubated with tFA, and in the presence of tCA, the half-life time extended from 91 to 114 minutes, (Thermostability increased 24minutes). Increased in the thermostability was reported for the BSA upon binding of ferulic acid (OJHA et al., 2012).

In terms of inhibition kinetics, the K_M values of *PcX1* increased by the addition of 1.0 mM or 4.0 mM of transferulic acid and the values of Vmax were not significantly changed, which indicates the addition of ferulic acid, decreased the affinity of *PcX1* for the substrate. Increased K_M and unchanged Vmax justify the definition of competitive inhibition. In agreement with our results, the ferulic acid showed the molecular docking at the catalytic site of *Aspergillus tamarii* xylanase (MONCLARO et al., 2019).

At low concentration (1.3 mM), K_M and Vmax increased and at high (5.4 mM) concentration of transcinnamic acid the K_M and Vmax decreased. The decrease in K_M was only 1.2 folds, which represents the affinity of *PcX1* slightly, increased for the substrate, but at the same time, Vmax decreased (3 folds) that characterised the transcinnamic acid might interfere with the residues important for substrate catalysis.

Opposite to *PcX1*, the K_M values of *PcX2* were decreased by the addition of transcinnmaic acid, though the decreased was 1.2 folds. Similarly, K_M decreased 1.82 and 1.1 folds with respective addition of 1.0 and 4.0 mM of transferulic acid. While apart from 4.0 mM of transferulic acid, the Vmax decreased in all scenarios. These results can be interpreted that the addition of phenolic acids increases the affinity of *PcX2* for substrate (oat spelt). Previous work of *Aspergillus terreus* discussed a similar result, where the K_M of 24 kDa xylanase decreased with the addition of 1mg ferulic acid. On the other hand, contrary to our findings, the addition of 6.7 mM transcinnamic acid increased the values of K_M for *A.terreus* xylanase (RIOS DE SOUZA MOREIRA et al., 2013).

Concerning the effect of phenolic acids on xylanase structure, the tryptophan band of *PcX1* has (12nm) redshift (328 to 340 nm) in the presence of tCA that notates the reorientation of tryptophan to the polar environment. The gradual increase of tCA the emission intensity decreased causing the quenching of fluorescence along with the unwinding of the protein molecule. Similarly, a slight red shift (338 nm to 340 nm) was also obtained with the addition of tFA. Moreover, the *PcX1* has exposed tryptophan at 338nm, as noticed in the biophysical section that confirm the emission band (338 nm) at pH 5.0. The interaction of phenolic acids with the aromatic residues of *PcX1* might responsible for the loss of activity.

As far as, the emission peak of *PcX2* did not change with the addition of phenolic acids as shown in (Fig IV.2B and IV.3B) emission peak at 326 nm, which is similar to that of the native enzyme, confirmed the quenching was due to the binding of phenolic acid and not due to the changed orientation of protein. Fluorescence study along with kinetics, activity and thermostability, *PcX2* results were better in comparison to *PcX1*. In both *PcX1* and *PcX2* spectrum there was an isosbestic point at 376 nm, in the presence of ferulic acid that might suggest the equilibrium between free and bound form tFA, further confirm the binding of transferulic acid to xylanases (OJHA et al., 2012; SGARBOSSA; LENCI, 2013). As the tFA is fluorophore that has emission at 420 nm.

The findings of biochemical analysis resonating well with the biophysical findings, *PcX2* was resistant to phenolic acids that were not interfacing with the protein conformation. Xylanase retained about 77% activity in the presence of 0.6 mg (tFA 3.0 mM and tCA 4.0 mM) of phenolic acids, thermostability as well increased and low values of K_M justify the affinity of *PcX2* increased with its substrate after the addition of phenolic acids.

Conclusion and perspectives

Penicillium chrysogenum is a filamentous fungus has the ability to degrade complex carbon sources by secreting the cell wall degrading enzymes. The initial objective of this study was to analyse the different biomass used as a carbon source to produced cost-effective enzymes. Our results conclude the sugarcane bagasse and straw were the best biomass to induce the secretion of xylanase and cellulase in comparison to avicel and orange peel (Chapter II).

Six different glycoside hydrolases: cellobiohydrolase, β-glucosidase, endoglucanase, mannanase, pectinase and xylanase were secreted, when *P. chrysogenum* cultured in the presence of sugarcane bagasse and corn straw used as sole carbon source (Chapter III). The experimental data helped to conclude the production of enzymes was time course and dependent on the type of carbon source. The production of xylanase was three times higher in comparison to other enzymes.

Enzymatic hydrolysis of sugarcane bagasse suggests the cooperative actions between endo-β-1, 4-xylanase and β-xylosidase, as 67% xylan was hydrolysed into xylose. Conversion of xylan was 44% higher than glucan that is due to the amorphous structure of hemicellulose and the activity of xylanase in the culture filtrate was higher than cellulase. The production of cellobiose predicts the presence of β-glucosidase activity. Significance results from enzymatic hydrolysis of pre-treated sugarcane bagasse indicate the potential role/application of *P. chrysogenum* enzymes in biorefinery.

Purified xylanases were sensitive to temperature and solution polarity. Physicochemical results showed that high temperature (> 50^{o}C) and change in pH caused the denaturation of both enzymes, that concludes physical environment dictate the protein folding important for its function. *PcX2* have a broader range of acting temperature (25^{o}C – 50^{o}C) than *PcX1,* signifies the application of *PcX2* in textile and food industry.

Effect of pH was almost equal on both xylanases; *PcX1* having acting pH ranges from (4.0 to 7.0) and *PcX2* was active at pH 5.0 to 7.0. The biochemical results showed that *PcX1* (GH10) was more thermostable at optimum pH than *PcX2* (GH11). From the biophysical analysis, we draw the conclusion that the stability of *PcX1* was attributed to the disulphide bond and the equilibrium of positive/negative charged side grouped on the surface of the protein. Contrary, *PcX2* lack disulphide bond (according to sequence alignment) and its stability was dependent upon α-helix that has hydrogen bond linkages break easily at high temperature and

denatured the protein. Our results confirm the fixed position of tryptophan was also a contributing factor in the stability of *PcX2.*

Moreover, both enzymes were resistant to some phenolic compounds, such as syringaldehyde ρ-coumaric acid and tannic acid. *PcX1* was also resistant to gallic acid and vanillin while *PcX2* was resistant to transferulic and transcinnamic acid. This feature is important for the applicability of these enzymes in the hydrolysis of pre-treated biomass.

Transferulic was responsible to unfold the protein structure as the concentration increased; the kinetics analysis showed the tFA caused the competitive inhibition of *PcX1*. Opposite to *PcX1*, transcinnmaic and transferulic acid were noncompetitive inhibitors of *PcX2* (Chapter IV), as the kinetics results were not significantly different (Appendix), we conclude the ferulic aicd bind to *PcX2* in a functionally neutral site.

The whole work concludes the *Penicillium chrysogenum* is a significant fungus in biotechnological point of view. However, this is the first study that deals with the biophysical characterisation of *PcX1* and *PcX2* and the effect of the phenolic acids on the activity/conformation of these xylanases. Findings of this work will definitely help in better understanding of GH10 and GH11 xylanases under bioindustry prospect and will improve the designing or development of future enzymes.

Acknowledgement

Firstly, I would like to express my sincere gratitude to my supervisor Professor Eliane Ferreira Noronha, for her continuous support of my PhD study and related research, for her patience, motivation, and immense knowledge. Her guidance helped me in all the time of research and writing of this thesis. I could not have imagined having a better advisor and mentor for my PhD study.

Besides my advisor, I would like to thank Professor Alice Nagata and Professor Tatsuya Nagata, for accepting my admission request and providing me a chance to be a student at the University of Brasilia. I feel privileged to meet these two wonderful people ever in my life.

My sincere thanks to Professor Sonia Freitas and Professor Joao Alexandre, who provided me an opportunity to work on Biophysical techniques, and gave me access to the laboratory and research facilities. Without their valuable support, it would not be possible to conclude the results of this research. I am also grateful to Prof. Sonia Maria Freitas and Prof. Aisel Valle Garay for accepting the invitation and attending my defence.

My special thanks to Mr. Nuno Domingues, mass spectrometry technician, for his untiring effort to sequence my enzymes. My sincere regards to Dr. Francilene Lopes, for helping me in the sequencing protocol of DNA and Protein. Identification was not possible without her assistance. Same gratitude for my workaholic co-author Dr. Amanada Souza, for helping with circular dichroism and fluorescence spectroscopy. Publication would not be easy without her collaboration. I also grateful to Dr. Geisianny Moreira, for her welcoming and helping gesture in need. Special thanks to Prof. Edivaldo Ximenes Ferreira for optimistic and encouraging gesture and Dr. Caio Silva for the courtesy to provide pre-treated sugarcane bagasse.

I express thanks to my fellows/lab mates, Mr. Alonso Ticona, Mr. Pedro Hamann, Mr. Mario Neto, Ms. Debora Costa, Ms. Hameli Takemastu, Ms. Jessica Silva along with Mrs. Diandra, Mrs. Andreza and Mrs. Raíssa, Ms.Carol for their cooperation to adjust me in the lab. To deal with the cultural lingual barrier would be not possible without serein behaviour of my lab fellows.

I appreciate the advice and helping hands of Dr. Brenda Camargo, Dr. Helder Gomes, Dr. Antonielle Monclaro. I also admire the effort of Ms. Gideane Oliveira to facilitate in homology structure.

I also thank the postgraduate program of Molecular Biology, and funding organizations (CNPq and Capes) for giving me the opportunity to complete my PhD pleasantly.

In the end, I admire the patience and courage of my parents specially my Mother, for sending her only child across the sea to seek knowledge. I further acknowledge their wisdom to enlighten me with both Science and Religion. Without their intellect, I would be neither a Hafiza nor a Doctor. My sincere regards for my Husband, for his absolute effort in my admission.

Above all, I express my gratefulness to the Almighty for making me able to achieve whatever I have

Sadia Fida Ullah

REFERENCES

ALAÑA, A. et al. Pectin Lyase Activity in a Penicillium italicum Strain. **Applied and environmental microbiology**, v. 56, n. 12, p. 3755–9, 1 dez. 1990.

ARDÈVOL, A.; ROVIRA, C. Reaction Mechanisms in Carbohydrate-Active Enzymes: Glycoside Hydrolases and Glycosyltransferases. Insights from *ab Initio* Quantum Mechanics/Molecular Mechanics Dynamic Simulations. **Journal of the American Chemical Society**, v. 137, n. 24, p. 7528–7547, 24 jun. 2015.

ATALLA, R. H. Chapter 13:Cellulose and the Hemicelluloses: Patterns for the Assembly of Lignin. In: [s.l: s.n.].

AVER, K. R. et al. Saccharification of ionic-liquid-pretreated sugar cane bagasse using Penicillium echinulatum enzymes. **Journal of the Taiwan Institute of Chemical Engineers**, v. 45, n. 5, p. 2060–2067, 1 set. 2014.

AYMARD, C.; BELARBI, A. Kinetics of thermal deactivation of enzymes: A simple three parameters phenomenological model can describe the decay of enzyme activity, irrespectively of the mechanism. **Enzyme and Microbial Technology**, v. 27, n. 8, p. 612–618, 2000.

BACKUS, M. P.; STAUFFER, J. F.; JOHNSON, M. J. Penicillin yields from new mold strains. **Journal of the American Chemical Society**, v. 68, n. 1, p. 152–153, 1946.

BALKAN, B.; ERTAN, F. Production of alpha-amylase from Penicillium chrysogenum under solid-state fermentation by using some agricultural by-products. **Food Technology and Biotechnology**, v. 45, n. 4, p. 439–442, 2007.

BARREIRO, C.; MARTÍN, J. F.; GARCÍA-ESTRADA, C. Proteomics shows new faces for the old penicillin producer Penicillium chrysogenum. **Journal of Biomedicine and Biotechnology**, v. 2012, 2012.

BARRETO, M. C.; HOUBRAKEN, J.; SAMSON, R. A. Taxonomic studies of the Penicillium glabrum complex and the description of a new species P . subericola. p. 23–33, 2011.

BELANCIC, A. et al. Penicillium purpurogenum produces several xylanases: Purification and properties of two of the enzymes. **Journal of Biotechnology**, v. 41, n. 1, p. 71–79, 1995.

BENITO, M. J. et al. Purification and characterization of an extracellular protease from Penicillium chrysogenum Pg222 active against meat proteins. **Applied and environmental**

microbiology, v. 68, n. 7, p. 3532–6, 1 jul. 2002.

BERG, M. A. VAN DEN et al. Genome sequencing and analysis of the filamentous fungus Penicillium chrysogenum. v. 26, n. 10, p. 1161–1168, 2008.

BERRIN, J. G. et al. Substrate and product hydrolysis specificity in family 11 glycoside hydrolases: An analysis of Penicillium funiculosum and Penicillium griseofulvum xylanases. **Applied Microbiology and Biotechnology**, v. 74, n. 5, p. 1001–1010, 2007.

BESOMBES, S.; MAZEAU, K. The cellulose/lignin assembly assessed by molecular modeling. Part 2: seeking for evidence of organization of lignin molecules at the interface with cellulose. **Plant Physiology and Biochemistry**, v. 43, n. 3, p. 277–286, 1 mar. 2005.

BIELY, P. et al. Endo-β-1,4-xylanase families: differences in catalytic properties. **Journal of Biotechnology**, v. 57, n. 1–3, p. 151–166, 16 set. 1997.

BORASTON, A. B. et al. Carbohydrate-binding modules : fine-tuning polysaccharide recognition. v. 781, p. 769–781, 2004.

BOUKARI, I. et al. Probing a family GH11 endo-β-1,4-xylanase inhibition mechanism by phenolic compounds: Role of functional phenolic groups. **Journal of Molecular Catalysis B: Enzymatic**, v. 72, n. 3–4, p. 130–138, 2011a.

BOUKARI, I. et al. Probing a family GH11 endo-β-1,4-xylanase inhibition mechanism by phenolic compounds: Role of functional phenolic groups. **Journal of Molecular Catalysis B: Enzymatic**, v. 72, n. 3–4, p. 130–138, 2011b.

BRADFORD, M. A rapid and sensitive method for the quantiWcation of microgram quantities of protein utilizing the principle of protein– dye binding. **Analytical Biochemistry**, v. 72, p. 248–254, 1976.

BUCHERT, J. et al. Application of xylanases in the pulp and paper industry. **Bioresource Technology**, v. 50, n. 1, p. 65–72, 1994.

BURANOV, A. U.; MAZZA, G. **Lignin in straw of herbaceous cropsIndustrial Crops and Products**, 2008. Disponível em: <https://www.sciencedirect.com/science/article/pii/S0926669008000630>. Acesso em: 22 jul. 2018

BUTT, M. S. et al. Xylanases and their applications in baking industry. **Food Technology and**

Biotechnology, v. 46, n. 1, p. 22–31, 2008.

CAMASSOLA, M.; DILLON, A. J. P. Steam-exploded sugar cane bagasse for on-site production of cellulases and xylanases by Penicillium echinulatum. **Energy and Fuels**, v. 26, n. 8, p. 5316–5320, 2012.

CANILHA, L. et al. Bioconversion of Sugarcane Biomass into Ethanol : An Overview about Composition , Pretreatment Methods , Detoxification of Hydrolysates , Enzymatic Saccharification , and Ethanol Fermentation. v. 2012, 2012.

CARDONA, C. A.; SÁNCHEZ, Ó. J. Fuel ethanol production: Process design trends and integration opportunities. **Bioresource Technology**, v. 98, n. 12, p. 2415–2457, set. 2007.

CARPITA, N. C.; GIBEAUT, D. M. Structural models of primary cell walls in flowering plants: consistency of molecular structure with the physical properties of the walls during growth. **The Plant Journal**, v. 3, n. 1, p. 1–30, 1 jan. 1993.

CHÁVEZ, R. et al. Differences in expression of two endoxylanase genes (xynA and xynB) from Penicillium purpurogenum. **Gene**, v. 293, n. 1–2, p. 161–168, 2002.

CHÁVEZ, R.; BULL, P.; EYZAGUIRRE, J. The xylanolytic enzyme system from the genus Penicillium. **Journal of Biotechnology**, v. 123, n. 4, p. 413–433, 2006.

CHEN, M. et al. Isolation and characterization of a β-glucosidase from Penicillium decumbens and improving hydrolysis of corncob residue by using it as cellulase supplementation. **Enzyme and Microbial Technology**, v. 46, n. 6, p. 444–449, 5 maio 2010.

COLLINS, T.; GERDAY, C.; FELLER, G. Xylanases, xylanase families and extremophilic xylanases. **FEMS Microbiology Reviews**, v. 29, n. 1, p. 3–23, 1 jan. 2005.

CROZIER, A.; CLIFFORD, M. N. **Terpenes, Plant Secondary Metabolites**. [s.l: s.n.].

DA COSTA SOUZA, P. N. et al. Production and chemical characterization of pigments in filamentous fungi. **Microbiology (United Kingdom)**, v. 162, n. 1, p. 12–22, 2016.

DAVIES, G.; HENRISSAT, B. Structures and mechanisms of glycosyl hydrolases. **Structure**, v. 3, n. 9, p. 853–859, 1 set. 1995.

DAVIES, G. J.; SINNOT, M. L. Sorting the diverse. **Biochemical Journal**, p. 26–32, 2008.

DAVIES, G. J.; WILSON, K. S.; HENRISSAT, B. Nomenclature for sugar-binding subsites in glycosyl hydrolases. **The Biochemical journal**, v. 321 (Pt 2, n. Pt 2, p. 557–9, 15 jan. 1997.

DE OLIVEIRA GORGULHO SILVA, C. et al. Mild hydrothermal pretreatment of sugarcane bagasse enhances the production of holocellulases by Aspergillus niger. **Journal of Industrial Microbiology & Biotechnology**, n. 0123456789, 2019.

DE OLIVEIRA GORGULHO SILVA, C.; FILHO, E. X. F. A Review of Holocellulase Production Using Pretreated Lignocellulosic Substrates. **Bioenergy Research**, v. 10, n. 2, p. 592–602, 2017.

DE SOUZA MOREIRA, L. R. et al. Two β-xylanases from Aspergillus terreus: Characterization and influence of phenolic compounds on xylanase activity. **Fungal Genetics and Biology**, v. 60, p. 46–52, 2013.

DE SOUZA MOREIRA, L. R. et al. Xylan-degrading enzymes from Aspergillus terreus: Physicochemical features and functional studies on hydrolysis of cellulose pulp. **Carbohydrate Polymers**, v. 134, n. December, p. 700–708, 2015.

DONALDSON, L. A. Lignification and lignin topochemistry — an ultrastructural view. **Phytochemistry**, v. 57, n. 6, p. 859–873, 1 jul. 2001.

DOYLE, E.; KELLY, C.; FOGARTY, W. The high maltose-producing -α-amylase by Penicillium expansum α-amylase by Penicillium expansum amylase of Penicillium expansum. **Applied Microbiology and Biotechnology**, v. 30, n. 5, p. 492–496, maio 1989.

DRYJAŃSKI, M. et al. Aspartic proteinase from Penicillium camemberti: Purification, properties, and substrate specificity. **Enzyme and Microbial Technology**, v. 17, n. 8, p. 719–724, 1995.

DUTTA, S.; WU, K. C. W. Enzymatic breakdown of biomass: Enzyme active sites, immobilization, and biofuel production. **Green Chemistry**, v. 16, n. 11, p. 4615–4626, 2014.

EBRINGEROVÁ, A. **Structural diversity and application potential of hemicelluloses**. Macromolecular Symposia. **Anais**...dez. 2006Disponível em: <http://doi.wiley.com/10.1002/masy.200551401>. Acesso em: 22 jul. 2018

EBRINGEROVÁ, A.; HEINZE, T. Xylan and xylan derivatives - Biopolymers with valuable properties, 1: Naturally occurring xylans structures, isolation procedures and properties. **Macromolecular Rapid Communications**, v. 21, n. 9, p. 542–556, 1 jun. 2000.

EDGAR, R. C. MUSCLE: Multiple sequence alignment with high accuracy and high throughput. **Nucleic Acids Research**, v. 32, n. 5, p. 1792–1797, 2004.

ERTAN, F. et al. Solid state fermentation for the production of α -amylase from Penicillium chrysogenum using mixed agricultural by-products as substrate. p. 657–661, 2006.

FAULDS, C. B.; WILLIAMSON, G. The role of hydroxycinnamates in the plant cell wall. **Journal of the Science of Food and Agriculture**, v. 79, n. 3, p. 393–395, 1 mar. 1999.

FERRER, M. et al. Purification and properties of a lipase fromPenicillium chrysogenum isolated from industrial wastes. **Journal of Chemical Technology & Biotechnology**, v. 75, n. 7, p. 569–576, 2000.

FLEMING, A. ON THE ANTIBACTERIAL ACTION OF CULTURES OF A PENICILLIUM, WITH SPECIAL REFERENCE TO THEIR USE IN THE ISOLATION OF B. INFLUENZ?1E. **British journal of experimental pathology**, v. 10, n. 3, p. 226–235, 1929.

FORSBERG, Z. et al. Structural and functional characterization of a conserved pair of bacterial cellulose-oxidizing lytic polysaccharide monooxygenases. **Proceedings of the National Academy of Sciences of the United States of America**, v. 111, n. 23, p. 8446–51, 2014.

FRISVAD, J. C.; SAMSON, R. A. Polyphasic taxonomy of Penicillium subgenus Penicillium: A guide to identification of food and air-borne terverticillate Penicillia and their mycotoxins. **Studies in Mycology**, v. 2004, n. 49, p. 1–173, 2004.

FRISVAD, J.; MYCOLOGY, R. S.-S. IN. Polyphasic taxonomy of Penicillium subgenus Penicillium. A guide to identification of food and air-borne terverticillate Penicillia and their mycotoxins. **Studies in Mycology**, v. 49, n. 1, p. 1–174, 2004.

FUNAGUMA, T. et al. Purification and some properties of xylanase from Penicillium herquei Banier and Sartory. **Agricultural and Biological Chemistry**, v. 55, n. 4, p. 1163–1165, 1991.

GILBERT, H. J.; HAZLEWOOD, G. P. Bacterial cellulases and xylanases. **Journal of General Microbiology**, v. 139, n. 2, p. 187–194, 1993.

GILKES, N. R. et al. Domains in microbial beta-1, 4-glycanases: sequence conservation, function, and enzyme families. **Microbiological reviews**, v. 55, n. 2, p. 303–15, 1 jun. 1991.

GOMES, H. A. DA R. Universidade de Brasília Perfil e caracterização de holocelulases secretadas por Penicillium fellutanum com ênfase em mananase . Perfil e caracterização de holocelulases secretadas por Penicillium fellutanum com ênfase em mananase . 2014.

GOMES, H. A. R. et al. Identification of multienzymatic complexes in the Clonostachys

byssicola secretomes produced in response to different lignocellulosic carbon sources. **Journal of Biotechnology**, v. 254, n. June, p. 51–58, 2017.

GRETHLEIN, H. E. The Effect of Pore Size Distribution on the Rate of Enzymatic Hydrolysis of Cellulosic Substrates. **Narure Biotechnology**, v. 3, n. 2, p. 155–160, fev. 1985.

GREUTER, WERNER, AND J. I. P. **Greuter, W., & Pitt, J. I. (1993). Names in current use in the families Trichocomaceae, Cladoniaceae, Pinaceae, and Lemnaceae. Published for the International Association for Plant Taxonomy by Koeltz Scientific Books**. [s.l: s.n.].

GREUTER, W.; PITT, J. Names in current use in the families Trichocomaceae, Cladoniaceae, Pinaceae, and Lemnaceae. 1993.

GUPTA, V. K. et al. Fungal Enzymes for Bio-Products from Sustainable and Waste Biomass. **Trends in Biochemical Sciences**, v. 41, n. 7, p. 633–645, 2016.

GUSAKOV, A. V; SINITSYN, A. P. Cellulases from *Penicillium* species for producing fuels from biomass. **Biofuels**, v. 3, n. 4, p. 463–477, 2012.

HAAS, H. et al. Purification, characterization and partial amino acid sequences of a xylanase produced by Penicillium chrysogenum. **Biochimica et Biophysica Acta (BBA) - General Subjects**, v. 1117, n. 3, p. 279–286, 1992.

HARRIS, P. J.; SMITH, B. G. Plant cell walls and cell-wall polysaccharides: Structures, properties and uses in food products. **International Journal of Food Science and Technology**, v. 41, n. SUPPL. 2, p. 129–143, 2006a.

HARRIS, P. J.; SMITH, B. G. Plant cell walls and cell-wall polysaccharides: structures, properties and uses in food products. **International Journal of Food Science and Technology**, v. 41, n. s2, p. 129–143, dez. 2006b.

HATAKKA, A.; HAMMEL, K. E. Fungal Biodegradation of Lignocelluloses. **Industrial Applications**, p. 319–340, 2011.

HAYASHI, H. et al. Nucleotide sequences of two contiguous and highly homologous xylanase genes xynA and xynB and characterization of XynA from Clostridium thermocellum. **Applied Microbiology and Biotechnology**, v. 51, n. 3, p. 348–357, 26 mar. 1999.

HAYES, D. J. An examination of biorefining processes, catalysts and challenges. **Catalysis Today**, v. 145, n. 1–2, p. 138–151, 2009.

HENRISSAT, B. A classification of glycosyl hydrolases based on amino acid sequence similarities. **The Biochemical journal**, v. 280, n. 2, p. 309–16, 1 dez. 1991.

HENRISSAT, B.; GRENOBLE, F. A Classification of Glycosyl Hydrolases Based on Sequence Similarities Amino Acid. **Journal of Biochemistry**, v. 280, p. 309–316, 1991.

HENRY, R. J. (ED.). **Plant diversity and evolution: genotypic and phenotypic variation in higher plants**. Wallingford: CABI, 2005.

HOU, Y. et al. Cloning, sequencing and expression analysis of the first cellulase gene encoding cellobiohydrolase 1 from a cold-adaptive Penicillium chrysogenum FS010. **Acta Biochimica et Biophysica Sinica**, v. 39, n. 2, p. 101–107, 2007a.

HOU, Y. et al. Cloning, Sequencing and Expression Analysis of the First Cellulase Gene Encoding Cellobiohydrolase 1 from a Cold-adaptive Penicillium chrysogenum FS010. **Acta Biochimica et Biophysica Sinica**, v. 39, n. 2, p. 101–107, fev. 2007b.

HOUBRAKEN, J.; FRISVAD, J. C.; SAMSON, R. A. Fleming ' s penicillin producing strain is not Penicillium chrysogenum but P . rubens. v. 2, n. 1, p. 87–95, 2011a.

HOUBRAKEN, J.; FRISVAD, J. C.; SAMSON, R. A. Taxonomy of Penicillium section Citrina. **Studies in Mycology**, v. 70, p. 53–138, 1 set. 2011b.

ISABIRYE, M. et al. Sugarcane Biomass Production and Renewable Energy. **Intech**, 2013.

JIM BIDLACK, MIKE MALONE, AND R. B. Molecular structure and component integration of secondary cell walls in plants. **ojs.library.okstate.edu**, v. 72, p. 51–56, 1992.

JØRGENSEN, H. et al. Production of cellulases and hemicellulases by three Penicillium species : effect of substrate and evaluation of cellulase adsorption by capillary electrophoresis. v. 36, p. 42–48, 2005.

JØRGENSEN, H.; OLSSON, L. Production of cellulases by Penicillium brasilianum IBT 20888—Effect of substrate on hydrolytic performance. **Enzyme and Microbial Technology**, v. 38, n. 3–4, p. 381–390, 1 fev. 2006.

KASANA, R. C. et al. A rapid and easy method for the detection of microbial cellulases on agar plates using Gram's iodine. **Current Microbiology**, v. 57, n. 5, p. 503–507, 2008.

KAYA, F.; HEITMANN, J. A.; JOYCE, T. W. Influence of lignin and its degradation products on enzymatic hydrolysis of xylan. **Journal of Biotechnology**, v. 80, n. 3, p. 241–247, 2000.

KHATRI, V.; MEDDEB-MOUELHI, F.; BEAUREGARD, M. New insights into the enzymatic hydrolysis of lignocellulosic polymers by using fluorescent tagged carbohydrate-binding modules. **Sustainable Energy & Fuels**, v. 2, n. 2, p. 479–491, 30 jan. 2018.

KIRK, P.M., CANNON, P.F., MINTER, D.W. & STALPERS, J. A. (EDS. . 2008.; DICTIONARY OF THE FUNGI. 10TH ED. WALLINGFORD, U. C. P. 505. **DICTIONARY OF THE FUNGI**. 10th. ed. UK: CABI.org, 2008.

KITTUR, F. S. et al. Fusion of family 2b carbohydrate-binding module increases the catalytic activity of a xylanase from Thermotoga maritima to soluble xylan. **FEBS Letters**, v. 549, n. 1–3, p. 147–151, 14 ago. 2003.

KNOB, A. et al. Production, purification, and characterization of a major penicillium glabrum xylanase using brewer's spent grain as substrate. **BioMed Research International**, v. 2013, 2013.

KOSHLAND.D.E. STEREOCHEMISTRY AND THE MECHANISM OF ENZYMATIC REACTIONS. **Biological Reviews**, v. 28, n. 4, p. 416–436, nov. 1953.

KOTIRANTA, P. et al. Adsorption and Activity of Trichoderma reesei Cellobiohydrolase I, Endoglucanase II, and the Corresponding Core Proteins on Steam Pretreated Willow. **Applied Biochemistry and Biotechnology**, v. 81, n. 2, p. 81–90, 1999.

LAEMMLI, U. K. Cleavage of Structural Proteins during the Assembly of the Head of Bacteriophage T4. **Nature**, v. 227, n. 5259, p. 680–685, 15 ago. 1970.

LAFOND, M. et al. GH10 xylanase D from Penicillium funiculosum: biochemical studies and xylooligosaccharide production. **Microbial Cell Factories**, v. 10, n. 1, p. 20, 2011.

LEE, C. C.; WONG, D. W. S.; ROBERTSON, G. H. Cloning and characterization of the Xyn11A gene from Lentinula edodes. **Protein Journal**, v. 24, n. 1, p. 21–26, 2005.

LEE, Y.-H.; FAN, L. T. Kinetic studies of enzymatic hydrolysis of insoluble cellulose: Analysis of the initial rates. **Biotechnology and Bioengineering**, v. 24, n. 11, p. 2383–2406, 1 nov. 1982.

LEITÃO, A. L. Potential of Penicillium Species in the Bioremediation Field. **International Journal of Environmental Research and Public Health**, v. 6, n. 4, p. 1393–1417, 9 abr. 2009.

LIAB, K. et al. Relationships between activities of xylanases and xylan structures. **Enzyme and Microbial Technology**, v. 27, n. 1–2, p. 89–94, 1 jul. 2000.

LIAO, H. et al. Insights into high-efficiency lignocellulolytic enzyme production by Penicillium oxalicum GZ-2 induced by a complex substrate. **Biotechnology for Biofuels**, v. 7, n. 1, p. 1–17, 2014.

LIAO, H. et al. Functional diversity and properties of multiple xylanases from Penicillium oxalicum GZ-2. **Scientific reports**, v. 5, n. 88, p. 12631, 2015.

LONG, T. M. et al. Cofermentation of glucose, xylose, and cellobiose by the beetle-associated yeast Spathaspora passalidarum. **Applied and environmental microbiology**, v. 78, n. 16, p. 5492–500, 15 ago. 2012.

MAEDA, R. N. et al. Enzymatic hydrolysis of pretreated sugar cane bagasse using Penicillium funiculosum and Trichoderma harzianum cellulases. **Process Biochemistry**, v. 46, n. 5, p. 1196–1201, 1 maio 2011.

MAMO, G.; HATTI-KAUL, R.; MATTIASSON, B. Fusion of carbohydrate binding modules from Thermotoga neapolitana with a family 10 xylanase from Bacillus halodurans S7. **Extremophiles**, v. 11, n. 1, p. 169–177, 9 jan. 2007.

MARTINS, L. F. et al. Comparison of Penicillium echinulatum and Trichoderma reesei cellulases in relation to their activity against various cellulosic substrates. **Bioresource Technology**, v. 99, n. 5, p. 1417–1424, 1 mar. 2008.

MATSUMOTO, S. et al. Identification of a novel Penicillium chrysogenum rhamnogalacturonan rhamnohydrolase and the first report of a rhamnogalacturonan rhamnohydrolase gene. **Enzyme and Microbial Technology**, v. 98, p. 76–85, 2017.

MCCANN, M.; WELLS, B, K. R. Direct visualization of cross-links in the primary plant cell wall. **Journal of cell sciences**, v. 96, p. 323–334, 1990.

MCCARTER, J. D.; STEPHEN WITHERS, G. Mechanisms of enzymatic glycoside hydrolysis. **Current Opinion in Structural Biology**, v. 4, n. 6, p. 885–892, 1994a.

MCCARTER, J. D.; STEPHEN WITHERS, G. Mechanisms of enzymatic glycoside hydrolysis. **Current Opinion in Structural Biology**, v. 4, n. 6, p. 885–892, 1 jan. 1994b.

MCCARTNEY, L. et al. Differential recognition of plant cell walls by microbial xylan-specific

carbohydrate-binding modules. **Proceedings of the National Academy of Sciences of the United States of America**, v. 103, n. 12, p. 4765–70, 21 mar. 2006.

MCNEIL, M. et al. Structure and Function of the Primary Cell Walls of Plants. **Annual Review of Biochemistry**, v. 53, n. 1, p. 625–663, jun. 1984.

MILAGRES, A. M. F.; LACIS, L. S.; PRADE, R. A. Characterization of xylanase production by a local isolate of Penicillium janthinellum. **Enzyme and Microbial Technology**, v. 15, n. 3, p. 248–253, 1993.

MILLER, G. L. Use of Dinitrosalicylic Acid Reagent for Determination of Reducing Sugar. **Analytical Chemistry**, v. 31, n. 3, p. 426–428, 1959.

MOERS, K. et al. Endoxylanase substrate selectivity determines degradation of wheat water-extractable and water-unextractable arabinoxylan. **Carbohydrate Research**, v. 340, n. 7, p. 1319–1327, 23 maio 2005.

MONCLARO, A. V. et al. Xylanase from Aspergillus tamarii shows different kinetic parameters and substrate specificity in the presence of ferulic acid. **Enzyme and Microbial Technology**, v. 120, p. 16–22, jan. 2019.

NG, I. S. et al. High-level production of a thermoacidophilic β-glucosidase from Penicillium citrinum YS40-5 by solid-state fermentation with rice bran. **Bioresource Technology**, v. 101, n. 4, p. 1310–1317, 2010.

NWODO, S. C. et al. **Xylanase Production of Aspergillus niger and Penicillium chrysogenum from Ammonia Pretreated Cellulosic WasteResearch Journal of Microbiology**, 2008.

O'SULLIVAN, A. C. Cellulose: the strcture slowly unravels. **Cellulose**, v. 4, p. 173–207, 1997.

OCTAVE, S.; THOMAS, D. **Biorefinery: Toward an industrial metabolismBiochimie**, 2009. Disponível em: <https://www.sciencedirect.com/science/article/pii/S0300908409000765>. Acesso em: 22 jul. 2018

OISE PAYAN, F. et al. The Dual Nature of the Wheat Xylanase Protein Inhibitor XIP-I STRUCTURAL BASIS FOR THE INHIBITION OF FAMILY 10 AND FAMILY 11 XYLANASES*□ S. 2004.

OJHA, H. et al. Spectroscopic and isothermal titration calorimetry studies of binding interaction of ferulic acid with bovine serum albumin. **Thermochimica Acta**, v. 548, n. December 2017, p. 56–64, 2012.

OLSEN, J. V et al. In-gel digestion for mass spectrometric characterization of proteins and proteomes. v. 1, n. 6, p. 2856–2860, 2007.

PAËS, G.; BERRIN, J. G.; BEAUGRAND, J. GH11 xylanases: Structure/function/properties relationships and applications. **Biotechnology Advances**, v. 30, n. 3, p. 564–592, 2012.

PALMQVIST, E. et al. The effect of water-soluble inhibitors from steam-pretreated willow on enzymatic hydrolysis and ethanol fermentation. **Enzyme and Microbial Technology**, v. 19, n. 6, p. 470–476, 1 nov. 1996.

PANAGIOTOU, G.; OLAVARRIA, R.; OLSSON, L. Penicillium brasilianum as an enzyme factory; the essential role of feruloyl esterases for the hydrolysis of the plant cell wall. **Journal of Biotechnology**, v. 130, n. 3, p. 219–228, 2007.

PANDA, T. **Penicillium abundance and diversity patterns associated with cashew plantations in coastal sand dunes, Odisha, IndiaJournal of Ecology and the Natural Environment**. [s.l: s.n.]. Disponível em: <http://www.academicjournals.org/jene>. Acesso em: 6 mar. 2019.

PENG, X. et al. Induced resistance toCladosporium cucumerinum in cucumber by pectinases extracted fromPenicillium oxalicum. **Phytoparasitica**, v. 32, n. 4, p. 377–387, ago. 2004.

PÉREZ, J. et al. Biodegradation and biological treatments of cellulose, hemicellulose and lignin: An overview. **International Microbiology**, v. 5, n. 2, p. 53–63, 2002.

PERTICAROLI, S. et al. Secondary structure and rigidity in model proteins. **Soft Matter**, v. 9, n. 40, p. 9548, 25 set. 2013.

POLIZELI, M. L. T. M. et al. Xylanases from fungi: Properties and industrial applications. **Applied Microbiology and Biotechnology**, v. 67, n. 5, p. 577–591, 2005.

PRATIMA BAJPAI. **Xylanolytic Enzymes**. [s.l.] Elsevier, 2014.

RAGHOTHAMA, S. et al. Solution Structure of the CBM10 Cellulose Binding Module from Pseudomonas Xylanase A,. **ACS Publications**, 2000.

RALPH, J.; GRABBER, J. H.; HATFIELD, R. D. Lignin-ferulate cross-links in grasses: active

incorporation of ferulate polysaccharide esters into ryegrass lignins. **Carbohydrate Research**, v. 275, n. 1, p. 167–178, 15 set. 1995.

RAPPSILBER, J.; MANN, M.; ISHIHAMA, Y. Protocol for micro-purification , enrichment , pre-fractionation and storage of peptides for proteomics using StageTips Protocol for micro-purification , enrichment , pre-fractionation and storage of peptides for proteomics using StageTips. n. May 2016, 2007.

RASHEEDHA BANU, A. et al. Production and characterization of pectinase enzyme from Penicillium chrysogenum. **Indian Journal of Science and Technology**, v. 3, n. 4, 2010.

REN, J. L.; SUN, R. C. **Hemicelluloses**. 1. ed. [s.l.] Elsevier, 2010.

RENNEBERG, R. et al. Enzymes: Molecular Supercatalysts for Use at Home and in Industry. In: **Biotechnology for Beginners**. [s.l.] Academic Press, 2017. p. 33–63.

RESHETNYAK, Y. K.; BURSTEIN, E. A. Decomposition of Protein Tryptophan Fluorescence Spectra into Log-Normal Components. II. The Statistical Proof of Discreteness of Tryptophan Classes in Proteins. **Biophysical Journal**, v. 81, n. 3, p. 1710–1734, 1 set. 2001.

RIOS DE SOUZA MOREIRA, L. et al. Two b-xylanases from Aspergillus terreus: Characterization and influence of phenolic compounds on xylanase activity. **Fungal Genetics and Biology**, v. 60, p. 46–52, 2013.

RODRUSSAMEE, N.; SATTAYAWAT, P.; YAMADA, M. Highly efficient conversion of xylose to ethanol without glucose repression by newly isolated thermotolerant Spathaspora passalidarum CMUWF1–2. **BMC Microbiology**, v. 18, n. 1, p. 73, 13 dez. 2018.

SAINI, R. et al. Enhanced cellulase production by Penicillium oxalicum for bio-ethanol application. **Bioresource Technology**, v. 188, p. 240–246, 1 jul. 2015.

SAKAMOTO, T. et al. A cold-adapted endo-arabinanase from Penicillium chrysogenum. **Biochimica et Biophysica Acta - General Subjects**, v. 1624, n. 1–3, p. 70–75, 2003.

SAKAMOTO, T. et al. Molecular characterization of a Penicillium chrysogenum exo-1,5-α-L-arabinanase that is structurally distinct from other arabinan-degrading enzymes. **FEBS Letters**, v. 560, n. 1–3, p. 199–204, 2004.

SAKAMOTO, T. et al. Biochemical characterization and gene expression of two endo-arabinanases from Penicillium chrysogenum 31B. **Applied Microbiology and Biotechnology**,

v. 93, n. 3, p. 1087–1096, 2012.

SAKAMOTO, T. et al. Biochemical characterization of a GH53 endo-β-1,4-galactanase and a GH35 exo-β-1,4-galactanase from Penicillium chrysogenum. **Applied Microbiology and Biotechnology**, v. 97, n. 7, p. 2895–2906, 2013a.

SAKAMOTO, T. et al. Substrate specificity and gene expression of two Penicillium chrysogenum ??-l-arabinofuranosidases (AFQ1 and AFS1) belonging to glycoside hydrolase families 51 and 54. **Applied Microbiology and Biotechnology**, v. 97, n. 3, p. 1121–1130, 2013b.

SALOHEIMO, M. et al. Swollenin, a Trichoderma reesei protein with sequence similarity to the plant expansins, exhibits disruption activity on cellulosic materials. **European Journal of Biochemistry**, v. 269, n. 17, p. 4202–4211, 2002.

SAMSON, R. A. Phylogenetic analysis of Penicillium subgenus Penicillium using partial β -tubulin sequences . Stud Mycol. n. January 2004, 2016.

SAMSON, R. A.; HADLOK, R.; STOLK, A. C. A taxonomic study of the Penicillium chrysogenum series. v. 43, p. 169–175, 1977.

SANDHU, S. K. et al. Penicillium: The next emerging champion for cellulase production. **Bioresource technology**, n. 2017, p. 131–140, 2018.

SCHMIDT, A.; GÜBITZ, G. M.; KRATKY, C. Xylan binding subsite mapping in the xylanase from Penicillium simplicissimum using xylooligosaccharides as cryo-protectant. **Biochemistry**, v. 38, n. 8, p. 2403–2412, 1999.

SCHOCH, C. L. et al. Nuclear ribosomal internal transcribed spacer (ITS) region as a universal DNA barcode marker for Fungi. **Proceedings of the National Academy of Sciences of the United States of America**, v. 109, n. 16, p. 6241–6, 17 abr. 2012.

SGARBOSSA, A.; LENCI, F. A Study for the Cause of Ferulic Acid-Induced Quenching of Tyrosine Fluorescence and Whether it is a Reliable Marker of Intermolecular Interactions or Not. **Journal of Fluorescence**, v. 23, n. 3, p. 561–567, 6 maio 2013.

SHARMA, A. et al. Effects of aromatic compounds on hemicellulose-degrading enzymes in Aspergillus japonicus. **Biotechnology and Bioengineering**, v. 27, n. 8, p. 1095–1101, 1985.

SHINOZAKI, A. et al. A novel GH43 ??-l-arabinofuranosidase of Penicillium chrysogenum

that preferentially degrades single-substituted arabinosyl side chains in arabinan. **Enzyme and Microbial Technology**, v. 58–59, p. 80–86, 2014.

SHINOZAKI, A. et al. Identification and characterization of three Penicillium chrysogenum ??-l-arabinofuranosidases (PcABF43B, PcABF51C, and AFQ1) with different specificities toward arabino-oligosaccharides. **Enzyme and Microbial Technology**, v. 73–74, p. 65–71, 2015.

SILVA, C. DE O. G. et al. Sugarcane Bagasse Hydrothermal Pretreatment Liquors as Suitable Carbon Sources for Hemicellulase Production by Aspergillus niger. **Bioenergy Research**, p. 1–14, 2018.

SILVA, C. O. G.; VAZ, R. P.; FILHO, E. X. F. Bringing plant cell wall-degrading enzymes into the lignocellulosic biorefinery concept. **Biofuels, Bioproducts and Biorefining**, v. 12, n. 2, p. 277–289, 2018.

SILVA, L. DE M. B. et al. Biochemical Properties of Carbohydrate-Active Enzymes Synthesized by Penicillium chrysogenum Using Corn Straw as Carbon Source. **Waste and Biomass Valorization**, p. 1–12, 22 jan. 2019.

SOUZA, A. A. et al. Trichoderma harzianum produces a new thermally stable acid phosphatase, with potential for biotechnological application. **PLoS ONE**, v. 11, n. 3, p. 1–18, 2016.

SUBRAMANIYAN, S.; PREMA, P. Biotechnology of microbial xylanases: Enzymology, molecular biology, and application. **Critical Reviews in Biotechnology**, v. 22, n. 1, p. 33–64, 2002.

SUGIMOTO, M. et al. Cloning and characterization of preferentially expressed genes in an aluminum-tolerant mutant derived from Penicillium chrysogenum IFO4626. **FEMS Microbiology Letters**, v. 230, n. 1, p. 137–142, 1 jan. 2004.

TAMURA, K.; NEI, M. Estimation of the number of nucleotide substitutions in the control region of mitochondrial DNA in humans and chimpanzees. **Molecular Biology and Evolution**, v. 10, n. 3, p. 512–526, 1 maio 1993.

TAVARES, E. Q. P.; BUCKERIDGE, M. S. Do plant cell walls have a code? **Plant Science**, v. 241, p. 286–294, 2015.

TERRASAN, C. R. F. et al. Production of xylanolytic enzymes by Penicillium janczewskii.

Bioresource Technology, v. 101, n. 11, p. 4139–4143, 2010.

TIAN, Y.; JIANG, Y.; OU, S. Interaction of cellulase with three phenolic acids. **Food Chemistry**, v. 138, n. 2–3, p. 1022–1027, 2013.

TÖRRÖNEN, A.; ROUVINEN, J. Structural and functional properties of low molecular weight endo-1,4-β -xylanases. **Journal of Biotechnology**, v. 57, n. 1–3, p. 137–149, 16 set. 1997.

ULLAH, S. F. et al. Structural and functional characterisation of xylanase purified from Penicillium chrysogenum produced in response to raw agricultural waste. **International Journal of Biological Macromolecules**, v. 127, p. 385–395, 2019.

VAAJE - KOLSTAD. **Methods of degrading or hydrolyzing a polysaccharide**, 5 ago. 2011. Disponível em: <https://patents.google.com/patent/US9758802B2/en>. Acesso em: 11 ago. 2019

VAISHNAV, N. et al. Penicillium : The next emerging champion for cellulase production. **Bioresource Technology Reports**, v. 2, p. 131–140, 1 jun. 2018.

VANGULIK, W. M. et al. Energetics of growth and penicillin production in a high-producing strain of Penicillium chrysogenum. **Biotechnology and Bioengineering**, v. 72, n. 2, p. 185–193, 2001.

VASELLA, A.; DAVIES, G. J.; BÖHM, M. Glycosidase mechanisms. **Current Opinion in Chemical Biology**, v. 6, n. 5, p. 619–629, 1 out. 2002.

VISAGIE, C. M. et al. Identification and nomenclature of the genus Penicillium. **Studies in Mycology**, v. 78, n. 1, p. 343–371, jun. 2014.

WERTZ, J.-L. et al. **Hemicelluloses and lignin in Biorefineries**. [s.l: s.n.].

WONG, K. K.; TAN, L. U.; SADDLER, J. N. Multiplicity of beta-1,4-xylanase in microorganisms: functions and applications. **Microbiological reviews**, v. 52, n. 3, p. 305–317, 1988.

WU, H. et al. High efficiency co-production of ferulic acid and xylooligosaccharides from wheat bran by recombinant xylanase and feruloyl esterase. **Biochemical Engineering Journal**, v. 120, p. 41–48, 2017.

XIMENES, E. et al. Enzyme and Microbial Technology Inhibition of cellulases by phenols. v. 46, p. 170–176, 2010.

YANG, Y. et al. A novel bifunctional acetyl xylan esterase/arabinofuranosidase from Penicillium chrysogenum P33 enhances enzymatic hydrolysis of lignocellulose. **Microbial Cell Factories**, v. 16, n. 1, p. 1–12, 2017.

YANG, Y. et al. The composition of accessory enzymes of Penicillium chrysogenum P33 revealed by secretome and synergistic effects with commercial cellulase on lignocellulose hydrolysis. **Bioresource Technology**, v. 257, n. December 2017, p. 54–61, 2018a.

YANG, Y. et al. The composition of accessory enzymes of Penicillium chrysogenum P33 revealed by secretome and synergistic effects with commercial cellulase on lignocellulose hydrolysis. **Bioresource Technology**, v. 257, n. February, p. 54–61, 2018b.

YUAN, J. S. et al. **Plants to power: bioenergy to fuel the futureTrends in Plant Science**, 2008. Disponível em: <https://www.sciencedirect.com/science/article/pii/S1360138508001775>. Acesso em: 22 jul. 2018

ZECHEL, D. L.; WITHERS, S. G. Dissection of nucleophilic and acid–base catalysis in glycosidases. **Current Opinion in Chemical Biology**, v. 5, n. 6, p. 643–649, 1 dez. 2001.

ZHANG, H.; SANG, Q. Production and extraction optimization of xylanase and ??-mannanase by Penicillium chrysogenum QML-2 and primary application in saccharification of corn cob. **Biochemical Engineering Journal**, v. 97, p. 101–110, 2015.

ZHANG, W.; GENG, A. Improved ethanol production by a xylose-fermenting recombinant yeast strain constructed through a modified genome shuffling method. **Biotechnology for Biofuels**, v. 5, n. 1, p. 46, 18 jul. 2012.

ZHANG, X. et al. Exploring the Effect of Cu2+ on Sludge Hydrolysis and Interaction Mechanism between Cu2+ and Xylanase by Multispectral and Thermodynamic Methods. **Water, Air, and Soil Pollution**, v. 228, n. 3, p. 99, 2017.

Waste and Biomass Valorization
https://doi.org/10.1007/s12649-019-00589-x

ORIGINAL PAPER

Biochemical Properties of Carbohydrate-Active Enzymes Synthesized by *Penicillium chrysogenum* Using Corn Straw as Carbon Source

Luísa de M. B. Silva[1] · Tainah C. Gomes[1] · Sadia F. Ullah[1] · Alonso R. P. Ticona[1] · Pedro R. V. Hamann[1] · Eliane F. Noronha[1]

Received: 13 June 2018 / Accepted: 14 January 2019

Abstract
Lignocellulosic material is an alternative, renewable and cheaper source of molecules to be applied in greener industrial processes. Its utilization for this purpose requests steps of pre-treatment and hydrolysis. Filamentous fungi are receiving attention as source of plant cell wall degrading enzymes to apply in lignocellulosic biomass hydrolysis. In the present study, a strain of *Penicillium chrysogenum* CCDCA10756 isolated from Brazilian Cerrado soil (Savannah like biome) was evaluated as a producer of plant cell wall degrading enzymes aiming industrial application. The fungus cultivated in the presence of corn straw as sole carbon source secreted cellulases (endo-β-1,4-glucanases, cellobiohydrolases, β-glucosidases), endo-β-1,4-xylanases, and pectinases. Endo-β-1,4-xylanases and pectinases presented earlier production reaching maximum values after 3 days of growth in comparison to cellulolytic activities mostly produced after 5 days. Cellobiohydrolases and endo-β-1,4-glucanases present maximal activity in acid pH (3 and 4) and at 50 °C, whereas β-glucosidase presents maximal activity at pH 5.0 and 60 °C. Pectinases showed maximum activity in pH 8 at 50 °C. Furthermore, endo-β-1,4-glucanases and cellobiohydrolases displayed remarkable thermostability at 40 °C. Lignin-derived compounds, trans-ferulic acid, 4-hydroxybenzoic and syringaldehyde inhibited cellobiohydrolases. Pectinolytic activity, instead, was improved in the presence of *p*-coumaric acid, trans-ferulic acid, and syringaldehyde.

Keywords Cellulases · Biorefinery · Lignocellulosic biomass · Bioethanol

Statement of Novelty

In the present work, we showed the potential use of a strain of *Penicillium chrysogenum* from Savannah-like biome in Brazil as model fungi to produce plant cell wall degrading enzymes using corn straw as a carbon source. In addition to previous works which showed *P. chrysogenum* as a producer of hemicellulases, we described a natural blend containing all the enzymes related to the complete hydrolysis of holocellulose. We provided also a detailed enzymatic characterization of produced enzymes and novel information concerning pectinases tolerance to lignin derived phenolics and activity on alkaline pH, as well as, cellulases' thermal stability. Data presented here will support the use of *P. chrysogenum*'s hollocellulases in industrial lignocellulose deconstruction processes.

Introduction

Lignocellulose is an abundant and renewable source of molecules with biotechnological interest, daily produced and discarded as waste worldwide in result of agro-industrial activities [1]. In Brazil, agriculture is a relevant economic sector corresponding to 21.6% of Brazilian Gross Domestic Product (Base year 2017 CEPEA/Esalq http://www.cepea.esalq.usp.br). Corn is the fourth largest crop of Brazil, in 2010 its production generated about 46 million tons of agricultural residues, which would be converted to 4.4 billion liters of cellulosic ethanol [2].

Lignocellulose mainly found in plant cell wall is constituted by cellulose (45–60%), hemicellulose (20–40%), pectin

Luísa de M.B.Silva and Tainah C. Gomes have equally contributed to this work.

✉ Pedro R. V. Hamann
pedrorvhamann@gmail.com

[1] Cell Biology Department, Enzymology Laboratory, Universidade de Brasilia, Brasilia 70910-900, Brazil

Published online: 22 January 2019

(5–10%) and lignin (10–40%) and its utilization as feedstock depends on its complete hydrolysis. Fermentable sugars, in special glucose, liberated by cellulose and hemicellulose deconstruction can be used into fuel production, ethanol and butanol [3, 4]. Lignin and hemicellulose-derived monomers also presented industrial applications [5, 6]. In fact, lignocellulose complete utilization is a desirable approach to reach an economically viable process based on the use of lignocellulose as feedstock [7].

Despite the potential use of lignocellulose as feedstock in biorefinery, technical barriers have been hampering its utilization on large scale industrial processes. Commercial feasibility of lignocellulose biodegradation into fermentable sugars and other derived monomers due its recalcitrance is one of the most important barriers to be overcome. The current process industrially used included a first step of pre-treatment, followed by saccharification. Pre-treatment is carried to disrupt lignocellulose fibers and remove lignin making hemicellulose and cellulose available to the further step. Saccharification is carried using plant cell wall degrading enzymes, in special *Trichoderma reseei* and *Aspergillus spp* enzymes [8].

Production of enzymatic cocktails is still costly and the commercially available blends present variable efficiency on hydrolysis, according to the source of lignocellulose and the presence of inhibitory molecules generated during pre-treatment. Therefore, a continued characterization of sources of such enzymes, together with an improved understanding of the mechanisms involved in enzyme efficiency are of fundamental importance for biorefineries based on lignocellulose as feedstock.

In addition, an efficient industrial process of enzymatic lignocellulose deconstruction should closely resemble natural ecosystems in which biodegradation of lignocellulose is accomplished by a consortium of diverse microorganisms and their enzymes rather than individuals. Microbial lignocellulose degradation is carried in nature by plant cell wall active enzymes presenting activity against cellulose, hemicelluloses, pectin and lignin. Cellulose acting enzymes included: cellobiohydrolases (EC 3.2.1.90), endo-β-1,4-glucanases (EC 3.2.1.4), and β-glucosidases (EC 3.2.1.21), which in synergism completely hydrolyze cellulose [9]. Hemicellulose deconstruction required a more diverse group of enzymes since is a ramified heteropolysaccharide. The major backbone of xylan is hydrolyzed by endoxylanases (EC 3.2.1.8), whereas xylooligosaccharides are converted to D-xylose units by the action of β-xylosidases (EC 3.2.1.37). Ramifications and acetyl groups associated to xylan main backbone are mostly removed by the action of α-L-arabinofuranosidases (EC 3.2.1.55), acetyl xylan esterase (EC 3.2.1.1), and feruloyl esterase (EC 3.1.1.73) [10, 11]. Pectin active enzymes included polygalacturonases (EC 3.2.1.15), pectinesterase (EC 3.1.1.11), and pectin lyase (EC 4.2.2.10) [12–14], these enzymes act in synergism aiming pectin main backbone degradation. At first, considered as accessory activities, hemicellulose and pectin degrading enzymes are essential to a complete deconstruction of lignocellulose.

Auxiliary activities such as: lytic polysaccharide monooxygenases (LPMOs), laccases and expansins are also required to the complete lignocellulose de-polymerization [16, 19–22]. LPMOs catalyze the oxidative breakdown of cellulose at C1 or C4 carbons increasing the number of reducing and non-reducing extremities available to cellobiohydrolases [15]. Laccases catalyze oxidation of lignin, modifying its structure and increasing hemicellulases and cellulases accessibility to plant cell wall carbohydrate core [16, 17]. Swollenins disrupted hydrogen bounds between cellulose's filaments increasing cellulases' accessibility to cellulose [18].

Previous literature has largely debated about *Trichoderma* and *Aspergillus* species particularly efficient in the production of cellulases and hemicellulases and their ability to deconstruct lignocellulose [8, 9]. However, other species also are focus of research due to their potential to produce in addition to cellulases, hemicellulases, pectinases and auxiliary activities [19–22].

Penicillium chrysogenum, previously studied as source of antimicrobial activities, nowadays is gaining attention as producer of cellulases, xylanases and pectinases [23]. This specie has been characterized as an efficient producer of xylanase rather than cellulases, secreting a larger number of hemicellulases, as endoxylanases, β-xylosidases, α-galactosidases, α-arabinofuranosidases, β-mannosidase, and carboxylesterases during growth on wheat bran plus microcrystalline cellulose as carbon source [24]. However, information regarding auxiliary activities, as well as, detailed enzymatic characterization are still scarce. Including, those related to tolerance/stability to industrial processes conditions (pH, temperature, salt concentration) and compounds liberated during lignocellulosic biomasses deconstruction.

Given the importance to develop enzymatic blends able to complete deconstruct lignocellulose compatible to industrial processes and reduction on enzyme production cost. In the present work, we evaluated the use of corn straw as carbon source by *P. chrysogenum* to produce plant cell wall hydrolases, as well as, characterized physical–chemical properties of the enzymatic mixture produced.

Methodology

Fungal Isolation and Maintenance

Soil samples obtained from Cerrado's soil (Unaí -Minas Gerais State, Brazil), were diluted in de-ionized water and

then plated on MYG solid media (yeast extract 2.5 g L^{-1}, malt extract 5 g L^{-1}, glucose 10 g L^{-1}, and agar 20 g L^{-1}), with addition of 50 mg L^{-1} of oxytetracycline to avoid bacterial growth. Fungi strains were isolated on basis of morphology and purified cultures were inoculated on MYG agar plate supplemented with 1% (*w*/*v*) oat-spelt xylan (Sigma-Aldrich, USA), or 1% (*w*/*v*) carboxymethylcellulose (CMC) (Dinâmica, Brazil). After growth, plates supplemented with carbohydrates were stained with 0.1% (*w*/*v*) congo red and then isolates that showed the highest degradation halo selected to further experiments. One of the isolates was classified as *P. chrysogenum*, on the base of ITS and β-calmodulin sequences, as well as, morphometricanalysis. This fungi strain was deposited in Universidade Federal de Lavras (Minas Gerais, Brazil), under the accession code CCDCA10756. Fungus preservation was done by adding two mycelial disks (Ø 1 cm) in cryotubes containing 50% (*v*/*v*) glycerol solution at − 80 °C.

Biomass Preparation, Enzyme Production and Sample Preparation

Corn straw was obtained from local farms (Brasilia—Df, Brazil), autoclaved for 1 h, rinsed with tap water, and oven-dried at 60 °C until reaching a constant weight. Dried biomass was subjected to milling by using industrial food blender [Skymsen, Brazil (Model TA-02-N 900W)], the resulted powder was then used to supplement growth media.

Enzyme production was carried out by culturing *P. chrysogenum* in minimum mineral media as described by [25] at 28 °C in a rotary shaker at speed of 120 rev min^{-1}. Mineral media supplemented with 1% (*w*/*v*) of corn straw was autoclaved and inoculated by mycelia disk (Ø 1 cm) collected from a 10 days old MYG fungi culture. An aliquot of 1 mL was withdrawn from inoculated culture media after every 24 h and used as a source of enzymes to plot enzyme production curves. Growth media from the 10th day was used as a source of enzymes for biochemical characterization. Shortly, the supernatant was vacuum filtered using filter paper (Whatman® number 5), and then centrifuged at 10,000 × *g* for 20 min at 4 °C, the final clarified broth was named culture filtrate.

Enzymatic Activity and Protein Quantification

For pectinase, xylanase, endoglucanase, and cellobiohydrolase activities quantification, standard enzymatic assays were carried out using 50 µL of culture filtrate and 100 µL of substrate at 0.5% (*w*/*v*) for oat-spelt xylan (Sigma Aldrich, USA), carboxymethylcellulose (Dinâmica, Brazil), citrus pectin (Sigma Aldrich, USA), and Avicel® PH101 (Sigma Aldrich, USA) dissolved in 100 mM sodium acetate buffer, pH 5.0. Enzymatic assays were incubated at 50 °C for 30 min (xylanase, endoglucanase, and pectinase) or 1 h (cellobiohydrolase), the reaction was stopped by addition of 300 µL of 3,5-dinitrosalycilic acid, and then boiled for 10 min, the colorimetric reaction was read in a spectrophotometer at 540 nm [26]. Standard curves were built using the monomeric sugars, D-glucose, D-xylose, and galacturonic acid. Activities of β-glucosidase and cellobiohydrolase (thermostability experiment) were determined using 100 µL of 4-nitrophenyl β-D-glucopyranoside at 2 mM, and 4-nitrophenyl β-D-cellobioside at 2 mM, dissolved in 100 mM sodium acetate buffer pH 5.0. The reaction was carried for 30 min at 50 °C, and stopped by adding 300 µL of sodium carbonate 1 M. Colorimetric reaction was read in a spectrophotometer at 405 nm, a standard curve was built using *p*-nitrophenol. One enzymatic unit (IU mL^{-1}) was defined as the amount of enzyme required to produce 1 µmol of product per minute. Protein quantification was performed by using Quick Start™ Bradford 1 × Dye Reagent (Bio-Rad Laboratories Inc., USA) following manufacturer instructions, bovine serum albumin was used standard, the reaction was read at 595 nm [27].

Temperature Analysis, pH Optima, and Stability in Different pH

The effect of temperature on holocellulases was carried out ranging the temperature from 30 to 80 °C using the standard enzymatic assay, above described. The pH effect was carried out changing the buffer system to phosphate-citrate buffer at 100 mM in a pH range from 3 to 8. Stability in different pHs was determined to measure residual activity after incubation for 1 h at 60 °C in 100 mM phosphate-citrate buffer pH 3–8.

Inhibition of Holocellulases by Lignin-Derived Compounds

The effect of lignin components on pectinase, cellobiohydrolase, endoglucanase, β-glucosidase, and xylanase activities was carried out using: tannic acid, vanillin, *p*-coumaric acid, trans-ferulic acid, 4-hydroxybenzoic, syringaldehyde, gallic acid and trans-cinnamic acid. Briefly, 50 µg o proteins were incubated with inhibitors for 12 h at 25 °C, lignin compounds were utilized in final concentration of 0.020 mg mL^{-1}, 0.100 mg mL^{-1}, and 0.200 mg mL^{-1}. These concentrations were used since they corresponds to a phenolic/protein ratio 0.4–4, within the interval on which cellulases of commercial mixtures were assayed in front of biomass inhibitory compounds, previously described by Ximenes et al. [29]. Activities were measured using the standard enzymatic assay.

Ions Effect on Enzymatic Activities

The effect of ions was evaluated using the following ions: sodium chloride, cobalt(II) chloride, magnesium chloride, zinc chloride, calcium chloride, iron(III) chloride, copper(II) chloride, potassium chloride, and ethylenediaminetetraacetic acid (EDTA). Based on current literature about enzymes involved in plant cell degradation, theses ions were chosen, and assayed in concentration 1–10 mM [30].

SDS-PAGE and Zymogram

SDS-PAGE (12%) was performed using proteins samples from culture filtrates pooled every 24 h growth time. Electrophoresis procedures were carried out as described by [31],protein precipitation was carried out by trichloroacetic acid preparation. After the electrophoresis run, protein bands were visualized by staining with Coomassie brilliant blue G-250 (USB Corporation, USA). The molecular mass standard used was Unstained Protein Marker #26610 (Thermo Scientific, USA), which contains β-galactosidase (116.0 kDa), bovine serum albumin (66.2 kDa), ovalbumin (45.0 kDa), lactate dehydrogenase (35.0 kDa), REase Bsp98I (25.0 kDa), β-lactoglobulin (18.4 kDa) and lysozyme (14.4 kDa).

For xylanase and endoglucanase zymograms were prepared polyacrylamide gels 12% co-polymerized with oat-spelt xylan 0.1% (*w*/*v*) or CMC 0.1% (*w*/*v*). Electrophoresis run was carried out in denaturing conditions [31]. Gels were washed with Triton™ X-100 (Sigma Aldrich, USA) 2.5% (*v*/*v*) for 1 h, followed by wash step with distilled water and incubated at room temperature for 1 h in 50 mM sodium acetate buffer pH 5.0. Then gels were incubated at 50 °C for 1 h, for xylanase zymogram, and 12 h for endoglucanases. After the incubation time, gels were soaked in a congo red solution 0.1% (*w*/*v*) for 15 min at room temperature. Right after the gels were washed with NaCl 1 M until the excess of congo red was removed from active bands. Acetic acid 0.5% (*v*/*v*) was added to the gels for better visualization.

Statistical Analyses

Statistical analyses were performed using SigmaPlot v.12.0 (Systat Software Inc, USA). Statistical significance was defined as $p < 0.05$.

Results and Discussion

Penicillium chrysogenum CCDCA10756 produced endo-β-1,4-glucanases, cellobiohydrolases, β-glucosidases, pectinases, and endo-β-1,4-xylanases during growth in liquid media containing corn straw as carbon source, reaching maximum protein secretion after 4 days of cultivation (Fig. 1a). Endo-β-1,4-xylanases and pectinases activities were earlier produced in comparison to cellulases, being detected in the first day of growth (Fig. 1c, f). On the other hand, cellobiohydrolase and endo-β-1,4-glucanase activities were detected after 3 and 6 days of growth, respectively. Endo-β-1,4-xylanases and pectinases activities presented a constant increase from day 1 to 6th, in which reaches their maximum values. Maximal endo-β-1,4-glucanase activity was obtained on the 8th day, meanwhile cellobiohydrolase was maximal after the 9th day (Fig. 1b, d). In agreement to our results a previous study showed a similar pattern of production of endo-β-1,4-xylanases and endo-β-1,4-glucanase by *P. chrysogenum* P33 growing on a mixture of wheat bran and microcrystalline cellulose as carbon source [24].

Co-production of cellulose, hemicellulose and pectin acting enzyme is a desirable feature for enzymatic blends applied to lignocellulosic materials hydrolysis. Pectin active enzymes seems to be critical to increase the level of xylose and glucose liberated, as previously showed for corncob hydrolysis by a mixture of xylanases and cellulases amended with a commercial pectinase [32].

β-glucosidase activity was obtained from the second day to 10th, reaching its maximum value after 8 days (Fig. 1e). This activity also presented a critical role in cellulose deconstruction, acting in synergism with endo-β-1,4-glucanases and cellobiohydrolases to complete hydrolyze cellulose. In addition to this cooperative effect, β-glucosidases consume cellobiose preventing its inhibitory effect on cellobiohydrolases [33]. As above discussed for pectinase activity, the enzymatic blend here described presented the remarkable feature to contain cellobiohydrolases, endo-β-1,4-glucanases alongside β-glucosidases. Currently, there is no record of microorganisms with enhanced production of these enzymes alongside.

Zymogram carried to detect endo- β-1,4-glucanases showed a single band of 35 kDa within the first 2 days and two additional activity bands with estimated molecular mass of 45 and 66 from the third to the fifth day of growth (Fig. 2a, b). As showed for endo- β-1,4-glucanases, isoforms of endo- β-1,4-xylanases were produced by *P. chrysogenum* CCDCA10756. Two major isoforms with estimated molecular masses of 16 and 25 kDa were detected within the first 24 h and a third one with estimated molecular mass of 18 kDa after the second day of growth (Fig. 2c). Endo-β-1,4-glucanase production profile using zymogram analysis was different from that showed in Fig. 1b. This difference might occur by difference on enzymatic sample preparation. Enzymatic samples for zymogram analysis were concentrated, whilst culture filtrate used in enzymatic assays was used as source of enzymes without previous concentration step.

Endo-β-1,4-glucanase, cellobiohydrolases, pectinases, endo-β-1,4-xylanases produced by *P. chrysogenum*

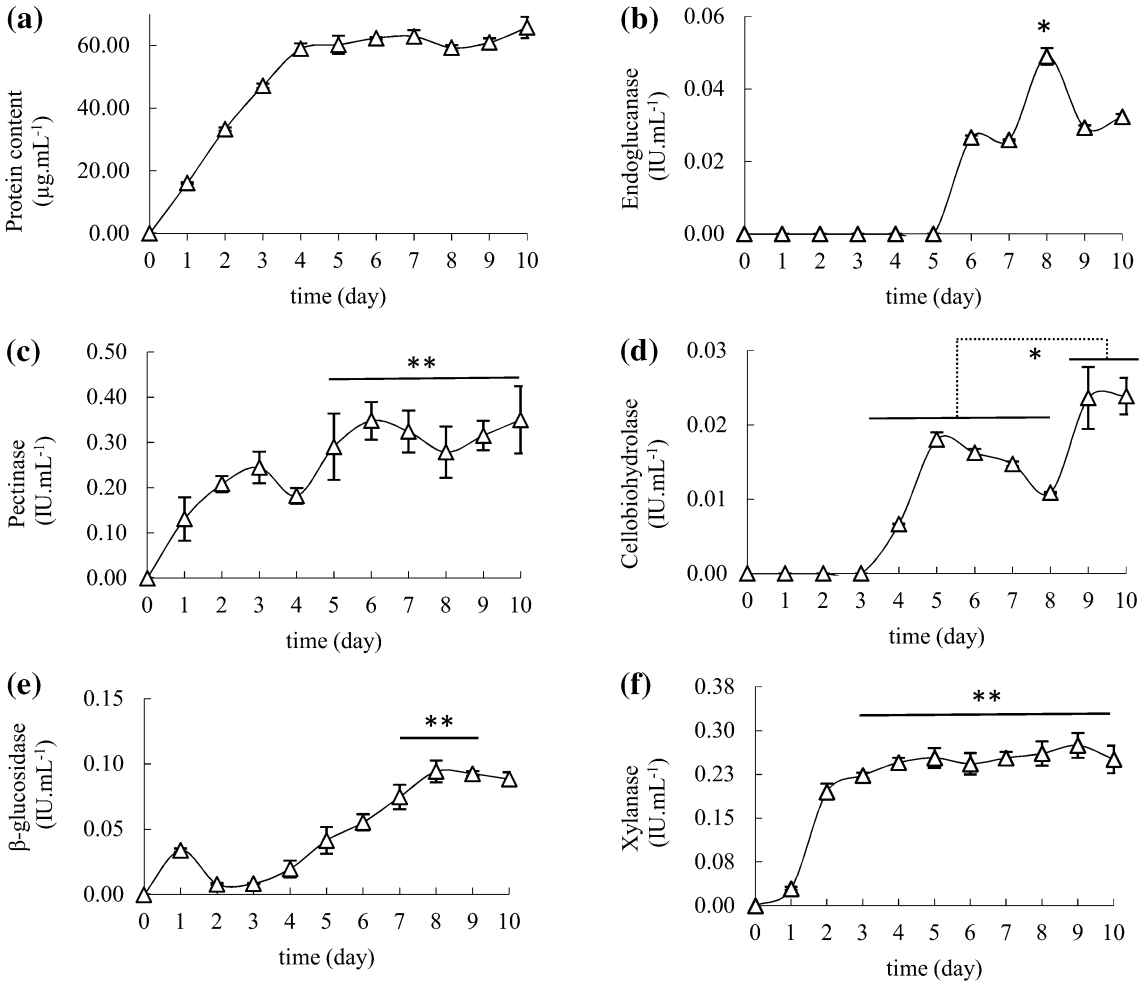

Fig. 1 Time course production of **a** proteins, and enzymatic activities: **b** endoglucanase, **c** pectinase, **d** cellobiohydrolase, **e** β-glucosidase and **f** xylanase produced by *P. chrysogenum* during growth in liquid media containing corn straw 1% (*w*/*v*) as a carbon source. Vertical bars represent standard deviation from biological triplicates. * $p < 0.05$, ** $p > 0.05$

presented highest activity at 50 °C and β-glucosidase at 60 °C (Fig. 3). Endo-β-1,4-xylanases and endo-β-1,4-glucanases presented a broader range of acting temperature in comparison to pectinases, β-glucosidases and cellobiohydrolases (Fig. 3). Haas et al. [34], in other hand, described maximum xylanolytic activity at 40 °C for a purified xylanase from *P. chrysogenum* Q 176. This difference might be related to the sample, since enzymatic characterization performed in our study used as sample the whole secretome instead of the purified enzyme.

β-glucosidase optimum temperature varies from 50 to 70 °C among *Penicillium* species [35, 36]. This contrasting profile between Penicillium β-glucosidases may lead these enzymes to different applications. Enzymes with maximum activity above 50 °C have their operational temperature in a range similar to commercial cellulases, and thus preferentially sought after for its use in lignocellulose saccharification.

Regarding pH effect, endo-β-1,4-glucanases and cellobiohydrolases presented maximum activities at pH 3 and 4, whereas maximum β-glucosidase activity was obtained in the range pH 5–6. Endo-β-1,4-xylanases presented activity over a broad pH range with maximum activity in pH 3 up to 6. Pectinases, instead, presented highest activity in alkaline pH, pH 8 (Fig. 4).

Our results are in agreement to optimum pH values detected for plant cell wall hydrolases produced by different *P. chrysogenum* isolates in exception to pectinase activity [34, 37, 38]. Activity at alkaline pH add a potential use of *P. chrysogenum* CCDCA10756 pectinases in other biotechnological applications, such as, textile processing, paper industry, and degumming of plant fibers [39].

In respect to stability in different pH, endo-β-1,4-glucanases and endo-β-1,4-xylanases retained, 18 and 5.76% of activity at pH 3, respectively (Fig. 5). Whereas maximum activity retention occurred in pH 7 for

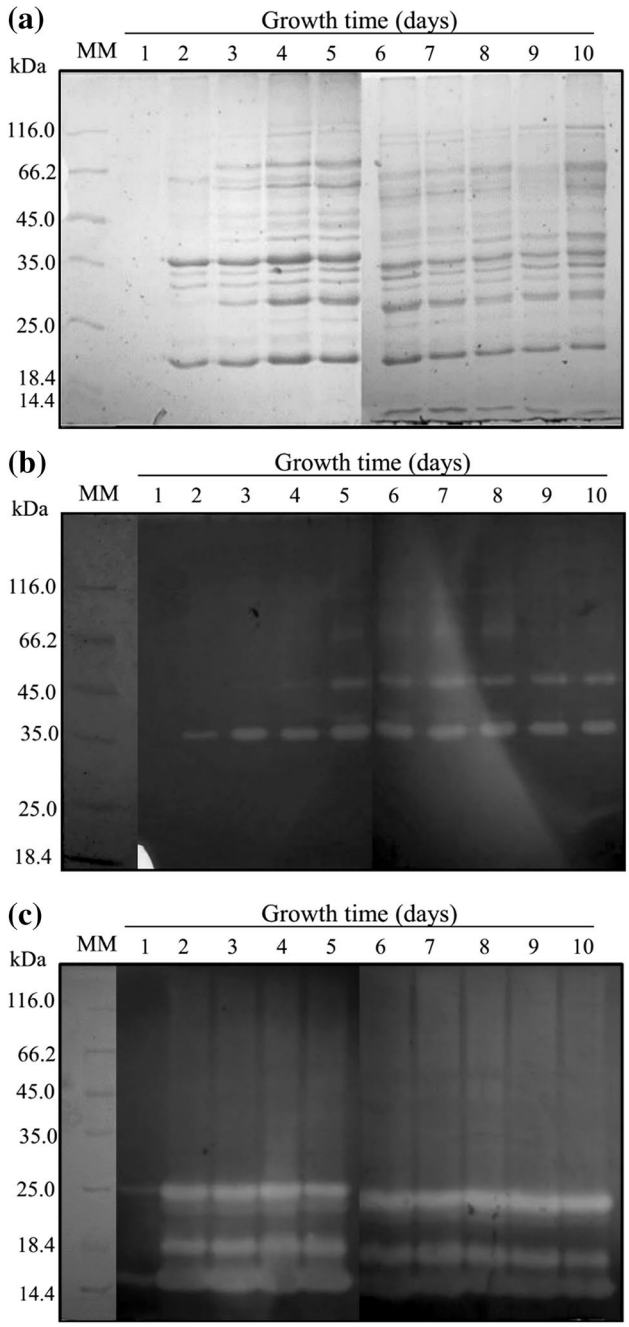

Fig. 2 Protein and enzymatic activity profile of pooled samples from culture filtrate electrophoresis SDS-PAGE in 12% gels (**a**); zymogram showing endoglucanase (**b**); and xylanase (**c**) activities. Lanes represent samples from different growth days from *P. chrysogenum* cultured in corn straw 1% (*w/v*), and mass marker (MM)

endo-β-1,4-glucanases, and pH 5 for endo-β-1,4-xylanases. Cellobiohydrolases in pH 4 and 6 presented no significant activity loss. β-glucosidases displayed maximum activity retention in pH 5 and 6. For pectinases, maximum activity was maintained in acid pH range from 3 up to 5. For pH values above six pectinases were more susceptible to activity

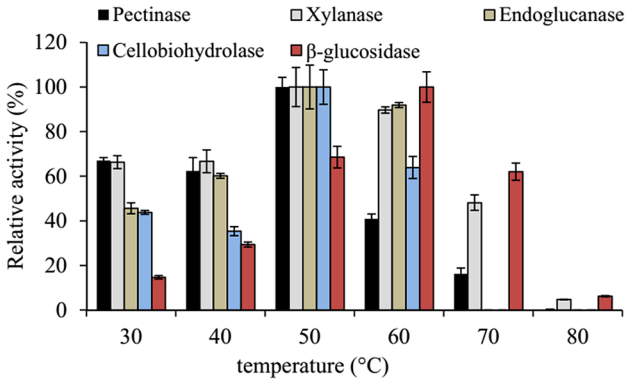

Fig. 3 Temperature effect on pectinase (black bars), endoglucanase (brown bars), xylanase (grey bars), cellobiohydrolases (blue bars), and β-glucosidases (red bars) activities produced by *P. chrysogenum* after 10 days growth time in the presence of corn straw 1% (*w/v*). Vertical bars represent standard deviation from technical triplicates. (Color figure online)

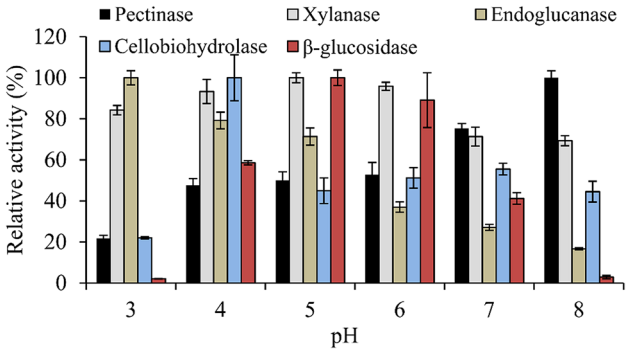

Fig. 4 pH effect on pectinase (black bars), endoglucanase (brown bars), xylanase (grey bars), cellobiohydrolases (blue bars), and β-glucosidases (red bars) activities produced by *P. chrysogenum* after 10 days growth time in the presence of corn straw 1% (*w/v*). Vertical bars represent standard deviation from technical triplicates. (Color figure online)

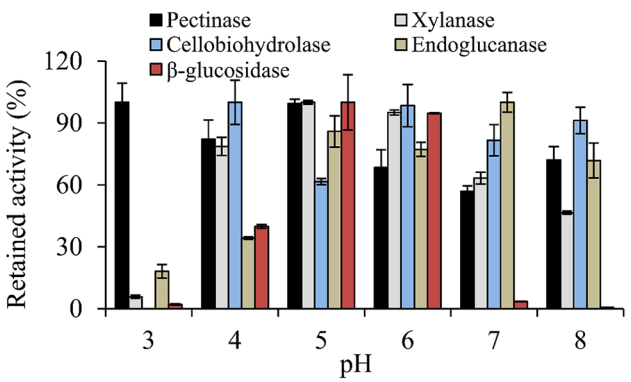

Fig. 5 pH stability of pectinase (black bars), xylanase (grey bars), cellobiohydrolase (blue bars), endoglucanase (brown bars), and β-glucosidases (red bars) activities produced by *P. chrysogenum* after 10 days growth time in the presence of corn straw 1% (*w/v*). Vertical bars represent standard deviation from technical triplicates. (Color figure online)

loss, retaining 72.10% of activity at pH 8. pH stability is an essential information to decide which application is suitable to enzyme preparations.

In the present study, β-glucosidase, endo-β-1,4-xylanases and endo-β-1,4-glucanases activities had stability in pH range close to 5, interval on which industrial enzymes are usually assayed. The lower stability observed to pectinases in more alkali pH in comparison to more acidic pH range, differ from the alkaline pectin lyase describe for *P.italicum* [40].

Cellulases (β-glucosidase, endo-β-1,4-glucanases and cellobiohydrolases) exhibited minor activity loss during time incubation at 40 and 50 °C (Fig. 6). Amongst cellulases, endo-β-1,4-glucanases had higher activity decay, after 72 h time incubation at 50 °C, half of the original activity value was detected. Endo-β-1,4-xylanase activity showed a similar activity decay profile at 40 and 50 °C, retaining close to 40% of original activity. As observed for endo-β-1,4-xylanase, the activity decay profile for pectinases was very similar between both temperatures, being 20% of activity maintained after 72 h time incubation.

Endo-β-1,4-glucanase activities secreted by *P. chrysogenum* reported in the present study, had minor activity loss when comparing to the endo-β-1,4-glucanase GH12 obtained from *Aspergillus terreus*, which was stable for 4 h at 50 °C [41]. Indeed, the thermostability of *Penicillium* cellulases have been reported to other species, in example, the β-glucosidase GH3 from *P.brazilianum* displayed no activity loss after 24 h at 60 °C [36].

Endo-β-1,4-glucanases are inhibited by $FeCl_2$, $CuCl_2$, and no effect was noticed by $CoCl_2$ at 10 mM. Endo-β-1,4-xylanase activity, instead, was increased about 10 and 20% by $CoCl_2$ at 1 and 10 mM, respectively (Table 1). Major activity loss for this activity occurred in the presence of EDTA, and $CuCl_2$ at 10 mM, resulting in 68.99 and 65.86% of activity, respectively (Table 1). For pectinase, as observed

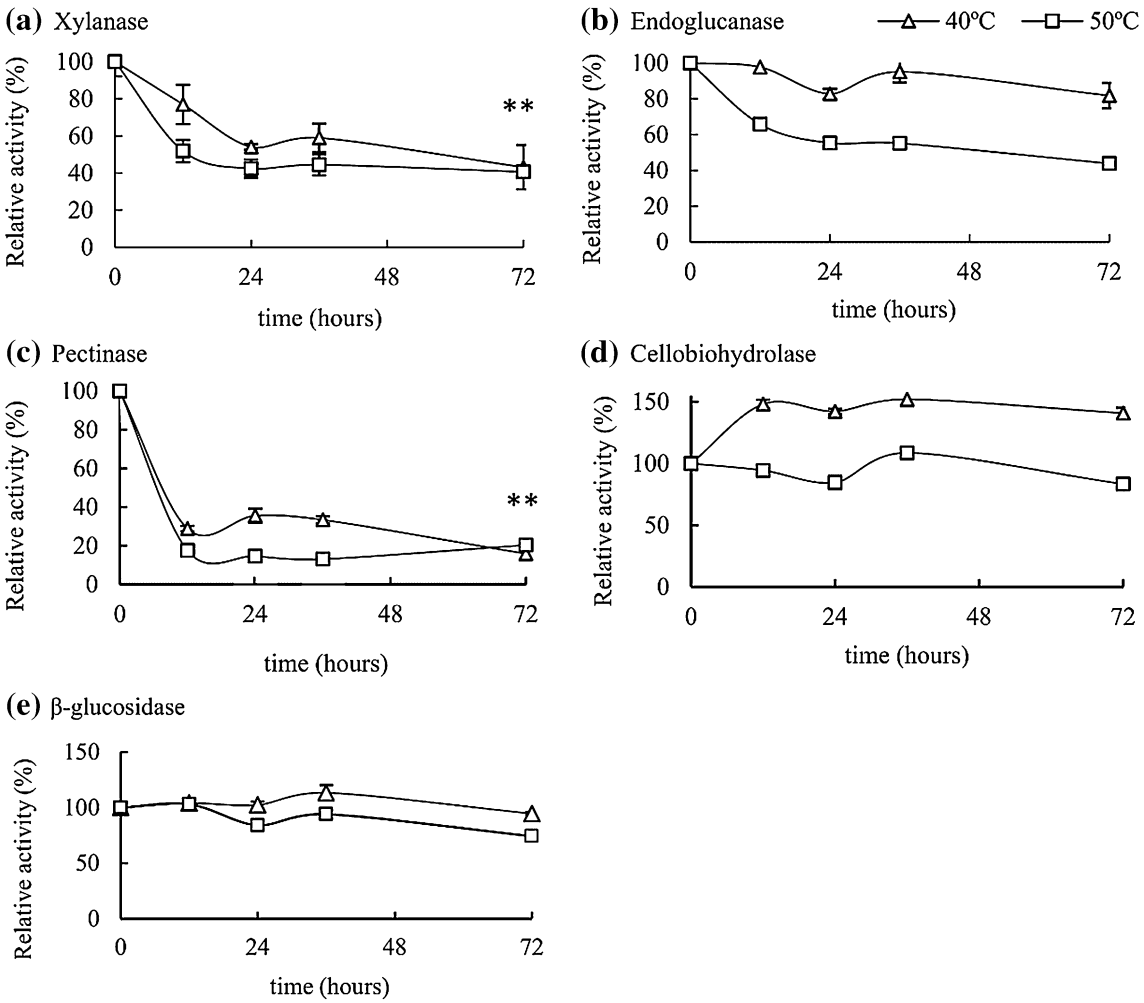

Fig. 6 Thermostability of **a** xylanase, **b** endoglucanase, **c** pectinase, **d** cellobiohydrolase, and **e** β-glucosidase activities produced by *P. chrysogenum* after 10 days growth time in the presence of corn straw 1% (*w*/*v*). Triangles and squares respectively represent incubation at 40 and 50 °C. Vertical bars represent standard deviation from technical triplicates. ** $p > 0.05$

Table 1 Ions (NaCl, $CoCl_2$, $MgCl_2$, $ZnCl_2$, $CaCl_2$, $FeCl_2$, $CuCl_2$, KCl) and EDTA effect over xylanase, pectinase, endoglucanase, cellobiohydrolase, and β-glucosidase activities produced by *P. chrysogenum*

		Xylanase	Pectinase	Endoglucanase	Cellobiohydrolase	β-Glucosidase
NaCl	1 mM	86.85 ± 3.69	92.10 ± 9.70	85.27 ± 4.56	**96.32 ± 8.81**	117.06 ± 2.15
	10 mM	94.82 ± 0.87	39.80 ± 6.18	63.41 ± 2.39	**80.20 ± 9.14**	78.97 ± 6.00
$CoCl_2$	1 mM	115.93 ± 2.5	**70.06 ± 6.10**	**100 ± 10.95**	27.50 ± 3.17	109.67 ± 0.89
	10 mM	136.52 ± 2.94	**72.80 ± 1.64**	**92.33 ± 4.70**	84.99 ± 3.20	75.90 ± 3.94
$MgCl_2$	1 mM	**92.49 ± 2.00**	**87.93 ± 6.92**	72.69 ± 5.13	26.42 ± 2.51	113.38 ± 0.89
	10 mM	**91.63 ± 0.06**	**101.09 ± 7.48**	100 ± 10.82	61.23 ± 3.42	82.93 ± 5.14
$ZnCl_2$	1 mM	86.65 ± 0.95	79.27 ± 4.21	**96.31 ± 7.66**	9.12 ± 0.49	113.43 ± 4.52
	10 mM	72.84 ± 3.38	39.91 ± 5.26	**90.94 ± 5.41**	119.28 ± 8.70	51.66 ± 7.42
$CaCl_2$	1 mM	**91.10 ± 3.63**	**62.60 ± 5.6**	92.94 ± 7.84	43.37 ± 1.13	**118.39 ± 1.33**
	10 mM	**88.24 ± 15.09**	**69.07 ± 6.15**	78.39 ± 3.86	79.06 ± 3.16	**100.80 ± 25.51**
$FeCl_2$	1 mM	**76.62 ± 5.87**	79.60 ± 8.51	67.48 ± 4.24	–	118.27 ± 2.33
	10 mM	**76.89 ± 1.94**	34.64 ± 6.86	42.50 ± 3.65	3.38 ± 0.24	–
$CuCl_2$	1 mM	83.66 ± 0.66	75.87 ± 6.39	72.39 ± 10.47	21.78 ± 3.55	43.77 ± 5.43
	10 mM	65.86 ± 0.87	33.55 ± 9.40	18.46 ± 3.34	41.85 ± 1.71	6.35 ± 1.10
KCl	1 mM	85.92 ± 1.67	52.74 ± 8.62	**72.39 ± 9.65**	**52.61 ± 4.53**	118.56 ± 3.05
	10 mM	79.88 ± 2.42	73.35 ± 1.24	**66.55 ± 8.02**	**59.69 ± 2.83**	91.60 ± 5.45
EDTA	1 mM	81.14 ± 0.88	76.09 ± 4.00	84.20 ± 4.00	**71.12 ± 3.47**	110.12 ± 2.50
	10 mM	68.99 ± 2.44	111.07 ± 4.88	59.23 ± 11.90	**80.57 ± 4.96**	90.33 ± 6.28

Activity not detected (−), standard deviation from technical triplicates (±). Numbers highlighted in bold $p>0.05$

for endo-β-1,4-glucanases, $FeCl_2$ and $CuCl_2$ caused highest activity loss, resulting in 34.64 and 33.55% of original activity. In respect to β-glucosidase activity, most assayed compounds at 1 mM increase its activity, an exception to copper chlorine, which inhibited enzymatic activity by 43.77 and 6.35%, at 1 and 10 mM, respectively.

Commonly, ions such as calcium have been reported as cellulases activators [42], however, in the present study, this ion showed an inhibitory effect over endo-β-1,4-glucanases, and cellobiohydrolases. Inhibition of cellulolytic enzymes by $CoCl_2$ has previously been reported by Akiba et al. [43] for a cellulase produced by *Aspergillus niger*. In addition, for a xylanase produced by *Aspergillus awamori* $CuSO_4$, and $CoCl_2$ at 10 mM occasioned minor inhibition [44].

The nature of activation or inhibition of holocellulases possibly arises from multiple interactions between enzymes and ions. However, the mechanism behind cellulases inhibition by copper and iron, have not been fully elucidated. Indeed, Tejirian and Xu [46] described that cellulases inhibition by ferrous/ferric compounds occurs by means of a redox reaction. Glycoside hydrolases achieve acid catalysis through the action of aspartate and/or glutamate amino acid residues working as a proton donor and nucleophile pair [47], a reaction that might be disrupted in the presence of alternative donor/acceptor. The fact that glycoside hydrolases have this conserved mechanism, may possibly explain the reason $FeCl_2$ caused major inhibition over cellobiohydrolases, endo-β-1,4-glucanases, β-glucosidases and pectinases as shown in this study.

In addition to protein/ion interaction, copper and iron compounds are able to interact with reducing sugars generated during cellulose/hemicellulose deconstruction, and then chemically modifying the substrate [46, 48]. This modification is critical for some cellobiohydrolases, which may recognize the substrate by reducing ends [49], leading this class of enzyme to not recognize cellulosic substrates and thus resulting in inhibition, as observed in the present study. In addition, the excess of copper can oxidase glucose at C1 and generate gluconic acid, which may represent a major inhibitor for β-glucosidases. Cannella et al. [50] demonstrated that β-glucosidases from commercial preparation are inhibited in a higher degree by gluconic acid in comparison to glucose, this information supports the inhibitory profile observed for *P. chrysogenum*'s β-glucosidases in interaction with copper chlorine.

Although, the nature of ions and its concentration may vary from biomass, as well as, hydrolises conditions *e.g* additives used for enzyme production, and water quality. The molarity range used in the present study is in accordance to the reported for characterization of cellulases [41], hemicellulases [51] and pectinases [52], bringing a good *proxy* in terms of comparison to others lignocellulosic enzymes Monti et al. [53] described that for different plant structures from energy crops, a distinguish mineral composition may be observed. Ions such as Al, Ca, Cl, Fe, K, Mg, Na are found in the lignocellulosic structure, however, it's not expected that all ions will be freely available in hydrolyses slurry for protein/ion interaction.

Penicillium chrysogenum's endo-β-1,4-glucanase were not inhibited by phenolic compounds at 0.02 mg/mL (0.4 phenolic/protein ratio), however; tannic acid and vanillin at 0.1 (2 phenolic/protein ratio) and 0.2 mg/mL (4.0 phenolic/protein ratio) caused slight activity increment (Fig. 7c). For others assayed compounds at 0.2 mg/mL, endo-β-1,4-glucanase had accentuate activity abatement, in special for *p*-coumaric-acid and gallic acid, causing almost all activity to be inhibited. Similar to the profile observed for endo-β-1,4-glucanase activity, phenolic compound at 0.02 mg/mL caused no activity change in endo-b-1,4-xylanases (Fig. 7a), however at 0.1 mg/mL tannic acid and vanillin caused moderate activity abatement ~ 25%. At higher concentration of phenolic compounds, endo-β-1,4-xylanase were inhibited, majorly by *p*-coumaric acid, trans ferulic acid and trans cinamic acid. β-glucosidases (Fig. 7e), displayed slight activity abatement at 0.02 mg/mL for tannic and vanillin ~ 20%. At 0.2 mg/mL *p*-coumaric acid, trans-ferulic acid, and trans cinamic acid caused major activity loss > 50%; whereas 4-hydroxybenzoic acid abolished β-glucosidase activity. Cellobiohydrolase (Fig. 7d) showed a dissimilar profile, tannic acid at 0.02 and 0.1 mg/mL caused slight activity increment, for trans cinnamic acid is observed actvity increment at 0.02 mg/mL. Despite these particular enhancements, phenolic compounds caused major activity abatement for cellobiohydrolases, being observed activity loss around 50% in the presence of vanillin, trans ferulic acid, and 4-hydroxybenzoic acid in all assayed concentrations of phenolic compounds. Pectinases (Fig. 7b) were mainly inhibited by tannic acid at 0.1 and 0.2 mg/mL, compounds such as *p*-coumaric acid, trans ferulic acid, 4-hydroxybenzoic acid, syringaldehyde and gallic acid caused a progressive enzyme activation from 0.1 to 0.2 mg/mL.

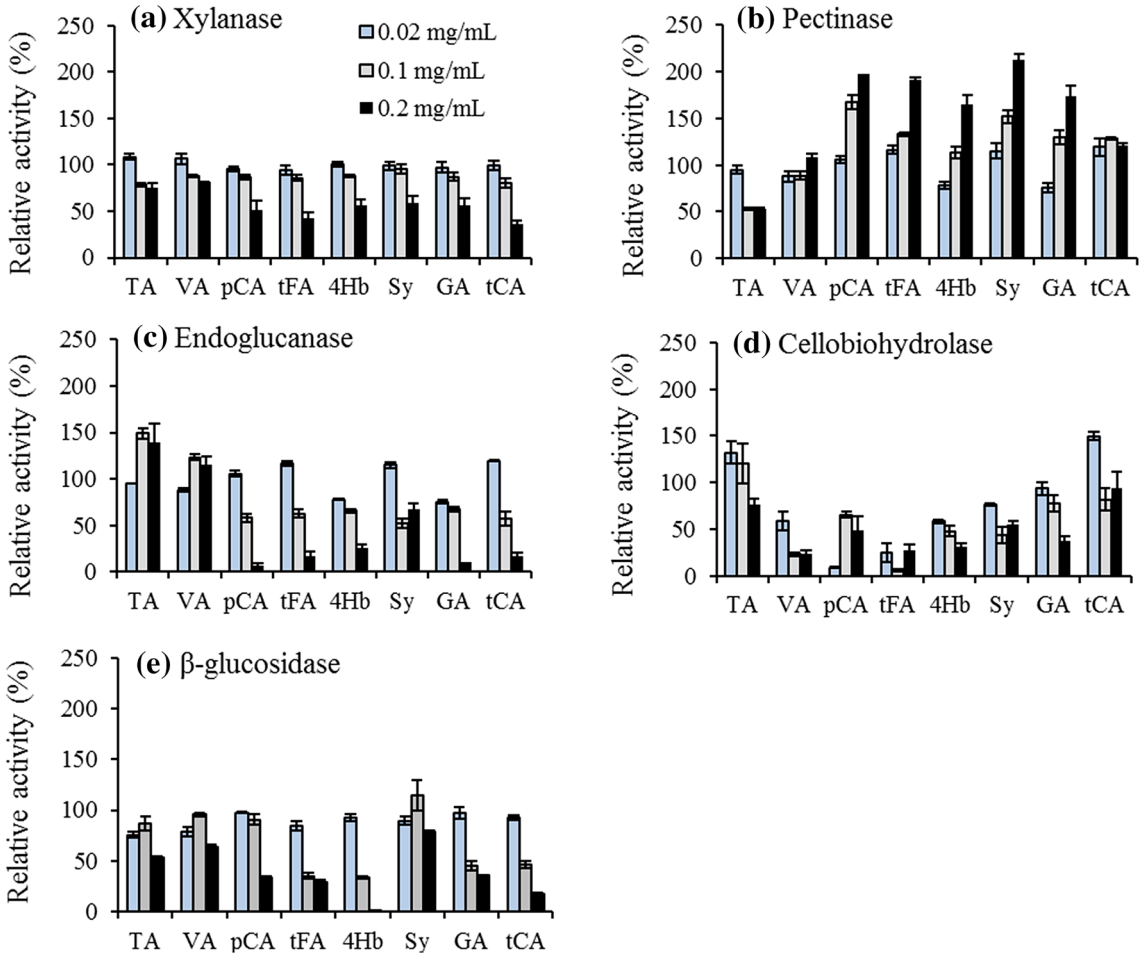

Fig. 7 Lignin derived phenolic compounds effect on **a** xylanase, **b** pectinase, **c** endoglucanase, **d** cellobiohydrolase, **e** β-glucosidase activities produced by *P. chyrsogenum* after 10 days growth time in the presence of corn straw (1% *w*/*v*). Blue, grey, and black bars represent 0.02, 0.1, and 0.2 mg/mL final concentration of phenolic compounds, respectively. tannic acid (TA), vanillin (VA), p-coumaric acid (pCA), trans-ferulic acid (tFA), 4-hydroxybenzoic (4Hb), syringaldehyde (Sy), galic acid (GA), trans-cinnamic acid (tCA). Vertical bars represent standard deviation from triplicates

Previously, Moreira et al. [30], reported that the filamentous fungus *Aspergillus terreus* produces a endo-β-1,4-xylanase in which phenolic compounds had little influence on its activity. This result is remarkably different to the observed in the present study, indicating that *P. chrysogenum's* xylanases might have different exposed aminoacids residues that could lead to nonproductive interaction with phenolics, and thus heading to activity abatement.

The activity boost observed for pectinases in the presence of phenolic compounds is unusual, given that in literature carbohydrate active enzymes are regularly reported as prone to activity loss in the presence of phenolic compounds [29]. The activation of pectinases by lignin derived compounds was briefly reported by Hong-Sheng et al [54]. Results found by these authors describe that pectinases secreted by *Fusarium oxysporum* were highly activated in the presence of gallic acid. Truly, how phenolic compounds modulate pectinase activity is not elucidate, and brings interest for further studies.

Lignin-derived components used in this study, are in their free form, not aggregated in lignin structure, in exception to tannic acid, which naturally has a polyphenolic structure with high molecular weight. Furthermore, the amount and nature of these compounds may be found in different levels accordantly to lignocellulosic biomass used as feedstock. For instance, grass crops as sugarcane may present higher content in ferulic acid, in comparison to wood crops.

Although isolate phenolic components do not represent the complex mixture of phenols and carbohydrates found in industrial reactors, and natural environments, the study of separate components makes possible better understanding the role of these compounds in every class of enzyme involved in lignocellulose deconstruction. For the development of more efficient processes of lignocellulose deconstruction, is vital to identify bottleneck points on which holocellulases may have their activity diminished, and as previously reported, lignin structures represents a major drawback to be overcome [28, 55, 56].

Indeed, the concentration of phenolic compounds may vary from biomass as well as pretreatment technology used. The most relevant data is the phenolic/protein ratio, since in industrial scale holocellulaces are usually concentrated in order to achieve substantial plant cell wall degrading activities. In this respect, the phenolic/protein ratio used in the present study is in accordance to previous studies [28].

In addition to biochemical properties of holocellulases secreted by *P. chrysogenum* CCDCA10756, how these proteins are deactivated /inhibited by lignocellulose hydrolysis end products is an important datum to further applications of these enzymes for lignocellulose biomass deconstruction.

As previous described in this study, pectinases had enhancement in the presence of lignin derived components, bringing the possibility of using this enzyme set to degrade more recalcitrant biomasses, as well as, carbohydrate portion from lignocellulose pretreatment residual slurry.

Conclusion

Penicillium chrysogenum CCDCA10756 isolated from the soil of Cerrado has potential to be used as a producer of plant cell wall degrading enzymes utilizing a renewable, cheaper and widely available carbon source, corn straw. Among the group of enzymes evaluated, cellulases secreted by *P. chrysogenum* CCDCA10756 showed to be more robust for future industrial applications. As a perspective, further experiments will be conducted to evaluate the potential of *P. chrysogenum* to produce others enzymes, such as LPMOs, as well as, investigating how lignocellulosic phenolic compounds interact with *P. chrysogenum*'s holocellulases.

Acknowledgements This work was supported by research grants from the University of Brasilia – UnB, CNPq, and FAPDF. Eliane F. Noronha is recipient of Brazilian Research Council (CNPq) research scholarship. Pedro R.V Hamann, and Alonso R.P. Ticona are recipient of CAPES doctoral degree scholarship, Sadia F. Ullah is the recipient of CNPq doctoral's degree scholarship.

References

1. Limayem, A., Ricke, S.C.: Lignocellulosic biomass for bioethanol production: current perspectives, potential issues and future prospects. Prog. Energy Combust. Sci. **38**, 449–467 (2012). https://doi.org/10.1016/j.pecs.2012.03.002
2. Ferreira-Leitao, V., Gottschalk, L.M.F., Ferrara, M.A., Nepomuceno, A.L., Molinari, H.B.C., Bon, E.P.S.: Biomass residues in Brazil: Availability and potential uses. Waste Biomass Valoriz. **1**, 65–76 (2010). https://doi.org/10.1007/s12649-010-9008-8
3. Soccol C.R., Vandenberghe L.P., Medeiros A.B., Karp S.G., Buckeridge M, Ramos L.P., Pitarelo A.P., Ferreira-Leitão V, Gottschalk L.M., Ferrara MA, da Silva Bon E.P., de Moraes L.M., Araújo Jde A, Torres F.A.: Bioethanol from lignocelluloses: Status and perspectives in Brazil. Bioresour. Technol. **101**, 4820–4825 (2010). https://doi.org/10.1016/j.biortech.2009.11.067
4. Demain, A.L.: Biosolutions to the energy problem. J. Ind. Microbiol. Biotechnol. **36**, 319–332 (2009). https://doi.org/10.1007/s10295-008-0521-8
5. Strassberger, Z., Tanase, S., Rothenberg, G.: The pros and cons of lignin valorisation in an integrated biore fi nery. RSC Adv. 25310–25318 (2014). https://doi.org/10.1039/c4ra04747h
6. Saha, B.C.: Hemicellulose bioconversion. J. Ind. Microbiol. Biotechnol. **30**, 279–291 (2003). https://doi.org/10.1007/s10295-003-0049-x
7. Anwar, Z., Gulfraz, M., Irshad, M.: Agro-industrial lignocellulosic biomass a key to unlock the future bio-energy: a brief

review. J. Radiat. Res. Appl. Sci. **7**, 163–173 (2014). https://doi.org/10.1016/j.jrras.2014.02.003
8. Singhania, R.R., Sukumaran, R.K., Patel, A.K., Larroche, C., Pandey, A.: Advancement and comparative profiles in the production technologies using solid-state and submerged fermentation for microbial cellulases. Enzyme Microb. Technol. **46**, 541–549 (2010). https://doi.org/10.1016/j.enzmictec.2010.03.010
9. Gilbert, H.J., Hazlewood, G.P.: Bacterial cellulases and xylanases. J. Gen. Microbiol. **139**, 187–194 (1993). https://doi.org/10.1099/00221287-139-2-187
10. Beg, Q.K., Kapoor, M., Mahajan, L., Hoondal, G.S.: Microbial xylanases and their industrial applications: a review. Appl. Microbiol. Biotechnol. **56**, 326–338 (2001). https://doi.org/10.1007/s002530100704
11. Polizeli, M.L.T.M., Rizzatti, A.C.S., Monti, R., Terenzi, H.F., Jorge, J.A., Amorim, D.S.: Xylanases from fungi: properties and industrial applications. Appl. Microbiol. Biotechnol. **67**, 577–591 (2005). https://doi.org/10.1007/s00253-005-1904-7
12. Jayani, R.S., Saxena, S., Gupta, R.: Microbial pectinolytic enzymes: a review. Process Biochem. **40**, 2931–2944 (2005). https://doi.org/10.1016/j.procbio.2005.03.026
13. Kashyap, D.R., Vohra, P.K., Chopra, S., Tewari, R.: Applications of pectinases in the commercial sector: a review. Bioresour. Technol. **77**, 215–227 (2001). https://doi.org/10.1016/S0960-8524(00)00118-8
14. Adeleke, A.J., Odunfa, S.A., Olanbiwonninu, A., Owoseni, M.C.: Production of cellulase and pectinase from orange peels by fungi\n. Nat. Sci. **10**, 107–112 (2012)
15. Forsberg, Z., Mackenzie, A.K., Sørlie, M., Røhr, ÅK., Helland, R., Arvai, A.S., Vaaje-Kolstad, G., Eijsink, V.G.H.: Structural and functional characterization of a conserved pair of bacterial cellulose-oxidizing lytic polysaccharide monooxygenases. Proc. Natl. Acad. Sci. USA. **111**, 8446–8451 (2014). https://doi.org/10.1073/pnas.1402771111
16. Bourbonnais, R., Paice, M.G., Reid, I.D., Lanthier, P., Yaguchi, M.: Lignin oxidation by laccase isozymes from Trametes versicolor and role of the mediator 2, 2'-azinobis (3-ethylbenzthiazoline-6-sulfonate) in kraft lignin depolymerization. Appl. Environ. Microbiol. 61, 1876–1880 (1995)
17. Ibrahim, V., Mendoza, L., Mamo, G., Hatti-Kaul, R.: Blue laccase from *Galerina sp*.: properties and potential for kraft lignin demethylation. Process Biochem. **46**, 379–384 (2011). https://doi.org/10.1016/j.procbio.2010.07.013
18. Saloheimo, M., Paloheimo, M., Hakola, S., Pere, J., Swanson, B., Nyyssönen, E., Bhatia, A., Ward, M., Penttilä, M.: Swollenin, a Trichoderma reesei protein with sequence similarity to the plant expansins, exhibits disruption activity on cellulosic materials. Eur. J. Biochem. **269**, 4202–4211 (2002). https://doi.org/10.1046/j.1432-1033.2002.03095.x
19. Ertan, F., Balkan, B., Balkan, S., Aktac, T.: Solid state fermentation for the production of α -amylase from *Penicillium chrysogenum* using mixed agricultural by-products as substrate. 657–661 (2006). https://doi.org/10.2478/s11756-006-0137-2
20. Ferrer, M., Plou, F.J., Nuero, O.M., Reyes, F., Ballesteros, A.: Purification and properties of a lipase from *Penicillium chrysogenum* isolated from industrial wastes. J. Chem. Technol. Biotechnol. 75, 569–576 (2000). https://doi.org/10.1002/1097-4660(200007)75:7%3C569::AID-JCTB258%3E3.0.CO;2-S
21. Nwodo, S.C., Uzoma, A.O., Thompson, N.E., Victoria, I.O.: Xylanase production of *Aspergillus niger* and *Penicillium chrysogenum* from ammonia pretreated cellulosic waste. Res. J. Microbiol. **3**(4), 246–253 (2008)
22. Vangulik, W.M., Antoniewicz, M.R., Delaat, W.T.A.M., Vinke, J.L., Heijnen, J.J.: Energetics of growth and penicillin production in a high-producing strain of *Penicillium chrysogenum*. Biotechnol. Bioeng. **72**, 185–193 (2001). https://doi.org/10.1002/1097-0290(20000120)72:2%3C185::AID-BIT7%3E3.0.CO;2-M
23. Backus, M.P., Stauffer, J.F., Johnson, M.J.: Penicillin yields from new mold strains. J. Am. Chem. Soc. **68**, 152–153 (1946). https://doi.org/10.1021/ja01205a518
24. Yang, Y., Yang, J., Liu, J., Wang, R., Liu, L., Wang, F., Yuan, H.: The composition of accessory enzymes of *Penicillium chrysogenum* P33 revealed by secretome and synergistic effects with commercial cellulase on lignocellulose hydrolysis. Bioresour. Technol. **257**, 54–61 (2018). https://doi.org/10.1016/j.biortech.2018.02.028
25. Duarte, G., Moreira, L., Gómez-Mendoza, D., Siqueira, F.G., De Batista, L., Amaral, L., Ricart, C., Filho, E.: Use of Residual biomass from the textile industry as carbon source for production of a low-molecular-weight xylanase from *Aspergillus oryzae*. Appl. Sci. **2**, 754–772 (2012). https://doi.org/10.3390/app2040754
26. Miller, G.L.: Use of dinitrosaiicyiic acid reagent for determination of reducing sugar. Anal. Chem. **3**, 426–428 (1959)
27. Bradford, M.M.: A rapid and sensitive method for the quantitation of microgram quantities of protein utilizing the principle of protein-dye binding. Anal. Biochem. **72**, 248–254 (1976). https://doi.org/10.1016/0003-2697(76)90527-3
28. Ximenes, E., Kim, Y., Mosier, N., Dien, B., Ladisch, M.: Inhibition of cellulases by phenols. Enzyme Microb. Technol. **48**, 54–60 (2011). https://doi.org/10.1016/j.enzmictec.2010.09.006
29. Ximenes, E., Kim, Y., Mosier, N., Dien, B., Ladisch, M.: Deactivation of cellulases by phenols. Enzyme Microb. Technol. **48**, 54–60 (2011). https://doi.org/10.1016/j.enzmictec.2010.09.006
30. De S. Moreira L.R., De Carvalho Campos, M., De Siqueira, P.H., Silva, L.P., Ricart, C.A., Martins, P.A., Queiroz, R.M., Filho, E.X..: Two β-xylanases from *Aspergillus terreus*: characterization and influence of phenolic compounds on xylanase activity. Fungal Genet. Biol. **60**, 46–52 (2013). https://doi.org/10.1016/j.fgb.2013.07.006
31. LAEMMLI, U.K.: Cleavage of structural proteins during the assembly of the head of bacteriophage T4. Nature. **227**, 680–685 (1970)
32. Zhang, M., Su, R., Qi, W., He, Z.: Enhanced Enzymatic Hydrolysis of Lignocellulose by Optimizing Enzyme Complexes. 1407–1414 (2010). https://doi.org/10.1007/s12010-009-8602-3
33. Goyal, A., Ghosh, B., Eveleigh, D.: Characteristics of fungal cellulases. Bioresour. Technol. **36**, 37–50 (1991). https://doi.org/10.1016/0960-8524(91)90098-5
34. Haas, H., Herfurth, E., Stöffler, G., Redl, B.: Purification, characterization and partial amino acid sequences of a xylanase produced by *Penicillium chrysogenum*. Biochim. Biophys. Acta—Gen. Subj. **1117**, 279–286 (1992). https://doi.org/10.1016/0304-4165(92)90025-P
35. Chen, M., Qin, Y., Liu, Z., Liu, K., Wang, F., Qu, Y.: Enzyme and microbial technology isolation and characterization of a [illegible] -glucosidase from *Penicillium decumbens* and improving hydrolysis of corncob residue by using it as cellulase supplementation. Enzyme Microb. Technol. **46**, 444–449 (2010). https://doi.org/10.1016/j.enzmictec.2010.01.008
36. Krogh, K.B.R.M., Harris, P.V., Olsen, C.L., Johansen, K.S., Hojer-pedersen, J., Borjesson, J., Olsson, L.: Characterization and kinetic analysis of a thermostable GH3 β -glucosidase from *Penicillium brasilianum*. 143–154 (2010). https://doi.org/10.1007/s00253-009-2181-7
37. Terrone, C.C., Freitas, C., De, Rafael, C., Terrasan, F., Almeida, A.F., De Carmona, E.C.: Agroindustrial biomass for xylanase production by *Penicillium chrysogenum*: purification, biochemical properties and hydrolysis of hemicelluloses. Electron. J. Biotechnol. **33**, 1–7 (2018). https://doi.org/10.1016/j.ejbt.2018.04.001
38. Sakamoto, T., Kawasaki, H.: Purification and properties of two type-B a-L-arabinofuranosidases produced by *Penicillium*

chrysogenum. Biochim. Biophys. Acta (BBA)-Gen. Subj. 1621, 204–210 (2003). https://doi.org/10.1016/S0304-4165(03)00058-8
39. Hoondal, G., Tiwari, R., Tewari, R., Dahiya, N., Beg, Q.: Microbial alkaline pectinases and their industrial applications: a review. Appl. Microbiol. Biotechnol. **59**, 409–418 (2002). https://doi.org/10.1007/s00253-002-1061-1
40. Alafia, A., Llama, M.J.: Purification and some properties of the pectin lyase from *Penicillhtm italicum*. 2, 335–340 (1991)
41. Narra, M., Dixit, G., Divecha, J., Kumar, K., Madamwar, D., Shah, A.R.: Production, purification and characterization of a novel GH 12 family endoglucanase from *Aspergillus terreus* and its application in enzymatic degradation of delignified rice straw. Int. Biodeterior. Biodegrad. **88**, 150–161 (2014). https://doi.org/10.1016/j.ibiod.2013.12.016
42. Johnson, E.A., Demain, A.L.: Probable involvement of sulfhydryl groups and a metal as essential components of the cellulase of *Clostridium thermocellum*. Arch. Microbiol. **137**, 135–138 (1984)
43. Akiba, S., Kimura, Y., Yamamoto, K., Kumagai, H.: Purification and characterization of a protease-resistant cellulase from *Aspergillus niger*. J. Ferment. Bioeng. **79**, 125–130 (1995)
44. Sposina, R., Teixeira, S., Souza, M.V., De Ximenes, E., Filho, F.: Purification and characterization studies of a thermostable b -xylanase from *Aspergillus awamori*. J. Ind. Microbiol. Biotechnol **37**, 1041–1051 (2010). https://doi.org/10.1007/s10295-010-0751-4
45. Tejirian, A., Xu, F.: Inhibition of cellulase-catalyzed lignocellulosic hydrolysis by iron and oxidative metal ions and complexes. Appl. Environ. Microbiol. **76**, 7673–7682 (2010). https://doi.org/10.1128/AEM.01376-10
46. Xu, F., Ding, H., Tejirian, A.: Detrimental effect of cellulose oxidation on cellulose hydrolysis by cellulase. Enzyme Microb. Technol. **45**, 203–209 (2009). https://doi.org/10.1016/j.enzmictec.2009.06.002
47. Davies, G., Henrissat, B.: Structures and mechanisms of glycosyl hydrolases. Structure. **3**, 853–859 (1995). https://doi.org/10.1016/S0969-2126(01)00220-9
48. Tejirian, A., Xu, F.: Inhibition of enzymatic cellulolysis by phenolic compounds. Enzyme Microb. Technol. **48**, 239–247 (2011). https://doi.org/10.1016/j.enzmictec.2010.11.004
49. Yaoi, K., Kondo, H., Hiyoshi, A., Noro, N., Sugimoto, H., Tsuda, S., Mitsuishi, Y., Miyazaki, K.: The Structural basis for the exo-mode of Action in GH74 oligoxyloglucan reducing end-specific cellobiohydrolase. J. Mol. Biol. **370**, 53–62 (2007). https://doi.org/10.1016/j.jmb.2007.04.035
50. Cannella, D., Hsieh, C.W.C., Felby, C., Jørgensen, H.: Production and effect of aldonic acids during enzymatic hydrolysis of lignocellulose at high dry matter content. Biotechnol. Biofuels. **5**, 1–10 (2012). https://doi.org/10.1186/1754-6834-5-26
51. Vieira, W.B., Rios, L., Moreira, D.S., Neto, A.M., Ximenes, E., Filho, F.: Production and Characterization of an Enzyme Complex From a New Strain of Clostridium Thermocellum With Emphasis on Its Xylanase Activity. Braz. J. Microbiol. **38**, 237–242 (2007)
52. Yu, P., Xu, C.: Production optimization, purification and characterization of a heat-tolerant acidic pectinase from *Bacillus sp*. ZJ1407. Int. J. Biol. Macromol. **108**, 972–980 (2018). https://doi.org/10.1016/j.ijbiomac.2017.11.012
53. Monti, A., Di Virgilio, N., Venturi, G.: Mineral composition and ash content of six major energy crops. Biomass Bioenergy. **32**, 216–223 (2008). https://doi.org/10.1016/j.biombioe.2007.09.012
54. Wu, H.S., Wang, Y., Zhang, C.Y., Bao, W., Ling, N., Liu, D.Y., Shen, Q.R.: Growth of in vitro *Fusarium oxysporum f. sp*. niveum in chemically defined media amended with gallic acid. Biol. Res. **42**, 297–304 (2009). https://doi.org/10.4067/S0716-97602009000300004
55. Duarte, G.C., Moreira, L.R.S., Jaramillo, P.M.D., Filho, E.X.F.: Biomass-derived inhibitors of holocellulases. Bioenergy Res. **5**, 768–777 (2012). https://doi.org/10.1007/s12155-012-9182-6
56. Silva, C., de O.G., Aquino, Ricart, E.N., Midorikawa, C.A.O., Miller, G.E.O., Filho, R.N.G.: E.X.F.: GH11 xylanase from emericella nidulans with low sensitivity to inhibition by ethanol and lignocellulose-derived phenolic compounds. FEMS Microbiol. Lett. **362**, 1–8 (2015). https://doi.org/10.1093/femsle/fnv094

Appendix: Chapter I

Trace elements solution

$CuSO_4$	0.5g
$ZnSO_4$	0.1g
H_2O	100mL

Sodium acetate buffer for gel filtration column (Sephadex) equilibration.

Sodium acetate	4.35g
Acetic acid	1.0 mL
NaCl	8.72g
Water Milliq	1000 mL
pH 5.0; 100mM	

*****Buffer without NaCl was used for dialysis and enzyme resuspension, and substrate preparation

12% Polyacrylamide gel electrophoresis

Tris-Hcl	2.6mL
Acrylamide/Bisacrylamide	4.2mL
SDS 10%	1.0mL
H_2O	2.38mL
TEMED	10µL
APS 10%	225µL

*For zymogram CMC or Xylan (2%) was added with the compensation of H_2O

Appendix Chapter II

Mass spectrometry results of *PcX1*

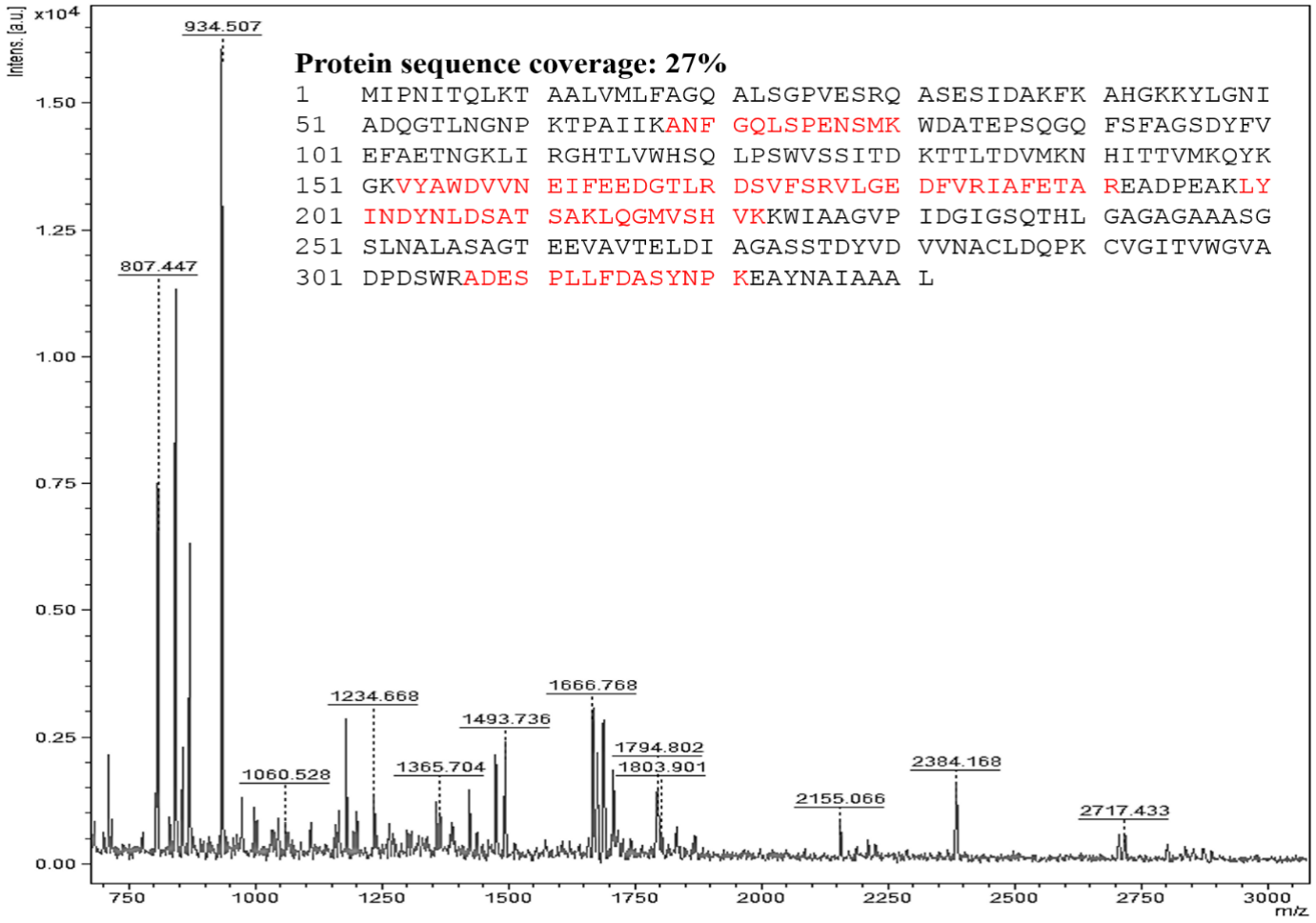

Figure showing identified peptides and spectra

Appendix Chapter III

Mass spectrometry results of *PcX2*

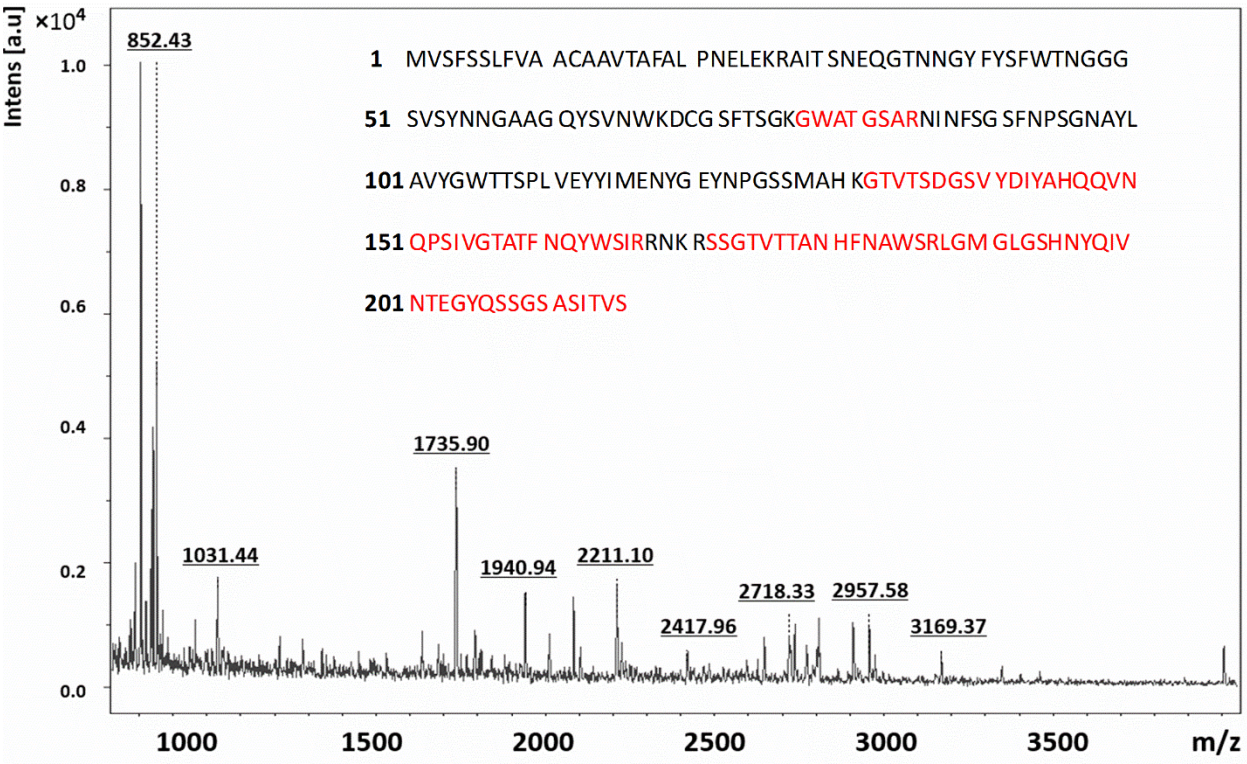

Figure showing identified peptides and spectra

HPLC Spectra

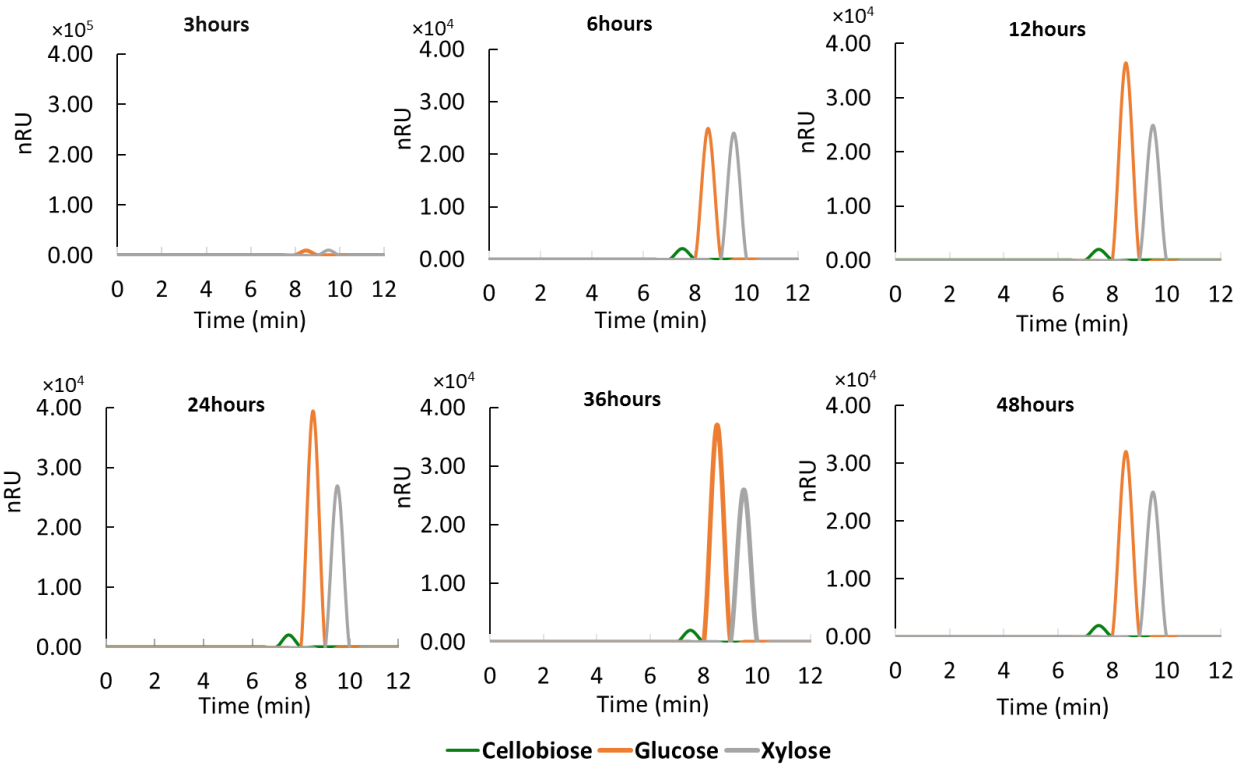

HPLC profile of reducing sugars, release during the enzymatic hydrolysis of hydrothermal pre-teated sugarcane bagasse during different intervals of time. Y.axis showing refrective index (nRU) X.axis showing the retension time (RT) of sugars. RT for Cellobiose = 7.50 min, Glucose = 8.82min, Xylose = 9.57min.

Appendix Chapter IV Statistical Reports

PcX1 Inhibition Kinetics

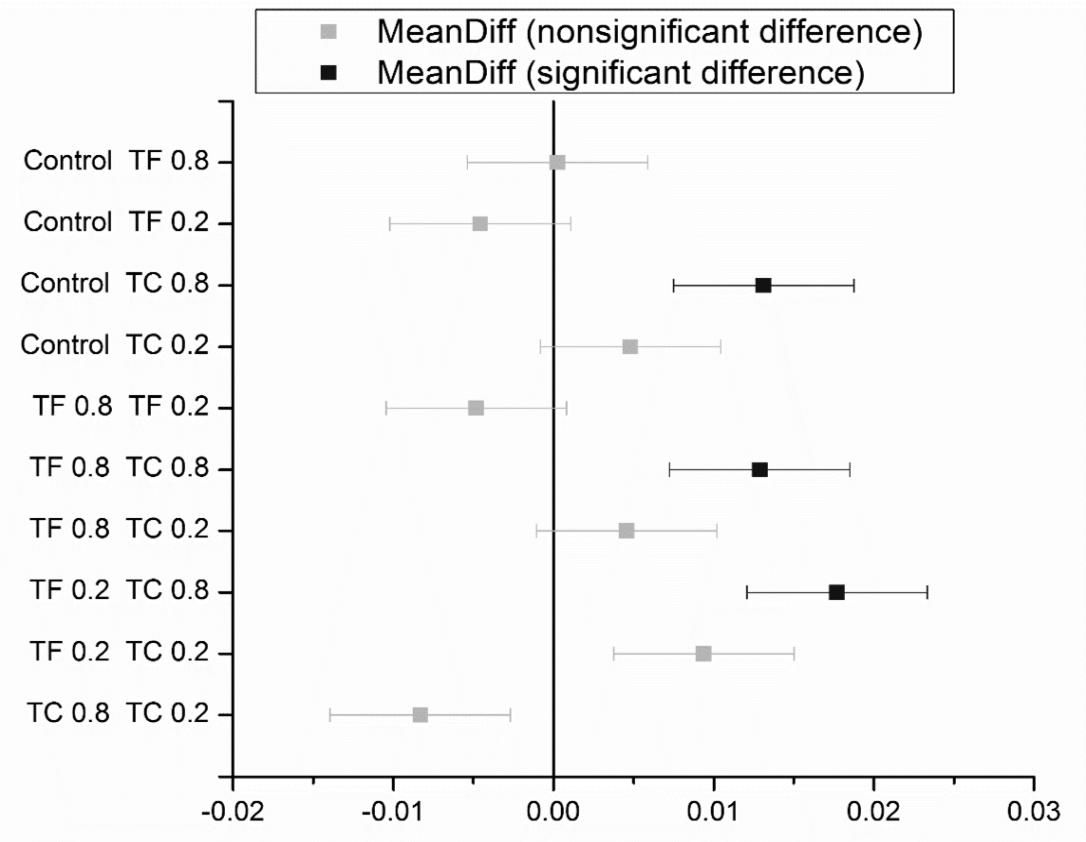

Pairwise LSD Fisher test

PcX2 Inhibition Kinetics

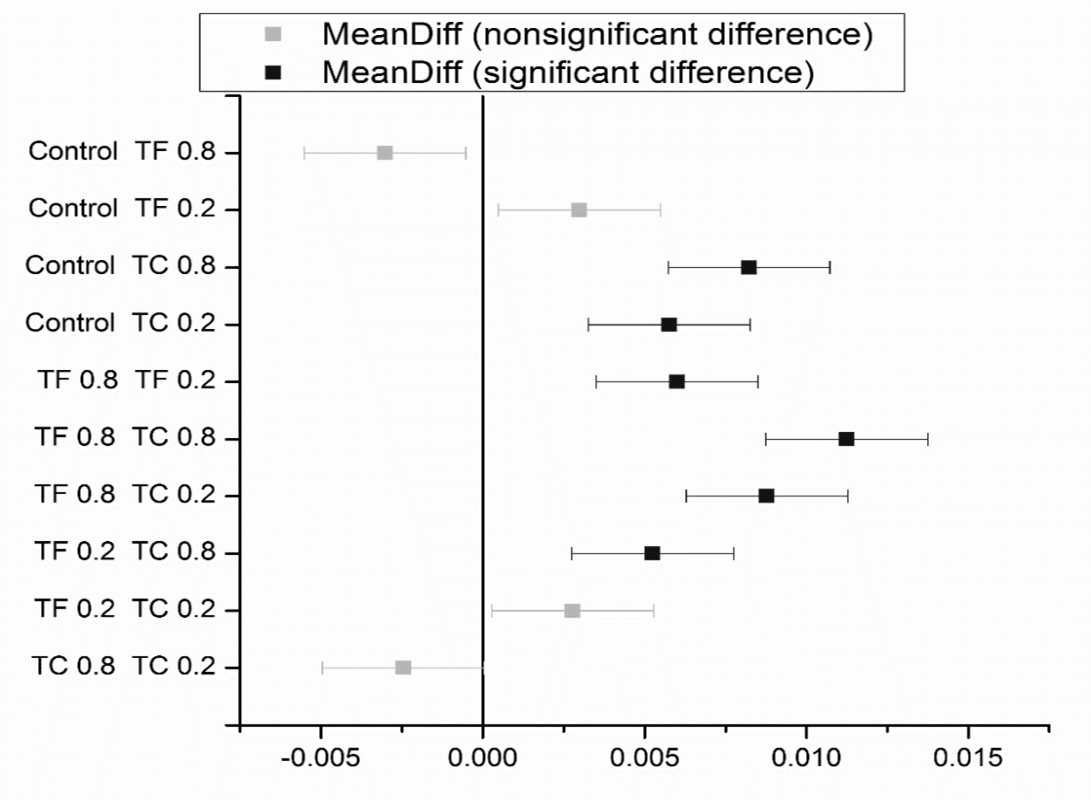

Pairwise LSD Fisher test

Appendix Chapter II, III, IV,

Properties of common amino acids in protein

Name	3 letter Code	1 letter code	Side chain class	pKa (COOH)	pKa ($NH3^{+}$)	pKa R group
Alanine	Ala	A	Aliphatic, nonpolar	2.4	9.9	--
Arginine	Arg	R	Basic	1.8	9	12.5
Asparagine	Asn	N	Acidic, polar	2.1	8.7	--
Aspartate	Asp	D	Acidic	2	9.9	3.9
Cysteine	Cys	C	Hydroxyl or Sulfur-Containing, polar	1.9	10.7	8.4
Glutamate	Glu	E	Acidic	2.1	9.5	4.1
Glutamine	Gln	Q	Acidic, polar	2.2	9.1	--
Glycine	Gly	G	Aliphatic, nonpolar	2.4	9.8	--
Histidine	**His**	**H**	**Basic**	**1.8**	**9.3**	**6**
Isoleucine	Ile	I	Aliphatic, nonpolar	2.3	9.8	--
Leucine	Leu	L	Aliphatic, nonpolar	2.3	9.7	--
Lysine	Lys	K	Basic	2.2	9.1	10.5
Methionine	Met	M	Hydroxyl or Sulfur-Containing, nonpolar	2.1	9.3	--
Phenylalanine	Phe	F	Aromatic	2.2	9.3	--
Proline	Pro	P	Cyclic	2	9.6	--
Serine	Ser	S	Hydroxyl or Sulfur-Containing, polar	2.2	9.2	--
Threonine	Thr	T	Hydroxyl or Sulfur-Containing, polar	2.1	9.1	--
Tryptophan	Trp	W	Aromatic	2.5	9.4	--
Tyrosine	Tyr	Y	Aromatic	2.2	9.2	10.5
Valine	Val	V	Aliphatic, nonpolar	2.3	9.7	--

Appendix Online Tools

In silico analysis and software

In the biochemical and biophysical characterization different online tools and software were used;

N-terminal and sequence alignment

- Complete sequences of Xylanase1 and Xylanase2 were accessed from NCBI https://www.ncbi.nlm.nih.gov/protein and
- Uniprot https://www.uniprot.org/
- The signal peptide were predicted by using SignalP an online tool http://www.cbs.dtu.dk/services/SignalP/.
- ProtParam, theoretical values of molecular mass and isoelectric point were retrieved from the Compute pI/Mw tool https://web.expasy.org/compute_pi/ according to predicted amino acid sequences resulted from mass spectrometry.
- Multiple sequence alignment was carried out with the Clustal Omega tool https://www.ebi.ac.uk/Tools/msa/clustalo/

Homology 3D structure

- The BLAST algorithm was applied to search the sequence homology. ESPript 3.0 http://espript.ibcp.fr/ESPript/ESPript/ was used to visualize the sequence alignment and the depiction of secondary structure.
- The sequence and 3D structure of the template protein were retrieved from the PDB_1B30 (*Penicillium simplicissimum*) holding 80% sequence similarity with *Xylanase1* https://www.rcsb.org/structure/1B31.
- Based on the high resolution crystal structure of the homologous protein, the model of xylanase1 was built using the homology modelling software MODELLER 9v18 and VMD.
- The best Modeller model was chosen based on the QMEAN analysis https://swissmodel.expasy.org/qmean/
- MolProbity http://molprobity.biochem.duke.edu/ evaluated the steric and geometric quality of the model. The structure depictions were generated using PyMol software

ProtParam

ProtParam

User-provided sequence:

```
        10         20         30         40         50         60
MVSFSSLFVA ACAAVTAFAL PNELEKRAIT SNEQGTNNGY FYSFWTNGGG SVSYNNGAAG

        70         80         90        100        110        120
QYSVNWKDCG SFTSGKGWAT GSARNINFSG SFNPSGNAYL AVYGWTTSPL VEYYIMENYG

       130        140        150        160        170        180
EYNPGSSMAH KGTVTSDGSV YDIYAHQQVN QPSIVGTATF NQYWSIRRNK RSSGTVTTAN

       190        200        210
HFNAWSRLGM GLGSHNYQIV NTEGYQSSGS ASITVS
```

References and documentation are available.

Number of amino acids: 216

Molecular weight: 23261.37

Theoretical pI: 7.75

Amino acid composition: CSV format

Ala (A)	19	8.8%
Arg (R)	6	2.8%
Asn (N)	21	9.7%
Asp (D)	3	1.4%
Cys (C)	2	0.9%
Gln (Q)	8	3.7%
Glu (E)	7	3.2%
Gly (G)	25	11.6%
His (H)	4	1.9%
Ile (I)	8	3.7%
Leu (L)	7	3.2%
Lys (K)	5	2.3%
Met (M)	4	1.9%
Phe (F)	10	4.6%
Pro (P)	5	2.3%
Ser (S)	30	13.9%
Thr (T)	17	7.9%
Trp (W)	6	2.8%
Tyr (Y)	15	6.9%
Val (V)	14	6.5%
Pyl (O)	0	0.0%
Sec (U)	0	0.0%
(B)	0	0.0%
(Z)	0	0.0%
(X)	0	0.0%

Total number of negatively charged residues (Asp + Glu): 10
Total number of positively charged residues (Arg + Lys): 11

Atomic composition:

Carbon	C	1028
Hydrogen	H	1512
Nitrogen	N	282
Oxygen	O	328
Sulfur	S	6

Formula: $C_{1028}H_{1512}N_{282}O_{328}S_6$
Total number of atoms: 3156

Extinction coefficients:

Extinction coefficients are in units of M^{-1} cm^{-1}, at 280 nm measured in water.

Ext. coefficient 55475
Abs 0.1% (=1 g/l) 2.385, assuming all pairs of Cys residues form cystines

Ext. coefficient 55350
Abs 0.1% (=1 g/l) 2.379, assuming all Cys residues are reduced

Estimated half-life:

The N-terminal of the sequence considered is M (Met).

The estimated half-life is: 30 hours (mammalian reticulocytes, in vitro).
>20 hours (yeast, in vivo).
>10 hours (Escherichia coli, in vivo).

Instability index:

The instability index (II) is computed to be 28.83
This classifies the protein as stable.

Aliphatic index: 54.68

Grand average of hydropathicity (GRAVY): -0.363

ProtParam

ProtParam

User-provided sequence:

```
        10         20         30         40         50         60
MIPNITQLKT AALVMLFAGQ ALSGPVESRQ ASESIDAKFK AHGKKYLGNI ADQGTLNGNP

        70         80         90        100        110        120
KTPAIIKANF GQLSPENSMK WDATEPSQGQ FSFAGSDYFV EFAETNGKLI RGHTLVWHSQ   W= 81, 117

       130        140        150        160 161    170        180
LPSWVSSITD KTTLTDVMKN HITTVMKQYK GKVYAWDVVN EIFEEDGTLR DSVFSRVLGE   W=124, 156

       190        200        210        220        230        240
DFVRIAFETA READPEAKLY INDYNLDSAT SAKLQGMVSH VKKWIAAGVP IDGIGSQTHL   W= 224

       250        260    267 270        280        290        300
GAGAGAAASG ALNALASAGT EEVAVTELDI AGASSTDYVD VVNACLDQPK CVGITVWGVA   W=297,305

       310        320        330
DPDSWRADES PLLFDASYNP KEAYNAIAAA L
```

References and documentation are available.

Number of amino acids: 331

Molecular weight: 35455.81

Theoretical pI: 4.90

Amino acid composition: CSV format

```
Ala (A)  43      13.0%
Arg (R)   7       2.1%
Asn (N)  15       4.5%
Asp (D)  22       6.6%
Cys (C)   2       0.6%
Gln (Q)  12       3.6%
Glu (E)  18       5.4%
Gly (G)  26       7.9%
His (H)   6       1.8%
Ile (I)  18       5.4%
Leu (L)  24       7.3%
Lys (K)  20       6.0%
Met (M)   6       1.8%
Phe (F)  12       3.6%
Pro (P)  13       3.9%
Ser (S)  26       7.9%
Thr (T)  21       6.3%
Trp (W)   7       2.1%
Tyr (Y)   9       2.7%
Val (V)  24       7.3%
Pyl (O)   0       0.0%
Sec (U)   0       0.0%

 (B)   0          0.0%
 (Z)   0          0.0%
 (X)   0          0.0%
```

Total number of negatively charged residues (Asp + Glu): 40
Total number of positively charged residues (Arg + Lys): 27

Atomic composition:

```
Carbon      C         1578
Hydrogen    H         2452
Nitrogen    N          418
Oxygen      O          495
```

Sulfur S 8

Formula: $C_{1578}H_{2452}N_{418}O_{495}S_8$
Total number of atoms: 4951

Extinction coefficients:

Extinction coefficients are in units of M^{-1} cm^{-1}, at 280 nm measured in water.

Ext. coefficient 52035
Abs 0.1% (=1 g/l) 1.468, assuming all pairs of Cys residues form cystines

Ext. coefficient 51910
Abs 0.1% (=1 g/l) 1.464, assuming all Cys residues are reduced

Estimated half-life:

The N-terminal of the sequence considered is M (Met).

The estimated half-life is: 30 hours (mammalian reticulocytes, in vitro).
>20 hours (yeast, in vivo).
>10 hours (Escherichia coli, in vivo).

Instability index:

The instability index (II) is computed to be 28.54
This classifies the protein as stable.

Aliphatic index: 83.50

Grand average of hydropathicity (GRAVY): -0.144